

University of Nottingham
UK | CHINA | MALAYSIA

A recombinant non-toxigenic *Clostridioides difficile* spore vaccine directed against toxigenic *C. difficile*

Carl Aston MSc

Thesis submitted to University of Nottingham for the Degree of Doctor of Philosophy

September 2021

Acknowledgements

I would like to thank Dr. Ruth Griffin for providing me with the opportunity to pursue this work and for use of the lab space, as well as for the advice she has given me throughout this project. I would also like to thank Professor Nigel Minton for his advice and support as my second supervisor. I would like to thank both the BBSRC DTP, as well as the Midlands Innovation and Commercialization Research Accelerator (MICRA) awarded to Ruth Griffin grant number CCF15-6840.

I am very grateful for the tireless help, advice and support offered to me by Dr. Jaime Hughes during this time. Her contributions in setting up cell lines and performing toxin neutralisation assays during the project have been invaluable and she has always been there to lend an ear and troubleshoot experiments.

I would also like to thank Miss Michelle Kelly for her contributions to the *in vivo* section of this project. Without her, those mornings spent in the animal unit would have passed much slower.

Thank you to Dr. David Onion and Miss Nicola Croxall for their guidance and expertise in FACS analysis, and thank you to Dr. Adam Dowle of the University of York for performing LC-MS.

I would also like to thank the other members of the Griffin Lab, Cansu Karyal, Liam Wood, and Barbora Martinkova for their help and support, as well as all the members of Lab B27.

Most of all, I would like to thank Miss (soon to be Dr.) Vicky Smith, who started the PhD with me as a stranger, but is finishing as my wife. Thank you for seeing us through the stress, the late nights, and the upheaval of moving cities. I wouldn't be here without you.

Covid Impact Statement

The immediate effect of the Covid-19 outbreak was the closure of the laboratory space. This completely prevented access to the laboratory between March and late July 2020. Upon returning to the laboratory, the systems by which we normally ordered and received supplies were heavily disrupted; this took the form of severe delays in the shipping of reagents, as well as necessitating the move to new, unfamiliar suppliers. This inevitably caused a large disruption to my ongoing project and my work was impacted significantly, even following the return to labs in July.

To overcome issues with social distancing and capacity, a shift system was put in place for laboratory and office space. Due to the number of hours available in labs being limited, this meant multiple protocols could not readily be performed as pre-Covid. For the early part of the return to work, this also eliminated the possibility of weekend and out of hours working, meaning a further compression of time within the laboratory.

Prior to lockdown, I was preparing samples for initiation of *in vivo* studies. However, following lockdown the Biosupport Unit at the University of Nottingham remained closed. It did not reopen until late Autumn of 2020, delaying the planning of *in vivo* studies significantly. Should the pandemic not have caused the lockdown and closure of laboratories, I would likely have had the opportunity to execute repeats/additional studies of the *in vivo* work described within this project.

In response to these events, much of the time spent in lockdown was spent working on my thesis, however the inability to continue generating data meant this time could not be utilised to its full potential. While communication across shifts allowed me to perform necessary experiments, severe restriction of time in labs has meant planned *in vivo* work was significantly delayed and therefore the predicted outcome of this data compared with the thesis plan was the most impacted.

Abstract

Clostridioides difficile (*C. difficile*) is the leading cause of hospital acquired diarrhoeal infection. Its pathology is mainly due to two toxins, TcdA and TcdB. The failure to treat recurrent infection can culminate in death and thus preventative measures are of urgent need. Current vaccine trials in humans are exclusively focused on parenteral delivery of toxin-based formulations. While these vaccines elicit toxin-neutralising serum antibody responses, they fail to provide protection against colonisation and therefore *Clostridium difficile* infection (CDI). Ideally a vaccine targeting *C. difficile* would aim to generate a local mucosal immune response (i.e., secretory IgA that directly targets the site of infection). In this study, a non-toxigenic strain of *C. difficile* (NTCD) was utilised as a delivery system, where immunisation with recombinant spores would allow direct delivery of vaccine candidates to the ileum. To provide a mechanism of release from the cell, as well as increase immunogenicity, a fragment of the TcdB receptor binding domain (previously shown to be immunogenic) was fused to the signal peptide of lipoprotein and colonisation factor CD0873 with a view to creating a TcdB antigen which is naturally lipidated. Both this TcdB construct, and full-length CD0873 were utilised as vaccine candidates. Recombinant episomal plasmids were engineered and conjugated into NTCD strain T7, generating strains capable of expressing these vaccine candidates following germination. Western immunoblotting demonstrated the ability of these strains to produce antigens which are secreted into the extracellular milieu. Spores of these recombinant strains were then used to immunise mice and hamsters. Tissues harvested from immunised animals demonstrated a high antigen-specific IgA and IgG titre compared to animals immunised with strains of the wild type T7 strain. They also demonstrated the ability to reduce binding of *C. difficile* to Caco-2 colorectal cells, and reduce cytotoxicity of TcdB and TcdA to Vero cells. This study provides important proof-of-concept data for use of NTCD strains as a delivery device for vaccine candidates, and paves the way for exploiting the ability of the signal peptide of CD0873 to lipidate and secrete attached antigens to the extracellular milieu.

Contents

Abstract **i.**

Contents **ii.**

Abbreviations **vii.**

Chapter 1. Introduction **5**

1.1 *Clostridioides difficile* 5

1.1.1 *C. difficile* infection 6

1.1.2 Risk factors associated with CDI 6

1.1.3 Economic impact 7

1.1.4 Pathogenesis and host defences 7

1.1.5 Clostridial spores 8

1.1.6 Germination 12

1.1.7 The role of the microbiota in spore germination 14

1.1.8 Colonisation 15

1.1.9 The S-layer and surface proteins 17

1.1.10 Toxin production 18

1.1.11 Sporulation 21

1.2 Lipoproteins 22

1.2.1 Acylation of bacterial lipoproteins 23

1.3 Current therapies and their limitations 25

1.3.1 Antibiotic therapy 25

1.3.2 Antibody Therapy 26

1.3.3 Faecal Microbiota Transplantation 27

1.3.4 Spore therapy 28

1.3.5 The need for a novel vaccine 29

1.4. Mucosal Immunity 29

1.4.1 Mucosa-associated lymphoid tissues (MALT) 29

1.4.2 Key differences between sIgA and IgG 32

1.4.3 The role of IgA in the mucosal immune response 32

1.5 Mucosal Vaccines 35

1.5.1 The benefits of mucosal vaccines 35

1.5.2 Challenges in developing mucosal vaccines 36

1.6 Factors to consider during vaccine development 38

1.6.1 Use of *in vivo* models 38

1.6.2 Antigen candidates 39

1.6.3 Deploying NTCD as a live oral vaccine strain 40

1.6.4 Antigenic presentation 41

1.7 Aims of this project 42

Chapter 2. Materials and Methods 44

2.1 General microbiological techniques 44

2.1.1 Bacterial strains and growth conditions 44

2.1.1.1 Bacterial strains 44

2.1.1.2 Growth medium and supplements 44

2.1.1.3 Glycerol stocks 46

2.1.1.4 Aerobic bacterial strains and culture conditions 46

2.1.1.5 Anaerobic bacterial strains and culture conditions 46

2.1.2 *C. difficile* spore preparation 46

2.1.2.1 Enumeration of *C. difficile* spores by phase-contrast microscopy 47

2.1.2.2 Quantification of *C. difficile* spores by serial dilution 47

2.1.3 Assessment of spores by TEM 47

2.2 Bioinformatics manipulations and tools 48

2.2.1 Basic Local Alignment Search Tool (BLAST®) 48

2.2.2 Generation of a Shotgun Sequence from T7 gDNA 48

2.2.3 Plasmid sequence maps 48

2.2.4 DNA Oligos 48

2.2.5 Sequence alignments 48

2.3 Liquid Chromatography Mass Spectrometry (LC-MS) investigation of clostridial lipoproteins 49

2.3.1 Preparation of culture supernatant 49

2.3.2 LC-MS of extracellular proteins 49

2.4 Genetic manipulations 51

2.4.1 Nucleic Acid Purification 51

2.4.2 Nucleic acid purification for use in genomic sequencing 51

2.4.3 Nucleic Acid Quantification 52

2.4.4 Polymerase chain reaction (PCR) and primers 52

2.4.5 Colony PCR 56

2.4.6 Agarose gel electrophoresis 56

2.4.7 Restriction digest 56

2.4.8 Dephosphorylation of plasmid vector 57

2.4.9 Ligation reactions 57

2.5 Transforming *E. coli* 58

2.5.1 Making competent *E. coli* cells 58

2.5.2 Transforming competent *E. coli* 58

2.5.3 Screening *E. coli* transformants 59

2.5.4 Verifying *E. coli* transformants 59

2.6 Transformation into *Clostridium difficile* 60

2.6.1 Transformation into conjugation strain sExpress 60

2.6.2 Transformation into *C. difficile* by conjugation 61
2.6.3 Screening of *C. difficile* transformants 61
2.7 Assessment of recombinant *C. difficile* strains 62
2.7.1 Growth curves and time sampling of clostridial species 62
2.7.2 Assessing the sporulation rate of recombinant strains 62
2.7.3 Assessment of plasmid retention by recombinant strains 63
2.8 Protein expression and purification 63
2.8.1 Protein expression 63
2.8.2 Protein extraction 63
2.8.3 Sodium dodecyl sulphate-polyacrylamide electrophoresis (SDS-PAGE) 64
2.8.4 Immobilized Metal Affinity Chromatography (IMAC) for purification of soluble recombinant His-tagged proteins 65
2.8.5 On-column solubilisation and purification of recombinant His-tagged proteins using IMAC 65
2.8.6 Solubilisation and purification by His-trap column 66
2.8.7 Purification by membrane filtration 66
2.8.8 Protein concentration determination using Bicinchoninic acid assay (BCA) 66
2.8.9 Western Immunoblotting 67
2.9 Fluorescent staining of T7 recombinant strains for use in FACS and confocal microscopy 67
2.9.1 Fluorescent staining of T7 recombinant strains 67
2.9.2 FACS analysis 69
2.9.3 Confocal microscopy 69
2.10 *in vivo* immunogenicity study using hamsters and mice 69
2.10.1 *in vivo* immunisation and sample collection 69
2.10.1.1 Serum and intestinal fluid preparations 70
2.10.1.2 ELISA 70
2.10.1.3 Toxin neutralisation assay using Vero cells 71
2.10.1.4 Adherence blocking assay using Caco-2 cells 72
2.10.3 Ethics statement 73
2.10.4 Statistical analysis 73

Chapter 3. Rational design of a vaccine against *C. difficile* 74
3.1 Introduction 74
3.2 Aims 75
3.3 Results 76
3.3.1 Identifying a suitable vaccine chassis strain 76
3.3.2 Comparison of sporulation efficiency of 4 strains of NTCD 79
3.3.3 TEM of spores 81
3.3.4 Analysis of the genome sequence of chosen NTCD chassis strain, T7 82

3.4 Identification of the most abundant extracellular lipoprotein 86
3.4.1 LC-MS to determine the most abundant extracellular lipoprotein 87
3.4.2 Determining the signal peptide region of CD0873 90
3.5 Selection of Toxin candidates 92
3.6 Discussion 94
3.7 Conclusion 95

Chapter 4. Creation of episomal shuttle vectors for lipidation and release of recombinant antigens in non-toxigenic *C. difficile* 97
4.1 Introduction 97
4.2 Aims 97
4.3 Results 98
4.3.1 Episomal shuttle *C. difficile* vector pMTL84123 98
4.3.2 Shuttle vector pMTL84123 engineered to harbour the SP and SPAP of CD0873 to create pMTL84123::08730_Signal and pMTL84123::08730_Signal+Anchor 99
4.3.3 Shuttle vectors pMTL84123::08730_Signal and pMTL84123::08730_Signal+Anchor plasmids engineered to fuse with in-frame TcdB RBD 102
4.3.4 Shuttle vectors pMTL84123::08730_Signal and pMTL84123::08730_Signal+Anchor plasmids engineered to fuse with in-frame TcdA RBD 107
4.3.5 Shuttle vectors pMTL84123 engineered to express full length CD0873 109
4.3.6 Integration of episomal constructs into non-toxigenic *C. difficile* strain T7 112
4.3.7 Confirmation of plasmid conjugation into non-toxigenic *C. difficile* 112
4.4 Discussion 113

Chapter 5. Phenotypic analysis of recombinant *C. difficile* strains 116
5.1 Introduction 116
5.2 Aims 117
5.3 Results 117
5.3.1 Purification of recombinant protein antigens of *C. difficile* 117
5.3.1.1 Purification of rTcdB for use in ELISA and Western blotting 117
5.3.1.2 Purification of r CD0873 for use as a control in ELISA and Western Blotting 123
5.3.2 Assessing growth rate of T7 recombinant strains harbouring plasmids 126
5.3.3 Assay to determine level of sporulation in recombinant strains 127
5.3.4 Assessment of expression of antigens in recombinant strains of T7 harbouring episomal plasmids. 128

5.3.4.1 Assessment of TcdB expression by Western immunoblotting 129
5.3.4.2 Assessment of CD0873 expression in T7-0873 by Western immunoblotting 131
5.3.6 Assessment of antigen expression on the surface of T7 recombinant strains by FACS 133
5.3.7 Further investigation of TcdB localisation in individual cells of recombinant strains of T7 by immunofluorescent confocal microscopy 136
5.4 Discussion 138
Phenotypic assessment of antigen candidates by Western immunoblotting 139
Examining the presence of antigen candidates on the cell surface by FACS 141
Examining the presence of antigen candidates on the cell surface by confocal microscopy 141
5.5 Conclusion 142

Chapter 6. Assessment of the immunogenicity of orally administered T7 recombinant strains in hamsters and mice 143
6.1 Introduction 143
6.2 Aims and Objectives 143
6.3 Results 144
6.3.1 Serum IgG titres detected in immunised hamsters by ELISA 144
6.3.2 Adherence blocking of *C. difficile* CD630 to Caco-2 cells by immunised hamster serum and intestinal fluid 148
6.3.3 Toxin neutralisation ability of immunised hamster serum and intestinal fluid as assessed by MTT assay 150
6.3.3.1 Conclusions from immunogenicity profiles of hamsters immunised with T7 recombinant strains 153
6.3.4 Serum IgG titres detected in immunised mice by ELISA 153
6.3.5 Adherence blocking of *C. difficile* CD630 to Caco-2 cells caused by immunised mouse serum and intestinal fluid 158
6.3.6 Toxin neutralisation ability of immunised mouse serum and intestinal fluid as assessed by MTT assay 161
6.3.6.1 Conclusions from immunogenicity profiles of hamsters immunised with T7 recombinant strains 165
6.4 Discussion 165
6.5 Conclusion 169

Chapter 7. Discussion 170

8. References 180

Abbreviations

ACE – Allelic coupled exchange

AP – Anchor peptide

APC – Antigen presenting cell

APD – Autoprocessing domain

BCA – Bicinchoninic acid assay

bp – Base pair

BSA – Bovine serum albumin

CbpA – Collagen binding protein A

CDC – Center for disease control

CDI – *Clostridioides difficile* infection

CFU – Colony-forming units

CIAP – Calf Intestinal alkaline phosphatase

CRISPR – Clustered regularly interspersed palindromic repeats

CROP – Combined repetitive oligopeptide

CSR – Class-switch recombination

CWP – Cell wall protein

DC – Dendritic cell

DD – Delivery domain

DPA – Dipicholinc acid

DMEM – Dulbecco's modified Eagle's medium

DMSO – Dimethyl sulfoxide

DTT – 1,4- Dithiothreitol

ECL – Enhanced chemiluminescence

EDA – Experimental design assistant

FAB – Fragment antibody binding

FACS – Fluorescence associated cell sorting

FBS – Fetal bovine serum

FC – Fragment Crystallisable

FL – Full length

FMT – Faecal microbiota transplant

GALT – Gut associated lymphoid tissue

GC – Germinal center

gDNA – Genomic DNA

GI – Gastrointestinal

GIT – Gastrointestinal tract

GR – Germinant receptor

GTD – Glucosyltransferase domain

HMW – High molecular weight

HRP – Horseradish peroxidase

iCDI – Initial *Clostridioides difficile* infection

IFR – Interfollicular region

IMAC – Immobilised metal affinity chromatography

IPTG – Isopropyl β- d-1-thiogalactopyranoside

IVC – Individually ventilated cage

LB – Luria-Bertani

LC-MS – Liquid chromatography mass spectrometry

Lgt – Diacylglyceryl transferase

LMW – Low molecular weight

Lnt – Apolipoprotein *N*-acyltransferase

Lol – Lipid outer-membrane localisation

LP – Lamina Propria

Lsp – Lipoproteins signal peptidase

MAL – Muramic-δ-lactam

MALT – Mucosa associated lymphoid tissue

MCS – Multiple cloning site

MGE – Mobile genetic element

MFI – Median fluorescence intensity

MLN – Mesenteric lymph nodes

MOI – Multiplicity of infection

MTT – 3-(4,5-dimethylthiazol-2-yl)-2,5- diphenyltetrazolium bromide

MWCO – Molecular weight cut-off

NAG – *N*-acetylglucosamine

NAM – *N*-acetylmuramic acid

NTCD – Non-toxigenic *Clostridioides difficile*

OD – Optical density

ORF – Open reading frame

PAGE – Polyacrylamide gel electrophoresis

PaLoc – Pathogenicity locus

PAMP – Pathogen-associated molecular patterns

PCI – Phenol/chloroform/isoamyl alcohol

PCR – Polymerase chain reaction

PG – Peptidoglycan

pI – Isoelectric point

pIgA – Polymeric IgA

pIgR – Polymeric immunoglobulin receptor

PP – Peyer's patches

RBD – Receptor binding domain

rCDI – Recurrent *Clostridioides difficile* infection

RT – Ribotype

SASP – Small acid-soluble proteins

SDS – Sodium dodecyl sulphate

SED – Subepithelial dome

SEM – Standard error of the mean

SIF - Small intestinal fluid

SLP – Surface-layer protein

SN – Supernatant

SP – Signal peptide

SPII – Signal peptidase II

SPAP – Signal peptide and anchor peptide

TAE – Tris-acetate- EDTA

TBS – Tris-buffered saline

TBST – Tris-buffered saline plus 0.1% Tween 20

TCD – Toxigenic *C. difficile*

TcdA – Clostridial toxin A

TcdB – Clostridial toxin B

TLR2 – Toll-like receptor 2

TMB – 3, 3',5 ,5'- Tetramethylbenzidine

WCL – Whole cell lysate

Chapter 1. Introduction

1.1 *Clostridioides difficile*

Clostridioides difficile (formerly *Clostridium difficile*) is a Gram-positive, spore-forming, anaerobic bacillus. All Gram-positive bacteria have a thick layer of peptidoglycan (PG) and a single plasma/cytoplasmic membrane. *C. difficile* is naturally present in the intestinal tract of humans and animals, but it is usually present in very low numbers (Galdys *et al*., 2014; Lawson *et al*., 2016). It was first isolated in 1935 by Hall and O'Toole (Hall, 1935) from the stool of a healthy infant and was believed to be part of the normal commensal flora only until the link was made to pseudomembranous colitis in 1978 (Lance George *et al*., 1978). Colonisation by *C. difficile* is suppressed by the more dominant anaerobes present within the normal gut flora. Thus, the rate of colonization in the human gut for *C. difficile* varies as the composition of the gut flora changes over time. Rate of colonisation is highest in early infancy as the composition of the gut flora is less diverse, though these colonisations are often asymptomatic (Adlerberth *et al*., 2014). It is estimated that approximately 5% of adults and 15–70% of infants are colonised by *C. difficile*, and the prevalence of colonisation is several times higher in patients in both hospitals and nursing homes (Leffler & Lamont, 2015).

C. difficile strain 630 (CD630) is one of the reference strains used widely in the laboratory. Its genome sequence was first published in 2006 after this strain was isolated from a patient with pseudomembranous colitis (Sebaihia *et al*., 2006). CD630 is resistant to a range of broad-spectrum antibiotics, including fluoroquinolones, macrolides, and cephalosporins (Pepin *et al*., 2005; Hensgens *et al*., 2012; Spigaglia, 2016). The genome of CD630 consists of a circular chromosome of 4.29 Mb and a plasmid, pCD630, of 7.8 kb, both of low GC content (29.06%) (Sebaihia *et al*., 2006). The GC content is highly variable across the genome. Indeed, as much as 11% of the CD630

genome is made up of mobile genetic elements (MGEs) such as *Tn5397* which confers resistance to tetracycline known also to be present in *Bacillus subtilis, Enterococcus faecalis* and *Streptococcus* species (Sebaihia *et al*., 2006; Spigaglia, 2016). The plasticity of the genome explains the organism's high rate of adaptability and propensity for acquisition of various antimicrobial resistance genes through horizontal gene transfer.

1.1.1 *C. difficile* infection

C. difficile has been recognised as the leading cause of hospital-acquired infection, which in worse cases manifests as a severe diarrhoea, pseudomembranous colitis, toxic megacolon, and bowel perforation (Paredes-Sabja *et al*., 2014; Peng *et al*., 2017; Smits *et al*., 2016). *C. difficile* is not only a problem in hospitals and care-homes but recent studies have shown that up to 30% of new *Clostridium difficile* infection (CDI) cases are now acquired from the community (Khanna *et al*., 2012). The emergence of hypervirulent strains for example 027/NAP1/BI which spread from North America to Europe, and antibiotic resistant strains have contributed to the dissemination of CDI in the community worldwide (Heimann *et al*., 2018).

1.1.2 Risk factors associated with CDI

Treatment with antibiotics is the main inducer of CDI (Tedesco *et al*., 1974) with up to 15% of hospital patients affected. In fact, almost all antibiotics have been associated with the development of CDI, but in particular broad spectrum antibiotics such as fluoroquinolones, clindamycin and cephalosporins (Bartlett *et al*., 1977; Bignardi, 1998; Leffler & Lamont, 2015). Antibiotic treatment causes fluctuations in the balance of the microbiota as whole populations of organisms are killed unintentionally by the treatment. This provides a niche for opportunistic pathogens such as *C. difficile* to colonise and establish infection (McFarland, 1999; Pepin *et al*., 2005). The risk of acquiring CDI is 8 to 10-fold higher during antimicrobial chemotherapy and 4 weeks thereafter, and 3-fold higher in the next 2 months (Hensgens *et al*., 2012). Age is another predisposing factor. Patients aged over 65 years have a

5-10-fold increased risk of acquiring CDI compared with patients below 65 years of age. This is also accompanied by a much higher likelihood of poor clinical outcome in terms of both severity and mortality (Czepiel *et al*., 2015). Recurrent CDI (rCDI) is common, occurring in up to 30% of patients who have received initial antibiotic treatment (Leffler & Lamont, 2015).

1.1.3 Economic impact

The Center for Disease Control and Prevention (CDC) reports approximately half a million cases of CDI in the United States each year and around 30,000 deaths, costing the US healthcare system about $4.8 billion each year (CDC, 2015). A recent report by Feuerstadt *et al.* (2020) calculated direct medical costs per patient with CDI to be nearly $72,000 for those with no recurrence and about $208,000 for those with 3 or more cases of recurrent CDI (rCDI) (Feuerstadt *et al*., 2020). CDI is a global public health threat (CDC, 2015) and cases in the UK are estimated to cost the NHS £14,212 per CDI patient with costs rising to £57,519 for patients with rCDI (Tresman *et al.,* 2018). Between March 2018 and March 2019, 13,369 new cases of CDI were reported in England (Public Health England, 2019).

1.1.4 Pathogenesis and host defences

The transmission of *C. difficile* is via its production of spores. Spores are ingested by a host and travel to the small intestine, where they begin to germinate into vegetative cells (Paredes-Sabja *et al*., 2014; Peter Setlow, 2003). The majority of spores are thought to germinate in the large intestine and the resulting vegetative cells colonise the colon, multiply and release clostridial toxins, which are responsible for the clinical symptoms observed in the host (Voth & Ballard, 2005; Di Bella *et al*., 2016; Aktories *et al*., 2017). New spores are produced by the vegetative cells which are released by the mother cells. Spores are then transmitted through faeces into the environment where they can survive harsh conditions and persist indefinitely on surfaces, promoting the spread of infection (Smits *et al*., 2016; Gil *et al*., 2017). Specifically, spores are transmitted from person to person by the faecal-oral

route (Paredes-Sabja *et al*., 2014), through poor hygiene practices or from ingesting polluted sources of food or water (**Figure 1.1).**

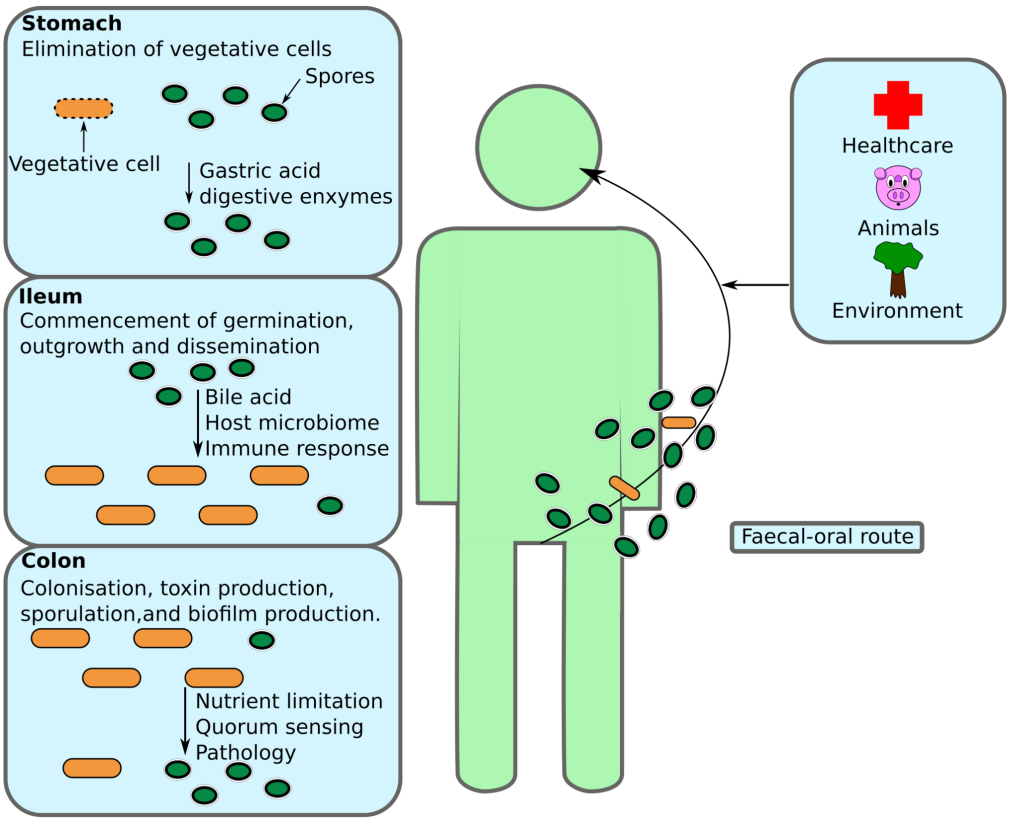


Figure 1.1: The life cycle of *Clostridioides difficile*. Spores are ingested from either environmental sources or enter by the faecal-oral route. Spores survive the stomach acidity and proteases and travel to the small intestine. Germination progresses down the gastrointestinal tract with the majority of spores germinating in the colon. Here, they are exposed to primary bile acids (**Section 1.1.6**), which stimulate them to germinate into vegetative cells. Vegetative cells colonise the colon, multiply and secrete toxins. The toxins cause the symptoms of *C. difficile* infection. Spores produced by vegetative cells in this stage are expelled in faeces into the environment to begin the cycle anew. Adapted from Smits *et al.*, 2016.

1.1.5 Clostridial spores

Spores are resistant to antibiotics and bleach-free cleaners which are now widely used in many healthcare establishments, including hospitals (Paredes-Sabja *et al*., 2014; Edwards *et al*., 2016). For this reason, many CDI prevention strategies are based around elimination of environmental spores using chlorinated surface cleaners (Dancer, 2016). Though the spore biology of *C. difficile* is not well understood, the process of sporulation and the structure of spores has been well studied in the closely related *Bacillus* genus, and similarities can be inferred between the two organisms. Bacterial spores

possess several different structural layers **(Figure 1.2)** that contribute to their robust properties.

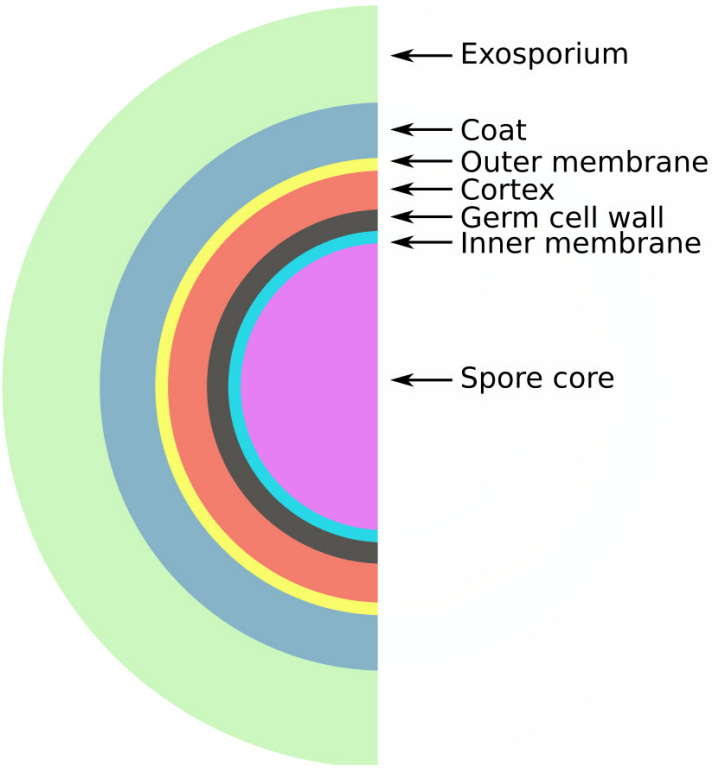


Figure 1.2: Structural layers of bacterial spores. The main layers of bacterial spore structure are shown (not drawn to scale). These structures are present in the spores of both *Bacillus* and *Clostridium* genera other than the exosporium layer which is only present in a subset of species, including *Bacillus cereus*, *Bacillus anthracis*, and *Clostridium difficile*. Adapted from Setlow, 2003.

The innermost compartment is the spore core, which contains the DNA, tRNA, and ribosomes. The enzymes of the organism are also stored here in their inactive zymogen state. Within the core, the low water content (25–55% of wet weight), elevated levels of dipicolinic acid (DPA) chelated 1:1 with calcium (Ca–DPA), (Slieman & Nicholson, 2001), and the saturation of DNA with a/b- type small acid soluble proteins (SASP) contribute to the spore's resistant properties (Slieman & Nicholson, 2001; Lawler, Lambert, and Worthington, 2020). Both DPA and SASPs protect the DNA from the damaging conditions of heat, moisture and UV radiation.

The core is surrounded by a compressed inner membrane, of a similar phospholipid composition to that of the plasma membrane of vegetative cells, but with low permeability to water and small molecules (Slieman & Nicholson, 2001, Nicholson *et al.,* 2020). The germ cell wall is made of peptidoglycan (PG) which surrounds the inner membrane and subsequently forms the main part of the cell wall of vegetative cells following spore germination. Specifically, PG of vegetative cell walls is composed of glycan chains of alternating *N*-acetylglucosamine (NAG) and *N*-acetylmuramic acid (NAM), where each molecule of NAM carries a peptide side chain. These peptide chains cross-link to form the cell wall (Irazoki*et al*., 2019). Surrounding the germ cell wall is another, thicker layer of PG, called the cortex. In the PG layer of the cortex, approximately every second NAM residue is substituted with muramic-δ-lactam (MAL) (**Figure 1.3**) (Popham *et al.*, 1996). The MAL residues are specifically recognized by the cortex lytic enzymes that hydrolyse the spore cortex but not the germ cell wall during germination (Paredes-Sabja *et al*., 2011).

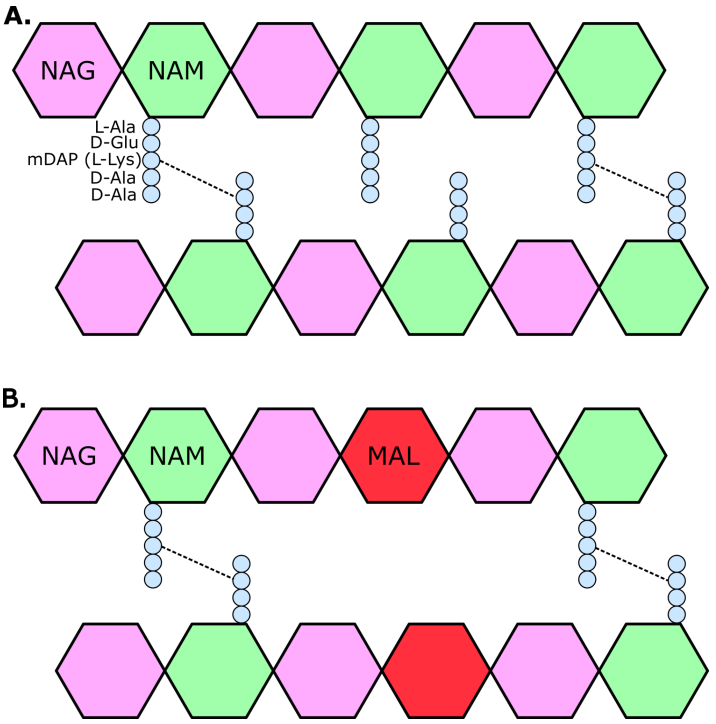


Figure 1.3: Comparison of the peptidoglycan (PG) component of the spore wall with that of the cell wall of vegetative cells. A. In *C. difficile* vegetative cells, the PG cell wall is composed of glycan chains of alternating *N*-acetylglucosamine (NAG) and *N*-acetylmuramic acid (NAM). Peptide chains attached to each NAM residue cross-link and form the cell wall. **B.** The cortex cell wall of *C. difficile* spores differ, in that every second NAM residue is substituted by a muramic-δ-lactam (MAL) residue. It is these MAL residues which are targeted by cortex-lytic enzymes during germination and allow hydrolysation of the spore cortex, while not targeting the cell wall of the developing vegetative cell. Adapted from Irazoki *et al*., 2019.

The PG is surrounded by an outer membrane derived from the mother cell which has been shown to be essential for spore formation but confers no resistance properties per se (Setlow, 2006; Calderón-Romero *et al*., 2018). A proteinaceous coat surrounds the outer membrane; in *B. subtilis*, the coat is composed of approximately 70 proteins unique to spores (Setlow, 2006). Though generally less well understood, investigations have been made into the *C. difficile* spore coat (Abhyankar *et al*., 2013) and several proteins have been discovered including orthologues CotE (Hong *et al*., 2017), and CotL (Alves Feliciano *et al*., 2019). Spore coat proteins are essential for the resistance of spores to commonly used decontaminants and disinfectants as well as playing

important roles in adherence to host cells (Paredes-Sabja & Sarker, 2011). In some species, such as *B. subtilis,* the spore coat is the outermost layer.

In other species, such as *B. anthracis* and *C. difficile*, an additional outer layer is present; the exosporium. The thickness of the exosporium layer is variable within and between species (Pizarro-Guajardo *et al*., 2016). The exosporium in some species, commonly those which are classed as pathogenic, possess hair-like projections formed by collagen-like BclA glycoproteins (Díaz-González *et al*., 2015; Pizarro-Guajardo *et al*., 2016). These projections have been observed to facilitate the binding of spores to gut epithelial cells and delay germination, as it has been shown that strains that carry mutated forms of *bclA1* which encodes BclA germinate faster than the wildtype (Phetcharaburanin *et al*., 2014).

Once within the host, spores must undergo germination into metabolically active vegetative cells in order to colonise the host by expression of adhesins, replicate and secrete toxins proteins ultimately establishing infection in the host.

1.1.6 Germination

Spore germination is the process by which spores are induced by external stimuli to mature into vegetative cells. In *C. difficile,* germination is triggered when spores sense specific molecules, termed germinants, through the Csp subtilisin-like serine proteases of the *cspBAC* locus (Francis *et al,* 2013; Bhattacharjee *et al.,* 2016; Shrestha *et al*., 2019). This locus encodes proteins CspA, CspB, and CspC. Of these proteins, CspC has been identified as the bile salt germinant receptor, which activate the proteolytic activity of CspB when stimulated (Francis *et al,* 2013; Bhattacharjee *et al.,* 2016).

In the GI tract, primary bile acids stimulate germination of *C. difficile* spores. Early work by Wilson *et al.* demonstrated that germination of *C.*

difficile spores could be induced *in vitro* by culturing spores in nutrient-rich media to which mammalian-specific primary bile acids sodium taurocholate and sodium cholate had been added (Wilson, 1983; Wilson *et al*., 1982). More recently, several studies have demonstrated that glycine, L-histidine, and hydrophobic amino acids that possess linear alkyl side branches can act as co-germinants. Although co-germinants alone are ineffective, together with cholate derivatives (bile salt components, i.e., taurocholate, glycocholate and cholate) they can promote germination (Sorg & Sonenshein, 2008; Howerton *et al*., 2011; Wheeldon *et al*., 2011).

The structure of *C. difficile* CspC, acognate germinant receptor (GR) CspC, a subtilisin-like serine pseudoprotease (Fimlaid *et al*., 2015; Gil *et al*., 2017; Makino & Moriyama, 2002) was recently solved, revealing natural mutations in key residues Arg456 and Gly457 promote greater sensitivity to taurocholate as a germinant, as well as to the above amino acids and calcium ions that act as co-germinants. These mutations were shown to be specific to CspC of *C. difficile* and allow spores to utilise a greater range of environmental signals to induce germination (Rohlfing *et al*., 2019).

Once the spore is activated by binding to germinants, CspC activates related CspB serine protease through proteolysis (Rohlfing *et al*., 2019). CspB cleaves the pro- cortex-lytic enzyme SleC zymogen, present in the dormant spore core forming SleC, which degrades the protective cortex layer (Paredes-Sabja *et al*., 2009). Only MAL residues present in the spore cortex are targeted, degrading the cortex while preventing degradation of the germ cell wall (Fimlaid *et al*., 2015; Gil *et al*., 2017). Degradation of the cortex leads to spore expansion and water uptake. Hydrolysis allows activation of enzymes and the initiation of metabolism, promoting spore outgrowth (Paredes-Sabja *et al*., 2014).

It is important to note that the ingestion of spores does not always lead to colonisation and infection as the conditions within the GI tract must be

favourable for germination to occur first. In addition, there is much competition for germinants and co-germinants by other members of the gut microbiota, thus ingested spores may transit directly through the body and out (Janoir *et al*., 2013; Jenior *et al*., 2017; Fletcher *et al*., 2018;)

1.1.7 The role of the microbiota in spore germination

The main barrier to the establishment of *C. difficile* in the intestine is the normal flora which provides a natural colonisation resistance barrier. Many factors including sex, ethnicity, age, geographical regions such as developing countries, and diet (Eckburg *et al*., 2005; De Filippo *et al*., 2010; David *et al*., 2014; Hollister *et al*., 2014) affect the composition of the microbiota of an individual. In addition, certain commensal organisms such as *Bacteroides fragilis*, *B. vulgatus*, *Clostridium scindens*, *Listeria monocytogenes* and several species of *Lactobacillus* and *Bifidobacterium,* produce enzymes which convert primary bile acids, such as taurocholate, into secondary bile acids, such as chenodeoxycholate, which inhibit the germination of spores (Gerard *et al*, 2014, Buffie *et al*., 2015; Theriot *et al*., 2016; Thanissery *et al*., 2017).

Furthermore, amino acid and carbohydrate metabolism can impact the establishment of *C. difficile* in the intestine (Janoir *et al*., 2013; Jenior *et al*., 2017). *C. difficile* is naturally auxotrophic for proline and branched-chain amino acids and is therefore reliant on their availability in the gut. Studies have shown that *C. difficile* colonisation rates are greatly diminished in the absence of such amino acids (Jackson *et al*., 2006' Battaglioli *et al*., 2018; Fletcher *et al*., 2018).

In a normal, healthy microbiome, these amino acids are sequestered by the organisms of the gut flora in a competitive manner. However, if the microbiome is disrupted, as during treatment with antibiotics, these amino acids are made more available due to reduced competition (Paredes-Sabja *et*

al., 2014; Riley *et al*., 2019). Thus for multiple reasons, CDI is attributed to dysbiosis (microbial imbalance) of the gut.

1.1.8 Colonisation

Colonisation is critical for the pathogenesis of *C. difficile.* It involves the attachment of the bacterium to the large intestine and multiplication. The interactions of clostridial surface proteins, such as colonisation factors, with colonic epithelial cells facilitate adherence of this pathogen to the gut (Rupnik *et al*., 2009). Although a number of colonisation factors have been identified and characterised in other bacterial pathogens, relatively little is known about the mechanism of colonisation in *C. difficile*.

The flagellar proteins FliC (flagellin) and FliD (flagellar cap protein) (Tasteyre *et al*., 2000; Tasteyre, Barc, *et al*., 2001; Tasteyre, Karjalainen, *et al*., 2001) have been linked to motility of the *C. difficile* vegetative cell; as observed for other species such as *Vibrio cholerae* and *Salmonella enterica* (Haiko & Westerlund-Wikström, 2013). It has been shown in some pathogens including *E. coli* and *Pseudomonas aeruginosa* that flagella promote adherence to host cells (Haiko & Westerlund-Wikström, 2013; Rossez *et al*., 2015). However, in *C. difficile,* this is not the case asstrains deleted for both FliC and FliD showed increased adherence to Caco-2 colonic epithelial cells compared to wild type (Dingle *et al*., 2011), suggesting environmental strains which lack flagella are potentially more virulent.

To date, several adhesins (surface factors which facilitate adherence to cells or surfaces) have been shown to promote attachment of *C. difficile* to the epithelium. The first adhesin to be identified in *C. difficile* was cell wall protein (CWP) 66 (Cwp66). Its role in cell adhesion was confirmed by using antibodies raised against a recombinant Cwp66 in cell binding studies. These antibodies partially blocked adhesion of *C. difficile* strain 79-685 to Vero kidney epithelial cells (Waligora *et al*., 2001). The role of the putative

adhesion, fibronectin binding protein (FbpA), was investigated by creating knockout strains. The loss of FbpA affected the rate of colonisation in murine models (as well as the rate of spore shedding), but to different extents in monoxenic and dixenic mice suggesting a role in adherence (Hennequin *et al*., 2003; Barketi-Klai *et al*., 2011).

Studies on the heat shock protein GroEL, a membrane-bound chaperone protein involved in protein folding, show polyclonal antibodies raised against it partially block *C. difficile* adhesion to Vero cells, implicating it in adherence (Hennequin, Collignon and Karjalainen, 2001; Hennequin *et al.*, 2001). Immunisation with recombinant GroEL has also been shown to decrease intestinal colonisation of *C. difficile* (Péchiné *et al*., 2013) corroborating the previous findings described.

The role of *C. difficile* collagen binding protein (CbpA) in colonisation and adherence has also been investigated. *Lactococcus lactis* was engineered to express recombinant *C. difficile* collagen binding protein CbpA on its cell surface and displayed enhanced ability to bind to collagen and murine intestinal cells *in vitro*. This binding activity was found to be blocked by antisera raised against the recombinant clostridial CbpA. However, the study also found that, when the antisera was used to block native CbpA activity, little difference was seen between a mutant strain of *C. difficile* with deletion of CbpA compared to the wild type (Tulli *et al*., 2013). This latter finding suggests CbpA is not required for adherence.

CD0873 is a lipoprotein found on the cell surface which was found to be sero-reactive when CDI patient sera were screened (Wright *et al*., 2008). CD0873 was hypothesised to be involved in adherence and knockout mutants and strains blocked with anti-CD0873 antibodies severely attenuated binding of *C. difficile* cells to Caco-2 cells, supporting its role as a colonisation factor (Kovacs-Simon *et al*., 2014). Additionally, immunisation of mice with recombinant CD0873 provided a protective effect through generation of

anti-CD0873 antibodies, preventing long-term gut colonisation (Bradshaw *et al*., 2019).

1.1.9 The S-layer and surface proteins

C. difficile possesses the typical features of a Gram positive cell wall consisting of a plasma membrane, surrounded by PG, with the PG layer being covered with a crystalline or paracrystalline array, formed by subunits of glycoproteins or proteins known as the S-layer (**Figure 1.4**) (Wheeldon *et al*., 2011). Lipoteichoic acid also traverses the PG layer, anchored in the cell membrane by a diacylglycerol (Broecker, *et al*., 2016).

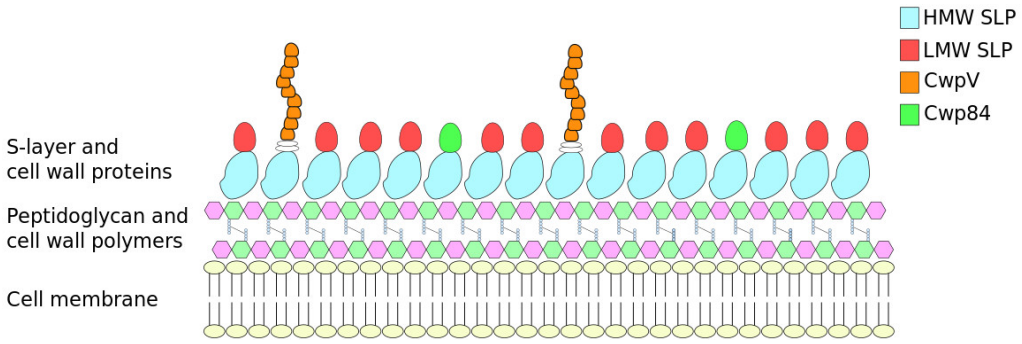


Figure 1.4: The cell wall of *C. difficile* vegetative cells. *C. difficile* possesses the typical features of a Gram positive cell wall consisting of a plasma membrane, covered by peptidoglycan (PG), with the PG layer further covered with a crystalline or paracrystalline array, formed by subunits of glycoproteins or proteins known as the S-layer. *C. difficile* has two superimposed and structurally different S-layer lattices, a high-molecular-weight (HMW) surface layer protein (SLP) (~40 kDa) and a low-molecular-weight (LMW) SLP (~35 kDa). LMW SLP appears to form additional complexes with several CWPs such as adhesin Cwp84 and aggregation factor CwpV. Adapted from Kirk *et al.,* 2017.

C. difficile has two superimposed and structurally different S-layer lattices, a high-molecular-weight (HMW) surface layer protein (SLP) (~40 kDa) and a low-molecular-weight (LMW) SLP (~35 kDa) (Cerquetti *et al.*, 2000; Calabi *et al.*, 2001). A single gene, *slpA*, that has a conserved genomic location among all *C. difficile* strains, encodes both SLPs. Specifically, *slpA* encodes a precursor protein, termed SlpA, that has three identifiable subdomains: an N-terminal secretion signal, followed by a highly variable

LMW region, and a HMW region containing three tandem cell wall binding 2 (CWB2) motifs (Takeoka *et al*., 1991). The precursor protein is then cleaved by protease Cwp84 to generate the two mature proteins.

Both HMW- and LMW-SLPs are linked by non-covalent interactions to form a tightly associated complex. LMW SLP appears to form additional complexes with several CWPs such as adhesins Cwp66, CD08730, and aggregation factor CwpV, all of which have been associated with increased virulence (Kirk *et al*., 2017). Early studies showed that removal of the SLPs through chemical treatment of vegetative cells with anti-SLP antibodies abolished adherence of *C. difficile* to murine cells and to HeLa cells (Takeoka *et al*., 1991). Later studies demonstrated that purified SLPs bind to intestinal tissues and several proteins of the extracellular matrix of gut epithelial cells such as fibronectin and collagen (Calabi *et al*., 2002), yet to date, the precise host receptor for SLP has not been identified.

1.1.10 Toxin production

Once colonisation has been established in the large intestine, vegetative cells begin producing clostridial Toxin A (TcdA) and Toxin B (TcdB). These toxins are encoded within a single operon, the pathogenicity locus (PaLoc), a 19.6-kb genetic locus, located between two insertion sequences, cdu 2/2′ and cdd 2-3 (Cohen *et al*., 2000).

The PaLoc contains the genes TcdA and TcdB *(tcdA* and *tcdB*, respectively) as well as three small open reading frames (ORFs) that encode putative regulatory genes (*tcdR/tcdD*, *tcdE*, and *tcdC*) (Cohen *et al*., 2000; Voth & Ballard, 2005). These genes are transcribed polycystronically according to the phase of growth (Hammond, Lyerly and Johnson, 1997; Hundsberger *et al.*, 1997). It is thought that the product of *tcdC* acts as an inhibitor of toxin production, as transcription is high in early exponential growth phase, but this remains to be proved (Paiva *et al*., 2019). It is thought

the product of *tcdR/tcdD* acts as a regulator of toxin production but has also been implicated in sporulation (Hammond, Lyerly and Johnson, 1997; Cohen *et al*., 2000; Girinathan *et al*., 2017) It is thought that the product of *tcdE*, is important for secretion of TcdA and TcdB. TcdE shares structural features with holin proteins produced by bacteriophages. Holins facilitate the release of progeny phages. It is hypothesised that TcdE acts in a similar way, acting in a bacteriolytic manner to facilitate the release of TcdA and TcdB from the vegetative cell (Govind & Dupuy, 2012; Olling *et al*., 2012). In non-toxigenic strains, the cdu insertion sequences exist, but the PaLoc and associated toxins are absent. Instead, a 115 bp DNA fragment is present (Hammond and Johnson, 1995).

TcdA and TcdB belong to the family of large clostridial glucosylation toxins and are 63% identical to one another at the amino acid sequence level (Wang *et al*., 2018). Their structural similarity is shown in **Figure 1.5**.

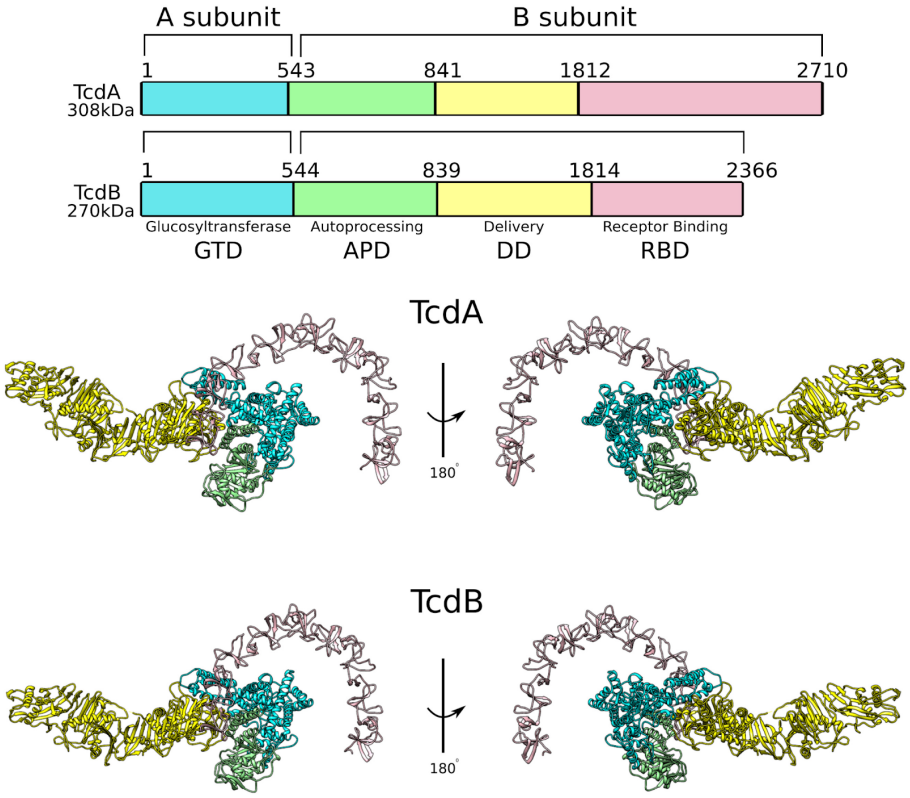


Figure 1.5: The structure of TcdA and TcdB. Protein structures generated using PHYRE2 Protein Fold Recognition Server (Kelley *et al.,* 2009).

TcdA and TcdB are secreted in the gut, where they damage the epithelial cell cytoskeleton, leading to disruption of tight junctions, fluid secretion, neutrophil adhesion and local inflammation. The disruption of the cytoskeleton is manifest by cell-rounding and apoptotic cell death (Libby, Jortner and Wilkins, 1982; Ciesla and Bobak, 1998; Voth and Ballard, 2005; Lyras *et al.*, 2009; Gerhard *et al.*, 2013; Cowardin *et al.*, 2016; di Bella *et al.*, 2016; Smits *et al.*, 2016). Actin is a key component of the cytoskeleton that is implicit in roles such as structural support and cell migration. TcdA and TcdB have been shown to inactivate Rho family GTPases; Rho GTPases have been shown to regulate various aspects of intracellular actin dynamics and therefore their inactivation disrupts cytoskeletal stability and integrity, often culminating in cell death (Jank, Giesemann and Aktories, 2007).

TcdA and TcdB bind to cell surface receptors via their receptor binding domains (RBD) which contain combined repetitive oligopeptide (CROP) structures. Studies have concluded that TcdA (Na *et al*., 2008) and TcdB (LaFrance *et al.*, 2015; Yuan *et al.*, 2015; Tao *et al.*, 2016) bind to different cell surface proteins. Binding begins the process of internalisation, whereby an endosome is formed which envelops the toxin. The endosome becomes acidified and the low pH causes a conformational change in the toxins' delivery domain (DD). This is accompanied by formation of a pore through which translocation of the glucosyltransferase domain (GTD) to the pore membrane and subsequent exposure to the cytosol is achieved. Inositol hexakisphosphate (InsP6) then binds to and activates the toxin's auto-processing domain (APD) causing cleavage and release of the GTD into the cytosol. The GTD acts to inactivate Rho family proteins by transferring the glucose moiety from readily available metabolism intermediate UDP-glucose to the switch I region of the GTPase (Just *et al*., 1995). This process of glucosylation disrupts GTPase signalling and leads to cytopathic 'rounding' effects and apoptotic cell death (**Figure 1.6**) (Chandrasekaran & Lacy, 2017).

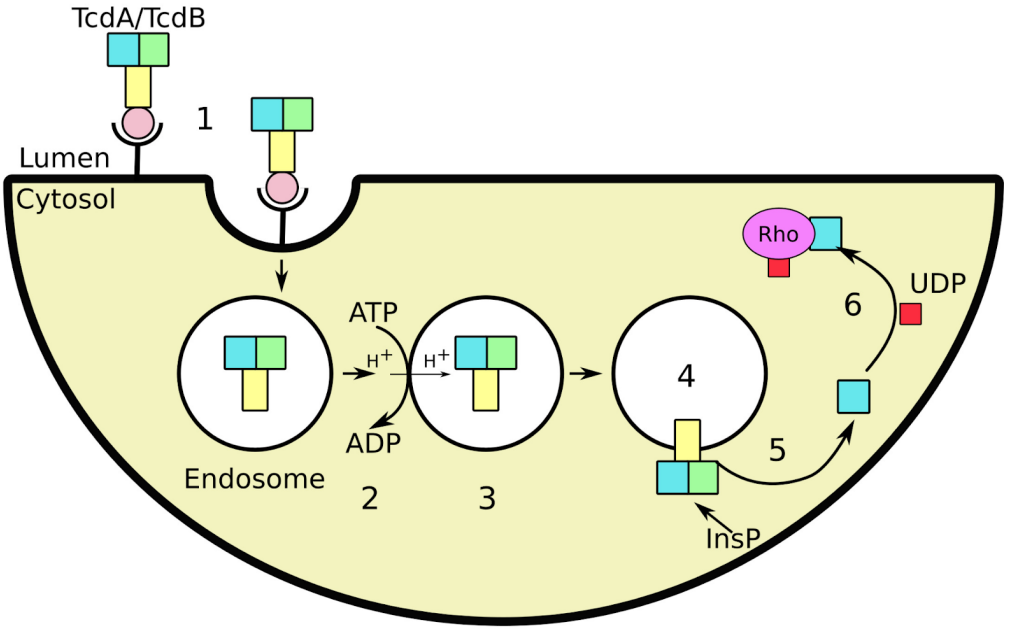


Figure 1.6: The action of TcdA and TcdB. 1) Binding to cell surface receptors and internalisation. 2) Acidification of the endosome. 3) Conformational change in the DD resulting in pore formation and 4) translocation of the GTD to the cytosol. 5) Inositol hexakisphosphate (InsP6) binds to and activates the APD causing cleavage and release of the GTD. 6) Monoglucosylation of Rho results in cell rounding and apoptotic cell death.

Hypervirulent *C. difficile* strains such as 027/BI/NAP1/078 produce a third toxin known as binary toxin or CDT. This toxin acts by ADP-ribosylating actin, causing major disruptions in microtubule formation and the cytoskeleton of host cells. These disruptions act to produce long protrusions from the membrane of the cell, facilitating greater adhesion by *C. difficile* to host cells (Gerding *et al.*, 2014b, 2014a)

1.1.11 Sporulation

Sporulation is the process by which spores are formed by and released from the vegetative mother cell. Each vegetative cell is expected to produce one spore then lyse (Paredes-Sabja, Shen and Sorg, 2014). The known triggers

which induce sporulation in *C. difficile* are predominantly environmental. The presence of the secondary bile acid deoxycholate inhibits sporulation by repressing expression of the master sporulation regulator *spo0A* (Usui *et al*., 2020; LaFrance *et al*., 2015). CDI has been associated with an increase in the pH of the gastrointestinal tract (GIT) and it has been shown that, in the presence of an alkaline pH, the sporulation rate of *C. difficile* vegetative cells increases (Wetzel & McBride, 2020). A recent report also described the importance of quorum sensing in *C. difficile* on sporulation rate (Darkoh, Odo and Dupont, 2016). In *Bacillus* species environmental signals such as nutrient deprivation and stress trigger sporulation (Steiner *et al.*, 2011; Higgins and Dworkin, 2012) and it remains to be proved whether these stimuli also induce sporulation in *C. difficile*. Once spores are released from their mother cells, they are shed into the environment in the faeces of the host. The hardiness of bacterial spores ensures their survival in the environment and propensity for transmission.

1.2 Lipoproteins

Bacterial lipoproteins collectively play diverse roles including germination, growth and division, adhesion, signalling, protein transport, nutrient uptake and spore formation and is thus described as a section on its own. (Schmaler *et al.*, 2009; Shahmirzadi, Nguyen and Götz, 2016; Nguyen *et al.*, 2017). Specific examples include OppA and AppA which are involved in sporulation (Edwards, Nawrocki and McBride, 2014; Charlton *et al.*, 2015), CD0873, an adhesion involved in colonisation (Bradshaw et al., 2019) and PrsA and PrsA2, extracellular chaperones, involved in lipoprotein secretion (Charlton *et al*., 2015) and GerS is required for spore germination (Diaz *et al*., 2018). In both Gram-negative and Gram-positive bacteria, lipoproteins possess a lipid moiety at their N-terminus which allows anchorage to the bacterial membrane (Zückert, 2014). In Gram-positive bacteria that lack the outer membrane such as *C. difficile*, lipoproteins are anchored to the cytoplasmic membrane (Schmaler *et al.*, 2009; Shahmirzadi, Nguyen and Götz, 2016; Nguyen *et al.*, 2017). The lipid domain is a pathogen-associated molecular

pattern (PAMP) that act to alert the immune system via their interaction with Toll-like receptor 2 (TLR2) found on antigen presenting cells (APCs) such as macrophages and dendritic cells (DCs) (Schmaler *et al.*, 2009; Zückert, 2014; Nguyen and Götz, 2016; Nguyen *et al.*, 2017). Upon PAMP recognition, TLRs recruit adaptor proteins that initiate signal transduction leading to the expression and regulation of cytokines and chemokines. The main functions of TLRs are induction of inflammation and establishment of adaptive immunity.

The number of acyl residues at the lipid moiety has been shown to affect their recognition by TLR2/1 or TLR2/6 receptors (Schmaler *et al.*, 2009). Gram-negative bacteria and some high-GC Gram-positive bacteria such as mycobacteria and streptomycetes produce triacylated lipoproteins, whereas most Gram-positive bacteria produce diacylated lipoproteins (Brülle, Tschumi and Sander, 2013).

1.2.1 Acylation of bacterial lipoproteins

Lipoproteins are synthesised in the cytoplasm as preprolipoproteins, which possess a characteristic N-terminal signal peptide ending in a conserved lipobox sequence composed of four amino acids with a conserved cysteine (**Figure 1.7)**. Following translocation of the preprolipoprotein across the cytoplasmic membrane, the thiol group of the invariant cysteine residue is modified to a diacylglyceryl moiety by lipoprotein diacylglyceryl transferase (Lgt). This diacylglyceryl moiety then acts as a membrane anchor (**Figure 1.7 A**). After lipidation, Lipoprotein signal peptidase (Lsp) cleaves the signal peptide (**Figure 1.7 B**). This results in the mature diacylated lipoprotein (**Figure 1.7 C**). In Gram-negative and a subset of Gram-positive bacteria, Lnt acts to add an amide-linked fatty acid to the N-terminal cysteine residue, resulting in a triacylated lipoprotein (**Figure 1.7 D**).

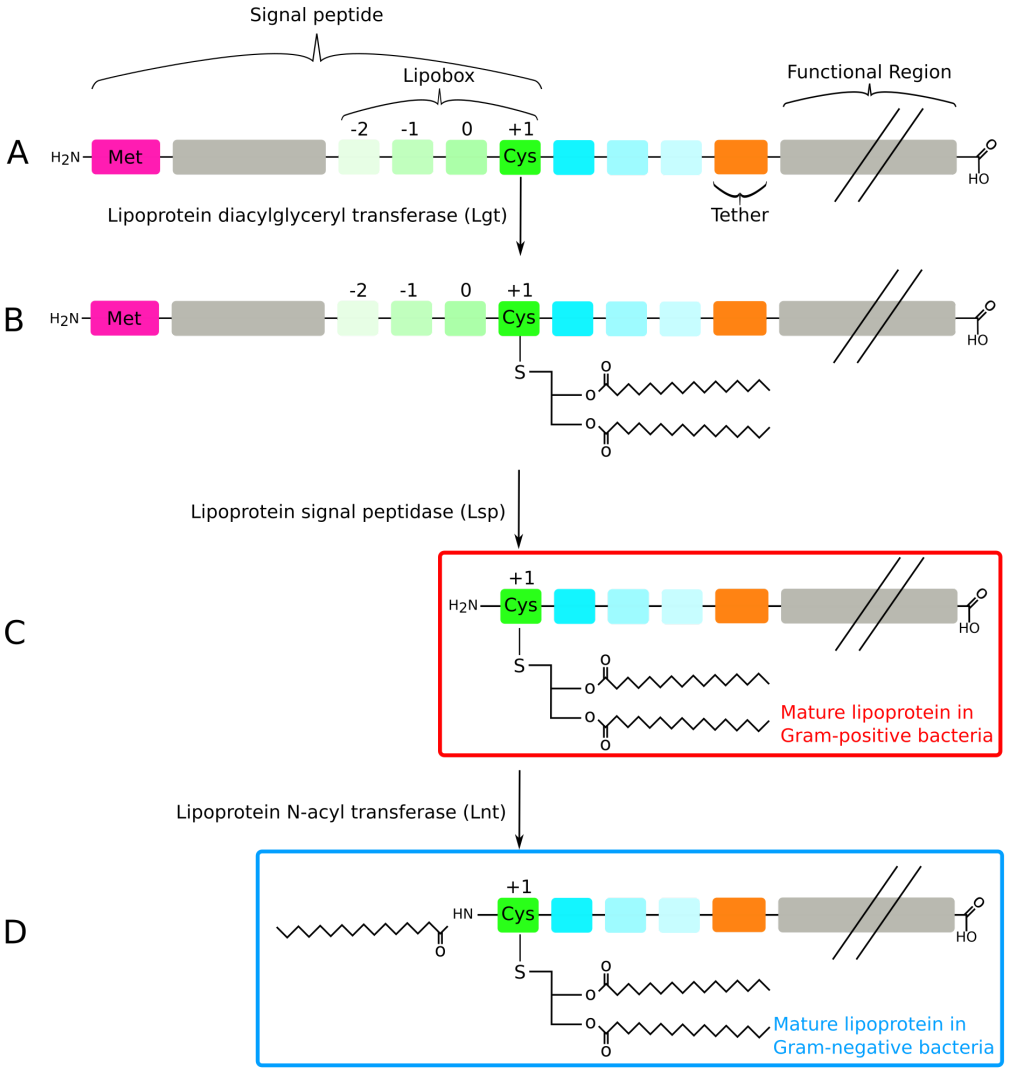


Figure 1.7: Biosynthesis of bacterial lipoproteins. A-C represents the two-step biosynthetic pathway in Gram-positive bacteria. A-D represents the three step biosynthetic pathway in Gram-negative bacteria and in some Gram-positive bacteria. A. Preprolipoproteins possess a characteristic N-terminal peptide containing a conserved lipobox sequence shown here as positions -2 - +1. B. During lipoprotein maturation, the thiol group of the invariant cysteine residue is substituted with a diacylglyceryl moiety which serves as a membrane anchor. C. After lipidation, Lipoprotein signal peptidase (Lsp) cleaves the signal peptide, leaving the cysteine as the new acylated amino-terminal residue. This forms the mature lipoprotein in most Gram-positive bacteria. D. In Gram-negative and some Gram-positive bacteria, the mature lipoprotein has an additional amide-linked fatty acid at the N-terminal cysteine residue attached by Lipoprotein N-acyl transferase (Lnt). Adapted from Zückert, 2014.

Lipoprotein biosynthetic enzymes Lgt, Lsp, and Lnt, are encoded in the genome of *C. difficile* CD630 strain: the CD630_2659 gene encodes Lgt, while CD630_2597 and CD630_1903 encode two distinct Lsps (Brülle *et al*., 2013;

Kovacs- Simon, 2013). and CD630_27370 encodes Lnt (Consortium *et al.*, 2021). The presence of Lnt suggests that in *C. difficile* lipoproteins are triacylated.

1.3 Current therapies and their limitations

Up to 19.3% (n=5,722) of cases of non-recurring CDI, and up to 7.6% (n=1,140) cases of rCDI in the UK resulted in death within 30 days of initial diagnosis between 2002 – 2013 (Enoch *et al.,* 2020). It is therefore vital that treatment commences immediately following diagnosis. Historically, the most common method of treatment has been antibiotic chemotherapy.

1.3.1 Antibiotic therapy

Three antibiotics currently form the foundation of CDI treatment; metronidazole, vancomycin and fidaxomicin (Nelson, Suda and Evans, 2017). Each drug possesses a different mode of action; metronidazole inhibits protein synthesis by interacting with DNA and causing strand breakage (Dingsdag & Hunter, 2018), vancomycin inhibits PG cell wall synthesis by binding to the terminal end of the growing peptide chain (Watanakunakorn, 1984) and fidaxomicin disrupts transcription by inhibiting bacterial RNA polymerase (Venugopal & Johnson, 2012).

Vancomycin has been found to be just as effective as metronidazole in preventing rCDI with recurrence after initial treatment being observed in between 20-60% of patients (Leffler & Lamont, 2015). However, treatment with vancomycin greatly reduces the 30-day mortality rate when compared to metronidazole (Stevens, *et al.*, 2017). rCDI remains a problem when treating with these broad spectrum antibiotics, because they severely disrupt the microbiota, predisposing treated patients to further episodes of CDI (Kelly, 2012). Treatment with vancomycin is problematic as vancomycin toxicity has been strongly associated with nephrotoxicity (Filippone, Kraft and Farber, 2017). In addition, the growing number of cases of resistance of

C. difficile strains to vancomycin is a major concern (Spigaglia, Mastrantonio and Barbanti, 2018). Similarly, the rate of treatment failure with metronidazole is high (Vardakas *et al*., 2012) and resistance has been observed in a growing number of hypervirulent ribotype (RT) 027 strains (Adler *et al.*, 2015; Miller-Roll *et al.*, 2016; Endres *et al.*, 2019).

It is thought that mobile genetic elements (MGEs) play a significant role in the ability of *C. difficile* to acquire resistance to antibiotics, whereby MGEs are frequently transferred between organisms by conjugation-mediated horizontal gene transfer (Spigaglia, 2016). Transposons *Tn5398* and *Tn6194*, which encode erythromycin resistance (Farrow, Lyras and Rood, 2001), and *Tn6164*, which encodes chloramphenicol resistance (Corver *et al*., 2012) are examples of such MGEs. The threat of acquisition of antibiotic resistance from other organisms justifies the requirement for measures to prevent rather than treat infection with antibiotics.

Fidaxomicin is macrocyclic, bacteriocidal, and has a narrow spectrum of action. Though it is effective against Gram positive pathogens, it has no significant influence on the natural gut flora and therefore is more repressive of recurrent CDI than both metronidazole or vancomycin (15% compared to 60%) (Cornely *et al*., 2012). However, fidaxomicin is extremely expensive with a 10 day course costing up to three times as much as comparable treatment with vancomycin (Smits *et al.*, 2016; Peng *et al.*, 2017; Nguyen *et al.*, 2018). Additionally, increasing resistance to fluoroquinolones has been observed, particularly in the hypervirulent RT 027/NAP1/BI strains suggesting fidaxomicin does not represent a long term solution to CDI (McDonald *et al*., 2005).

1.3.2 Antibody Therapy

Treatment with humanised monoclonal antibodies against TcdA and TcdB as a means to prevent the symptoms rCDI has been evaluated in clinical

trials for patients with rCDI. Passive immunity provided by these antibodies has been shown to alleviate CDI symptoms (Corthier *et al.*, 1991; O'Brien *et al.*, 2005; McDonald *et al.*, 2005; Babcock *et al.*, 2006; Qiu *et al.*, 2016; Wilcox *et al.*, 2018). Regarding rCDI, actoxumab (a humanised anti-TcdA monoclonal antibody) failed to demonstrate prevention of recurrent disease, however, bezlotoxumab (a fully humanized IgG1/kappa anti-TcdB monoclonal antibody) has shown encouraging results (Wilcox *et al.*, 2017; Navalkele and Chopra, 2018). The antibodies work by blocking the action of TcdA and TcdB on epithelial cells in the GI tract, thereby preventing associated disease symptoms (Navalkele & Chopra, 2018).

However, there is a significant drawback with this method of treatment; the protection offered is transient. Literature states that the antibody is not intended to treat the colonisation of the host, but the symptoms themselves and thus, symptoms will resume if treatment is stopped (Deeks, 2017). As this treatment does not target colonisation but simply transiently mops up the toxins, patients will continue to be colonised with spores shed into the environment. Passive immunisation, therefore, does not prevent transmission of CDI. Finally, the cost of treatment is extremely high due to high production costs of the antibodies (San-Juan-Rodriguez *et al*., 2018) and is therefore not a suitable system for treatment of rCDI globally.

1.3.3 Faecal Microbiota Transplantation

Faecal microbiota transplantation (FMT) provides another option for patients with rCDI. FMT is the administration of a solution of faecal matter from a donor into the intestinal tract of a recipient in order to restore the recipient's gut microbial composition (Smits *et al.*, 2013; Gupta, Allen-Vercoe and Petrof, 2016). FMT can be administered in a variety of ways: infusion of stool via colonoscopy, enema, orogastric tube, or orally in the form of a capsule (Gupta, Allen-Vercoe and Petrof, 2016; Bafeta *et al.*, 2017). Several factors must be taken into account when selecting a donor; the donor must not carry any autoimmune, metabolic or malignant diseases which could

potentially be passed on to the recipient. Any matter collected with the intent of donation must be subject to screening processes to check for pathogens (DeFilipp *et al*., 2019).

FMT has been shown to promote restoration of gut microbial communities in a sustained manner (Khoruts *et al.*, 2009; Hamilton *et al.*, 2013). However, uptake by patients is low. The paucity of placebo-controlled studies leads to uncertain estimates of FMT efficacy and optimal dosing and administration routes are unknown (Bafeta *et al.*, 2017; Tariq *et al.*, 2019). Safety concerns have been amplified by recent reports of transmission of bacterial infections and emerging viral infections after FMT, highlighting the need for mandatory donor screening guidelines (DeFilip *et al*., 2019). Development of any microbiome therapeutics, such as FMT, need to include manufacturing steps that inactivate pathogens to mitigate risks to recipients of donated matter (DeFilipp *et al*., 2019; Holshue *et al*., 2020). In terms of long-term adverse effects of FMT, there exists the possibility of undetected infectious disease transfer or stimulation of chronic disease (e.g. obesity, diabetes, atherosclerosis, etc.) development due to alteration of the gut microbiota (Alang and Kelly, 2015; Gupta, Allen-Vercoe and Petrof, 2016).

1.3.4 Spore therapy

Ser-109 is a spore-based treatment developed by Seres Therapeutics, which has recently undergone phase 2 clinical trials (McGovern *et al*., 2020). The treatment consists of an orally administered capsule containing the spores of Firmicutes isolated and purified from several donors (McGovern *et al*., 2020). As with FMT, the purpose of this treatment is to restore the protective properties of the microbiota in patients suffering rCDI. This therapy has been shown to reduce rCDI in those ≥ 65 years of age when compared to a placebo (45.2% versus 80% respectively), however there was no significant difference in younger patients in the rate of recurrence versus placebo (44.1% versus 53.3% respectively) (McGovern *et al*., 2020).

1.3.5 The need for a novel vaccine

It is clear from the current state of play regarding available CDI treatment options that prevention is the only way forward. Several vaccines have recently been developed in an attempt to tackle this problem.

Sanofi-Pasteur, Pfizer (Pfizer Inc., 2017) and Valneva (Bézay *et al*., 2016) have each produced toxin-based vaccines given as three intramuscular injections which have entered clinical trials. Pfizer based their vaccine on full-length TcdA and TcdB proteins which have been genetically inactivated and chemically inactivated. Valneva used a chimeric protein consisting of portions of the rRBDs of both TcdA and TcdB fused together (Bézay *et al*., 2016). In December 2017, Sanofi-Pasteur announced discontinuation of their phase III clinical trial of their vaccine, based on formalin-inactivated full length TcdA and TcdB. All three vaccines elicit systemic toxin-neutralising antibody responses (IgG), as shown in *in vitro* assays (Bézay *et al.*, 2016; Riley, Lyras and Douce, 2019). However, upon testing of vaccinated sera, Sanofi's vaccine conferred no protection against CDI (Pasteur, 2013). Since all three vaccines share the same route of immunisation to produce a systemic immune response as opposed to a local protective response, it is anticipated that the two vaccines still in development will also fail. Furthermore, as these vaccines only target secreted clostridial toxins as opposed to the bacteria itself, it is likely that colonisation by *C. difficile* will not be prevented in infected individuals.

1.4. Mucosal Immunity

1.4.1 Mucosa-associated lymphoid tissues (MALT)

The body's mucosal surfaces provide a physical barrier to defend against pathogens and protection of these surfaces is ensured by the mucosal immune system. The mucosa-associated lymph tissue (MALT) consists of mucus layers and epithelial cells, along with lymphoid tissues within the

lamina propria (LP) (Perez-Lopez *et al.*, 2016; Boyaka, 2017). In the gastrointestinal tract (GIT), Peyer's patches (PP) have been studied in detail as a major inductive site for mucosal immune responses. The selective delivery of pathogens and foreign bodies to the gastrointestinal-associated lymphoid tissue (GALT) is performed by a specialized type of highly invaginated enterocyte, the M (microfold) cell.

M cells ingest pathogens by phagocytosis and pass them to underlying antigen presenting cells (APC) such as dendritic cells (DC) and macrophages in the subepithelial dome region. After antigen processing APCs activate T cells residing in the interfollicular region (IFR). Activated T cells produce cytokines such as IL-2, IL-6, and CD40L, which function to stimulate B cells present in secondary lymphoid organs such as the lymph nodes and PPs (Jackson and Elsawa, 2015). These activated B cells mature to become either antigen secreting cells which secrete large amounts of secretory immunoglobulin A (sIgA) or memory B cells which can become activated and secrete antibodies during secondary infections. (**Figure 1.8**) (Corthsy, 2009; Jackson and Elsawa, 2015; Dillon & Lo, 2019).

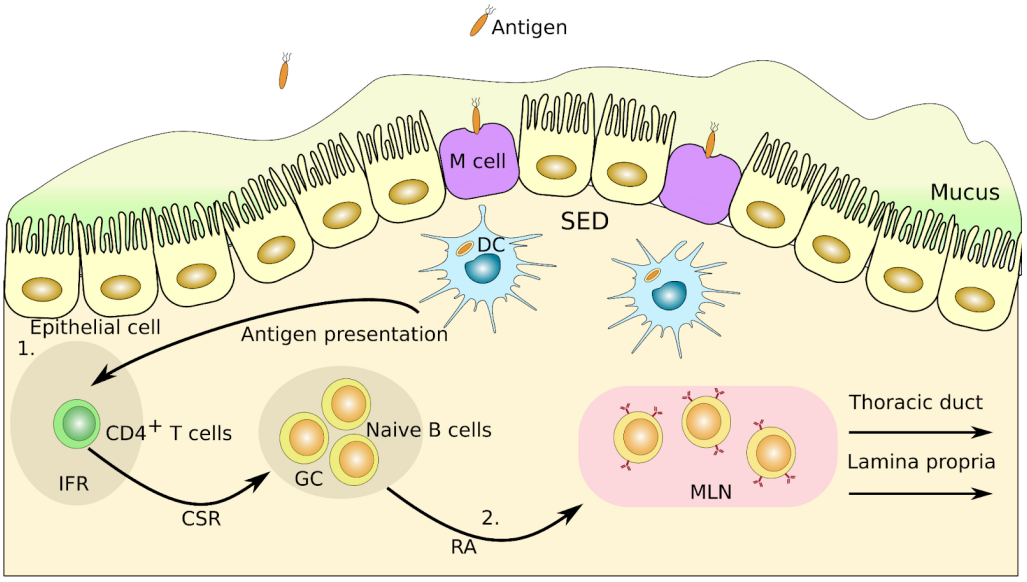


Figure 1.8: Schematic representation of the gut-associated lymphoid tissue (GALT) and generation of secretory IgA (sIgA). Following selective sampling by M cells in Peyer's patches(PP), antigens are captured by antigen-presenting cells including dendritic cells (DC) in the subepithelial dome (SED) region. [1] In the interfollicular region (IFR). Presentation to CD4+ T cells induces class switch recombination and somatic hypermutation of naïve B cells in the germinal center (GC) into IgA-expressing B lymphocytes. [2] Migration of IgA+ B lymphocytes to draining mesenteric lymph nodes (MLN), and further homing via the thoracic duct and circulation to distant effector sites in the intestinal lamina propria (LP). Adapted from Corthsy, 2009; Dillon & Lo, 2019

Activation of the CD40 receptor, a membrane bound receptor found in naive mature B cells, by CD40L induces class-switch recombination (CSR). This process stimulates naive mature B cells to stop producing IgM and IgD, and instead produce either IgG, IgA, or IgE (Stavnezer, Guikema and Schrader, 2008).

Immune responses in MALTs generate mainly secretory sIgA which travels back to their tissue of origin, effectively priming the tissue against subsequent attack. Specifically, once activated in PP by the engagement of their CD40 receptor, B cells that have undergone IgA CSR become IgA+ effector B cells, including memory B cells and plasmablasts (MacPherson *et al*., 2008). These cells upregulate the expression of the gut-homing receptors α4β7, CCR9, and/or CCR10, recirculate via the thoracic duct, and travel to the

intestinal LP (Mora *et al*., 2006) where they bind to addressin cell-adhesion molecules found on endothelial cells.

Among epithelial tissues, it is uncommon for cells to capture and transport foreign bodies from the apical face for transport and release at the basolateral side; thus, M cells have a unique and important function.

1.4.2 Key differences between sIgA and IgG

sIgA is the predominant antibody isotype in mucosal tracts, including the GIT, respiratory tract, vaginal tract, and in tears, saliva and colostrum. It is also the second most prominent immunoglobulin in the circulation, with IgG being the most abundant. Mucosal immunisation or natural immunity to mucosal pathogens results in mainly a local sIgA response but may also induce a systemic IgG response thus providing two layers of defence.

1.4.3 The role of IgA in the mucosal immune response

sIgA is structurally equipped to resist chemical degradation in the harsh environment of mucosal surfaces, such as digestion by host enzymes. IgA exists in both monomeric and dimeric (also known as polymeric (pIgA)) forms (**Figure 1.9**). In the common dimeric form, two IgA molecules are linked by a joining chain (J-chain), a small polypeptide, attached to the penultimate cysteine residues of their Fc regions, the tail region of an antibody which commonly interacts with cell surface FC receptors as well as some proteins of the complement system (Brandtzaeg & Prydz, 1984). pIgA is subsequently transported across the mucosal barrier, and upon secretion is classified as sIgA (Corthsy, 2009).

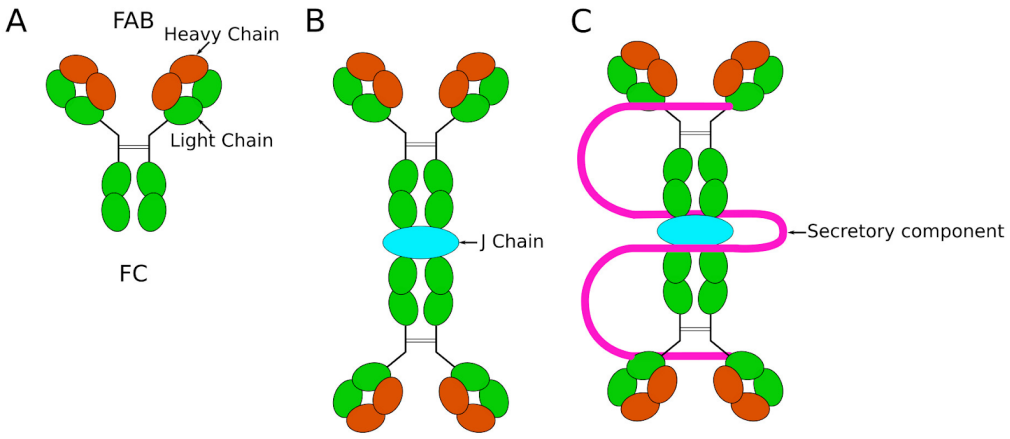


Figure 1.9: A visual representation of antibody configurations. A) A monomeric antibody. This configuration is typical of IgG. The enzyme is split into the fragment antigen-binding (FAB) and fragment crystallisable (FC) regions, with its heavy chains (green) and light chains (orange). B) An example of a dimeric antibody. This is the typical configuration of dimeric IgA, also referred to as polymeric IgA (pIgA). The two antibodies are linked at their FC regions by a J chain, a small glycopeptide of 15 kDa. C) The structure of secretory IgA (sIgA). After pIgA is transported across the epithelium to the luminal side of a mucosal tissue via the polymeric immunoglobulin receptor, part of the receptor, known as the secretory component (SC) remains bound to the pIgA **(Figure 1.10)**. This SC confers benefits such as resistance to peptidases and acids found in the GI tract, as well as ensuring the proper localisation of the sIgA molecule by virtue of its carbohydrate residues (Phalipon *et al.,* 2002). Adapted from Invitrogen, *Secretory IgA and the mucosal immune system* [online] Available at https://www.invivogen.com/review-iga [Accessed 21st September 2021].

Prior to transferring to the luminal side of the LP, pIgA binds to the polymeric immunoglobulin receptor (pIgR) on the basolateral side of the epithelium and is transported to the luminal side. The pIgA-binding portion of the pIgR is cleaved to form the molecule sIgA (**Figure 1.10)** (Kaetzel, Mestecky and Johansen, 2017)**.** The pIgR fragment forms the secretory component (SC), which enhances stability and protects the sIgA from degradation by microbial and host proteolytic enzymes as well as ensuring the proper localisation of the sIgA molecule by virtue of its carbohydrate residues (Phalipon *et al.,* 2002; Johansen & Kaetzel, 2011).

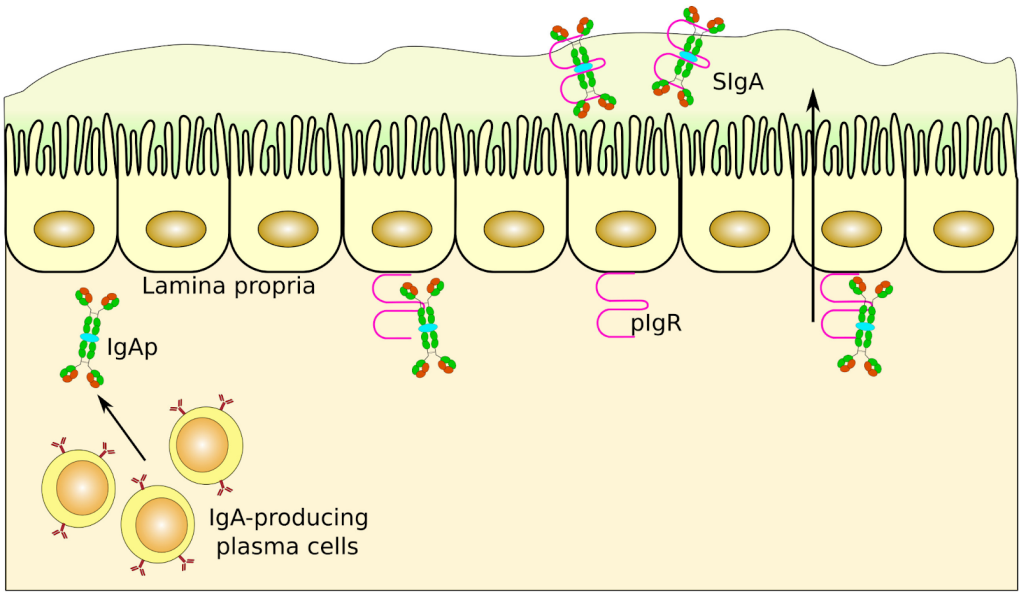


Figure 1.10: Transport of IgAp across the gut epithelium. Terminal maturation into plasma cells producing high-affinity polymeric IgA (IgAp) occurs under the influence of local cytokines (IL-6, IL-10) and growth factors (TGF-β) within the Lamina propria. Upon binding to polymeric Ig receptor (pIgR)expressed at the basolateral pole of epithelial cells, IgAp is exported as secretory IgA (SIgA) into luminal secretions for defence functions such as immune exclusion of pathogens and toxins. Adapted from Corthsy, 2009; Dillon & Lo, 2019

Immune exclusion is the primary mechanism by which sIgA blocks microorganisms and toxins from attaching to mucosal target epithelial cells – this prevents surface damage, colonisation and subsequent invasion (Corthsy, 2009; Leusen & Nimmerjahn, 2013).

The mucosal immune response can be exploited by means of a mucosal vaccine directed to specific MALTs priming them for future infections.

1.5 Mucosal Vaccines

1.5.1 The benefits of mucosal vaccines

In contrast with injected vaccines, needle-free vaccines administered via mucosal routes such as the oral, nasal, vaginal, or rectal routes have the potential to induce mucosal sIgA and in some cases systemic IgG (Boyaka, 2017).

Mucosal vaccines not only have the potential to elicit both antigen-specific sIgA responses and systemic IgG responses, mimicking our natural first and second lines of defence against pathogens, they are extremely practical in terms of vaccine administration and long-term storage. The lack of requirement for use of sterile needles and syringes means professional medical personnel are not required and large numbers can be vaccinated with relative ease. Yet, despite these advantages over parenteral vaccination, there are relatively few mucosal vaccines licensed for use in humans (**Table 1.1**)

Table 1.1: Mucosal vaccines currently licensed for human use. Adapted from (Miquel-Clopés *et al*., 2019)

Pathogen	Trade name	Delivery route (form)	Formulation (± adjuvant)
Vibrio cholerae	Dukoral ®	Oral (liquid)	Inactivated (recombinant cholera toxin subunit B)
	ShanChol ®		Inactivated
	Euvichol ®		
	Vaxchora ®		Live attenuated
Influenza type A and B virus	FluMist ™	Intranasal spray	Live attenuated
Polio virus	Biopolio ™	Oral (liquid)	Live attenuated
	- OPVs		
Rotavirus	Rotarix ® and RotaTeq ®	Oral (liquid)	Live attenuated
Salmonella typhimurium	Typhi Vivotif ®	Oral (capsules)	Live attenuated
Adenovirus	No trade name Approved for military	Oral (tablets)	Live attenuated

1.5.2 Challenges in developing mucosal vaccines

The initial question when producing a mucosal vaccine is which route of administration will be used? The preferred route will produce an immune response in the specific MALT exposed to the pathogen.

One of the largest challenges for oral vaccines is overcoming the mucosal tissue's inherent tolerance to foreign matter. Vaccine antigens must be sufficiently immunogenic or recognised as "foreign" to be selected and taken up by M cells. For this, vaccine adjuvants are used. Adjuvants are molecules that act to potentiate and/or modulate the immune response of an individual; in this case, they work with the vaccine antigen to improve their immunogenicity.

For parenteral vaccines, aluminium-containing adjuvants, particularly alum, are some of the most widely used adjuvants which have been used for almost a century (Kool, Fierens and Lambrecht, 2012). Many antigens adsorb to aluminium-containing adjuvants, facilitating phagocytosis and slowing the diffusion of antigens from the injection site, allowing more time for the host immune response to occur (HogenEsch, 2012). It is suggested that aluminium-containing adjuvants also stimulate recruitment of immune cells by promoting necrosis in vaccinated muscle tissue (Oleszycka & Lavelle, 2014).

Unfortunately, this adjuvant is not effective at triggering the molecular events that support IgA CSR or homing of effector B and T cells in mucosal tissues (Boyaka, 2017). Adjuvants such as cholera toxin and type 1 labile toxin from *E. coli* have been shown to successfully increase the immunogenicity of antigens given orally but issues around safety of these native toxins remain (Mowat, 2003; Bilsborough and Viney, 2004; Uddin *et al.*, 2009; Mestecky, Russell and Elson, 2014).

Another important factor for vaccine development is that the vaccine formulation needs to be protected to reach the target site, for oral vaccines targeting the intestine, the PP Vaccine antigens will be exposed to various challenges including proteolytic enzymes and unfavourable pH in the stomach (Mowat, 2003; Perez-Lopez *et al*., 2016). Strategies such as administration inside protective enteric-coated capsules and in polylactic acid nanoparticles, both of which dissolve only at a specific pH, have been observed to sufficiently protect antigens en route to the intestine by preventing dissolution in the stomach. They provide a more controlled and targeted release of vaccine antigen by ensuring release is halted until the targeted mucosal tissue is reached (Mason *et al*., 2007; Uddin *et al*., 2009).

Once the antigen has been safely delivered to the target site, uptake and processing for presentation by APCs is vital. This can be aided by mucoadhesive substances, such as chitosan, to allow the antigen to come into

close contact with the mucosal membrane, and resist clearance by mucus (Garg *et al.*, 2010; Domm *et al.*, 2011). Where liposomes or nanoparticles are used for either encapsulation or surface display of vaccine antigens, these can additionally carry surface ligands known to enhance mucoadhesion or uptake. Additionally, M cells can be targeted directly through the addition of known M cell-directed motifs within the structure of vaccine candidates (Rakoff-Nahoum *et al.*, 2004; Holmgren and Czerkinsky, 2005; Paredes-Sabja and Sarker, 2012).

1.6 Factors to consider during vaccine development

In order to produce an effective vaccine, several factors must be considered. These include route of administration, delivery method, and antigen candidates. Ultimately any vaccine candidates produced will need to be tested *in vivo* to assess their efficacy and safety before reaching the clinical trial phase. To that end, the suitability of animal models must be considered.

1.6.1 Use of *in vivo* models

Hamsters have been used as an animal model for CDI since the 1960's (Small, 1968). One reason for its suitability as a model is that the pathology of CDI in hamsters, particularly Syrian hamsters, is very similar to that in humans (Price, Larson and Crow, 1979; Best, Freeman and Wilcox, 2012).

Like humans, hamsters are particularly susceptible to CDI upon disruption of their gut microbiota with antibiotics such as clindamycin. This allows colonisation by *C. difficile,* making hamsters a robust model in which to investigate *C. difficile* colonisation. An important difference between CDI in hamsters and humans is that it is often rapidly fatal in hamsters (often 2-3 days post infection) occurs. This allows hamsters to be utilised as a survival model.

Mice models by contrast have historically been less susceptible to fatal CDI (Price, Larson and Crow, 1979). Work undertaken by Chen *et al.* in 2008 sought to address the issue of the lack of commercially available hamster antibodies by establishing a new mouse model which more closely resembled CDI in humans using C57BL/6 mice. Since then, C57BL/6 mice In addition C57Bl/6 mice as well as Balb/c mice have been used to study the life cycle of *C. difficile* including spore transmission (Lawley, *et al.,* 2009) and the role of bile salt metabolism in spore germination (Giel, *et al.,* 2010). More recently, a refined mouse model has been established whereby a cocktail of antibiotics is given which allows *C. difficile* to establish infection (Aubry, *et al.,* 2020).

1.6.2 Antigen candidates

In terms of antigen candidates targeting *C. difficile*, previous work has focused on TcdA and TcdB as key targets (**Section 1.3.5**). Recombinant fragments of the RBD of both TcdA and TcdB, as well as full length and chimeric TcdA/TcdB proteins, have been shown to confer protection against *C. difficile* infection in mice and hamsters (Huang *et al*., 2015; Tian *et al*., 2017). These parenterally administered vaccines alleviated symptoms associated with toxin production, but did not prevent colonisation in the intestine itself and thus did not block transmission of pathogenic spores.

Recent work has shown that CD0873 from strain CD630, the lipoprotein and putative adhesin, is a bona fide colonisation factor and has immunogenic properties in mice. Immunisation with recombinant CD0873 produced antigen-specific responses 10-fold higher in mice that had been immunised compared to naïve animals (Bradshaw *et al*., 2019). This makes CD0873 an attractive vaccine candidate. Immunisation with recombinant CD0873 would prevent colonisation by blocking native CD0873 from performing its role in colonisation thus interfering with an early stage of pathogenesis. The use of CD0873 as an antigen candidate, combined with previously utilised TcdA and TcdB antigens would potentially allow a single

vaccine to target more than one stage of pathogenesis and combat the major virulence factors responsible for causing disease symptoms.

1.6.3 Deploying NTCD as a live oral vaccine strain

As previously discussed, oral administration of a vaccine is the preferred route to elicit a mucosal immune response in the GALT; which should be effective for targeting *C. difficile*. To this end, commensal gut bacteria can be exploited as vaccine vehicles that naturally direct themselves to the intestine. Moreover deploying gut spore-forming bacteria means that spores can be administered that naturally germinate in the intestine.

Early work by Wilson & Sheagren (1983) demonstrated that, following administration of the antibiotic cefotaxime to kill the normal gut flora in hamsters, colonisation by NTCD prior to infection with pathogenic *C. difficile* increased hamster survival from 21% to 93%. It is likely that in this case, the NTCD colonisation is monopolising germinants and nutrients, thereby denying access to the pathogenic *C. difficile.*

Clinical trials have been performed with the aim of developing a stable therapeutic option for prevention of rCDI using oral preparations of NTCD spores (Gerding *et al.*, 2015; Gerding, Sambol and Johnson, 2018). The ability of spores to survive harsh conditions for long periods of time makes them ideal for storage. Their robust structure means they are specially adapted to survive the harsh conditions of the stomach, before germinating in the small intestine and colonising the large intestine, making them attractive vehicles for specifically targeting the GALT.

Administration of NTCD spores alone into a patient with an established pathogenic *C. difficile* infection would not be sufficient for providing protection against the symptoms associated with the current infection caused

by TcdA and TcdB. The lack of TcdA and TcdB would mean administration of NTCD alone would be insufficient to raise antibodies against the toxins present in the infected gut. However, NTCD-M3 spores are under investigation for their ability to prevent recurrent infection by providing transient colonisation as a barrier to reinfection (Gerding *et al.,* 2015a).

1.6.4 Antigenic presentation

Once successful administration to the MALT has been achieved, the selected antigen must be presented to the host immune system in a manner suitable to elicit an appropriate immune response. A system has been developed in *B. subtilis* which allows the expression of recombinant protein fragments on the surface of its spores (Isticato *et al.*, 2001; Potot *et al.*, 2010; Fantappie *et al.*, 2017; Guoyan *et al.*, 2019). Such a system has been engineered to successfully express *C. difficile* protein fragments in such a manner (Negri *et al*., 2013).

However, expression of proteins on the spore surface would expose them to host factors which could degrade or damage them. This is especially likely if administered orally, as acids and proteases within the stomach could denature the proteins prior to reaching the target site. Additionally, such epitopes are normally expressed on the vegetative cell; by forcing expression on the outer spore coat, it is possible their conformation may differ significantly from that presented naturally on the vegetative cell. This would prevent an immune response occurring against the bona fide epitope, and therefore against an active *C. difficile* infection, and thus such a strategy is problematic. It would thus be preferable to express the antigen candidates on the surface of the vegetative cell.

Though effective, an alternative strategy would be to have these fragments recombinantly expressed as lipidated surface antigens for maximal

presentation, potentially enhancing immunogenicity associated with the lipid moieties of lipoproteins as discussed previously.

A combination of all the above work, i.e. an orally administered spore-based vaccine containing *C. difficile* cells capable of expressing immunogenic triacylated antigen fragments on its cell surface, would likely provide the most efficacious attempt at a vaccine to date.

A successful vaccine against CDI must target the bacterial cell in addition to the toxins, and importantly, produce a local protective sIgA antibody response in the gut. A multivalent approach using domains of both toxins and a surface antigen would increase the probability of generating an effective vaccine. This would not only alleviate symptoms associated with toxins, but would also target the vegetative cell itself, blocking attachment to the gut epithelium. To that end, an orally administered, spore-based vaccine utilising lipidated antigen candidates should be produced to directly target the GALT and provide long lasting local protection.

1.7 Aims of this project

In this study, we set out to develop an oral vaccine against *C. difficile* utilising a non-toxigenic strain of the same species as a chassis for delivery of antigen candidates directly to the ileum. Additionally, we planned to utilise lipoprotein moieties to direct antigen fragments to be shed into the extracellular milieu, in order to boost the associated immune response. This project can be broadly defined by the following aims:

- Screening of non-toxigenic *C. difficile* strains for ability to sporulate and ease of purification of spores;
- Sequencing of the selected strain to confirm the absence of toxins TcdA and TcdB;

- Identification of suitable vaccine candidates and a lipoprotein which will facilitate lipidation and release of antigen candidates into the extracellular milieu;
- Cloning of selected candidates with the lipoprotein of choice and integration of the episomal construct into the selected non-toxigenic strain of *C. difficile*;
- Confirmation of antigen expression and viability of the recombinant strains;
- Test the ability of spores of the recombinant strains to generate an *in vivo* immune response in both mice and hamsters.

Chapter 2. Materials and Methods

2.1 General microbiological techniques

2.1.1 Bacterial strains and growth conditions

2.1.1.1 Bacterial strains

All bacterial strains used in this study are shown in **Table 2.1**. *E. coli* TOP10 (Invitrogen) was used throughout for the purpose of cloning and expressing recombinant proteins. The *E. coli* conjugation donor strain sExpress (lab collection) was used for plasmid transfer into *Clostridium*.

Table 2.1: Bacterial strains used in this study and culture conditions

Name	Function	Genotype	Source
E. coli Top10	Cloning strain	F- mcrA Δ(mrr-hsdRMS-mcrBC) φ80lacZΔM15 ΔlacX74 nupG recA1 araD139 Δ(ara-leu)7697 galE15 galK16 rpsL(StrR) endA1 λ-	Invitrogen
E. coli sExpress	Conjugation strain	fhuA2 [lon] ompT gal sulA11 R(mcr-73:miniTn10--TetS)2 [dcm] R(zgb-210:Tn10--TetS) endA1 Δ(mcrC-mrr)114:IS10 + R702 plasmid	Laboratory collection
C. difficile CD37	Host/expression strain	Non-toxigenic *C. difficile*	Laboratory collection
C. difficile M3	Host/expression strain	Non-toxigenic *C. difficile*	Dale Gerding
C. difficile M23	Host/expression strain	Non-toxigenic *C. difficile*	Dale Gerding
C. difficile T7	Host/expression strain	Non-toxigenic *C. difficile*	Dale Gerding
C. difficile CD630	Pathogenic control		Trevor Lawley

2.1.1.2 Growth medium and supplements

All media was autoclaved by heating to 121°C for 10 minutes and allowed to cool to 56°C prior to addition of appropriate supplements. All

media and supplements used in this study are stated in **Table 2.2** and **Table 2.3**.

Table 2.2: Media for bacterial growth and components used throughout this study

Media	Components	g/l
Luria-Bertani (LB) broth	Sodium	5
	Tryptone	10
	Yeast extract	10
LB Agar	Sodium	5
	Tryptone	10
	Yeast extract	10
	Agar	10
Brain Heart Infusion supplemented (BHIS) broth	Brain heart infusion	37
	Yeast extract	5
	L-cysteine	1
BHIS agar	Brain heart infusion	37
	Yeast extract	5
	L-cysteine	1
	Agar	10

Table 2.3: Growth medium supplements and antibiotics used throughout this study

Supplement	Stock concentration mg/ml	Working concentration µg/ml	Solvent
Ampicillin	100	100	dH_2O
Chloramphenicol	25	25	100 % EtOH
Thiamphenicol	50	50	50 % EtOH
***C. difficile* selective supplement**			
D-cycloserine	62.3	250	dH_2O
Cefoxitin	2	8	dH_2O

2.1.1.3 Glycerol stocks

Bacterial cells were stored at -80°C in 15% (v/v) glycerol prepared by mixing 500 µl broth culture with 500 µl of 30% (v/v) sterile glycerol.

2.1.1.4 Aerobic bacterial strains and culture conditions

All *E. coli* strains were routinely grown in Luria-Bertani (LB) broth or agar at 37°C, with liquid cultures shaken at 200 rpm. LB broth and agar was supplemented with either ampicillin (100 µg/ml) or chloramphenicol (25 µg/ml in agar or 12.5 µg/ml in broth) when appropriate.

2.1.1.5 Anaerobic bacterial strains and culture conditions

All *Clostridium* strains were grown in an anaerobic cabinet (MG1000 Mark II, Don Whitley Scientific Ltd, Bingley, UK) with an atmosphere of CO_2 (10%), H_2 (10%) and N_2 (80%) at 37°C. *C. difficile* strains were routinely grown in BHIS broth or on BHIS agar. All liquid media was pre-reduced overnight, with agar pre-reduced for a minimum of 4 hours in anaerobic conditions before use. Media was supplemented as appropriate with *C. difficile* selective supplement (cycloserine 250 µg/ml and cefoxitin 8 µg/ml) and thiamphenicol (15 µg/ml).

2.1.2 *C. difficile* spore preparation

A single *C. difficile* colony which had been grown on BHIS agar (supplemented with 15 µg/ml thiamphenicol as appropriate), was used to set up a 10 ml inoculum in BHIS broth (supplemented with 15 µg/ml thiamphenicol as appropriate) and incubated anaerobically at 37°C overnight. The culture was diluted 1:100 into a fresh flask of 200 ml BHIS broth supplemented as necessary. Following a 5 day incubation period, the culture was removed from the anaerobic cabinet and incubated overnight at 4°C. The suspension was heat shocked at 60°C for 30 minutes for the removal of vegetative cells and then centrifuged at 16, 000 x *g* for 3 minutes. The supernatant was discarded and the pellet was washed in 1 ml sterile water and centrifuged again. This wash step was repeated until observation of the solution using a phase contrast

microscope showed the suspension to be free of vegetative cells. The final pellet was re-suspended in 1 ml sterile water and stored at -80°C.

2.1.2.1 Enumeration of *C. difficile* spores by phase-contrast microscopy

Sporulation cultures were set up as described in **Section 2.1.2**. Following incubation in BHIS broth for five days, spores were enumerated by phase-contrast microscopy using a Bright-Line haemocytometer (Sigma, United Kingdom). To load the haemocytometer, a drop of water was placed on each corner of the coverslip. The coverslip was then placed in the appropriate position, and 10 µl of *C. difficile* spore culture was loaded onto the haemocytometer. *C. difficile* spores were then visualised by phase-contrast microscopy. Spores were counted in 10, 200 µm haemocytometer squares, averaged, and expressed as spores/ml using the appropriate dilution factors.

2.1.2.2 Quantification of *C. difficile* spores by serial dilution

Frozen stocks of spores were enumerated as colony forming units per ml (CFU/ml). Spores were serially diluted 1:10 (10^{-1} to 10^{-8}) in PBS and plated onto BHIS agar plates containing *C. difficile* selective supplement and 0.1% sodium taurocholate (**Table 2.3**) to promote germination. Each dilution was plated in triplicate in 10 µl aliquots before overnight anaerobic incubation at 37°C. Dilutions which gave the most separate colonies were used for enumeration.

2.1.3 Assessment of spores by TEM

Spores of *C. difficile* were prepared as described in **Section 2.1.2**. Spores were fixed in 3% PFA, 0.1 M cacodylate buffer 24 hours before imaging. Imaging was performed by the School of Life Sciences Imaging department at the University of Nottingham.

2.2 Bioinformatics manipulations and tools

2.2.1 Basic Local Alignment Search Tool (BLAST®)

Similarity in nucleotide or protein sequences with available sequenced genomes of *C. difficile* in National Centre for Biotechnology Information (NCBI) was analysed using the BLASTn or BLASTp tool; https://blast.ncbi.n.lm.nih.gov/Blast.cgi.

2.2.2 Generation of a Shotgun Sequence from T7 gDNA

Shotgun sequencing was performed by Illumina sequencing by the DEEPSEQ department at the University of Nottingham. The sequence was then annotated using the previously compiled CD630 genome as a reference by Gareth Little using the PROKKA programme.

2.2.3 Plasmid sequence maps

All plasmid sequence maps were generated using the Benchling online tool available at https://www.benchling.com/.

2.2.4 DNA Oligos

All primers were purchased from Merck (Merck group, Darmstadt, Germany) or IDT (Integrated DNA technologies, Leuven, Belgium) . Primer sequences were manually designed and analysed for secondary structure using the Eurofins oligo analysis tool.

2.2.5 Sequence alignments

Sequence alignments were analysed using the Benchling online alignment tool and the Clustal Omega tool for multiple alignments available at https://www.ebi.ac.uk/Tools/msa/clustalo/.

2.3 Liquid Chromatography Mass Spectrometry (LC-MS) investigation of clostridial lipoproteins

2.3.1 Preparation of culture supernatant

Non-toxigenic *C. difficile* strain T7 was grown in 100 ml minimal media in glass flasks at 37°C in an anaerobic workstation (Don Whitley Scientific, Bingley, UK) with an atmosphere of CO_2 (10%), H_2 (10%) and N_2 (80%). Three flasks were grown to mid-log phase (A600~0.6) and 3 flasks to stationary phase (A600~1.0). 10 ml of each culture was centrifuged at 3000 rpm for 2.5 min at 4°C and the supernatant harvested and filter-sterilised to remove any bacterial cells. SIGMAFAST™ protease inhibitors (Sigma) were added and the supernatant concentrated down to the volumes shown in Table 2.4 using Vivaspin columns: 3 kDa cut-offs, with centrifugation at 4000 rpm for typically 1 hour at 4°C The protein concentration of each concentrated sample was determined by BCA assay. Samples were frozen at -80°C.

Table 2.4: Concentration and volume of supernatant samples of non-toxigenic Clostridioides difficile strain T7. Samples 1-3 were taken from mid-log phase cultures and samples 4-6 from stationary phase cultures.

Non-toxigenic *C. difficile* sample	Volume (ml)	Conc (mg/ml)	Total protein (mg)
1 (OD 1.29)	0.37	6.23	2.31
2 (OD 1.00)	0.58	6.48	3.76
3 (OD 0.95)	0.3	6.25	1.88
4 (OD 0.74)	0.8	6.6	5.28
5 (OD 0.72)	0.75	5.89	4.41
6 (OD 0.50)	0.75	7.44	5.58

2.3.2 LC-MS of extracellular proteins

For all samples, an aliquot equivalent to 100 µg of protein was taken for analysis. Protein was denatured with addition of 8 M urea before reduction with DTT, alkylation with iodoacetamide and digestion overnight with a mixture of trypsin and LysC proteases. Following digestion, peptides were desalted by Strata C18 SPE, dried-down under vacuum and reconstituted in aqueous 0.1% TFA for LC-MS.

LC-MS acquisitions were performed with elution from a 50 cm C18 PepMap EasyNano C18 column over 1 h driven by a Waters mClass UPLC. Eluted peptides were analysed in DDA mode using an Orbitrap Fusion Tribrid mass spectrometer.

LC-MS chromatograms were aligned in Progenesis QI and a consensus, concatenated MS/MS peak list exported in .mgf format for database searching using Mascot. Searching was performed against *Clostridioides difficile* T7 protein sequences appended with common proteomic contaminates. Matching peptides were filtered to 1% FDR as assessed against a reversed database search using the Percolator algorithm. Accepted protein identifications made against the *Clostridioides difficile* T7 strain were downloaded as sequences in .FASTA format then mapped to *Peptoclostridium difficile* 630 protein annotations in String-DB (Szklarczyk et al. Nucleic Acids Res 47.D1 (2018): D607-D613.2) using Smith–Waterman bit scores as a proxy for protein homology, where original scores are computed by similarity matrix of proteins SIMAP1 (doi: 10.1093/nar/gkj106). The String-DB-derived annotations and scores were then mapped back onto the QI-derived quantification data by accession.

Peptide identifications were imported into Progenesis QI and identifications mapped between samples for quantification through MS1 precursor intensities. For relative quantification, data were normalised against all "*Clostridioides difficile*" identified peptides. Data were further filtered to remove matches to contaminants such as keratins and to require a minimum of two peptide matches per accepted protein. A top 3 quantification approach was chosen, which although providing less precision for fine differences between samples, provide a more comparable intensity measurements between different proteins to gauge relative inter-protein abundance within samples i.e. to see which proteins are most abundant in the sample.

To assess changes between mid-log phase samples (1-3) and stationary phase samples (4-6), samples were grouped as (1-3) and (1-4) and ANOVA

comparison was conducted within Progenesis QI, with multiple-test correction to q-values also in QI. To aid visualisation of intra-protein abundance between sample groups normalised intensities were converted to relative percent intensity.

2.4 Genetic manipulations

2.4.1 Nucleic Acid Purification

Plasmids were extracted using an NEB Monarch Nucleic Acid Purification Kit, as per the manufacturer's instructions. PCR products were purified using Monarch PCR & DNA Cleanup Kit. Protocol was followed according to the manufacturer's instructions. Where DNA was run on an agarose gel and excised, DNA was purified using a Jena Biosciences gel extraction kit as per the manufacturer's instructions. The purified vector was eluted in 20 µl of elution buffer provided with each kit.

2.4.2 Nucleic acid purification for use in genomic sequencing

Genomic DNA was extracted from *C. difficile* for gDNA sequencing and use in PCR amplification. To achieve this, 10 ml of overnight culture was centrifuged and the supernatant discarded. The pellet was then resuspended in 180 µl of 10 mg/ml lysozyme in PBS before incubation at 37°C for 1 hour with gentle agitation every 15 minutes.

To remove any RNA from the sample, 20 µl RNase solution was added before incubating at room temperature for 10 minutes. 25 µl proteinase K (Qiagen) was then added along with 85 µl ddH_2O, and 110 µl 10% SDS solution. The solution was mixed by inversion and incubated at 65°C for 1 hour with gentle agitation every 15 minutes.

The solution was transferred to a Phasemaker™ tube (Thermo Fisher) and an equal volume of Phenol/chloroform/isoamyl alcohol (PCI) solution (25:24:1) (Sigma Aldrich) added before centrifugation at 16 000 × g for 5

minutes. The upper fraction was removed and added to a fresh Phasemaker™ tube with an equal volume of PCI solution and centrifuged once more.

The upper phase was removed and 0.1 volume of 3 M NaAc and 2.0 volume of 100% EtOH previously chilled to -80°C were added before incubation at -80°C for 1 hour.

Sample was centrifuged at maximum speed for 15 minutes at 4°C. The supernatant was gently removed and the pellet air-dried for 45 minutes before resuspension in 50 µl ddH_2O.

2.4.3 Nucleic Acid Quantification

To determine the concentration and purity of plasmid preparations the absorbance at a ratio of 260:280 nm was measured by NanoDrop (Lite Spectrophotometer, ThermoFisher) or by fluorometrically by Qubit (Qubit 4 fluorometer, Invitrogen).

2.4.4 Polymerase chain reaction (PCR) and primers

DNA amplification was carried out using Q5 ® High-Fidelity DNA Polymerase (NEB) for cloning genes and Taq DNA polymerase (NEB) for confirming cloning. The PCR reaction was conducted using the components and conditions shown in **Table 2.5 and 2.6. A**ll reactions were performed in 25 µl volumes, following the manufacturer's instructions. The reactions were conducted in an Eppendorf® Mastercycler® (Eppendorf, Hamburg, Germany). All primer annealing temperatures were calculated using the NEB ™ calculating tool available at; https://tmcalculator.neb.com/. On occasions where regular PCR was unable to provide suitable conditions for reliable incorporation of novel bases to form elements such as restriction sites within PCR products, touch-down PCR was employed. The conditions for these reactions are shown in **Table 2.7.** All touch-down PCR reactions used Q5 High

fidelity polymerase. All primers are shown in **Table 2.8**. PCR products were then purified (**Section 2.4.1**).

Table 2.5: Components of PCR using Q5® High-Fidelity DNA Polymerase and Taq DNA polymerase.

Components	DNA (µl)	No DNA (µl)
Q5 High-fidelity polymerase		
5x Q5 reaction buffer	5	5
dNTP mix (10 mM)	0.5	0.5
Primers (10 µl)	1.25	1.25
Template DNA (50-100 ng)	1	0
Q5 High fidelity DNA Polymerase	0.25	0.5
Nuclease free water	up to 25 µl	up to 25 µl
Taq DNA polymerase		
10 x Standard Taq buffer	2.5	2.5
dNTP mix (10 mM)	0.5	0.5
Primers (10 µl)	0.5	0.5
Template DNA (50-100 ng)	1	0
Taq DNA polymerase	1	0
Nuclease free water	up to 25 µl	up to 25 µl

Table 2.6: The conditions used for PCR when using Q5® High-Fidelity DNA Polymerase and Taq DNA polymerase

	Q5 High-fidelity polymerase			**Taq DNA polymerase**		
Step	**Temperature (°C)**	**Time**	**Cycle**	**Temperature (°C)**	**Time**	**Cycle**
Initial denaturation	98	30 secs	1	95	30 sec	1
Denaturation	98	30 sec	35	95	30 sec	35
Annealing	Dependent on Primer T_m	30 sec		Dependent on Primer T_m	60 sec	
Extension	72	20-30 secs / kb		68	1 min / kb	
Final extension	72	2 min	1	68	5 min	1

Table 2.7: The conditions used for Touch-down PCR when using Q5® High-Fidelity DNA Polymerase

	Step	Temperature (°C)	Time	Cycle
	Initial denaturation	98	30 sec	1
Phase 1	Denaturation	98	30 sec	14
	Annealing	-10 °C below Tm, increase by 1°C each cycle	30 sec	
	Extension	72	20-30 secs / Kb	
Phase 2	Denaturation	98	30 sec	20
	Annealing	72	30 sec	
	Extension		20-30 secs / Kb	
	Final extension	72	2 min	1

Table 2.8: PCR primers used in this study

Primer		Sequence	Restriction site
08730_signal_FWD	Forward	GCCGCCGAGCTCAGTTAAAATTACAATAATTATGG	*SacI*
08730_signal_REV	Reverse	GCCGCCTCTAGAACACCCTGTAAGCATAG	*XbaI*
08730_anchor_REV	Reverse	GCCGCCTCTAGAAACCAGTTGAGTTATACCA	*XbaI*
TcdB_FWD	Forward	AGTAAATTCTAGAACTGGATTTGTGACTG	*XbaI*
TcdB_REV	Reverse	ACATATCTCGAGCTATTCACTAATCACTAAT	*XhoI*
TcdB_FWD+Start	Forward	AGTAAATTCTAGAATGCCTGGATTTGTGACTGTAGGCG	*XbaI*
TcdA_FWD	Forward	AGTAAATTCTAGAAAAGCAGTTACTGGATGGCAAACCA	*XbaI*
TcdA_REV	Reverse	ACATATCTCGAGTTAGCCATATATCCCAGGGGCTTTT	*XhoI*
TcdA_FWD+Start	Forward	AGTAAATTCTAGAAATGAAGCAGTTACTGGATGGCAAACCA	*XbaI*
08730_FL_FWD	Forward	GCGGCGGAGCTCTTACAATAATTATGGTTA	*SacI*
08730_FL_REV_XBAI	Reverse	*GGCGCCCTAGACTATTCTTGTTTAGTCTT*	*XbaI*
M13F_Nested	Forward	CTGGCGAAAGGGGGAT	
M13R_Nested	Reverse	AGCAAGGCAAGACCGATC	
Sequencing Primers			
M13F	Forward	GTTTTCCCAGTCACGAC	
M13R	Reverse	CAGGAAACAGCTATGAC	

2.4.5 Colony PCR

Colony PCR was conducted as a method for quick screening of multiple colonies where necessary without the need for genomic extraction. Briefly, individual colonies were picked using a sterile 1 µl loop and suspended gently in 30 µl of nuclease free water. The suspension was heated at 95°C for 5 minutes and 1 µl of this was used as template DNA to conduct PCR amplification as described in **Section 2.4.3** using the Taq DNA polymerase (NEB) (**Tables 2.5 and 2.6**).

2.4.6 Agarose gel electrophoresis

The size of DNA fragments were verified by electrophoresis using 1% (w/v) agarose gel stained with 0.01% (v/v) SYBR-Safe DNA gel stain (Invitrogen™) in 1X Tris-acetate- EDTA buffer (TAE) (ThermoFisher Scientific). The X-Cell SureLock (Bio-Rad) electrophoresis chamber was used and electrophoresis was conducted at 100 volts for 50 minutes. 1 kb Plus DNA ladder (Invitrogen™) and GeneRuler 1 kb Plus DNA ladder (Invitrogen™) were used as a size marker for agarose gels. Verification was performed by loading each gel with a total volume of 6 µl containing 1 µl 6X gel loading dye (NEB) and 5 µl PCR product. DNA loading for gel extractions was carried out in a total volume of 50 µl containing 5 µl 6X gel loading dye (NEB) and 25 µl PCR product. All agarose gels were imaged using the Gel Doc™ XR+ with the Image Lab software (BioRad, California, USA).

2.4.7 Restriction digest

Restriction digests of PCR products and plasmid DNA were performed in a total volume of 50 µl containing the components listed in **Table 2.9**. All enzymes were purchased from NEB. Compatible reaction buffers were selected for each double digest according to manufacturer's recommendations. All reactions were carried out at 37°C for 2 hours followed by gene clean or gel extraction for plasmid digest as described in **Section 2.4.1**.

Table 2.9: Components of a typical restriction digest

Components	Volume (µl)
DNA (1 µg)	Variable
NEBuffer (10 X)	5
Restriction enzyme 1	1
Restriction enzyme 2	1
Nuclease free water	Up to 50 µl

2.4.8 Dephosphorylation of plasmid vector

To prevent self-ligation of vector DNA, plasmid DNA was dephosphorylated following digestion using Calf Intestinal Alkaline Phosphatase (CIAP) (Invitrogen™). The reaction was performed by adding 1 µl CIAP enzyme into the restriction digest reaction and incubating for an additional 5 minutes at 37°C followed by either gene clean or gel extraction (**Section 2.4.1**).

2.4.9 Ligation reactions

In order to determine the concentration of insert required for ligation reactions, the following formula was applied:

$$ng\ of\ insert\ required\ = \left(\frac{ng\ of\ vector \times base\ pair\ of\ insert}{base\ pair\ of\ vector}\right) \times\ molar\ ratio\left(\frac{insert}{vector}\right)$$

All ligation reactions were performed with a constant vector concentration of 25 ng and a molar ratio of 1:6, vector to insert. Each reaction contained the required quantity of insert DNA and plasmid vector, 1 µl T4 DNA ligase (NEB), 1 µl T4 DNA ligase buffer (10X) (NEB) and nuclease-free water to a total volume of 10 µl. Ligations were incubated overnight at 4°C. A vector-only reaction was included alongside all ligation reactions as a negative control.

2.5 Transforming *E. coli*

2.5.1 Making competent *E. coli* cells

Using an overnight *E. coli* culture, 500 µl were used to inoculate 50 ml LB broth containing ampicillin (**Table 2.3**) in a 250 ml flask and incubated at 37^{o}C with 200 rpm shaking until an optical density at 600 nm wavelength (OD 600) 0.2-0.4 was reached. Cells were then transferred to a 50 ml falcon tube and incubated on ice for 30 minutes followed by centrifugation at 4000 rpm for 10 minutes at 4^{o}C. The pellet was gently re-suspended in 20 ml sterile 0.1 M $MgCl_2$ and incubated on ice for 30 minutes followed by further centrifugation. The pellet obtained was re-suspended in 12.5 ml sterile 0.1 M $CaCl_2$ and incubated on ice for 30 minutes followed by centrifugation. The final pellet was resuspended in 2 ml 0.1 M $CaCl_2$ and stored in 15% (v/v) sterile glycerol in 50 µl volumes at ‑80^{o}C.

2.5.2 Transforming competent *E. coli*

All ligations were transformed into Top10 *E. coli* (Invitrogen) and then verified as per **Sections 2.5.3 and 2.5.4**. The heat shock method was used for all transformations (Froger and Hall, 2007). In brief, 50 µl of competent cells were thawed on ice followed by the addition of 1-5 µl of ligation reaction and mixed gently. Cells were incubated on ice for 30 minutes followed by heat shock for 30 seconds at 42°C then transferred onto ice immediately. All contents were transferred into a 15 ml falcon tube with 950 µl of LB broth and were left shaking horizontally at 200 rpm for 1 hour at 37^{o}C.

Following this, 200 µl of the cell suspension were plated onto LB agar containing ampicillin. The remaining cells were transferred to a 1.5 ml Eppendorf tube and centrifuged for 3 minutes at 6000 rpm. Most of the supernatant was removed and the remainder used to resuspend the pellet for plating onto LB agar containing ampicillin. Plates were incubated overnight at 37^{o}C.

2.5.3 Screening *E. coli* transformants

The transformation plates were assessed for the presence of colonies subject to confirmation of zero growth on the vector-only negative control plates. Single colonies were picked and used to inoculate 10 ml LB broth containing ampicillin. Following overnight incubation at 37°C with 200 rpm, plasmid DNA was extracted as described (**Section 2.5.1**) and quantified (**Section 2.5.2**).

2.5.4 Verifying *E. coli* transformants

Two transformants were selected from each transformation and the expected size base pair (bp) for the insert was verified by PCR amplification (**Section 2.5.3**). Recombinant constructs were verified using primers *M13F* and *M13R*. The *M13R* intein primer anneals from 232 bp upstream of the *SapI* restriction site and the *M13F* reverse primer anneals from 47 bp downstream of the *XhoI* site of vector plasmid pMTL84123. Plasmids were further confirmed by sequencing (Source Bioscience, Nottingham). A longer fragment was first amplified using *M13F_Nested* (which binds 95 bp downstream of the *XhoI* site) and *M13R_Nested* (which binds 319 bp upstream of the *SapI* site) primers, before *M13F* and *M13R* were used to sequence them. Internal primers listed in **Table 2.10** were used for constructs where full-length sequencing reads were not obtained. All constructs produced are listed in **Table 2.11**

Table 2.10: Internal primers used for sequencing

Primer		Sequence
S+TcdB_Internal_FWD	Forward	GAAGAAGGTGAAGAAATC
S+TcdB_Internal_REV	Reverse	ACTTTGAACCATCCTCTA
SA+TcdB Internal_FWD	Forward	ATTTTGATGATTCATTTA
SA+TcdB_Internal_REV	Reverse	CCATCATTTATTAATGAC

Table 2.11: Plasmids used in this study and their function

Plasmid	Purpose	Created by
pMTL84123	Parental plasmid	Sarah Chapman
pMTL84123::08730_Signal	Intermediate stage	This study
pMTL84123::08730_Signal+Anchor	Intermediate stage	This study
pMTL84123::TcdB	No-signal peptide control	This study
pMTL84123::08730_Signal::TcdB	Used to overexpress TcdB	This study
pMTL84123::08730_Signal+Anchor::TcdA	Used to overexpress rTcdA	This study
pMTL84123::08730_Signal+Anchor::TcdB	Used to overexpress rTcdB	This study
pMTL84123::08730_FL	Used to overexpress 08730	This study
pTWIN1.HIS	Expression vector	NEB
pTWIN1_CO_TcdA.HIS	Used to express rTcdA	Cansu Karyal
pTWIN1_CO_TcdB.HIS	Used to express rTcdB	Cansu Karyal
pTWIN1_CO_TcdA_17.HIS	Used to express rTcdA_17	Cansu Karyal
pTWIN1_CO_TcdA_28.HIS	Used to express rTcdA_27	Cansu Karyal
pTWIN1_CO_TcdA_30.HIS	Used to express rTcdA_30	Cansu Karyal

2.6 Transformation into *Clostridium difficile*

2.6.1 Transformation into conjugation strain sExpress

All expression constructs were conjugated into the *E. coli* conjugation strains sExpress or CA434 following the heat-shock method outlined in **Section 2.5.2**.

2.6.2 Transformation into *C. difficile* by conjugation

Cultures of sExpress containing expression plasmids were cultured overnight in LB + chloramphenicol (**Table 2.3**) broth at 37 ° C. The *C. difficile* strain T7 was also cultured overnight anaerobically at 37 °C in BHIS broth. The following day, 1 ml of sExpress was centrifuged at 3, 000 *g* for 2.5 minutes and washed twice with PBS. The pellet was then resuspended in 200 µl of the T7 overnight culture and the mixture was plated onto BHI agar which had previously been reduced in the anaerobic cabinet. This was done in 20 µl droplets. Plates were incubated for 24 hours at 37 °C anaerobically.

500 ul of PBS was subsequently added to the plates and colonies scraped off. 100 µl of cell suspension was then added to BHI agar plates containing *Clostridium difficile* selective supplement (Oxoid) and 15 ng/ml thiamphenicol. Plates were inverted and left to grow for 72 hours before colonies were harvested for verification.

2.6.3 Screening of *C. difficile* transformants

To assess the purity of the transformants. Colonies were harvested from transformation plates and grown overnight in BHIS containing *C. difficile* selective supplement and thiamphenicol 15 ng/ml thiamphenicol. These cultures were then used to perform a PCR using Q5 High-fidelity polymerase using the primers shown in **Table 2.12.** Primers *E.coli_uspA_FWD* and *E.coli_uspA_REV* were used to confirm the presence of the gene *uspA* in *E. coli* and primers *C.diff_Spo0A_FWD* and *C.diff_Spo0A_REV* were used to confirm the presence of the *Spo0A* gene in *C. difficile.* This method of selection would ensure recombinant strains used going forward were solely *C. difficile* and contained no *E. coli* contaminants.

Table 2.12: Primers used to detect *E. coli* contamination in T7 recombinant strains

Primer		Sequence
E.coli_uspA_FWD	Forward	CCGATACGCTGCCAATCAGT
E.coli_uspA_REV	Reverse	ACGCAGACCGTAGGCCAGAT
C.diff_Spo0A_FWD	Forward	GCAGATGACAATAAGGATTTT
C.diff_Spo0A_REV	Reverse	CCTCCATTGCATGTCTTATTGC

2.7 Assessment of recombinant *C. difficile* strains

2.7.1 Growth curves and time sampling of clostridial species

To assess the growth rate and generation times of *C. difficile* strains, cultures were grown for two consecutive overnights in BHIS medium or BHIS + 15 ng/µl thiamphenicol where appropriate, ensuring that on day three, only actively growing cells were used for the assay. Cells were diluted 1:100 in BHIS or BHIS + 15 ng/µl thiamphenicol where appropriate, and added in triplicate to a 48-well plate. Optical density (A_{600}) was measured continuously for 24 hours in a spectrophotometer (Promega GloMax-multi detection system).

2.7.2 Assessing the sporulation rate of recombinant strains

To assess the rate at which each of these recombinant strains sporulate, cultures were grown over the course of 5 days in selective medium where appropriate, and two samples were taken for each strain. One sample was heat treated at 65°C for 30 minutes to kill all vegetative cells within the sample, and the other was not. Serial dilutions were created for each sample and spotted onto medium containing 0.1 % taurocholate and 15 ng/µl thiamphenicol where appropriate in triplicate as per **Section 2.1.2.2**. Colony forming units (CFUs) were counted and rate of sporulation assessed.

2.7.3 Assessment of plasmid retention by recombinant strains

To assess the rate at which expression plasmids are lost from T7-recombinant strains in the absence of selective pressure, 10^3 spores from each recombinant strain were inoculated into BHIS broth and grown anaerobically at 37°C for 6 hours. Serial dilutions were then performed and spotted onto selective and non-selective media in triplicate as per **Section 2.1.2.2**. After anaerobically incubating overnight at 37 °C, CFUs were enumerated.

2.8 Protein expression and purification

2.8.1 Protein expression

Expression of proteins was conducted using the T7 express competent *E. coli* cells (NEB). Using a single colony following an overnight plate incubation (**Section 2.1.1.4**), 10 ml LB broth containing ampicillin was inoculated (**Table 2.3**) and incubated with 200 rpm shaking at 37°C overnight. The following day, 10 ml of overnight culture was used to inoculate 1 L LB broth containing ampicillin in a sterile 2.5 L flask incubated with shaking at 200 rpm at 37°C until an OD_{600} 0.6-0.7 was reached. The cultures were then induced for protein expression using 0.3 mM Isopropyl β-D-1-thiogalactopyranoside (IPTG) with an overnight incubation at room temperature with shaking at 200 rpm. Non-induced controls were included in this experiment to distinguish expression of the target protein from native proteins. The cultures were then transferred to 500 ml Nalgene® centrifuge bottles and centrifuged at 5, 000 x g for 10 minutes at 4°C.

2.8.2 Protein extraction

Proteins were extracted using a binding buffer composed of 20 mM Tris-HCl, 1 M NaCl and 40 mM imidazole at pH 7.4, which formed the basis for all buffers used throughout the purification process. The proceeding steps were conducted on ice and the bacterial cells were lysed in the following manner. The cell pellets were re- suspended in 100 ml refrigerated binding buffer and sonicated in 40 ml volumes with 10 seconds on and 30 seconds off

pulse for 18-20 minutes at 40% amplitude using the Fisherbrand™ Q500 sonicator-500 W, 20kHz (ThermoFisher Scientific) with a 13 mm diameter probe tip. Lysed cells were then centrifuged at 19, 000 x *g* for 30 minutes at 4^{o}C. The supernatant containing proteins in the cytosol (soluble fraction) was harvested. In order to check if the protein of interest had formed inclusion bodies or aggregated, the pellet (insoluble fraction) was further re-suspended in 40 ml of binding buffer. A sample of both the soluble fraction and insoluble fraction were analysed by sodium dodecyl sulphate-polyacrylamide electrophoresis (SDS-PAGE) (**Section 2.8.3**).

2.8.3 Sodium dodecyl sulphate-polyacrylamide electrophoresis (SDS-PAGE)

All cell lysates were fractionated using 10% (w/v) Tris-glycine SDS-PAGE gels. The lysate samples were prepared by using 20 µl of 2X SDS sample buffer containing 100 mM Tris-HCl, 4% (w/v) SDS, 0.2% (w/v) bromophenol blue, 20% (v/v) glycerol and 200 mM 1,4- Dithiothreitol (DTT), mixed with 20 µl cell lysate followed by incubation at 95°C for 5 minutes. Each lysate including the non-induced negative control was loaded in a 10 µl volume along with 3 µl Colour Pre-stained Protein standard (NEB) on each gel.

Gels were run using 1X Tris-glycine buffer containing 25 mM Tris, 192 mM glycine, 0.1% (w/v) SDS at pH 8.3 in the X-Cell SureLock (Bio-Rad) tank at 120 volts for 1 hour and 30 minutes. The protein gels were then Coomassie blue stained using 1% (w/v) Coomassie brilliant blue, 50 % (v/v) methanol and 40% (v/v) diH 2 O with incubation at room temperature for 20 minutes and gently shaking. This was followed by incubation with a destain solution containing 50% (v/v) methanol, 10% (v/v) glacial acetic acid and 40% (v/v) diH 2 O for 1 hour with further removal of Coomassie blue stain by incubating the gels overnight in diH_2O. Gels were imaged using the Gel Doc™ XR+ with the Image Lab software (Bio-Rad).

2.8.4 Immobilized Metal Affinity Chromatography (IMAC) for purification of soluble recombinant His-tagged proteins

Following verification of expression, crude cell lysates were passed through an Ni^{2+} - charged affinity column using the nickel-nitrilotriacetic acid HisPur TM Ni-NTA Resin (Thermo Scientific, Rockford, USA) and all steps performed at room temperature. Binding buffer was used for all wash steps. The target protein was eluted using increasing concentrations of imidazole elution buffers containing 0.1 M Tris-HCl and 2.5 M NaCl with 50 mM, 100 mM, 250 mM and 500 mM imidazole

Purification steps were as follows. In a PD-10 column (GE Healthcare Life Sciences), 3 ml of resin slurry was loaded obtaining a 1.5 ml bed volume of resin. The resin was washed with 5X bed volume of dH_2O followed by the same amount of binding buffer. Using a 10 ml volume, lysates were loaded onto the resin and the flow-through collected. The resin was then washed with 10X bed volume with binding buffer for the removal of non-bound proteins and the flow-through collected.

The protein was then eluted using increasing concentrations of imidazole; 50 mM, 100 mM, 250 mM and 500 mM. All eluates were collected and fractionated by SDS-PAGE (**Section 2.8.3**). All elutions containing protein were combined and dialysed in PBS overnight for downstream applications using the Biodesign™ Cellulose Dialysis Tubing strip with a 14 kDa molecular weight cut off (MWCO) (Fisher Scientific, Leicestershire, UK).

2.8.5 On-column solubilisation and purification of recombinant His-tagged proteins using IMAC

On-column solubilisation was performed for insoluble proteins found within cell lysates pellets (**Section 2.8.2**). The binding buffer containing 20 mM Tris-Hcl, 500 mM NaCl and 40 mM imidazole, pH 7.4 was used throughout with decreasing concentrations of urea. The insoluble pellet was resuspended in breaking buffer containing binding buffer with 6 M

guanidine-HCl and incubated by stirring at 100 rpm for 1 hour at 4°C. This was then centrifuged at 19, 000 x *g* for 30 minutes at 4°C.

The supernatant was loaded onto Ni^{2+} columns prepared, washed and equilibrated in breaking buffer as described in **Section 2.8.4**. The column was flushed through with 20X bed volume washes of binding buffer containing 6 M, 4 M, 2 M urea and 1 mM reduced and 0.1 mM oxidized glutathione respectively. The protein was then eluted in increasing concentrations of imidazole and visualised using 10% (w/v) Tris-glycine SDS-PAGE gels (**Section 2.5.3** and **2.5.4**).

2.8.6 Solubilisation and purification by His-trap column

Samples were loaded onto a His-trap Fast Flow column (5 ml) at a rate of 0.8 ml/min using a fast protein liquid chromatography system (Bio Rad Standard BioLogic LP System) and left overnight at 4°C. The column was then washed with 50 ml of each solubilisation buffer as discussed in **Section 2.2.5** stepwise, at a rate of 0.8 ml/min. The sample was then eluted with increasing concentrations of imidazole ranging from 100-500 mM in volumes of 20 ml at a rate of 1 ml/min. A sample of the final eluate was taken to assess purity using SDS-PAGE as per **Section 2.8.3**.

2.8.7 Purification by membrane filtration

Samples purified by IMAC or His-trap column were added to Vivaspin centrifugal concentrator columns (GE Healthcare Vivaspin) with a 10kDa cut off. Samples were centrifuged at 8, 000 x *g* for 10 minutes at a time until all but 1 ml of the sample had passed through the filter.

2.8.8 Protein concentration determination using Bicinchoninic acid assay (BCA)

Protein concentration was determined using the Pierce™ BCA protein assay kit (ThermoFisher Scientific), following manufacturer's instructions. Purified bovine serum albumin (BSA) standards ranging from 200-2000 µg/ml

were prepared in PBS. Protein was serially diluted 2-fold (1:2-1:32) to ensure detection. A total of 25 µl of each sample, standards and PBS control were dispensed in duplicates into a 96-well plate Costar™ (ThermoFisher Scientific). BCA reagents A and B were pre-mixed using a ratio of 50:1 and added to each well in a total volume of 200 µl. The plate was briefly mixed using the plate shake setting and incubated at 37^{o}C for 30 minutes. Absorbance values were measured at 562 nm using the CLARIOstar Plus (BMG LABTECH, Aylesbury, UK) plate reader.

2.8.9 Western Immunoblotting

Tris-glycine SDS-PAGE gel (**Section 2.8.3**) was transferred to the pre-cut blotting transfer pack (Trans-Blot® Turbo™ Mini PVDF Transfer Packs) (Bio-Rad) and positioned directly above the PVDF membrane in between two stacks of wet filter paper. The transfer was conducted using the Trans-Blot® Turbo™ Transfer system (Bio-Rad) at 25 volts for 7 minutes. Once transferred, the membrane was blocked for 1 hour in 5% milk made from dry, powdered milk dissolved in Tris-buffered saline (TBS) containing 0.1% (v/v) Tween-20 (TBST). The membrane was then incubated overnight at 4^{o}C with the primary antibody diluted in 1% milk in TBST. The membrane was then washed for 30 minutes in TBST with solution changes every 10 minutes. This was followed by an hour incubation with HRP-conjugated secondary antibody diluted in 1% milk in TBST. The membrane was then washed in TBST for 1 hour with 15 minute interval solution changes. Protein bands were detected using 3, 3',5 ,5'- Tetramethylbenzidine (TMB) (Sigma-Aldrich) or enhanced chemiluminescent (ECL) (Bio-Rad) substrate and visualised using the Gel Doc™ XR+ with the Image Lab software (Bio-Rad).

2.9 Fluorescent staining of T7 recombinant strains for use in FACS and confocal microscopy

2.9.1 Fluorescent staining of T7 recombinant strains

To stain surface antigens, 1 ml of overnight culture was harvested for each strain and washed twice with 1x TBS plus 0.1% Tween 20 (TBST) (all

centrifugations to be performed at 3,000 xg for 2.5 minutes). The pellets were resuspended in 1 ml of TBST plus 5% milk to block non-specific binding sites before incubating for 1 hour shaking at room temperature.

Samples were centrifuged and resuspended in 2 ml of a 1:1000 dilution of primary MAb (**Table 2.13**) in TBST + 1% milk (w/v) and incubated shaking at 4^{o}C overnight. Samples were then washed for 30 minutes in TBST with solution changes every 10 minutes before resuspension in 2 ml of a 1:1000 dilution of secondary MAb (**Table 2.13**) in TBST + 1% milk (w/v) and incubation for 2 hours shaking at room temperature. Samples were washed in TBST for 1 hour with 15 minute interval solution changes.

Table 2.13: Table of antibodies used in this study

Target antigen	Host animal	Conjugated to	Primary/ secondary	Poly/ monoclonal	Supplier
C. difficile	Rabbit	n/a	Primary	Polyclonal	Abcam
TcdB	Mouse	n/a	Primary	Polyclonal	Native antigen company
CD0873	Rabbit	n/a	Primary	Polyclonal	Stephen Mitchell
Rabbit IgG	Goat	Alexa fluorophore 488	Secondary	Monoclonal	Thermo Fisher
Mouse IgG	Donkey	Alexa fluorophore 568	Secondary	Monoclonal	Thermo Fisher
Mouse IgG	Rabbit	Horseradish peroxidase (HRP)	Secondary	Monoclonal	Cell signalling technology
Rabbit IgG	Goat	HRP	Secondary	Monoclonal	Cell signalling technology
Hamster IgG	Goat	Biotin	Secondary	Monoclonal	Sigma-Aldrich
Biotin	Streptavidin	HRP	Secondary	N/A	RD Systems

Pellets were resuspended in 500 µl 4% paraformaldehyde and incubate shaking at room temperature for 30 minutes before being washed twice using TBST and finally resuspended in 1 ml TBST. The negative control consists of

cells incubated solely with the secondary antibody as well as the wildtype strain.

2.9.2 FACS analysis

Samples of cells prepared as per **Section 2.9.1** were passed through a MoFlo Astrios EQ cell sorter (Beckman Coulter) within the Flow Cytometry Facility (University of Nottingham). A 488 nm laser was used to measure green fluorescence, and a 468 nm laser was used to measure red fluorescence. The data was visualised and density plots were produced using the FlowJo 7.6 Software (Becton, Dickinson and Company; 2019).

2.9.3 Confocal microscopy

Cells were prepared as stated in **Section 2.9.1** before being added to microscopy slides in 10 µl aliquots and allowed to dry. Coverslips containing 10 µl ProLong^{TM} glass antifade mountant were then added and allowed to dry for 5 days before being stored in a sealed container at 4^{o}C. Slides were imaged using a ZEISS Elyra 7 with Lattice SIM confocal microscope (SLiM facility, University of Nottingham).

2.10 In vivo immunogenicity study using hamsters and mice

2.10.1 In vivo immunisation and sample collection

Female Golden Syrian hamsters (12-14 weeks old) weighing approximately 150 g and Female C57BL/6J (8-10 weeks old) weighing approximately 20 g were purchased from Janvier Labs and used for the in vivo immunisation, all housed individually using individually ventilated cages (IVCs). All animal experiments were conducted under project licence-PPL14712E8BB. Each animal received a total of 3 immunisations of 1x10^{6} spores, hamsters were orally gavaged using the Luer lock dosing applicator, 9hEC device and mice with gavage on day 1, 15 and 30. Animals were weighed prior to each immunisation. All animals were euthanised using exposure to CO_2 in a gas chamber (3 ml/L) followed by cervical dislocation 14 days post final immunisation. Blood samples were collected via cardiac

puncture and faecal pellets were extracted from the large intestines and stored at -80°C. A small portion (~ 2 cm) of small intestine (ileum), large intestine and caecum were removed and stored at -80°C. The remainder of the small intestine was placed in 5 ml PBS containing 1X SIGMAFAST™ protease inhibitor tablet (Sigma-Aldrich).

2.10.1.1 Serum and intestinal fluid preparations

Biological fluids were prepared as described below and stored at -80°C for subsequent use in in vitro assays.

Serum

Blood withdrawn at the experimental endpoint was collected in 2 ml Eppendorf tubes and allowed to clot overnight at 4°C. The tubes were then centrifuged at 2, 000 x g for 10 minutes at 4°C and the supernatant collected and stored at -80 °C.

Small intestine

The small intestine was placed in 5 ml PBS containing 1X SIGMAFAST™ protease inhibitor cocktail (Sigma-Aldrich), vortexed for 20 seconds and flushed through twice with 1 ml of the suspension in a 50 ml falcon tube. The suspension was then centrifuged at 2, 500 x g for 30 minutes at 4°C. The supernatant was collected and stored at -80°C.

2.10.1.2 ELISA

Anti-IgG levels in serum were detected using indirect ELISA. All incubation steps were performed with gentle shaking at 50 rpm followed by gentle removal of contents and 5 washes with 200 µl PBST (PBS containing 0.01% Tween 20). In brief, 96-well Nunc MaxiSorp ™ plates (Thermo Fisher Scientific) were coated with 100 µl purified recombinant proteins at a concentration of 2.5 µg/ml in 0.2 M sodium bicarbonate, pH 9.4 and incubated overnight at 4°C.

Wells were blocked with 200 µl of 5% dry-milk in PBST for 2 hours at room temperature. Wells were then incubated overnight at 4°C with 100 µl serum at 1:10 dilution in PBST. This was followed by a 2 hour incubation at room temperature with 100 µl goat anti-hamster IgG (H +L) highly cross adsorbed- Biotin antibody (Sigma-Aldrich) at a 1: 20 000 dilution in PBST and then a 2 hour incubation with Strepavidin-HRP (RD Systems-Fisher Scientific) at 1:200 dilution in PBST.

Absorbance measurements were taken following incubation with 100 µl of TMB (Sigma-Aldrich) for 15 minutes at room temperature at 650 nm wavelength using the CLARIOstar Plus (BMDLABTECH) plate reader. Detection of anti-IgA levels in the faecal and intestinal fluid samples was not possible due to the lack of availability of anti-hamster IgA secondary antibody.

2.10.1.3 Toxin neutralisation assay using Vero cells

Vero cells were maintained in a T25 cell culture flask (Corning®) using 15 ml Dulbecco's Modified Eagle's Medium (DMEM) containing 10% (v/v) fetal bovine serum (FBS) and 1% (w/v) penicillin/streptomycin (Gibco™-ThermoFisher Scientific) at 37°C with 5 % CO_2. Cells were passaged 2-3 times weekly and reseeded at a ratio of 1:5. Cells counts were determined using a haemocytometer under the Motic AE2000 light microscope and seeded onto 96-well plate (Corning®) at a density of 1 x 10 5 /ml in a volume of 100 µl per well 24 hours prior to the assay.

The serum and intestinal fluid were filter-sterilised using the Costar Spin-X centrifuge tubes (0.22 µm) (Corning®) at 14, 000 x g. All dilutions were conducted in DMEM containing 1% (w/v) penicillin/streptomycin. Serum and intestinal fluid were added to a separate 96-well plate in triplicates in a volume of 25 µl with a series of 2-fold dilution in non-supplemented DMEM. Full-length toxin A and toxin B *C. difficile* VPI043 strain (FL-TcdA and FL-TcdB) (Public Health England) was added to each well in a volume of 25 µl to a final concentration of 50 ng/ml and 0.25 ng/ml respectively. The plate was incubated at 37°C with 5% CO_2 for 1 hour. Following removal of

DMEM from Vero cells, each serum/intestinal fluid + toxin suspension was added to these cells and incubated for 20 hours at 37°C with 5% CO_2.

As controls, cells only and FL- TcdB and FL-TcdA added to cells were also included. A colorimetric assay was used to detect cell death/cell rounded with 3-(4,5-dimethylthiazol-2-yl)-2,5- diphenyltetrazolium bromide (MTT) solution (Sigma-Aldrich) added to each well in 50 µl volume at 0.5 mg/ml and incubated for 4 hours 37°C with 5% CO_2 . MTT solution was removed and wells incubated with 75 µl of dimethyl sulfoxide (DMSO) for 10 minutes at room temperature. Absorbance measurements were taken at 570 nm wavelength using the CLARIOstar Plus (BMDLABTECH) plate reader.

2.10.1.4 Adherence blocking assay using Caco-2 cells

Caco-2 cells were maintained and passaged as stated in **Section 2.10.1.3** using DMEM supplemented with 10% (v/v) FBS and 1% (w/v) penicillin/streptomycin (Gibco™- ThermoFisher Scientific). For the adherence assay, Caco-2 cells were seeded at a density of 1 x 10 5 /ml in a total volume of 500 µl per well in a 24 well plate (Corning). Cells were left to grow for 14 days and the media changed every 2-3 days. The medium was also changed 24 hours prior to conducting the assay.

Caco-2 cell counts were performed by first removing the medium and adding 200 µl 1X trypsin-EDTA (Sigma-Aldrich) to the monolayer of cells to detach the cells from the bottom of the well. Detached cells were harvested and the wells washed with 300 µl PBS and added to the 200 µl of detached cells. Cell counts were determined using a haemocytometer under the Motic AE2000 light microscope.

The entirety of the assay was performed under anaerobic conditions at 37°C in the following manner. A 10 ml overnight grown *C. difficile* strain 630 culture was centrifuged at 5, 000 x g for 6 minutes and washed once in PSB followed by a repeat centrifugation step. The pellet was resuspended in serum-free DMEM. For retrospective multiplicity of infection (MOI)

determination, 100 µl of the cell suspension was serially diluted 1 in 10 in PBS (10 -1 to 10 -7) and 100 µl of each dilution was plated onto BHIS plates containing *C. difficile* selective supplement.

50 µl of serum (1:5) /intestinal fluid (1:2) were added to 50 µl of bacterial cells of the different dilutions and incubated for 1 hour. This mixture was then added to Caco-2 cells following removal of medium and incubated for 2 hours. This suspension was then removed and the Caco-2 cells washed 3 times with 500 µl PBS and then incubated with 200 µl 1X trypsin-EDTA. The detached cells were removed and re-suspended in 300 µl DMEM containing 10% (v/v) FBS. This cell suspension was then serially diluted (10 -1 to 10 -3) in PBS and 100 µl plated on BHIS plates supplemented with *C. difficile* selective supplement and incubated overnight for CFU/ml counts.

2.10.3 Ethics statement

Animal experiments were proceeded using the Experimental Design Assistant (EDA) online tool and both Golden Syrian hamster and C57BL/6J mouse models were utilised correspondingly with the UK Home Office Inspectorate under the Animals (Scientific Procedures) Act 1986. Approval for experimental procedure was granted by the University of Nottingham Animal Welfare and Ethical Review Body and the UK Home Office under project licence- PPL14712E8BB. Animals were euthanised with CO_2 followed by cervical dislocation.

2.10.4 Statistical analysis

All statistical analysis was conducted using the GraphPad Prism 7 software. All data were tested for normality using the D'Agostino & Pearson and the Shapiro-Wilko normality test. A parametric one way ANOVA test was performed followed by Dunn's multiple comparison test to compare means of control groups with experimental groups for ELISA and adherence blocking assays.

Chapter 3. Rational design of a vaccine against *C. difficile*

3.1 Introduction

The purpose of this PhD project was to utilise a commensal spore-forming organism as a chassis, here non-toxigenic *C. difficile* (NTCD) in which lipidated, heterologous antigens of *C. difficile* could be engineered. Spores will be used for oral administration of this vaccine, exploiting the spores' thermostability for storage, natural hardiness and resilience against the low pH of the stomach and against proteases and their natural target site for germination into metabolically active vegetative cells, the ileum. Lipidated antigens would be released from the host cell in the ileum for uptake by M cells, and possess natural adjuvant afforded by the lipid moiety to induce a humoural immune response. It was essential that before cloning began, appropriate elements for each part of the proposed system were identified. These included a suitable commensal spore-forming organism, a lipoprotein to direct expression and lipidation of the chosen antigen and its release into the extracellular milieu, and promising vaccine antigens.

This chapter first sets out to identify NTCD chassis strains from the literature and select one strain to take forward based on its sporulation efficiency. Secondly, the chapter sets out to sequence the genome of the chosen strain to confirm the absence of paLoc and to identify the non-toxin vaccine candidates the strain possesses that are in common with the toxigenic reference strain 630, which may provide a background level of protection against toxigenic *C. difficile*. Finally, the chapter sets out to identify the most abundant lipoprotein that localises to the extracellular milieu by LC-MS analysis of culture supernatants so that appropriate fusion constructs can be engineered with the chosen antigen and expressed in the chassis strain (**Chapter 4**). The ideal lipoprotein would be one that is naturally released in abundance in the

extracellular milieu. The N-terminal leader sequence of this lipoprotein could then be fused with the chosen antigen.

Vaccine candidates must be strongly immunogenic to induce an immune response particularly in the small intestine of the host as they have to be capable of overcoming immunotolerance in the GALT, yet they must not be toxic to the host. Vaccines in clinical trials have exploited *C. difficile* toxoids, or toxin fragments given intramuscularly. Unfortunately they do not provide local protection against colonisation in the colon or shedding of spores which results in transmission.

It is likely that two or more antigen candidates will be required in an effective vaccine. Ideally Both toxins, TcdA and TcdB, should be targeted as well as a protein on the bacterial cell surface to ensure the main cell body is targeted. It must be taken into consideration that the clostridial toxins are very large (TcdA is 308 kDa and TcdB is 270 kDa) (Giannasca *et al.,* 1999; Chandrasekaran and Lacey, 2017) and would therefore be difficult to clone into plasmids in their entirety for expression and would be toxic to the host (Phelps, *et al.,* 1991; Tang-Feldman *et al*., 2002). Therefore, a fragment of these proteins is likely the best solution that has previously been shown to be capable of inducing an immune response (Huang, 2015; Huang, Shen, *et al*., 2015; Huang, Wu, *et al*., 2015).

3.2 Aims

- Identify a NTCD strain for use in this project;
- Identify a lipoprotein which will facilitate lipidation and release of antigen candidates into the extracellular milieu;
- Identify a suitable vaccine antigen to be lipidated and released by the NTCD chassis strain.

3.3 Results

3.3.1 Identifying a suitable vaccine chassis strain

There are several factors to consider when selecting a suitable chassis strain;

- They must possess no toxigenic activity for good safety and therefore suitable for administration to the immuno-compromised.
- Any immune response is induced by the introduced vaccine candidates alone.
- They must produce spores efficiently to facilitate rapid production and purification.

Using a strain of NTCD as a vaccine chassis is beneficial given the repertoire of antigens these strains are likely to possess in common with toxigenic *C. difficile* (TCD). The commonality of antigens between NTCDs and TCDs means a natural level of protection should be afforded against TCD. By further engineering NTCD to express immunogenic domains of toxins downstream of the signal peptide of a lipoprotein that is abundantly released from the cell, the toxin fragments can be lipidated and released to engage the mucosal immune system.

Work performed by Senoh *et al.* in 2018 showed that colonisation by four separate strains of TCD was reduced by up to 99% and survival increased by 30% in mice that had been administered an intrarectal preparation of the membrane fraction of NTCD strain JND13-023. The immunisation was shown to have stimulated production of both systemic IgG and intestinal IgA within the mice. This demonstrates that the NTCD possessed sufficiently similar

immunogenic components within its membrane to that of TCD to mount an effective immune response against the latter. This also demonstrates that individual antigens, as would be found in membrane fractions, are likely taken up by M cells to stimulate adaptive immune responses.

Sambol *et al.* (2002) used NTCD strains M3, M23, and T7 because of their high prevalence in asymptomatic patients with CDI to assess the effect that immunisation with NTCD would have on inhibiting TCD colonisation, TCD strains B1, J9 and K14 were chosen due to their potency as outbreak strains in recent human epidemics. Hamsters were selected as the animal model for this study; their high sensitivity to CDI normally results in death up to three days after an initial infection with 100 spores of TCD. This makes them an ideal lethality model to determine protective efficacy of vaccine strength (Wang *et al*., 2018). Hamsters were administered 30 mg/kg clindamycin to clear their gut flora before being immunised with 10^6 NTCD spores. On day 7, hamsters were then challenged with 100 spores from TCD strains which were administered orogastrically. The results of this experiment are summarised in **Table 3.1.**

Table 3.1: Results of NTCD immunisation as performed by Sambol *et al.* (2002)

Strain	% of hamsters colonised with NTCD	% disease prevention
M23	90	93
M3	97	100
T7	90	100
TCD control	0	0

These data indicate a strong correlation between NTCD colonisation and reduction of future colonisation by TCD (as seen by an increase in %

disease reduction) resulting in prevention of CDI symptoms. As the challenge was made after only 7 days of colonisation, it is likely that the prevention of symptoms is due to colonisation resistance rather than true immunity.

A subsequent study performed by Nagaro *et al.* in 2013 took a similar approach in testing the ability of colonisation with NTCD strains M3 and T7 to prevent CDI caused by hypervirulent B1/NAP1/027 TCD strains B11 and B16. It was concluded from this study that NTCD strains T7 and M3 are 100% effective in preventing colonisation by TCD strain B11. However, T7 and M3 conferred protection in only 60% and 90% of hamsters respectively against TCD strain B16. This suggests that not all strains of NTCD will be equally effective when used to immunise against TCD and emphasises that immunisation with NTCDs alone is not a suitable solution to vaccination and genetic modifications to the strains may be required.

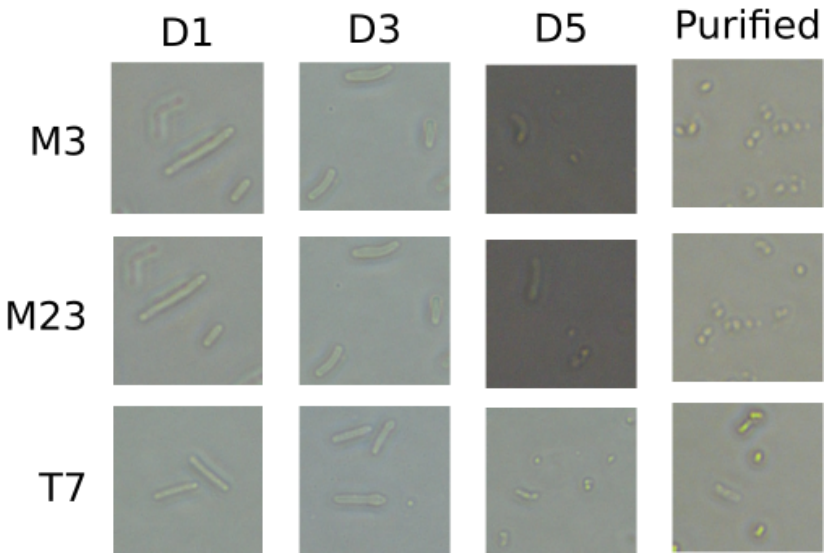
The suitability of NTCD for use in humans as a therapy (as opposed to a vaccine) to treat CDI has been shown by Gerding *et al.* in 2015. In a Phase 1 randomised, double-blind, placebo trial, CDI patients (n=173). were administered varying concentrations of NTCD strain M3 spores or placebo over the course of 7-14 days. The results of this study suggest that using NTCD isolates to colonise the GI tract reduces recurrent CDI. Specifically, the rate of recurrence decreased from 31% in the placebo group to 2% in the group administered M3 spores. They found that administering 10^7 spores/day for 7 days and 10^7 spores/day for 14 days had a very similar effect on reducing recurrence rates, and, as such the extra 7 days of treatment was not necessary. It was also discovered that NTCD colonisation eliminated TCD from the gastrointestinal tract which would reduce the rate of transmission and be extremely beneficial in high-risk environments such as hospitals. Thus, NTCD could be used as a therapeutic in addition to a prophylactic.

The purpose of this PhD was to exploit NTCD as a vaccine chassis but to improve its immunogenicity by engineering the organism to induce antibodies specifically against TCD, rather than merely confer a colonisation resistance benefit.

With all three NTCD strains M3, M23 and T7 showing protective effects against CDI, the first objective of this chapter was to compare their sporulation rates and select one strain to take forwards.

3.3.2 Comparison of sporulation efficiency of 4 strains of NTCD

Initially, it was essential to confirm that these strains are capable of forming spores which can then be easily purified in a quick and efficient manner (for practical mass production). To this end, a sporulation assay was conducted comparing the levels of sporulation between strains. Cultures were grown anaerobically in BHIS broth at 37℃ over 5 days. An aliquot of culture was taken each day and examined microscopically to compare the proportion of spores in the culture and therefore assess efficiency of sporulation **(Figure 3.1)**.



Strain	Average spores/ ml
M3	4.3×10^8
M23	3.8×10^8
T7	5×10^8

Figure 3.1: Sporulation of NTCD strains over the course of 5 days. All strains sporulated well however by day 5, the T7 culture appeared to be mostly spores, whereas vegetative cells were still found in the M3 and M23 cultures. Enumeration of spores after purification confirmed T7 to have returned the highest yield.

This assay confirmed that, although each of the strains sporulate well, by day 5, the T7 culture was predominantly spores, whereas vegetative cells were more commonly found in M3 and M23 cultures. T7 was also the most efficient to purify using the technique described in **Section 2.1.2** returning 5×10^8 spores per ml on average compared to 4.3×10^8 and 3.8×10^8 spores per ml for M3 and M23 respectively after purification.

3.3.3 TEM of spores

It has been observed that some strains of *C. difficile* possess hair-like projections on their spore coat which reduce the germination rate (Phetcharaburanin *et al.*, 2014; Pizarro-Guajardo *et al.*, 2016). When selecting a chassis strain, it was preferable to choose one that lacks these hair-like projections and ensure the spores germinate effectively into vegetative cells in the ileum for antigen to be expressed, lipidated and released prior to the organism being cleared by the host.

In order to determine the presence of hair-like projections on the surface of spores, TEM was performed on isolated and purified spore preparations from each of the 3 NTCD strains ((**Section 2.1.3**); **Figure 3.2**).

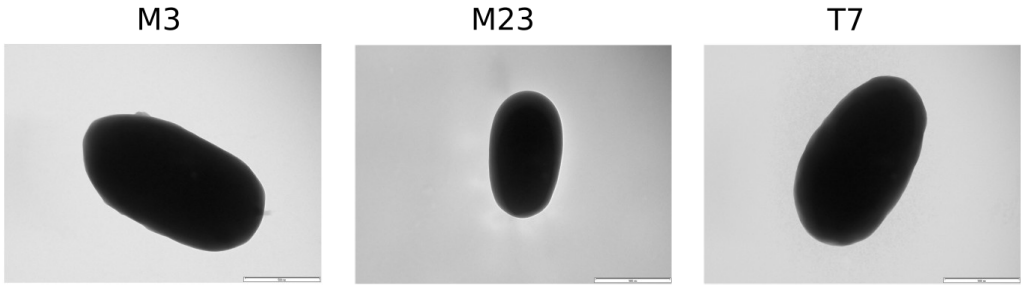


Figure 3.2: TEM of spores isolated from NTCD strains M3, M23, and T7. Each spore coat appears smooth with no hair-like projections detected as observed previously for spores of other *C. difficile* species (Paredes-Sabja *et al*., 2014; Malyshev & Baillie 2020).

The lack of detection of hair-like projections on the spores of all three strains would make them equally suitable to take forwards. This result, taken with the previous sporulation data, suggested T7 would be the most suitable strain due to its sporulation efficiency and the ease with which spores were isolated compared to the other two strains.

3.3.4 Analysis of the genome sequence of chosen NTCD chassis strain, T7

The genes for *C. difficile* toxins A and B (*tcdA* and *tcdB* respectively) are part of a 19.6 kb pathogenicity locus (PaLoc) that also includes the genes *tcdD*, *tcdE*, and *tcdC*. In order to be classified as NTCD, a strain must not possess the PaLoc region and therefore will be incapable of producing toxins (**Figure 3.3**).

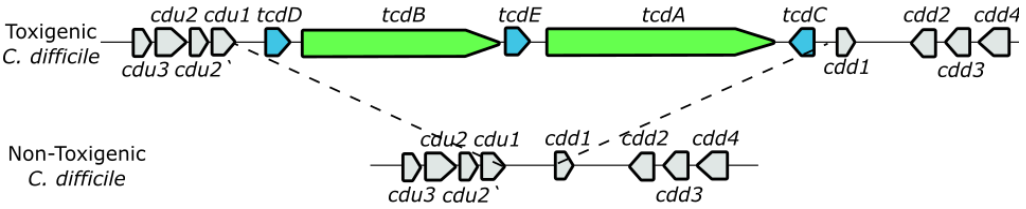


Figure 3.3: The pathogenicity locus in *Clostridioides difficile.* Clostridial toxins TcdA and TcdB are encoded by genes *tcdA* and *tcdB* respectively. These genes are found within the pathogenicity locus (PaLoc), a 19.6 kb genetic region which also contains genes *tcdC, tcdD,* and *tcdE*. The PaLoc is not present in non-toxigenic *C. difficile.* Instead, a 115 bp DNA fragment exists in its place.

Confirmation that T7 is non-toxigenic was obtained by isolating gDNA and performing Illumina sequencing to produce a shotgun genome. The sequences for *tcdA* and *tcdB* were found to be absent from T7, and instead of the PaLoc, a 115 bp region was present between the genes *cdu1* and *cdd1* (**Figure 3.3; Figure 3.4**).

```
CLUSTAL O(1.2.4) multiple sequence alignment

Query 1        Atttgttgtttaaaaagagttttgtaatagtttatctacaattataaaactctttttaaa 60
Sbjct 42630    atttgttgtttaaaaagagttttgtaatagtttatctacaattataaaactctttttaaa 42689
               ************************************************************

Query 61       tgtttaaatttaatttaaaataatttgatattagcagagtaaaaaataaatata 114
Sbjct 42690    tgtttaaatttaatttaaaataatttgatattagcagagtaaaaaataaatata 42744
               ******************************************************
```

Figure 3.4: Alignment of the T7 Shotgun sequence with 115 bp region present between *cdu1* and *cdd1.* This demonstrates the absence of the pathogenicity locus within the T7 genome.

Several non-toxin antigens encoded by TCD have been previously investigated and found to be immunogenic. Should these vaccine candidates also be present in T7, its use as a chassis strain is further justified; any immune response raised against these factors will provide a background level of protection against TCD. **Table 3.2** lists known and tested vaccine candidates; the gene sequence of the corresponding gene was taken from TCD strain CD630 and a BLAST search was performed for each against the T7 genome.

Table 3.2: Blastn results of vaccine candidates from CD630 against NTCD-T7.

Gene	Annotated function	Percentage match (%)	Associated references
fliC	Flagellin	100	(Bruxelle *et al.*, 2017)
fliD	Flagellar filament capping protein	100	(Péchiné *et al.*, 2018)
pilA	Type IV pilin	100	(Maldarelli *et al.,* 2014)
cwp84	Cell wall-binding cysteine protease	99	(Péchiné *et al.*, 2011)
groEL	60 kDa molecular chaperone	99	(Péchiné *et al.*, 2013)
CD0873	ABC transporter substrate-binding protein	99	(Kovacs-Simon et al., 2014, Bradshaw *et al.*, 2019, Karyal et al., 2021)
cdeC	Exosporium morphogenetic protein	99	(Pizarro-Guajardo *et al.*, 2018)
cdeM	Exosporium morphogenetic protein	99	(Rosales-Mendoza *et al.*, 2021)
bclA1	Putative exosporium glycoprotein	94	(Ghose *et al.*, 2016)
slpA	S-layer precursor protein	80	(Mori and Takahashi, 2018)
cwp66	Cell wall-binding repeat-containing protein	77	(Péchiné, Janoir and Collignon, 2005)

Flagella encoded by genes such as *fliC,* and the cap protein encoded by *fliD,* are globular proteins which exist on the surface of certain bacterial cells and are typically involved in cell adhesion and motility (Péchiné *et al.*, 2013). The genes which govern the assembly of flagella are variant between *C. difficile* species (Janoir, 2016), making them an unsuitable vaccine candidate in

their own right but nonetheless, they are immunogenic (Ghose *et al.,* 2016) and could potentially be included in a multivalent vaccine.

Pili are surface projections typically involved in colonisation (Janoir, 2016). Pili may also be involved in the conjugal transfer of DNA between bacteria (Janoir, 2016). Though conserved between strains of *C. difficile*, their C-termini are often variable between strains (Maldarelli *et al*., 2014), making PilA an unsuitable choice for our vaccine candidate.

GroEL is a heat shock protein which is released by the cell after heat shock and has been proven to be capable of binding to epithelial cells (Hennequin *et al*., 2001). Though it has been proven to be immunogenic, its shared homology with other bacterial species in the normal microbiota (Péchiné *et al.*, 2013) preclude it from being a suitable vaccine candidate in this instance.

SlpA is an S-layer precursor protein which produces high molecular weight and low-molecular weight SLPs after cleavage by Cwp84 (de la Riva *et al.*, 2011). These proteins have also been shown to be capable of adhering to epithelial cells (Calabi *et al.*, 2002). However, their variability between strains means SlpA is not suitable for use as a vaccine candidate which should be active against all strains of *C. difficile.*

Cwp84 is a cysteine protease of *C. difficile*, found to be associated with the SLPs, putatively playing a role in their maturation (de la Riva *et al.*, 2011). It has been found to be highly immunogenic (Pechine *et al*., 2005). Production of Cwp84 is vital for the colonisation phase of *C. difficile* pathology. However, it is unsuitable for our purposes as Cwp84 is not a lipoprotein. Similarly, Cwp66, a protein which plays a part in adhesion to host cells, plays an important role in *C. difficile* colonisation. However, its high variability between strains makes it unsuitable for use as a vaccine candidate (Dingle *et al.,* 2013).

CdeC, CdeM are two cysteine-rich proteins found in abundance in the exosporium of *C. difficile* spores (Ghose *et al.,* 2016) with *cdeM* being the

most highly upregulated gene during sporulation (Janoir *et al.,* 2013). Collagen-like protein BclA1 is also found on the exosporium. In *Bacillus anthracis* and *Bacillus cereus*, BclA1 forms hair-like projections on the surface of spores (Pizarro-Guajardo *et al,* 2014). It is unusual then that *bclA1* is found to be present in the T7 genome, as TEM has shown that no hair-like projections exist on the surface of its spores (**Figure 3.2).** Though abundant, these proteins are only found on the surface of spores and, therefore, would be unsuitable for vaccines as antibodies generated against them would not target vegetative cells.

CD0873 is a lipoprotein which functions as an adhesin involved in colonisation (Kovacs-Simon et al., 2014, Bradshaw *et al.,* 2019). It was previously shown to be seroreactive in patients with CDI and when given intraperitoneally to mice stimulated a strong immune response. Serum antibodies were shown to block adhesion to Caco-2 cells by *C. difficile* strain 630 cells (Bradshaw et al., 2019). Further work in hamsters by Karyal *et al.,(* 2021) demonstrated that oral immunisation with CD0873 resulted in antibodies in the small intestine and in the bloodstream that blocked adhesion by TCD cells to Caco-2 cells. CD0873 was further shown to elicit partial protection from CDI in hamsters upon challenged with spores of a hypervirulent strain (Karyal et al., 2021).

3.4 Identification of the most abundant extracellular lipoprotein

In order to be more readily taken up by M cells, it is desirable that the antigens engineered in the vaccine chassis strain are secreted into the extracellular milieu. To that end, it was hypothesised that fusing antigen candidates to the signal peptide of a clostridial lipoprotein (which is observed to be secreted) should provide the desired effect. Additionally the lipid moiety should enhance the immunogenicity of the protein antigen to which the SP is fused. To assess the lipoproteins secreted naturally by T7, supernatants were analysed by mass spectrometry.

3.4.1 LC-MS to determine the most abundant extracellular lipoprotein

The supernatant of three mid-log-phase cultures and three early stationary phase cultures were harvested (**Section 2.3.1**), analysed by LC-MS (**Section 2.3.2**) and the proteins identified ranked according to their abundance. The sequence of each identified peptide when then obtained from NCBI and a Blast search performed against the translated shotgun sequence of T7 (**Section 2.2.1**). These sequences were then matched with the corresponding annotated orthologue strain of CD630. The LipoP programme was then used to predict which of these proteins are lipoproteins with a Signal peptidase II (SPII)-recognisable signal peptide. The most abundant lipoprotein identified in the supernatant of mid log-phase cultures is *appA,* ranked as the 6th most abundant protein, and the second most abundant was CD0873 which ranked 13th out of 352 total protein hits (**Table 3.3**).

Table 3.3: Most abundant proteins identified in the supernatant of mid-log-phase cultures of T7 (with annotated homologue from strain 630 shown). Only the top 13 protein hits are shown here, ending at lipoprotein CD0873.

630 Gene	Description	Peptide count	Lipoprotein
slpA	S-layer protein SlpA	64	No
pfo	Pyruvate:ferredoxin (flavodoxin) oxidoreductase	60	No
thlA1	Acetyl-CoA acetyltransferase	49	No
cwp20	Cell wall-binding protein Cwp20	47	No
gluD	NAD-specific glutamate dehydrogenase	44	No
appA	ABC transporter substrate-binding protein	36	Yes
eno	Enolase	36	No
CD36640	PLP-dependent aminotransferase family protein	34	No
cwp2	Cell wall-binding protein Cwp2	34	No
groL	Molecular chaperone GroEL	34	No
cwp84	Cell wall-binding cysteine protease Cwp84	30	No
prdA	D-proline reductase (dithiol) proprotein PrdA	30	No
CD0873	ABC transporter substrate-binding protein	29	Yes

For stationary phase cultures CD0873 was identified as the most abundant lipoprotein ranking 9th in abundance out of the 269 proteins identified from stationary phase cultures (**Table 3.4**).

Table 3.4: Most abundant proteins identified in the supernatant of stationary-phase cultures of T7 (with annotated homologue from strain 630 shown). Only the top 9 protein hits are shown here, ending at lipoprotein CD0873.

630 Gene	Description	Peptide count	Lipoprotein
slpA	S-layer protein SlpA	55	No
thlA1	Acetyl-CoA acetyltransferase	41	No
adhE1	Bifunctional acetaldehyde-CoA/alcohol dehydrogenase	41	No
gapA	Type I glyceraldehyde-3-phosphate dehydrogenase	28	No
prdA	D-proline reductase (dithiol) proprotein PrdA	28	No
gluD	NAD-specific glutamate dehydrogenase	26	No
fusA	Elongation factor G	26	No
groL	Molecular chaperone GroEL	25	No
CD0873	ABC transporter substrate-binding protein	24	Yes

Vaccine antigens , GroEL, SlpA, Cwp84 and CD0873 were all detected by LC-MS in the supernatant of T7 suggesting that these antigens are readily released from the cells of T7 holding promise for their likelihood to be taken up by M cells in vivo and induce some residual protection against TCD.

Importantly, the experimentally confirmed lipoprotein and CD0873 was found in abundance in the supernatant of T7 in both mid-log phase early stationary phase cultures. Furthermore, this lipoprotein is known to be immunogenic and confer partial protection from CDI (Kovacs-Simon et al., 2014, Bradshaw et al., 2019, Karyal et al., 2021). For the above reasons, the SP of CD0873 was chosen for fusion to the antigens.

3.4.2 Determining the signal peptide region of CD0873

In order to lipidate (and release) antigens into the extracellular milieu, fusion to the lipoprotein signal peptide is required. To that end, identification of the signal peptide itself was needed. Additionally, the region immediately downstream of the SP, known as the anchor peptide (AP) which is a disordered tether-like structure facilitates protrusion of the protein across the cell wall, facilitating surface exposure (Zückert, 2014; Fantappie *et al*., 2017) and has been shown to be important in the expression of fusion proteins (Chen et al., 2009). Thus identification of the putative AP of CD0873 was also required for designing appropriate fusion constructs.

To this end, the protein sequence of CD0873 was analysed by Phyre which predicts the structure of proteins. A disordered region was predicted by the PredictProtein programme as existing between residue 28 and 42 (**Figure 3.5**).

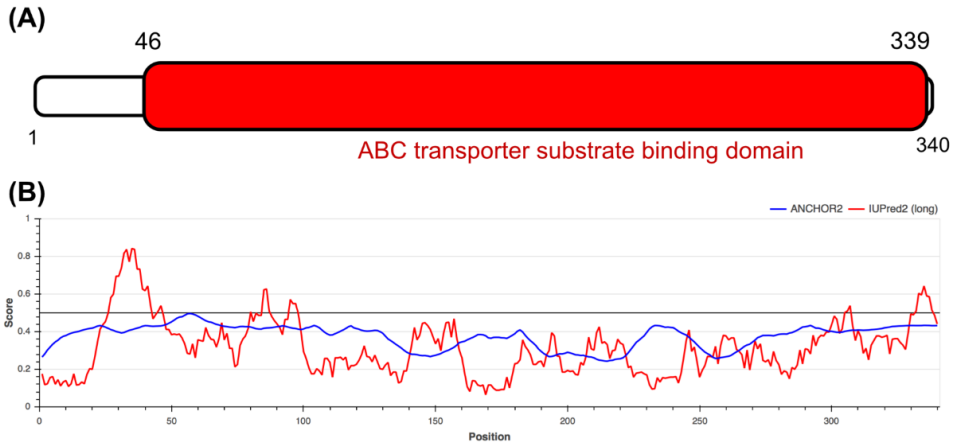


Figure 3.5: Structural disorder within CD0873. (A) Domain analysis of CD0873 sequence performed using Pfam (domains not to scale). The first 45 amino acids are not annotated as a bona fide domain. (B) IUPRED2A plot mapping regions of disorder (red) and disordered binding regions (blue). A peak can be seen between ~1-50 amino acids, suggesting disorder at this location. Made using IUPred2A (Mészáros *et al*., 2018).

Additionally by comparing CD0873 with another putative lipoprotein, CD0876 that is not known to be surface exposed but shares 70% amino acid identity with CD0873, it was speculated that differences may lie in the AP region further enabling identification of the AP in CD0873.in the literature to support CD0876 being surface exposed.

Both proteins possess an N-terminal signal peptide (SP) terminating in a lipobox, characteristic of lipoprotein SPs which are cleaved by SPII (Brülle, Tschumi and Sander, 2013; Zückert, 2014; Buddelmeijer, 2015) (**Figure 3.6**). Homology between CD0876 and CD0873 sharply decreases in the region immediately downstream of the lipobox from L21 to K46, rendering this particular region the most divergent between the two proteins. This agrees with the disordered region identified by PredictProtein and has therefore been deemed the putative anchor peptide.

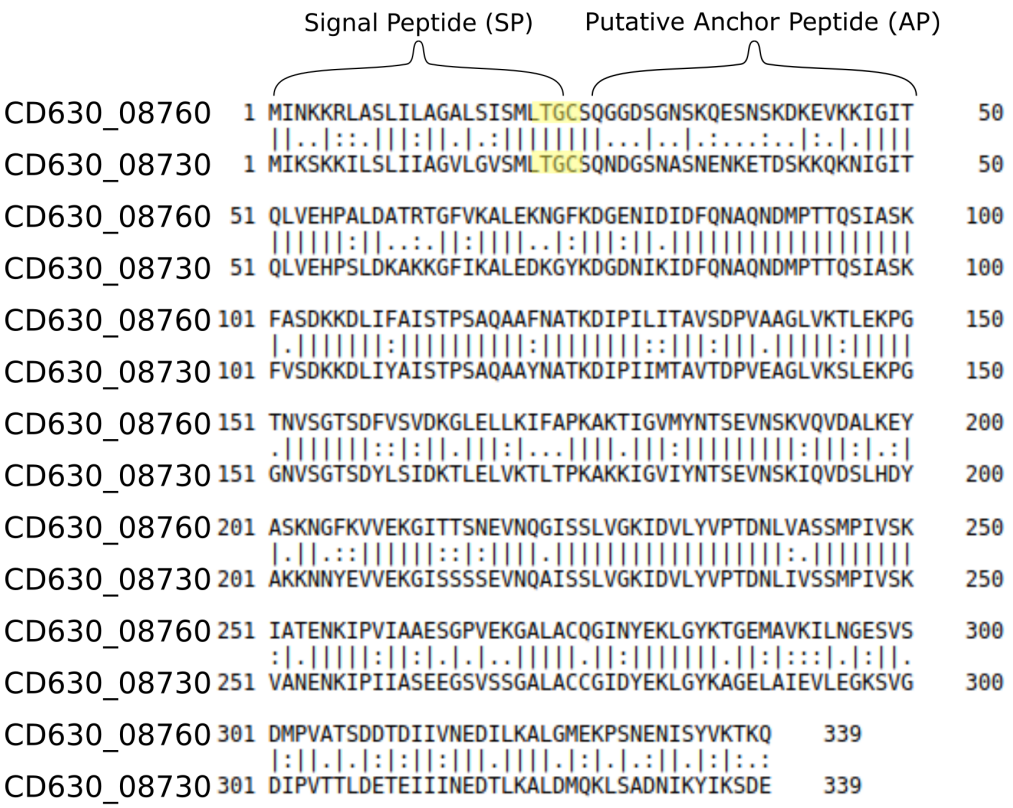


Figure 3.6: Alignment of CD0876 with CD0873. Sequence homology of the two genes lowers sharply after the lipobox region (highlighted in yellow). This region has been designated as the putative anchor peptide.

Based on this information, it was decided to fuse the region including the signal and putative anchor peptide of CD0873 to recombinant antigens to lipidate the attached antigen and facilitate expression as shown previously to be important for expression in a study by Chen et al., (2009) who fused the SP and AP of meningococcal Ag473 to a domain of the Dengue virus. Additionally, another version of the fusion protein would be designed that only included the SP in case the AP was not required for expression.

3.5 Selection of Toxin candidates

The clostridial toxins TcdA and TcdB have attracted strong interest as vaccine candidates (Huang, 2015; Huang, Shen, *et al*., 2015; Huang, Wu, *et al*., 2015; Bézay *et al*., 2016; Pfizer Inc., 2017). Engineering full-length toxins would not be appropriate given their toxicity. Toxoids or toxin fragments have been shown to induce toxin neutralising antibody responses. Previous work by

Huang *et al.* (2015) investigated the immunogenic properties of fragments of the receptor binding domain (RBD) of the toxins. These studies divided the RBD of TcdA and TcdB into three fragments (named F1, F2, and F3) designed to incorporate a number of repeat regions, identified by Huang as lectin-binding receptor-sites (**Figure 3.7**), and compared the immunogenic properties of each when used to immunise mice by intramuscular injection. A subsequent study (Huang, 2015) repeated the methodology, but for TcdB, producing a consensus sequence based on analysis of the RBDs repeat regions.

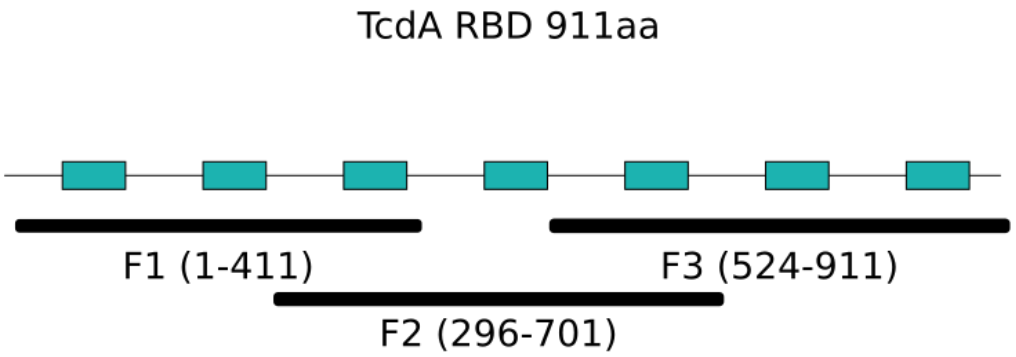


Figure 3.7: Fragments of the TcdA receptor binding domain as designed by Huang *et al.*, 2015. Each fragment was designed to incorporate a number of lectin-like receptor-binding sites (shown here in blue).

These studies found that the F3 region of TcdA was the most immunogenic and conferred protection against TCD cell binding and against cytotoxic activity. Another study performed by Liu *et al*. (2017) tested the equivalent domain of TcdB (residues 1852-2363). The study used recombinant TcdB encapsulated within nanoparticles composed of γ-PGA and chitosan. Mice were immunised three times intraperitoneally, and a high yield of anti-TcdB antibodies was produced as a result. The immunisation also afforded protection against challenge by *C. difficile* strain R20291 spores. It is for these reasons that the C-terminal regions of both TcdA and TcdB RBDs were selected as the basis for our toxin-based vaccine candidates in this study.

3.6 Discussion

The aims of this chapter were to: identify a suitable NTCD vaccine chassis strain for use in this project, investigate a suitable lipoprotein which will be used to lipidate the chosen antigen and facilitate its secretion into the extracellular milieu, and select a promising vaccine antigen to test the platform.

After an investigation of the literature into various NTCD strains, M3, M23 and T7 were selected to determine which would be the most suitable chassis strain. All three strains have previously been confirmed to confer colonisation resistance against TCD in mice and hamsters (Sambol *et al,* 2002; Nagaro *et al.,* 2013; Gerding *et al.,* 2015). None of these strains possess hair-like protrusions on their endospore, which can potentially delay germination (Phetcharaburanin *et al.*, 2014; Pizarro-Guajardo *et al.*, 2016), and all of these strains sporulate efficiently. Strain T7 however proved to be the most efficient sporulator, and its spores were easier to purify than for the other two strains. Further investigation by sequencing and bioinformatics confirmed strain T7 lacks the PaLoc and therefore cannot produce the two toxins. Furthermore, T7 was found to possess several antigens in common with TCD strains which may confer some residual protection against CDI.

LC-MS analysis of the extracellular proteome was performed to investigate which lipoprotein is most abundant and could be exploited for lipidating and secreting the chosen antigen. It was discovered that CD0873 was found to be the second most abundant lipoprotein in mid-log, and most abundant lipoprotein in stationary phase, and was therefore chosen. CD0873 has previously been shown itself to be a very promising vaccine (Bradshaw et al., 2019, Karyal et al., 2021). Interestingly, several other vaccine candidates that had been found to be encoded in the genome of T7 were detected in the supernatant including Cwp84, GroEL, and SlpA and all four antigens may provide a residual level of protection against CDI. The secretion or release of these antigens by T7 and potentially by the other two NTCD strains tested

previously may partly account for their protection observed by these strains against TCD (Senoh *et al.,* 2018).

As previously mentioned, Wright *et al*. (2008) first demonstrated the potential of CD0873 as a vaccine candidate when they found it was sero-reactive in CDI patients. Kovacs-Simon characterised the protein and found that it was a surface-exposed lipoprotein (Kovacs-Simon *et al*., 2014). Bradshaw *et al*. (2019) performed intra-peritoneal immunisations in mice with CD0873 and found it to be highly immunogenic with vaccine-induced antibodies inhibiting colonisation. Finally work in the Griffin lab demonstrated that CD0873 given orally to hamsters was partially protective against CDI (Karyal *et al*., 2021). Thus using the episomal expression system in NTCD strain T7 described in chapter 4, it was decided to over-express this lipoprotein on its own in T7 as part of a panel of recombinant strains to test *in vivo*.

Selection of the toxin fragment vaccine candidates was based on work performed by Huang *et al.,* (2015) and Liu *et al*., (2017). The rationale here is the inclusion of repeat regions which are hypothesised to act as PAMPs, which alert the immune system via their interaction with TLR2. While these regions have been proven to be immunogenic and confer protection against CDI, further genetic engineering to produce vaccine candidates which are lipidated and released from the cell will further enhance their efficacy (Leng *et al.,* 2015*).*

3.7 Conclusion

By using spores of NTCD strain T7 as a chassis for our vaccine, we are ensuring the vaccine candidates can be delivered to the GALT target site. The use of a vaccine vehicle that is the same species as the target organism will provoke generation of antibodies against factors in common to both organisms in addition to the vaccine candidates we shall introduce.

Utilising the signal peptide of CD0873 exploits native cellular machinery which will potentially allow our vaccine candidates to be lipidated and released from the cell in order to more efficiently provoke an immune response *in vivo*.

Vaccine candidates CD0873 and RBD fragments of both TcdA and TcdB will serve to form antibodies against both the toxins themselves and factors on the cell surface, allowing more effective targeting and clearance of pathogens by the host.

Chapter 4. Creation of episomal shuttle vectors for lipidation and release of recombinant antigens in non-toxigenic *C. difficile*

4.1 Introduction

It has previously been shown that heterologous *C. difficile* antigens can be expressed in NTCD vegetative cells and generate protective immune responses (Wang *et al.*, 2018). It was hypothesised that plasmids encoding recombinant antigens fused to the signal and anchor peptide region of a native lipoprotein found to be abundant in the supernatant of our chosen NTCD strain, T7 (**Chapter 3**) would allow the expression and release from the cell of lipidated recombinant antigens. The goal is for these antigens with enhanced immunogenicity afforded by the lipid moiety (Nguyen *et al*., 2017; Nguyen & Götz, 2016) to be readily taken up by M cells in the ileum for induction of sIgA and serum IgG responses. Even if the recombinant lipidated antigens are not secreted per se, it is anticipated there will be a degree of sloughing off of surface factors in the small intestine, including these antigens. This chapter describes the creation of expression vectors designed to produce lipidated antigen candidates for expression and release by vegetative cells of NTCD strain T7.

4.2 Aims

- Amplify CD0873 signal peptide and the terminal portion of the receptor binding domains (RBD) of TcdB and TcdA;
- Ligate these fragments into a suitable vector;
- Transform expression vectors into NTCD strain T7.

4.3 Results

It was first necessary to make a panel of constructs to test whether the SP alone would facilitate lipidation and extracellular release of the fused domain of TcdB, or whether the region incorporating both the SP and AP were required for expression as previously reported for the fusion of a meningococcal lipoprotein SP to a domain of Dengue viral protein E3 (Chen et al., 2009). As a negative control, the TcdB domain alone was cloned into the same vector without fusion to the SP or SPAP.

4.3.1 Episomal shuttle *C. difficile* vector pMTL84123

The shuttle vector pMTL84123 was selected derived from the pMTL8000 series of modular shuttle plasmids (Heap *et al.*, 2009; Minton *et al.*, 2016), previously constructed by Sarah Chapman (Chapman, 2020) (**Figure 4.1**). This plasmid contains the pCD6 origin of replication from *C. difficile, E. coli* genes *repA*, *orfB*, *p15a* and *traJ* gene which is necessary for plasmid transfer. A *catP* resistance cassette provides chloramphenicol resistance in *E. coli* and thiamphenicol resistance in *C. difficile* for downstream selection in NTCD strain T7. To allow constitutive strong expression of genes, a ferredoxin promoter (*p.fdx*) is included immediately upstream of a multiple cloning site.

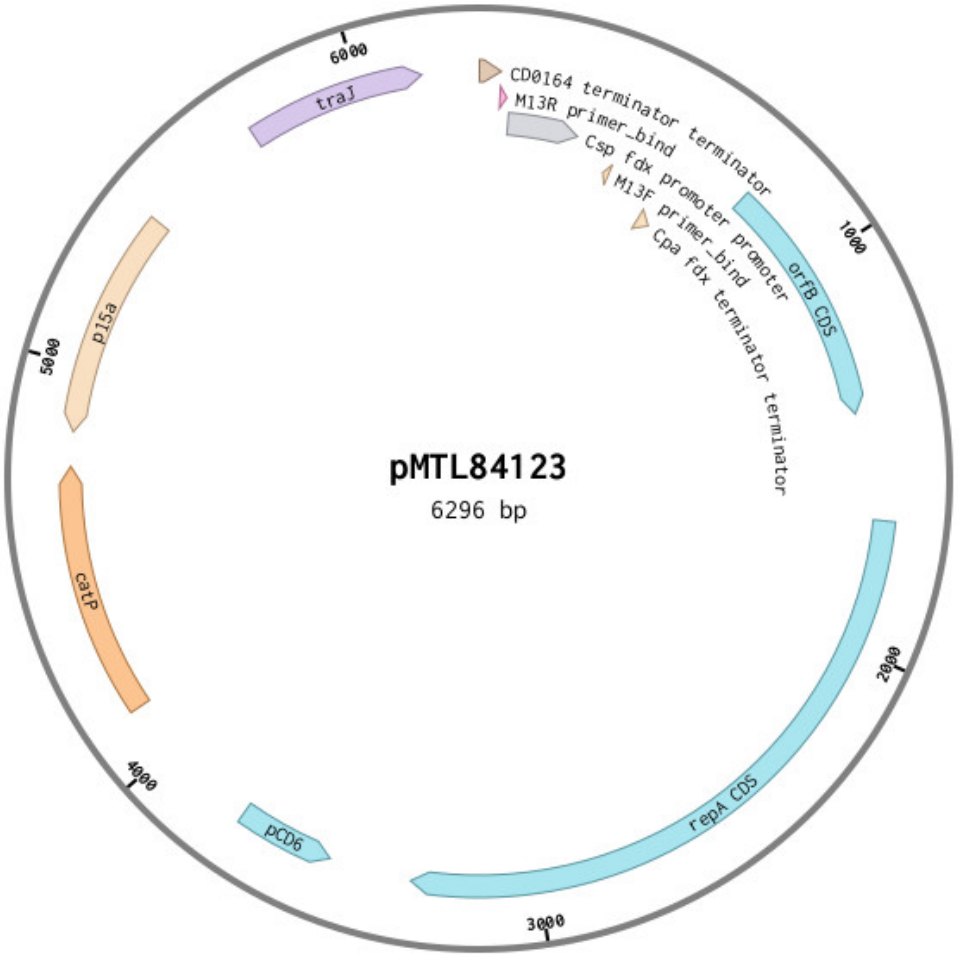


Figure 4.1: Shuttle vector pMTL84123. Plasmid pMTL84123 encodes the pCD6 origin of replication from *C. difficile, E. coli* genes *repA, orfB* and *p15a*, plus the *traJ* gene which is necessary for plasmid transfer A *catP* resistance cassette provides chloramphenicol resistance in *E. coli* and thiamphenicol resistance in *C. difficile* for downstream selection. To allow constitutive strong expression of genes, a ferredoxin promoter (*p.fdx*) is included adjacent to a multiple cloning site. Constructed by Sarah Chapman (Chapman, 2020).

4.3.2 Shuttle vector pMTL84123 engineered to harbour the SP and SPAP of CD0873 to create pMTL84123::08730_Signal and pMTL84123::08730_Signal+Anchor

Primers *08730_signal_FWD* incorporating a *SacI* site and *08730_Signal_REV* incorporating an *Xba*I site were used to amplify a 162 bp fragment including the CD0873 SP from genomic DNA (gDNA) of *C. difficile* strain T7 and its putative promoter, predicted by CNNPromoter_b (Umarov, & Solovyev, 2017) . Primers *08730_signal_FWD* incorporating a *Sac*I site and *08730_Signal+Anchor_REV* incorporating an *Xba*I site were used to amplify

the 250 bp region including the CD0873 SP and putative AP from gDNA of *C. difficile* strain T7 as well as native promoter (**Figure 4.2**). Despite the plasmid harbouring the constitutive strong Fdx promoter to drive expression of genes cloned downstream of this, the native promoter was included in the constructs as previous work in the Griffin lab discovered that the inclusion of the native promoter in addition to the plasmid promoter is sometimes required for efficient expression (da Silva *et al*., 2019). The PCR products were digested with *SacI* and *XbaI* and inserted into the *Sac*I-*Xba*I sites of pMTL84123 to create intermediate plasmids pMTL84123::08730_Signal and pMTL84123::08730_Signal+Anchor respectively (**Figure 4.3**).



Figure 4.2: Schematic of the amplified regions of CD0873. The signal only region (top) and signal + anchor region (bottom) are shown. Primers *08730_signal_FWD*, *08730_signal_REV*, and *08730_anchor_REV* introduce *Sac*I and *Xba*I restriction sites as shown. The putative start codon is highlighted in red, and the cysteine residue of the lipobox in yellow.

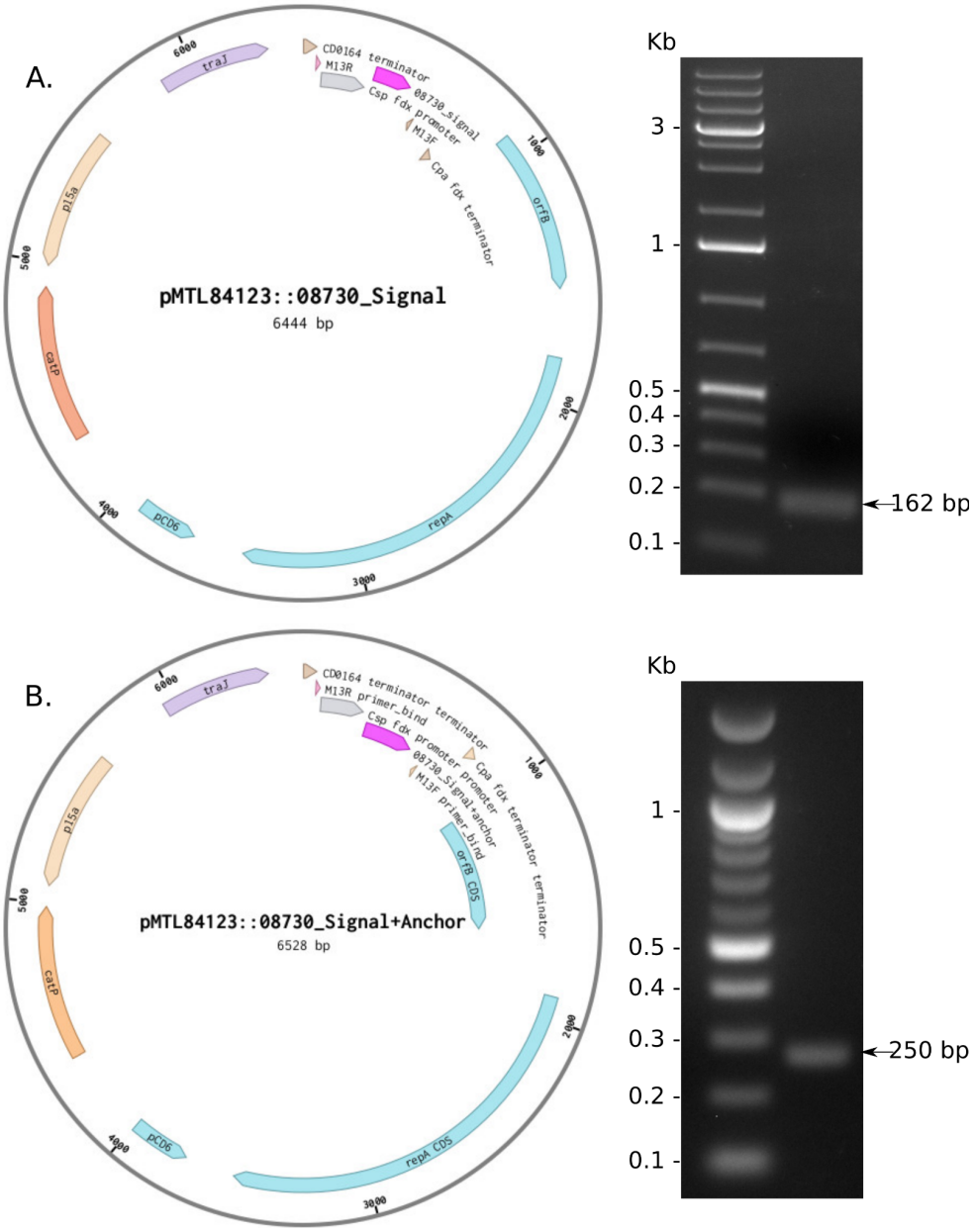


Figure 4.3: Insertion of signal and signal + anchor fragments into pMTL84123. (A) The 162 bp signal peptide PCR product was digested with *Sac*I and *Xba*I and cloned into corresponding sites within pMTL84123 to give plasmid pMTL84123::08730_Signal. (B) The 250 bp signal + anchor PCR product was cloned into the MCS in the same manner as above, giving rise to plasmid pMTL84123::08730_Signal+Anchor.

The successful integration of the SP and SP plus AP region was verified by colony PCR using primers *M13F* and *M13R,* which anneal 255 bp upstream and 71 bp downstream of the inserted fragments, yielding a final product of 496 bp for the SP insertion and 580 bp for signal + AP insertion

(Figure 4.4). Plasmids were further confirmed by first amplifying a fragment using *M13F_Nested* (which binds 95 bp downstream of the *Xho*I site) and *M13R_Nested* (which binds 319 bp upstream of the *Sac*I site) then *M13F* and *M13R* primers for sequencing the amplicon generated.

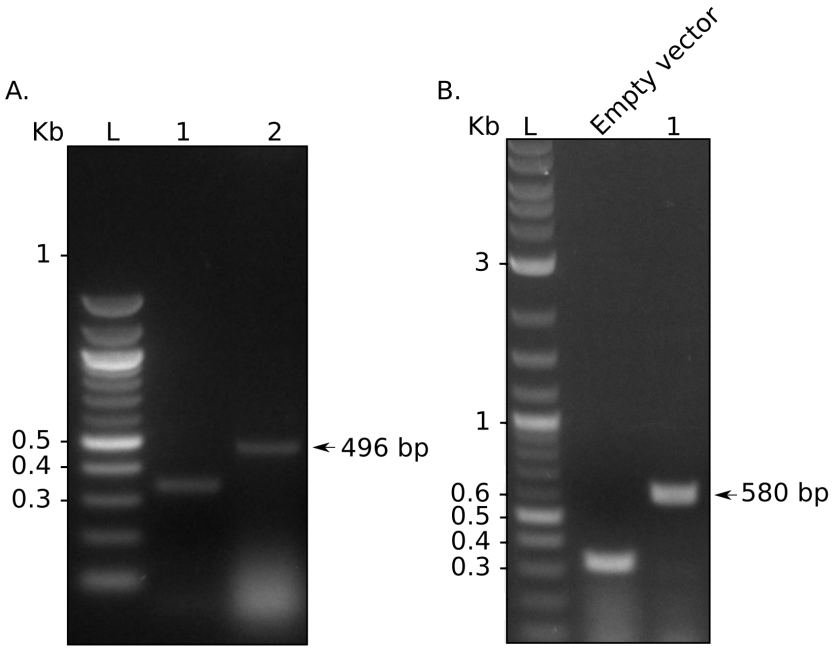


Figure 4.4: Colony PCR to confirm the successful ligation of SP and SPAP peptides into pMTL84123. (A) Colony PCR of SP insertion into vector pMTL84123. The correct band size of 496 bp is shown by the arrow. Each lane contains DNA from individual colonies and are shown against a 100 bp Plus DNA ladder (L) (NEB) (B) Colony PCR of SPAP insertion into vector MTL84123. The correct band size of 580 bp is shown by the arrow. Lane 1 contains DNA from an individual colony against a 1 kb+ Generuler (L) (ThermoFisher).

4.3.3 Shuttle vectors pMTL84123::08730_Signal and pMTL84123::08730_Signal+Anchor plasmids engineered to fuse with in-frame TcdB RBD

Primers *TcdB_FWD* and *TcdB_FWD+Start,* incorporating an *Xba*I site, and *TcdB_Rev,* incorporating a *Xho*I site, were used to amplify the 1543 bp (TcdB -ATG), and 1541 bp (TcdB +ATG) respectively from the C-terminus of TcdB, including the stop codon, from the gDNA of *C. difficile* strain CD630 **(Figures 4.5 & 4.6)**. A two bp difference exists rather than three to ensure the upstream sequence fused to the vaccine candidate remains in-frame. A start codon was also included as the first codon of TcdB in the TcdB-ATG fragment

even though the initiation codon of the SP would be exploited for translation of the fusion protein.

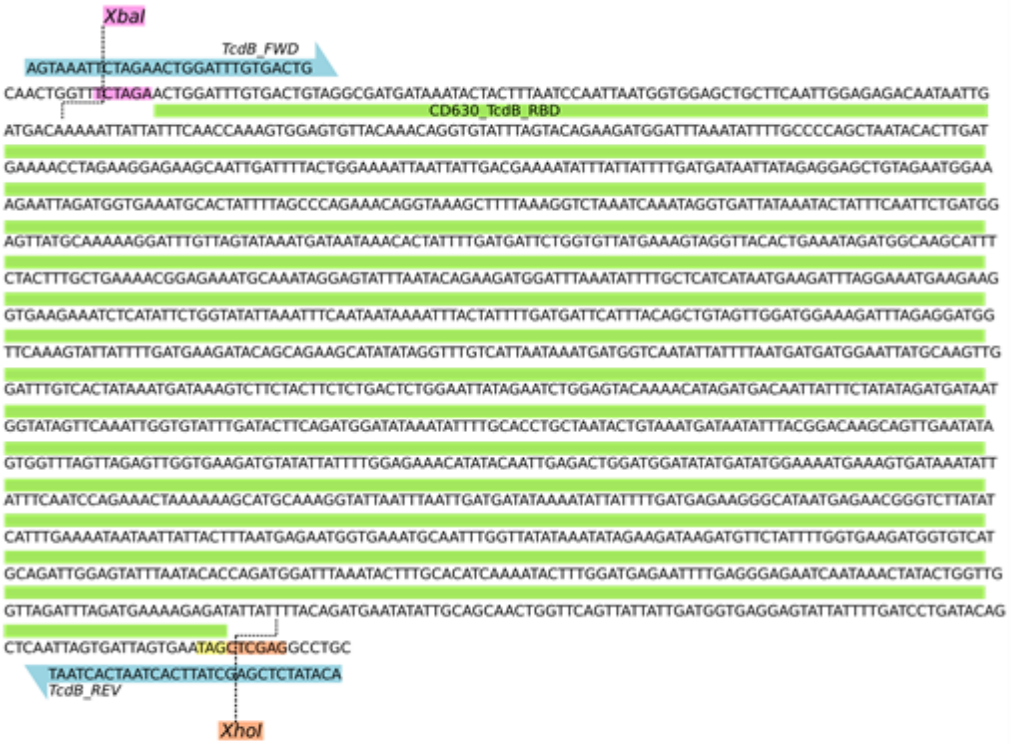


Figure 4.5: Amplified fragment of the TcdB receptor binding domain. Primers *TcdB_FWD* Forward) and *TcdB_Rev* (reverse) are shown in blue (*TcdB_FWD+Start* maps to the same position as *TcdB_FWD,* but includes an artificial ATG at the beginning of the sequence) . Restriction sites *Xba*I and *Xho*I are highlighted in pink and orange respectively. The stop codon is shown in yellow.

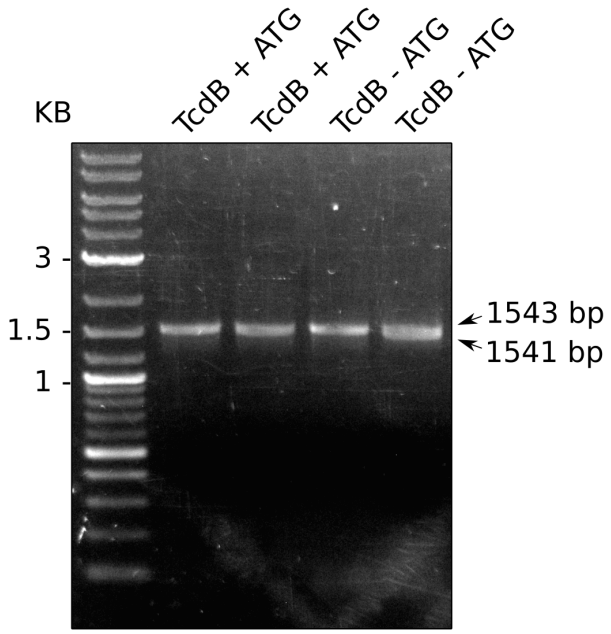


Figure 4.6: Agarose gel showing the amplified fragments of TcdB. The terminal 1541 bp of the TcdB receptor binding domain were amplified from the genomic DNA of *C. difficile* strain 630. Shown against a 1kb+ Generuler ladder (NEB). Correct sizes both without (1541 bp) and with (1543 bp) an artificially inserted start codon are shown by the arrow.

TcdB -ATG fragments were digested with *Xba*I and *Xho*I and inserted into plasmids pMTL84123::08730_Signal and pMTL84123::08730_ Signal+Anchor at corresponding restriction sites. This gave rise to plasmids pMTL84123::08730_Signal::TcdB and pMTL84123::08730_ Signal+Anchor::TcdB respectively. TcdB +ATG was digested with *Xba*I and *Xho*I and inserted into pMTL874123 at corresponding sites. This gave rise to plasmid pMTL84123::TcdB+ATG. Successful insertion of the TcdB region into each of the previous plasmids was confirmed by a diagnostic digest using enzymes *Sac*I and *Xho*I (**Figures 4.7, 4.8, & 4.9**).

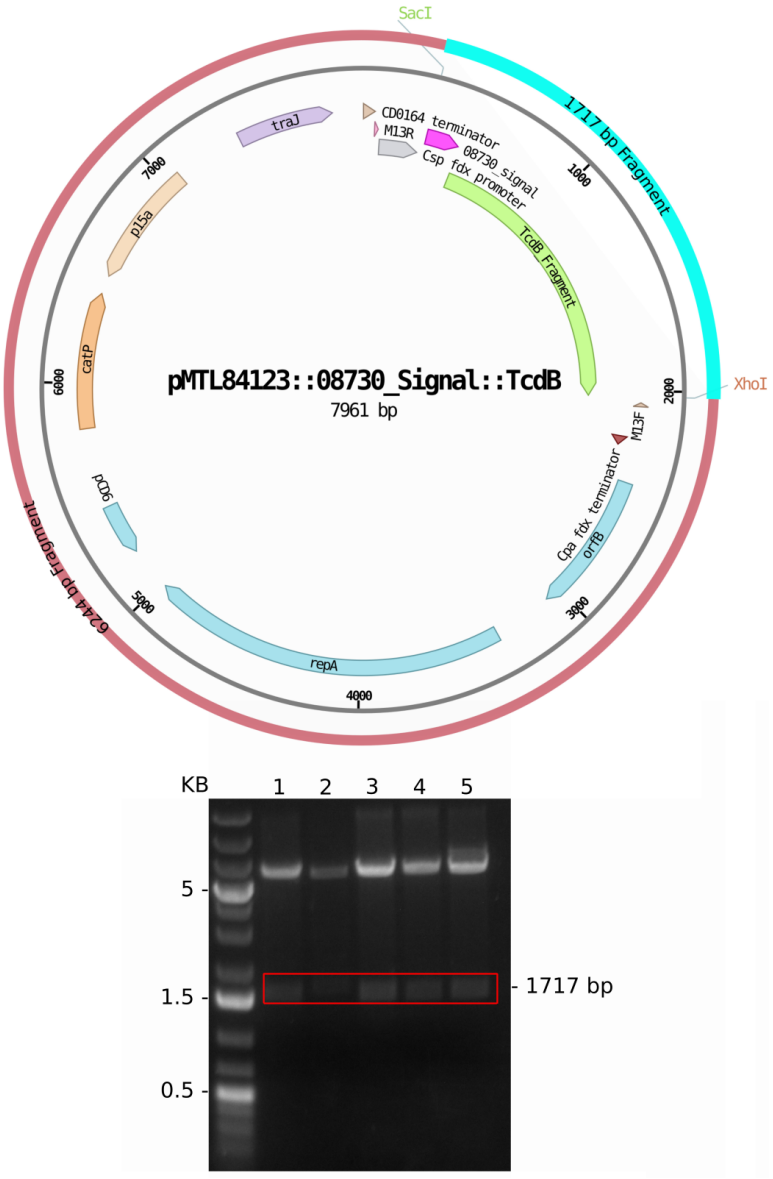


Figure 4.7: Map of pMTL84123::08730_Signal::TcdB and the results of a diagnostic digest to confirm correct integration of the TcdB-ATG fragment. The fragments obtained by diagnostic digest are shown in blue and red as well as the *Sac*I and *Xho*I restriction sites. Digest shows signal peptide + rTcdB with the correct fragment size of 1717 bp highlighted in red against 1kb + DNA ladder (NEB). Each lane contains digested DNA from individual clones.

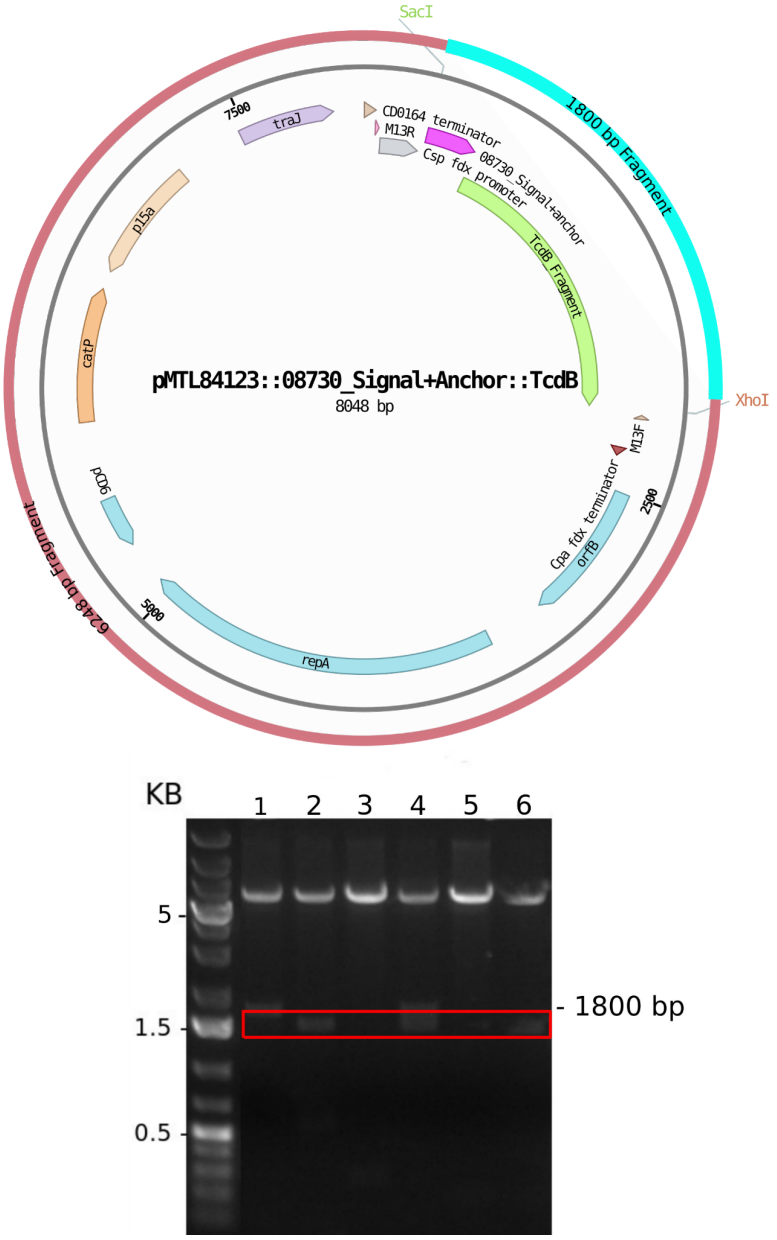


Figure 4.8: Map of pMTL84123::08730_Signal+Anchor::TcdB and the results of a diagnostic digest to confirm correct integration of the TcdB-ATG fragment. The fragments obtained by diagnostic digest are shown in blue and red as well as the *Sac*I and *Xho*I restriction sites. Digest shows Signal+Anchor peptide + rTcdB with the correct fragment size of 1800 bp highlighted in red against 1kb + DNA ladder (NEB). Each lane contains digested DNA from individual clones.

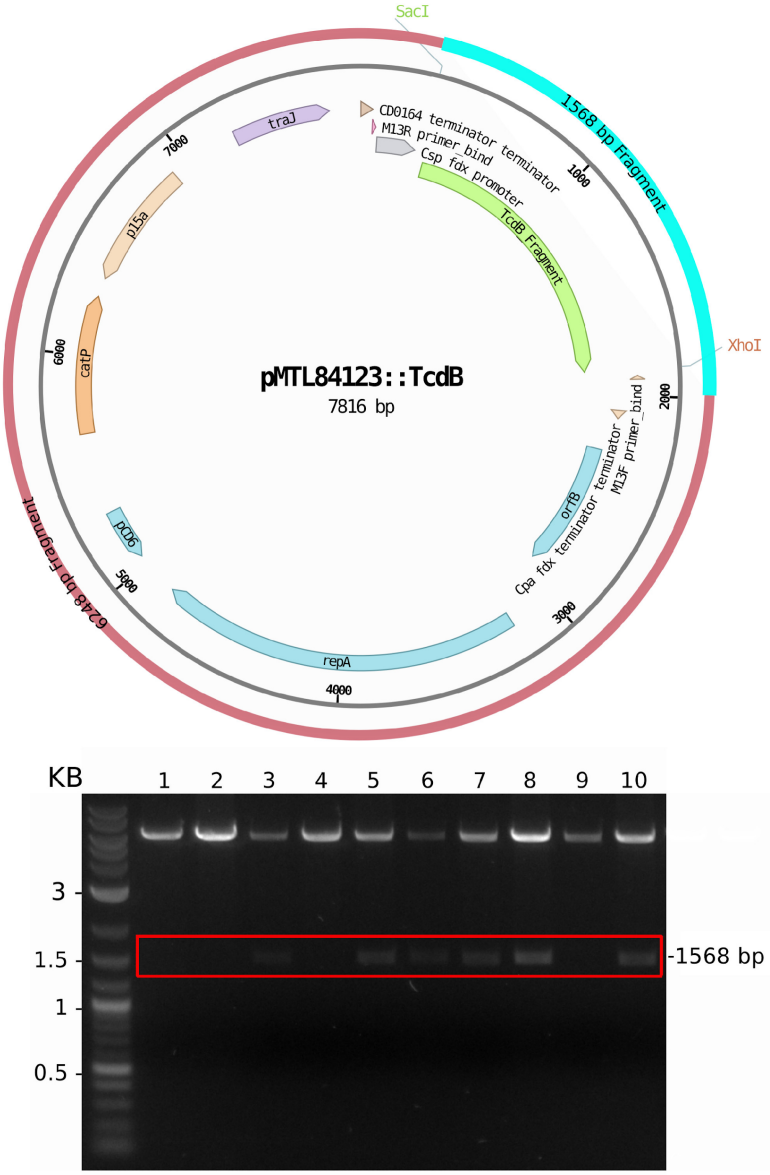


Figure 4.9: Map of pMTL84123::TcdB+ATG and the results of a diagnostic digest to confirm correct integration of the TcdB+ATG fragment. The fragments obtained by diagnostic digest are shown in blue and red as well as the *Sac*I and *Xho*I restriction sites. Digest shows TcdB with the correct fragment size of 1568 bp highlighted in red against 1kb Generuler (ThermoFisher). Each lane contains digested DNA from individual clones.

4.3.4 Shuttle vectors pMTL84123::08730_Signal and pMTL84123::08730_Signal+Anchor plasmids engineered to fuse with in-frame TcdA RBD

Primers *TcdA_FWD* incorporating an *Xba*I site, and *TcdA_Rev* incorporating an *Xho*I site were used to amplify the final 1192 bp from the

C-terminus of TcdA, including the stop codon, from gDNA of *C. difficile* strain CD630 **(Figure 4.10)**.



Figure 4.10: Amplified fragment of the TcdA receptor binding domain. Primers *TcdA_FWD* incorporating an *Xba*I site, and *TcdA_Rev* incorporating a *Xho*I site used in its construction are shown in blue. Restriction sites *Xba*I and *Xho*I are coloured pink and orange respectively. The stop codon is shown in yellow.

The PCR product was digested with *Xba*I and *Xho*I and inserted into plasmid pMTL84123::08730_ Signal+Anchor. This gave rise to plasmid MTL84123::08730_ Signal+Anchor::TcdA. Successful insertion of the rTcdA region into the plasmid was confirmed both by PCR, and by diagnostic digest using enzymes *SacI* and *XhoI* (**Figure 4.11**).

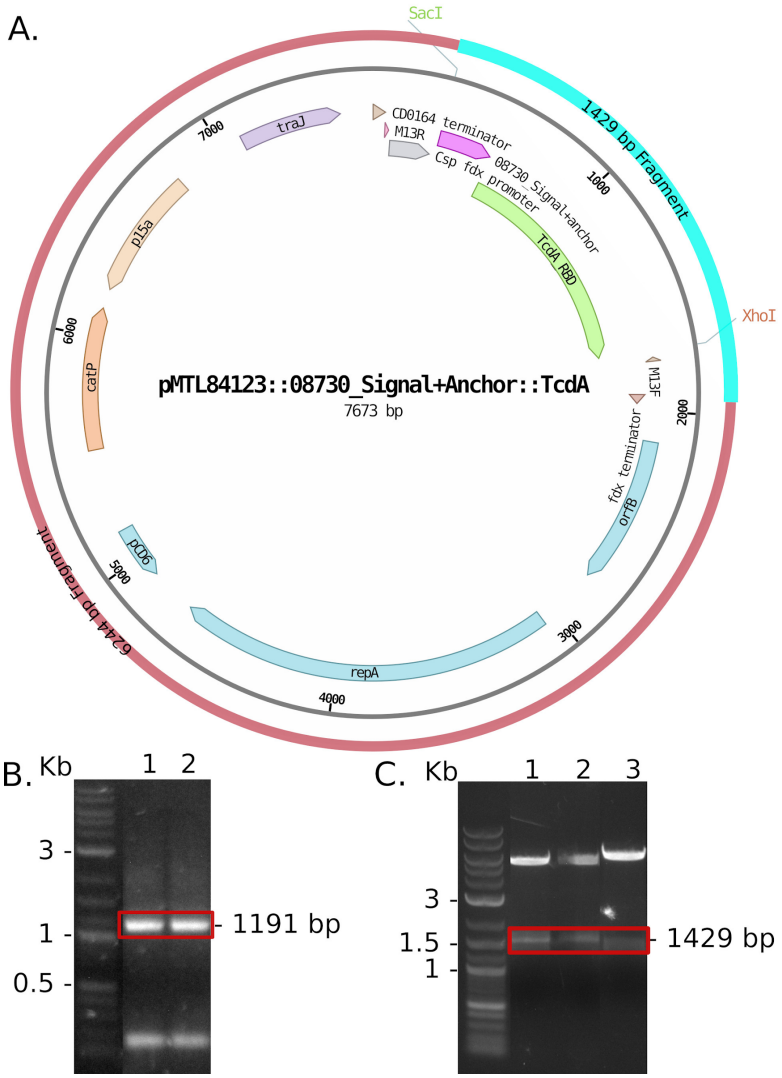


Figure 4.11: Map of pMTL84123::08730_Signal+Anchor::TcdA and the results of a diagnostic digest to confirm correct integration of the rTcdA fragment. (A) The fragments obtained by diagnostic digest are shown in blue and red, as well as the *Sac*I and *Xho*I restriction sites. (B) Colony PCR shows amplified rTcdA 1191 bp in length highlighted in red. (C) Digest shows rTcdA with the correct fragment size of 1429 bp highlighted in red against a 1kb+ Generuler (NEB). Each lane contains digested DNA from individual clones.

4.3.5 Shuttle vectors pMTL84123 engineered to express full length CD0873

Primers *08730_FL_Fwd* incorporating a *Sac*I site and *08730_FL_REV+XbaI* incorporating an *Xba*I site were used to amplify the full length 1108 bp open reading frame of CD0873 from gDNA of *C. difficile* strain T7 (**Figure 4.12**).



Figure 4.12: The amplified region of the full open reading frame of CD0873. Primers *08730_FL_FWD* incorporating an *Sac*I site, and *08730_FL_Rev_XbaI* incorporating an *Xba*I site used in its construction are shown in blue and restriction sites *Sac*I and *Xba*I in pink and orange respectively.

The PCR product was digested with *Sac*I and *Xba*I and inserted into the pMTL84123 vector at corresponding sites to create plasmid pMTL84123::08730_FL (**Figure 4.13**).

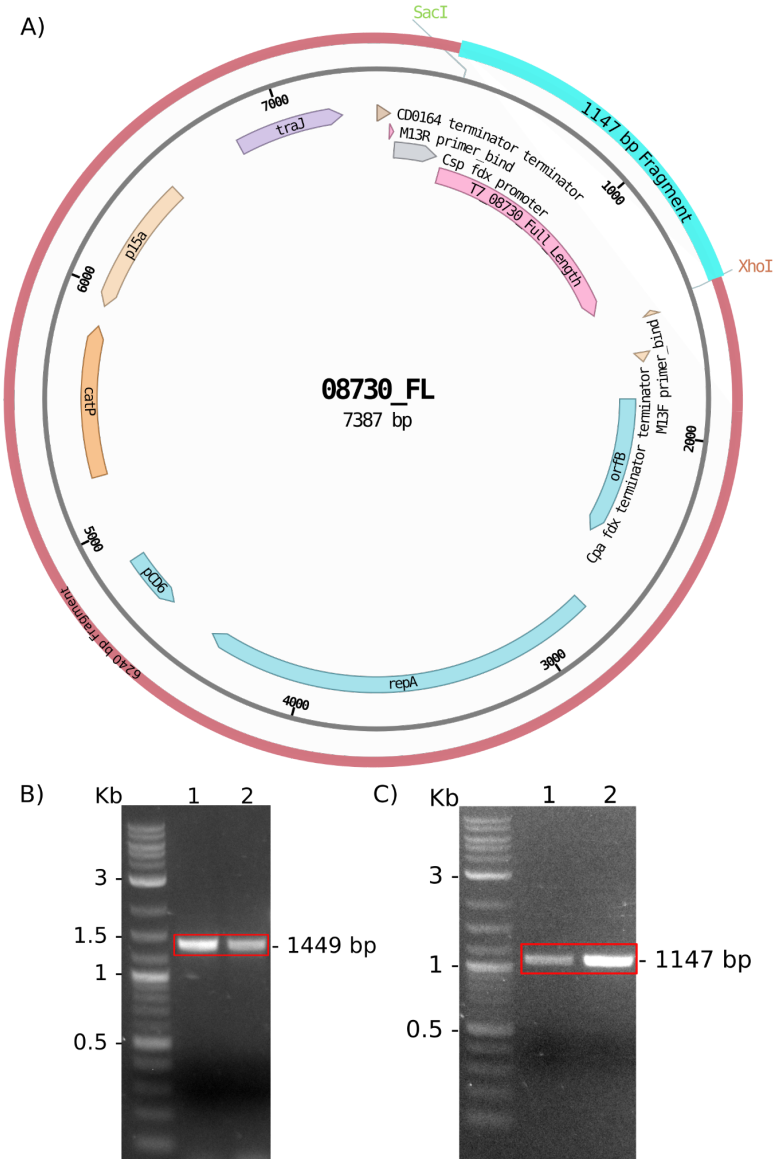


Figure 4.13: Map of pMTL84123_08730_FL and the results of a diagnostic digest to confirm integration of the full length CD0873 open reading frame.. (A) The fragments obtained by diagnostic digest are shown in blue and red as well as the *Sac*I and *Xho*I restriction sites. (B) Colony PCR shows amplified CD0873 1449 bp in length highlighted in red. (C) Digest shows rTcdA with the correct fragment size of 1147 bp highlighted in red against a 1kb+ Generuler (NEB). Each lane contains digested DNA from individual clones.

These plasmids were subsequently transformed into the sExpress strain of *E. coli* (Woods, *et al*., 2019) to facilitate conjugation into the non-toxigenic *C. difficile* strain T7.

To summarise, the construction of these plasmids aimed to facilitate expression of lipidated antigens that could be released into the extracellular space. Post-translational modification and extracellular release of recombinant TcdB is expected to ensue due to its fusion to the SP and its expression level facilitated due to inclusion of the AP component of CD0873. TcdB with neither SP nor SPAP component (TcdB) will likely accumulate in the cytosol due to its lack of lipoprotein processing signals.

4.3.6 Integration of episomal constructs into non-toxigenic *C. difficile* strain T7

Conjugation of plasmids pMTL84123, pMTL84123::TcdB, pMTL84123::08730_Signal, pMTL84123::08730_Signal+Anchor, and pMTL84123::08730_FL respectively into NTCD strain T7 gave rise to strains, T7-pMTL84123, T7-TcdB, T7-STcdB, T7-SATcdB, and T7-0873. These plasmids were maintained episomally by growing cells in the presence of thiamphenicol. It was not possible to successfully conjugate pMTL84123::08730_Signal+Anchor::TcdA and thus the project proceeded with only TcdB- and CD0873-based strains.

4.3.7 Confirmation of plasmid conjugation into non-toxigenic *C. difficile*

To confirm that conjugated strains did not contain *E. coli* contaminants, colony PCRs were performed on individual colonies of strain T7 streaked onto agar containing thiamphenicol that had the appearance of *C. difficile*. Primers *E.coli_uspA_FWD* and *E.coli_uspA_REV* are designed to amplify an 884 bp fragment of the gene *uspA,* present only in *E. coli* and absent in *C. difficile.* This has previously been shown to be a robust method for the detection of numerous *E. coli* strains (Chen & Griffiths, 1998). In parallel, primers *C.diff_Spo0A_FWD and C.diff_Spo0A_REV* are designed to amplify a 661 bp region of the *C. difficile* sporulation regulatory gene *Spo0A,* absent from *E. coli.* These PCRs confirmed that there was no *E. coli* contamination present in the conjugated *C. difficile* strains generated (**Figure 4.14**).

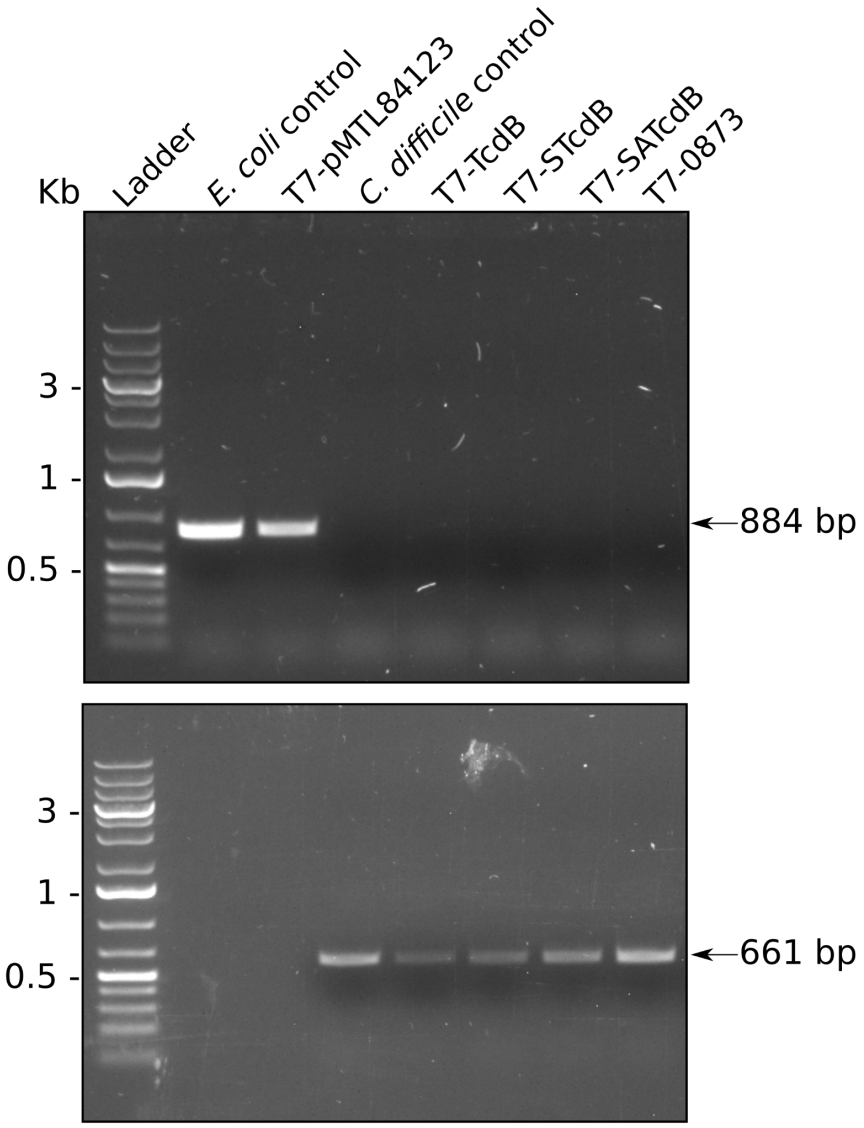


Figure 4.14: Colony PCR to confirm the absence of *E. coli* contamination in *C. difficile* transconjugants. The absence of *uspA* (884 bp; upper gel) and presence of *spo0A* (661 bp; lower gel) indicates that all transconjugants are solely *C. difficile except for* T7-pMTL84123 which contains the *E. coli* amplicon only and not the *C. difficile* amplicon indicating that this conjugation has not been successful.

4.4 Discussion

Previous studies have confirmed the possibility of displaying recombinant protein fragments on the surface *B. subtilis* spores (Isticato *et al*., 2001; Potot *et al*., 2010; Fantappie *et al*., 2017; Guoyan *et al*., 2019), including proteins from *C. difficile* (Negri *et al.*, 2013). It has also been shown that

recombinant proteins can be expressed in NTCD vegetative cells (Wang *et al.*, 2018). However, it has yet to be shown whether it is possible to express lipidated recombinant proteins that can further be released from the cell to elicit a potent immune response.

Here, overexpression plasmids were created in which toxin fragments were fused to the SP and putative AP region of lipoprotein CD0873. All verified fusion construct plasmids were subsequently conjugated into a NTCD strain T7.

Problems were encountered for TcdA during the cloning process. Specifically, insertion of the TcdA fragment was problematic and required multiple rounds of cloning to achieve a construct which, when digested with *Sac*I and *Xho*I, returned bands of the expected size. Sequencing confirmed that the PCR product obtained using the CD630 genomic template was correct. However, once this was ligated into the backbone vector, any sequence returned shared little homology with TcdA of strain 630, leading us to conclude that either ligation into the backbone vector, or subsequent amplification within *E. coli* was causing this problem. This could be a result of TcdA's toxicity in *E. coli* promoting the accumulation of SNPs within the plasmid. Further experimentation examining alternative origins of replication would be necessary in order to determine why such difficulty was encountered. The plasmid copy number may have some influence on the toxicity of this fragment. Using origins of replication which allow for a lower copy number may have resulted in this issue being resolved sooner. After several rounds of cloning, a successful construct was obtained and confirmed by sequencing.

Attempting to address the problem of conjugation, different ratios of *E. coli* and *C. difficile* were used during the mating step to assess whether increasing or decreasing the number of available mating partners on both sides yielded a more efficient result. Mating times were assessed between 8 and 48 hours to see if increasing mating time resulted in a greater number of successfully conjugated cells or if a shorter time resulted in fewer

unconjugated cells and allowed cells which had successfully conjugated to grow more easily. Droplets of 10 µl were also used in an attempt to reduce the amount of space between cells and facilitate more efficient mating. None of these amendments to the original protocol resulted in success.

Future work would be to persist with conjugating pMTL84123::Signal+Anchor::TcdA into T7 to demonstrate how this construct compares to its TcdB counterpart. Further work could also investigate whether exploiting individual promoters as opposed to both the native and pfdx promoters is beneficial particularly for the TcdA construct by adjusting the expression level in *E. coli*. Furthermore, identifying the optimum promoter or promoter combination for enhanced expression of antigens would be desirable for vaccine purposes.

Chapter 5. Phenotypic analysis of recombinant *C. difficile* strains

5.1 Introduction

Construction of overexpression vectors, and confirmation of their sequence and successful conjugation into *C. difficile* was demonstrated in the previous chapter. In this next chapter, a number of phenotypic analyses are conducted to confirm expression of these genes or fusion genes in strain T7 and to assess their localisation; whether they are retained in the cytoplasm or released extracellularly or both. The intended mode-of-action of this vaccine is for the antigen fragments to be released from T7 within the gut following germination of spores, therefore it is important to determine where the antigen localises to. To assess expression level and cellular localisation, a CD0873-specific antibody and a TcdB-specific antibody were used as markers for detection of these antigens in a number of assays. The findings generated are critical for proceeding with testing these vaccine strains *in vivo*.

In order to mass-produce the spores required for the vaccine strains, the presence of the plasmid within these strains must not have a deleterious effect on either their growth rate or rate of sporulation. Should the overexpression of the fragments reduce the ability of the strain to divide or sporulate, this would have major implications for downstream manufacturing of spore preparations.

Recognition of the candidates by antibodies against the full-length proteins would not only ensure that the *in-situ* constructs were expressing the fragments as intended, but also provide essential confirmation that the antigen candidates produced are recognisable. This would also lend support to the hypothesis that, *in vivo*, antibodies raised against these vaccine candidates would be capable of targeting the corresponding epitopes found in CD0873 and the RBD of TcdB in clinical infections. The intended mode-of-action of this vaccine would rely on surface expression and secretion of the vaccine candidates within the gut following germination of spores, therefore it will also

be important to define the localisation of the antigen fragment to ensure a response will be generated *in vivo*.

LC-MS work discussed in Chapter 3 revealed that CD0873 is the most abundant lipoprotein of T7 found extracellularly. As such, the N-terminal portion of CD0873 fused to our vaccine candidates should produce a high yield of lipidated antigen that is released from the cell increasing its chances of generating an immune response *in vivo.*

5.2 Aims

- Generate and purify TcdB and CD0873 from *E. coli* for use in Western blots as positive controls and for coating ELISA plates to be used in Chapter 6;
- Confirm the presence of episomal plasmids in strain T7 does not affect the viability of cells of the recombinant strains (specifically growth rate and sporulation rate);
- Assess the expression level and localisation of TcdB and CD0873 in recombinant strains by Western immunoblotting, Fluorescence associated cell-sorting (FACS), and immunofluorescent microscopy.

5.3 Results

5.3.1 Purification of recombinant protein antigens of *C. difficile*

5.3.1.1 Purification of rTcdB for use in ELISA and Western blotting

A construct for the overexpression and purification of a receptor binding domain (RBD) fragment of TcdB (pTWIN_CO_TcdB.HIS) from *E. coli* was previously generated by Cansu Karyal from cloning a codon-optimised gene string encoding the RBD into the pTWIN1.HIS modified backbone vector prior (Karyal *et al.,* 2021). pTWIN1.HIS features a T7 bacteriophage promoter for inducible expression of the protein, and an

N-terminal intein tag incorporating a chitin-binding domain, as well as a C-terminal His_{10}-tag for downstream purification of the protein.

rTcdB is a 61.5 kDa protein with an isoelectric point (pI) of 5.01 as predicted by the ExPASy pI/Mw tool (https://web.expasy.org/compute_pi/). Construct pTWIN1_CO_TcdB.HIS was used for expression and purification of rTcdB in *E. coli* strain T7 Express (NEB) following induction with isopropyl β- d-1-thiogalactopyranoside (IPTG). Soluble and insoluble fractions were harvested and examined by fractionation with 10% (w/v) Tris-glycine SDS-PAGE gels followed by staining with Coomassie blue (**Figure 5.1**).

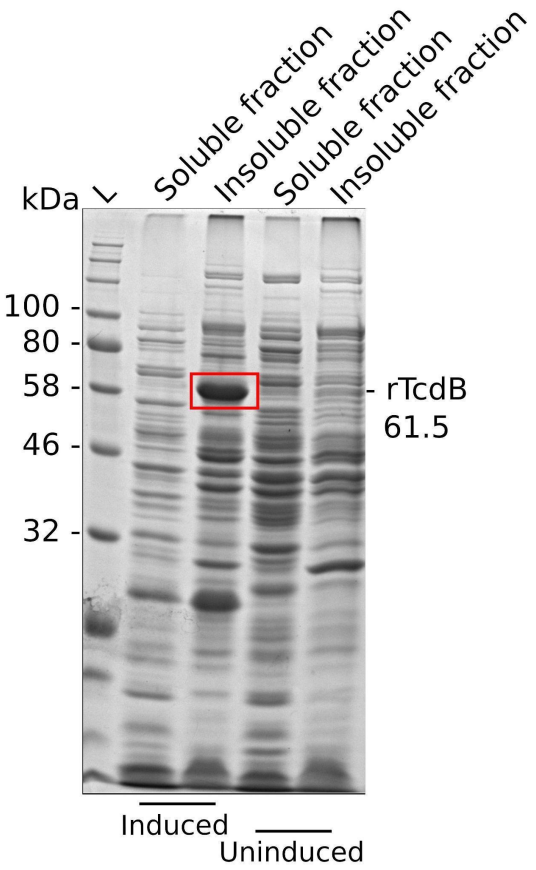


Figure 5.1: Expression of recombinant TcdB (rTcdB). *E coli* T7 Express cells (NEB) transformed with pTWIN_CO_TcdB.HIS were induced at room temperature using 0.3 mM IPTG. Non-induced controls were included. Soluble and insoluble fractions were visualised on 10% (w/v) Tris-glycine SDS-PAGE gels stained with Coomassie blue. L: Colour Pre-stained Protein standard (NEB). rTcdB is shown in the red box migrating at 61.5 kDa.

Preliminary experiments using cell lysates of both induced and uninduced cell lysate fractions showed that rTcdB is insoluble when expressed. It therefore required solubilisation prior to purification.

Solubilisation of rTcdB

The entire insoluble fraction was denatured first by resuspending in 6 M guanidine-HCl then allowing the proteins within to refold by dialysing in 1.4 kDa dialysis tubing (ThermoFisher) against buffers with a gradual reduced molarity of urea over the course of 3 days (**Section: 2.8.5**). The refolded rTcdB within the solution was then purified using Ni^{2+} immobilised metal affinity chromatography (IMAC) (**Figure 5.2**).

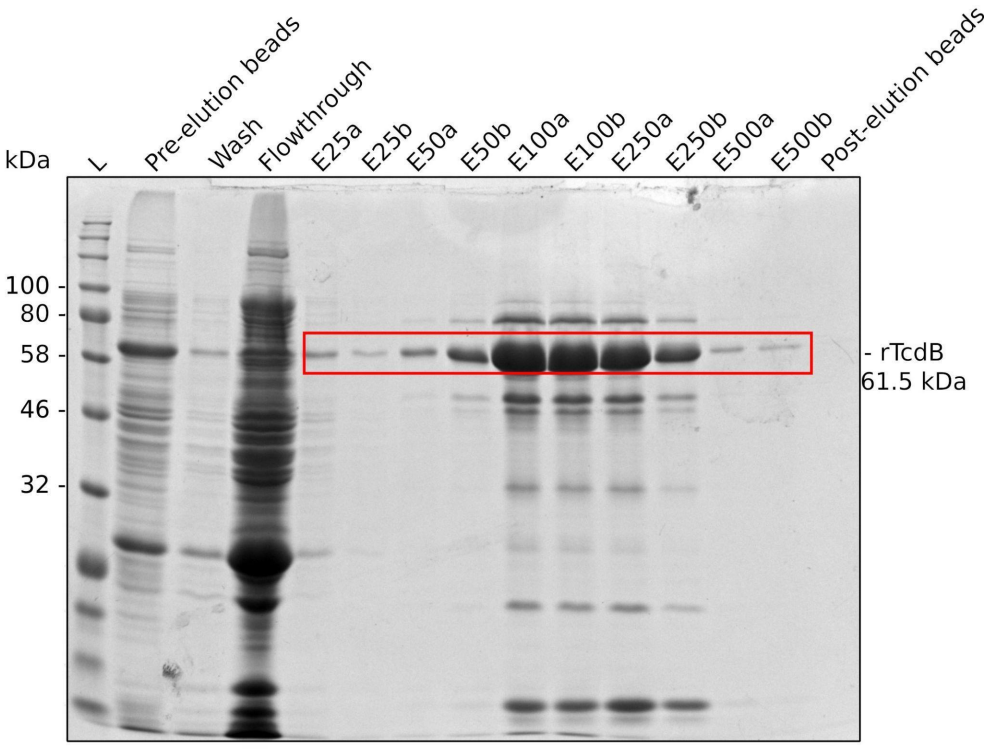


Figure 5.2: Affinity purified recombinant His-tagged TcdB. rTcdB was purified using a Ni^{2+} column with HisPurTM Ni-NTA Resin (Thermo Scientific) and eluates visualised by 10% (w/v) Tris-glycine SDS-PAGE with staining by Coomassie blue. L: Colour Pre-stained Protein standard (NEB), purified soluble recombinant TcdB shown in red box. Lanes E25-E500 denote elutions with the specified molarity of imidazole in mM with a and b denoting replicates.

rTcdB was predominantly detected in eluates containing between 100-250 mM imidazole with very little protein remaining attached to the beads. This method of refolding by dialysis, while successful, took an average of four days to complete and used a large amount of urea to create the necessary buffers. There were also an unacceptable number of histidine-containing contaminants present in the sample, suggesting this methodology was not the optimal protocol for purification.

His-trap purification of rTcdB

An alternative method for on-column solubilisation was attempted using a specialist His-trap column (Cytiva) as opposed to the previously used dialysis method followed by Ni^{2+} - charged affinity column (HisPur TM Ni-NTA Resin; Thermo Scientific) (**Section: 2.7.4**). This method, in comparison to the previous denaturation and refolding by dialysis, required much smaller volumes of solubilisation buffers, which were washed over the sample at very low speed and pressure. Fractions from all washes and eluates were taken and examined by SDS-PAGE to assess the level of purity (**Figure 5.3)**.

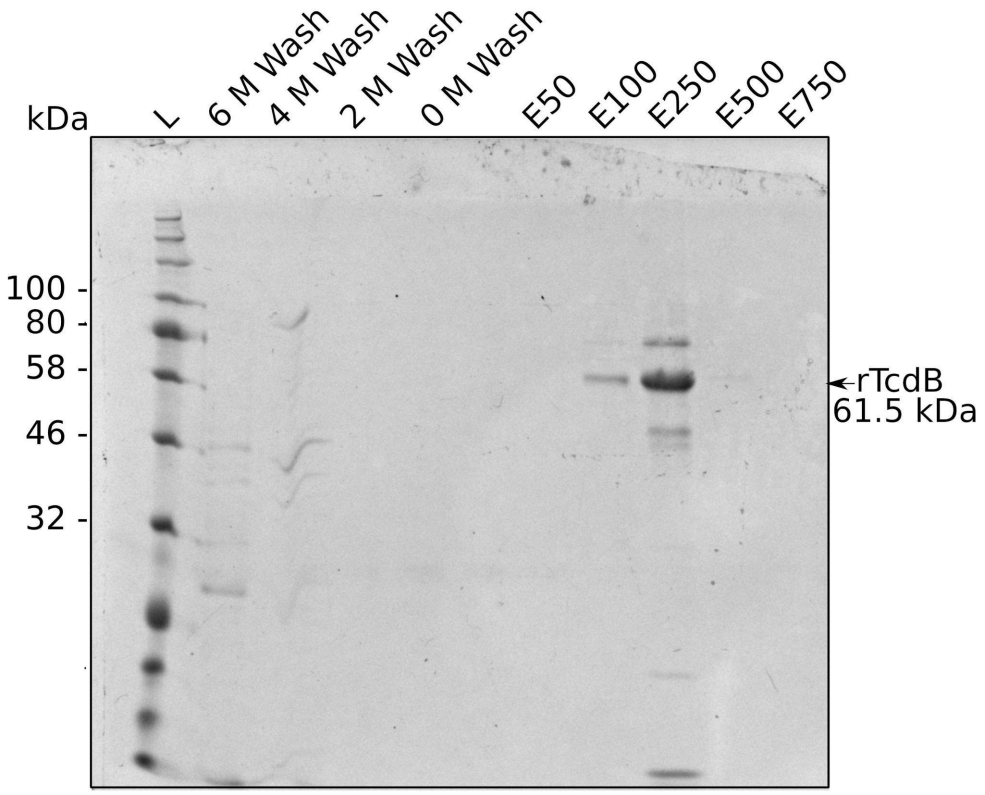


Figure 5.3: Affinity purification of recombinant His tagged TcdB by His-trap column. rTcdB was purified using a Ni^{2+} HisTrap High Performance column (Cytiva) and eluates visualised by 10% (w/v) Tris-glycine SDS-PAGE with staining by Coomassie blue. L: Colour Pre-stained Protein standard (NEB) purified soluble recombinant TcdB indicated by the arrow. Lanes E50-E750 contain elutions with the molarity of imidazole in mM.

rTcdB was detected in eluates containing between 100-250 mM imidazole, with the majority this time detected in the 250 mM eluate. The protein contaminants observed after washing off the column with 6 M and 4 M urea were lost upon subsequent washes with 2 M and 0 M urea. A higher level of purity was achieved using this HisTrap method, with far fewer contaminants seen below 46 kDa when eluting with 250 mM imidazole compared to any elution from the previous two-step dialysis approach followed by IMAC (**Figure 5.2**).

In an attempt to increase the purity of rTcdB, the insoluble fraction was loaded onto the His-trap column, as before, but with an increased incubation

time of 16 hours (previously 1 hour) in breaking buffer followed by elution with imidazole. This increased incubation resulted in a pure sample of rTcdB to be recovered. Confirmation of the presence of rTcdB was achieved by Western immunoblotting (**Figure 5.5**).

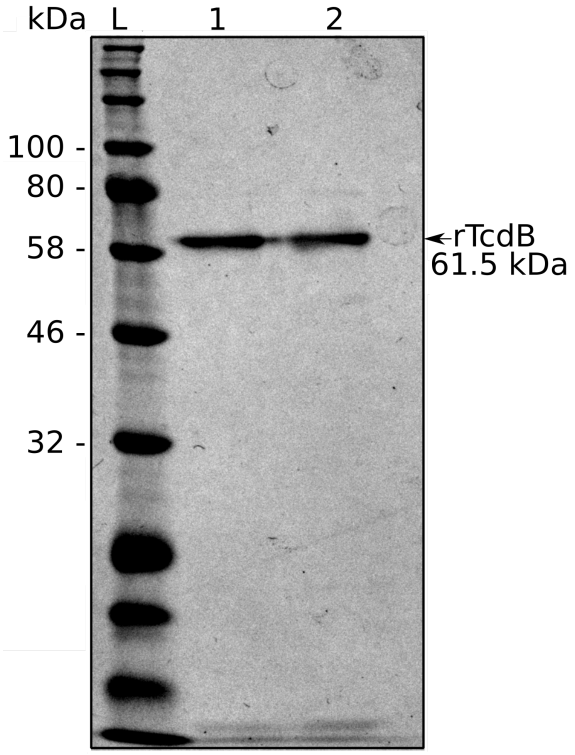


Figure 5.5: Western immunoblot to confirm purification of rTcdB following extended incubation of insoluble fraction on HisTrap-column. Insoluble fractions of rTcdB were loaded onto a HisTrap High Performance column (Sigma) and incubated for 16 hours before the established elution procedure was performed. Eluates were fractionated by 10% (w/v) Tris-glycine SDS-PAGE and transferred onto PVDF membrane. The membrane was probed with mouse anti-TcdB antibody (1:5000; Native antigen company), followed by corresponding anti-mouse IgG HRP (1:1000; CST) antibody and visualised using ECL. L: Colour Pre-stained Protein standard (NEB), rTcdB shown by arrow migrating at expected size (61.5 kDa).

Several rounds of protein purification using the optimised His-trap methodology were performed; each time eluates were assessed for purity by SDS-PAGE (data not shown) and samples which possessed a satisfactory level of purity were pooled for downstream applications.

5.3.1.2 Purification of r CD0873 for use as a control in ELISA and Western Blotting

A construct for the overexpression of purification of rCD0873 (pTWIN_CO_08730.HIS) was previously generated by Cansu Karyal by cloning a codon-optimised gene string encoding the gene *CD0873* minus its signal peptide into the backbone vector p.TWIN1.HIS prior to this project (Karyal *et al.,* 2021).

rCD0873 is a 36 kDa protein with an isoelectric point (pI) of 4.37 as confirmed by the ExPASy pI/Mw tool (https://web.expasy.org/compute_pi/). The method used to induce protein expression in pTWIN_CO_08730.HIS-containing *E. coli* T7 Express cells was the same as that outlined for rTcdB. Investigation of soluble and insoluble fractions by SDS-PAGE (10% w/v stained with Coomassie blue) revealed rCD0873 is soluble (**Figure 5.6**).

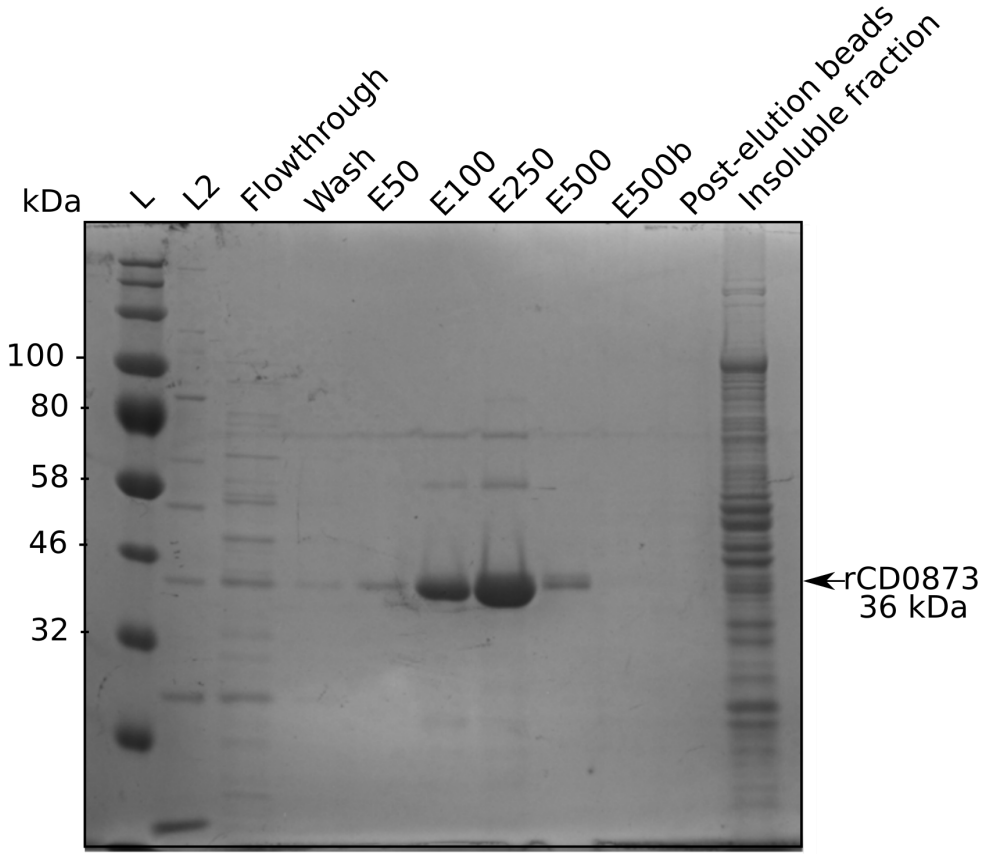


Figure 5.6: Expression and purification of recombinant CD0873 (rCD0873). rCD0873 was expressed in T7 Express cells (NEB) and induced at room temperature using 0.3 mM IPTG. rCD0873 was then purified using a Ni^{2+} column with HisPurTM Ni-NTA Resin (Thermo Scientific). Eluates and the insoluble fractions were visualised on 10% (w/v) Tris-glycine SDS-PAGE gel stained with Coomassie blue. L: Colour Pre-stained Protein standard (NEB), L2: Magic Mark XP Western Protein Standard (Thermo Scientific). Lanes E50-E500 denote elutions with the molarity of imidazole in mM, E500b is a second elution performed with 500 mM imidazole.

The predicted band size of 36 kDa was observed, primarily eluted at 100 mM and 250 mM imidazole, though there are also a number of unknown histidine-containing contaminants at predominantly 58 and 70 kDa. A Western blot was subsequently performed using rabbit anti-CD0873 antibody (kindly provided by Stephen Michell, University of Exeter) followed by anti-rabbit IgG HRP antibody (CST) (**Figure 5.7**).

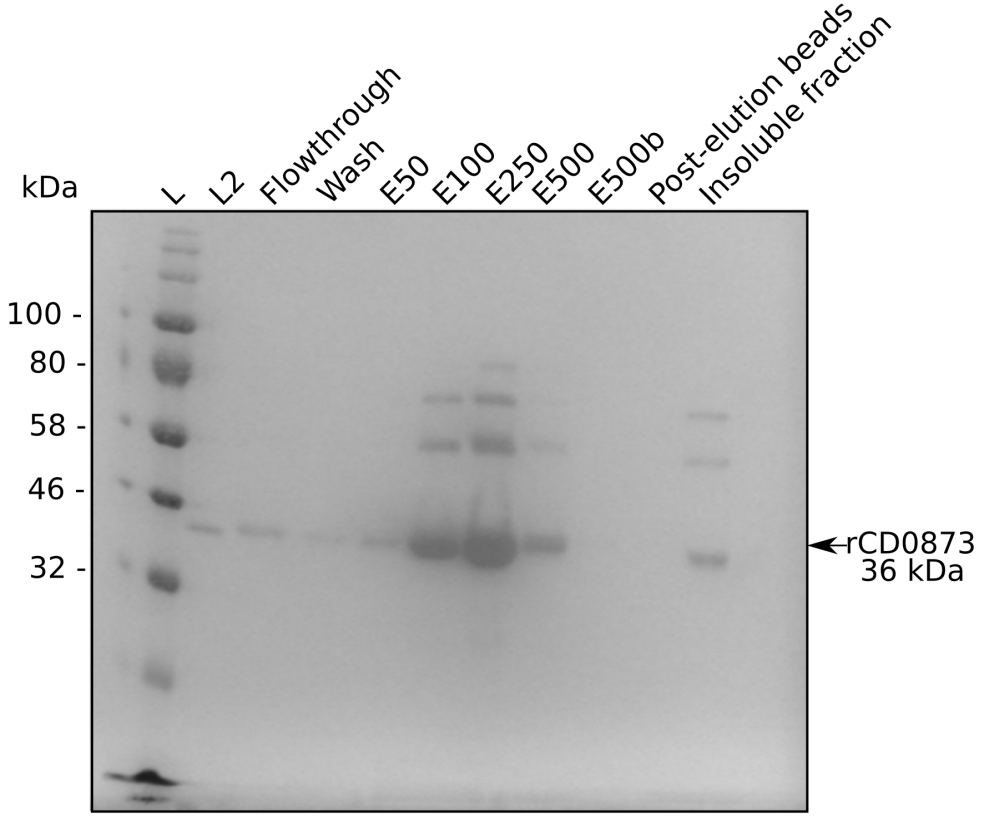


Figure 5.7: Visualisation of purified recombinant CD0873 by Western immunoblotting. Confirmation of purification of rCD0873 expression was assessed by Western immunoblotting. Eluates and the insoluble fraction were loaded onto a 10% (w/v) Tris-glycine SDS-PAGE gel and transferred to a PVDF membrane using a Trans-Blot Turbo Transfer system (Bio-Rad). Membranes were blocked with 5% dry-milk in TBST for 1 hour followed by an hour incubation with rabbit anti-CD0873 antibody (1: 10,000) and then anti-rabbit IgG HRP antibody (1:1000) in TBST and visualised using TMB. L: Colour Pre-stained Protein standard (NEB), L2: Magic Mark XP Western Protein Standard (Thermo Scientific) rCD0873 present at 36 kDa.

The Western blot confirmed successful purification of rCD0873. The 500 mM eluate was chosen for use in downstream applications due to the low level of contaminants compared to CD0873 eluates at 100 mM and 250 mM imidazole.

5.3.2 Assessing growth rate of T7 recombinant strains harbouring plasmids

In order to determine whether the presence of episomal plasmids and expression of the cloned antigens were detrimental to the growth of the recombinant strains of T7, a growth assay was performed. Strains were grown for two consecutive overnights (strain T7 in BHIS medium and all recombinant strains in BHIS containing thiamphenicol where appropriate), ensuring that on day three only actively growing cells were used for the assay. Cells were diluted 1:100 in BHIS broth or BHIS broth containing thiamphenicol as appropriate, and added in triplicate to a 48-well plate, which was then sealed. Optical density (A_{600}) was measured continuously for 24 hours in a spectrophotometer outside of the anaerobic cabinet (Promega GloMax-multi detection system), allowing the plotting of growth curves for each strain (**Figure 5.8**).

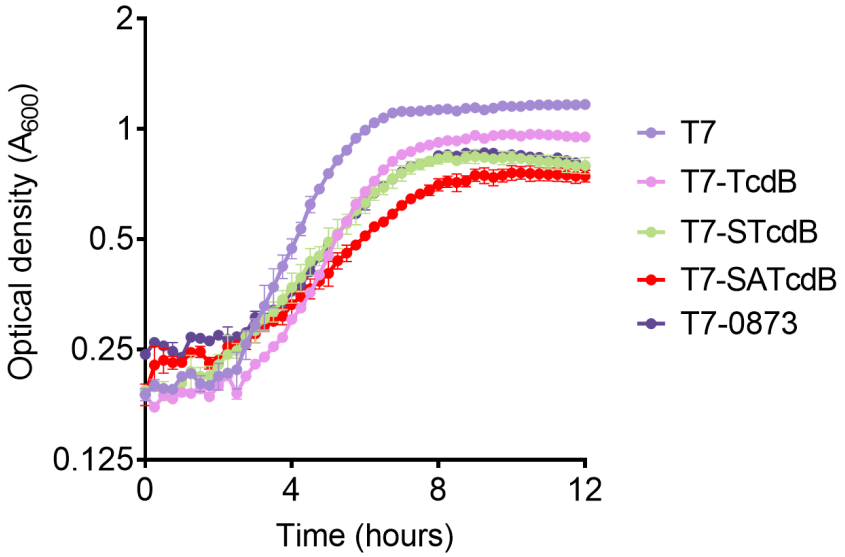


Figure 5.8: Growth curves of *C. difficile* strain T7 and recombinant T7 strains harbouring expression plasmids. Strains were grown in BHIS medium for two consecutive overnights before being diluted and plated. All strains (n=2) were incubated in a single 48-well plate and measured simultaneously for optical density (A_{600}) using a Promega GloMax-multi detection system.

These data demonstrate that all recombinant strains harbouring an episomal plasmid have a reduced growth rate when compared to wild type strain T7. However, while the doubling time is increased (longer) compared to T7, as seen by the less steep gradient, particularly in the case of T7-SATcdB, the recombinant strains can still grow to reach optical densities which were suitable for our needs.

5.3.3 Assay to determine level of sporulation in recombinant strains

Since the vaccine platform being developed relies on administration of spores, it was important to ensure the presence of episomal plasmids within T7 did not have a negative impact on the ability of the strain to generate spores (sporulation). To assess the rate at which the recombinant strains sporulate, cultures were grown in BHIS broth over 5 days (in the presence of thiamphenicol where appropriate). Two samples were taken for each strain: one was heat-treated at 65°C for 30 minutes to kill all vegetative cells within

the sample, and the other was not heat-treated harbouring both vegetative cells and spores. Serial dilutions were performed for each sample and spotted in triplicate onto medium containing 0.1 % taurocholate (and 15 ng/µl thiamphenicol where appropriate). Colony forming units (CFUs) were counted and the rate of sporulation assessed (**Figure 5.9**).

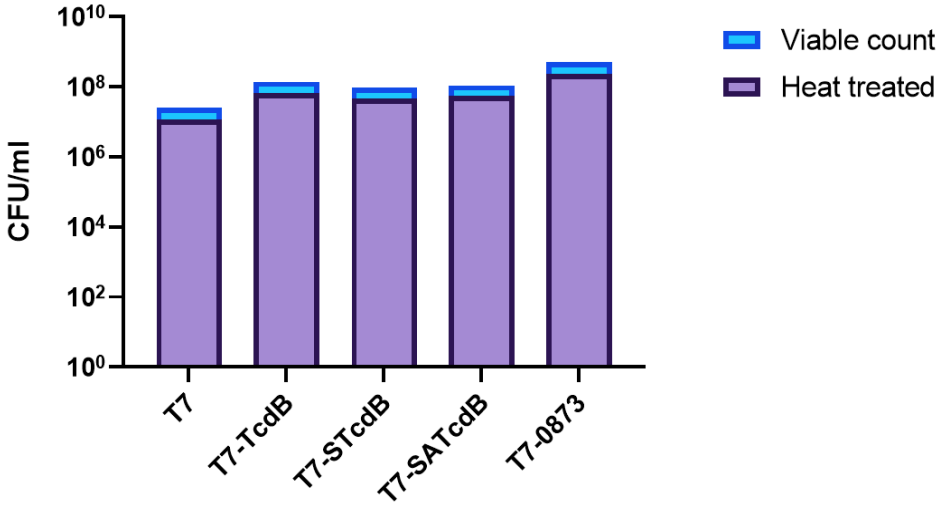


Figure 5.9: Enumeration of total viable cells vs spores after culturing in broth for 5 days. 50 ml cultures of T7, T7-TcdB. T7-STcdB, T7-SATcdB, and T7-0873 were assessed for their ability to produce spores over a period of 5 days to assess sporulation rate compared to the wild type strain T7. Culture was harvested after 5 days of anaerobic incubation and for each strain, one sample was heat-treated to kill vegetative cells and the other not heat-treated. Serial dilutions were made from both samples and plated in triplicate onto BHIS agar containing selective supplement and 0.1 % taurocholate. Plates were incubated anaerobically at 37°C and CFU enumerated.

All recombinant strains had a sporulation rate comparable to the wild type strain, T7. Additionally, the data suggest that by day 5 of growth in broth, almost all cells are harbouring spores.

5.3.4 Assessment of expression of antigens in recombinant strains of T7 harbouring episomal plasmids.

In order to assess whether the cloned vaccine candidates were being produced, 10 ml of late log culture were taken and spun down. For supernatant

analysis, the culture supernatant was harvested, protease inhibitors were added, samples were concentrated down to 1 ml by Vivaspin column (**Section 2.3.1**), and an equal volume of 2x sample buffer was added.. For analysis of whole cell lysate, the pellet from 1 ml of culture was resuspended in 50 µl of PBS and 50 µl of 2x SDS sample buffer. Equal volume of samples was fractionated by SDS-PAGE and Western immunoblotted to assess abundance of antigen within cells and supernatant.

5.3.4.1 Assessment of TcdB expression by Western immunoblotting

Western blots were performed on whole cell lysates (WCL) and supernatants (SN) of each recombinant strain, alongside wild type strain T7, to determine not only whether the antigen of interest is expressed (and can be detected by anti-TcdB or anti-CD0873 antibodies), but also whether these proteins are being released extracellularly and can be detected in culture supernatants. For each Western blot, the appropriate recombinant protein, rTcdB or rCD0873 (**Sections 5.3.1.1 and 5.3.1.2**), was used as a positive control.

Due to the presence of the SP leader sequence from CD0873 cloned upstream of the TcdB RBD fragment in the episomal plasmid of T7-STcdB and T7-SATcdB, 2 different size predictions were made by the LipoP prediction programme) depending on whether the antigen was processed (cleaved and lipidated) or not. For T7-SATcdB, which harbours both signal peptide and anchor peptide, the unprocessed form had a predicted molecular weight of 64.67 kDa and the processed form, a molecular weight of 62.3 kDa. For T7-STcdB, which only harbours the signal peptide, the unprocessed form has a predicted molecular weight of 61.69 kDa and the processed form, 59.31 kDa. Strain T7-TcdB lacks the CD0873 signal peptide and therefore is expected to exist as one size; 59.09 kDa.

WCLs and SNs of strain T7 and recombinant strains T7-TcdB, T7-STcdB, and T7-SATcdB were probed with an anti-TcdB antibody (Native

Antigen Company) to assess the level of TcdB found both intracellularly and extracellularly **(Figure 5.10)**

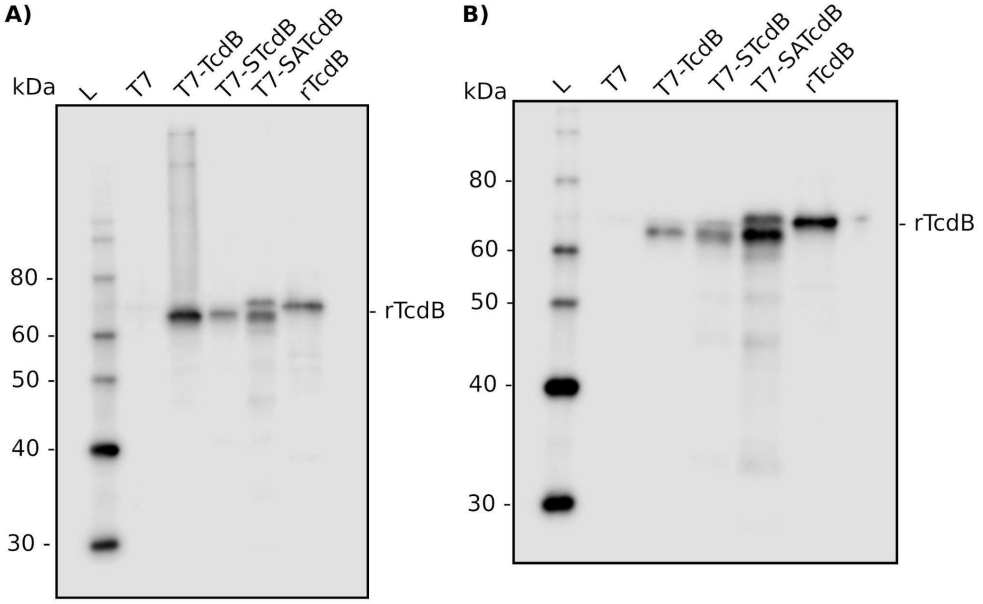


Figure 5.10: Confirmation of TcdB expression by recombinant strains of T7 by Western immunoblot. Western blot was performed with (A) whole cell lysates and (B) supernatants from TcdB recombinant strains T7-TcdB, T7-STcdB, and T7-SATcdB with rTcdB used as a positive control and T7 as a negative control. Samples were fractionated by 10% (w/v) Tris-glycine SDS-PAGE and transferred onto PVDF membrane. Membranes were probed with mouse anti-TcdB antibody (1:5000; Native antigen company) followed by corresponding anti-mouse IgG HRP (1:1000; CST) antibodies and visualised using ECL. L: Magic Mark XP Western Protein Standard (Thermo Scientific).

T7-TcdB, T7-STcdB, and T7-SATcdB were all found to express TcdB within the cell. T7-STcdB appears to produce the lowest level of TcdB overall, with T7-TcdB showing the highest level of TcdB detected in WCL with little detected in the SN, and T7-SATcdB the highest level of TcdB in the SN, with less detected in the WCL. Two distinct bands can be seen for T7-SATcdB. This suggests the presence of both processed and unprocessed species. A single band was detected for T7-STcdB at ~69 kDa, indicating the presence of only the processed species. It is matched in mobility (size) by the single band of the T7-TcdB sample, which possesses no signal peptide and therefore exists in only one form. This data supports the work performed by Chen *et al.,* 2009.

who showed that the inclusion of the AP downstream of the SP is important for facilitating expression of the fusion construct.

5.3.4.2 Assessment of CD0873 expression in T7-0873 by Western immunoblotting

As with the TcdB fragments, full-length CD0873 can potentially exist in two distinct forms, depending on whether the lipoprotein has been processed or not. The unprocessed form has a predicted molecular weight of 36.07 kDa, while the processed form has a predicted weight of 33.68 kDa. WCLs and SNs of wild type strains T7 and recombinant strain T7-0873 were prepared in the same manner described for TcdB recombinant strains, fractionated by SDS-PAGE, blotted and probed with a rabbit anti-CD0873 antibody **(Figure 5.11)**.

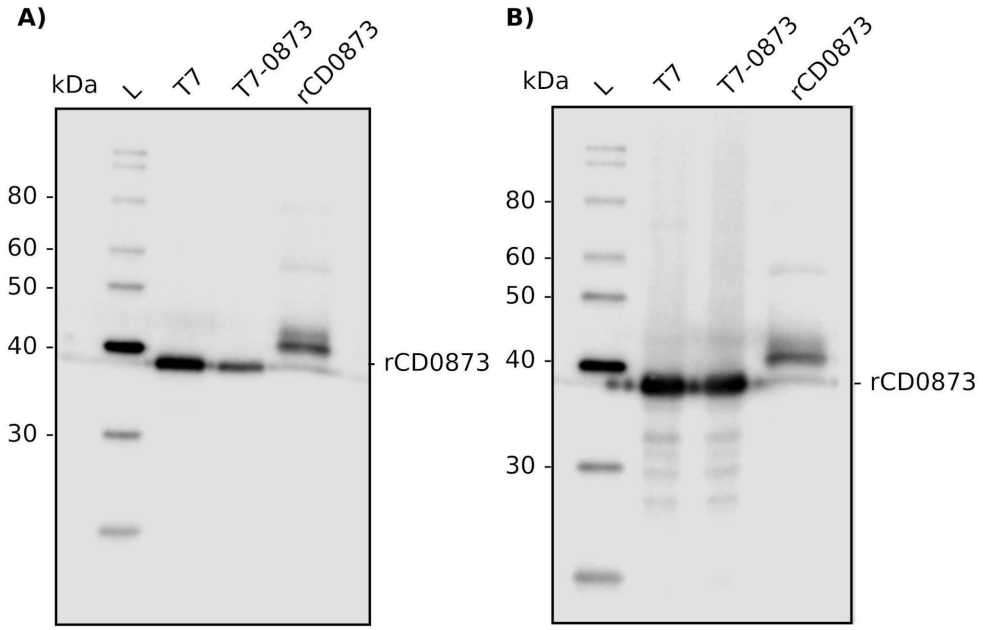


Figure 5.11: Confirmation of CD0873 expression in recombinant strain T7-0873 by Western immunoblot. Western blots were performed with (A) whole cell lysates and (B) supernatants from CD0873 recombinant strain T7-0873 with rCD0873 used as a positive control. Samples were fractionated by 10% (w/v) Tris-glycine SDS-PAGE and transferred onto PVDF membrane. Membranes were probed with rabbit anti-CD0873 antibody (1:1000) and bands were detected by anti-rabbit IgG HRP (1:10, 000) and visualised using ECL. L: Magic Mark XP Western Protein Standard (Thermo Scientific).

The size of the bands observed for T7-0873 samples suggests that CD0873 is found in its processed form as observed for T7 which expresses native CD0873 which is known to be processed. The molecular weight of these bands is visibly lower than that of rCD0873 which possesses the 10 His tag. A greater abundance of CD0873 was found in the supernatant, supporting our previous finding from LC-MS analysis of the supernatant of T7 (**section 3.4.1**).

To assess total protein loaded onto each SDS-PAGE gel, samples were fractionated by 10% (w/v) Tris-glycine SDS-PAGE before staining with Coomassie blue to confirm equal loading of samples (**Figure 5.12**).

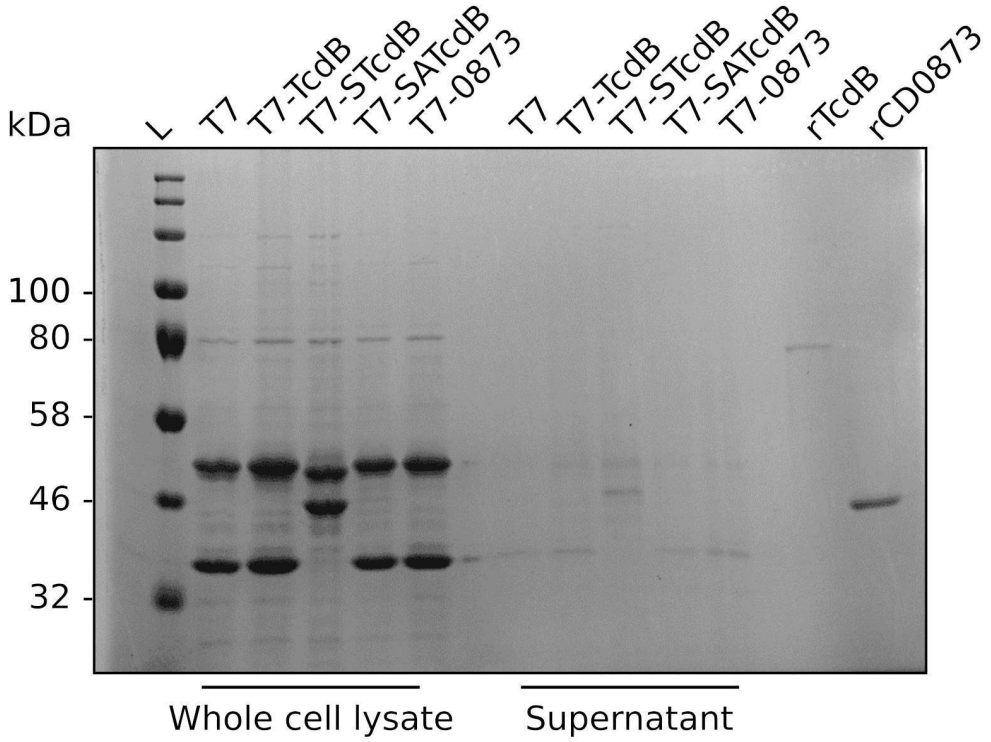


Figure 5.12: Coomassie stain of all recombinant strains (and wild type strain T7) to confirm equal loading. 1 ml of culture was harvested and both whole cell lysates (WCL) and supernatants (SN) were harvested for wild type strain T7, and recombinant strains T7-TcdB, T7-STcdB, T7-SATcdB, and T7-0873. Total protein load was visualised by fractionation by 10% (w/v) Tris-glycine SDS-PAGE with staining by Coomassie blue. L: Colour Pre-stained Protein standard (NEB).

Although total protein content of each sample loaded appears to be comparable within WCL and SN groups, it is clear that protein content is higher in WCL samples, which is to be expected. Interestingly, the pattern produced by these proteins is dissimilar only in the T7-STcdB sample where the lower MW band seen in other samples at ~38 kDa is not present. Instead a band is observed at ~46 kDa which is not present in the other samples.

5.3.6 Assessment of antigen expression on the surface of T7 recombinant strains by FACS

Having established that TcdB is released effectively into the extracellular milieu of T7-SATcdB and likewise, CD0873 of T7-CD0873, it was questioned whether some antigen remains cell-associated after translocation from the cytoplasm or whether it is predominantly released from the cell. In order to assess this question FACS analysis of whole cells of each of the recombinant strains was performed and compared to the wild type strain. Briefly, 1 ml of overnight culture was prepared for each strain and stained with either mouse anti-TcdB antibody (Native antigen company) and Donkey anti-Mouse IgG (H+L) Highly Cross-Adsorbed Secondary Antibody, Alexa Fluor 568 (red), or rabbit anti-CD0873 antibody (Stephen Michell, University of Exeter) and Goat anti-Rabbit IgG (H+L) Cross-Adsorbed Secondary Antibody, Alexa Fluor 647 (green) where appropriate (**Section: 2.9.1)**. Samples were then passed through a MoFlo Astrios EQ cell sorter (Beckman Coulter) and visualised using the FlowJo™ 7.6 Software (Becton, Dickinson and Company; 2019) (**Figures 5.13 and 5.14**).

Anti CD0873

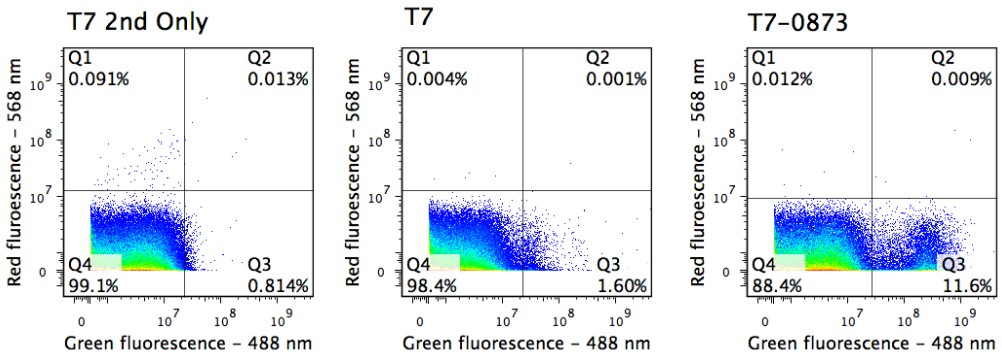


Figure 5.13: Representative FACS density-plot of wild type T7 and recombinant strain T7-0873. Cells were stained with rabbit anti-CD0873 antibody (1:1000) (and Goat anti-Rabbit IgG (H+L) Cross-Adsorbed Secondary Antibody, Alexa Fluor 647 (1:1000; green). Horizontal axis displays red fluorescence and the vertical axis displays green fluorescence. Density plots were used to determine the median fluorescence intensity (MFI) using the X-median values determined by the FlowJo 7.6 software. From left to right, T7 cells stained only with the secondary antibody, T7 cells stained with both primary and secondary antibodies, T7-0873 cells stained with both primary and secondary antibodies.

From these density plots, it was concluded that T7-0873 displays a higher level of staining as indicated by a shift to the right (green fluorescence) and the formation of a new sub-population compared to T7 which expresses native levels of this antigen. Overall the number of events indicating CD0873 molecules have been detected on the cell surface is 9-fold higher in the T7-0873 sample (11.6%) when compared to the wild type T7 (1.6%). This indicated that the recombinant strain possesses a larger number of CD0873 molecules on its cell surface when compared to the wild type.

Anti-TcdB

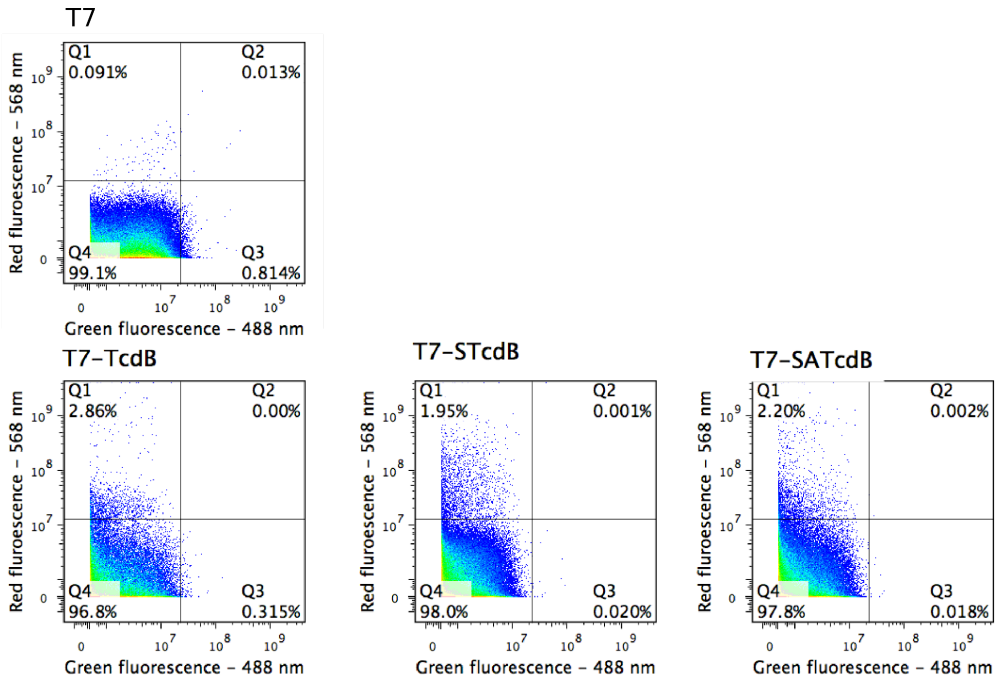


Figure 5.14: Representative FACS density-plot of wild type T7, T7-TcdB, T7-STcdB, and T7-SATcdB. Cells were stained with mouse anti-TcdB antibody (1:5000) (Native antigen company) and Donkey anti-Mouse IgG (H+L) Highly Cross-Adsorbed Secondary Antibody, Alexa Fluor 568 (1:1000; red). Horizontal axis displays red fluorescence and the vertical axis displays green fluorescence. Density plots were used to determine the median fluorescence intensity (MFI) using the X-median values determined by the FlowJo 7.6 software.

From these density plots, it appears the level of staining is generally comparable for each strain tested. This would imply that none of the recombinant strains possess any significant amount of TcdB on their cell surface as the level of fluorescence measured does not reach beyond that of the background. It is important to note that T7 does not encode TcdB and therefore the level of staining seen in the T7 plot must be as a result of non-specific staining.

We infer from the FACS data and Western immunoblotting results that TcdB in T7-TcdB remains in the cytosol and as expected is not surface-exposed. For T7 strains with TcdB fused to either SP or SP and AP, the data suggest that some TcdB is retained in the cytosol as shown by its presence

in WCL while the rest is released extracellularly with little or none remaining cell-associated. (The FACS procedure requires considerable washing of cells in between addition of antibodies and thus any protein loosely associated is likely to be removed.)

5.3.7 Further investigation of TcdB localisation in individual cells of recombinant strains of T7 by immunofluorescent confocal microscopy

To further assess the localisation of the engineered TcdB fragment, individual cells were assessed by immunofluorescent confocal microscopy. 1 ml of overnight culture was harvested and stained using Anti-*Clostridium difficile* Cell Surface Protein antibody (ab93728, Abcam plc) and mouse anti-TcdB antibody (Native antigen company). Samples were then stained using both Donkey anti-Mouse IgG (H+L) Highly Cross-Adsorbed Secondary Antibody, Alexa Fluor 568 (1:1000), and Goat anti-Rabbit IgG (H+L) Cross-Adsorbed Secondary Antibody, Alexa Fluor 647 **(Section 2.9.1**). Slides were then imaged using a ZEISS Elyra 7 with Lattice SIM confocal microscope (**Figure 5.15**).

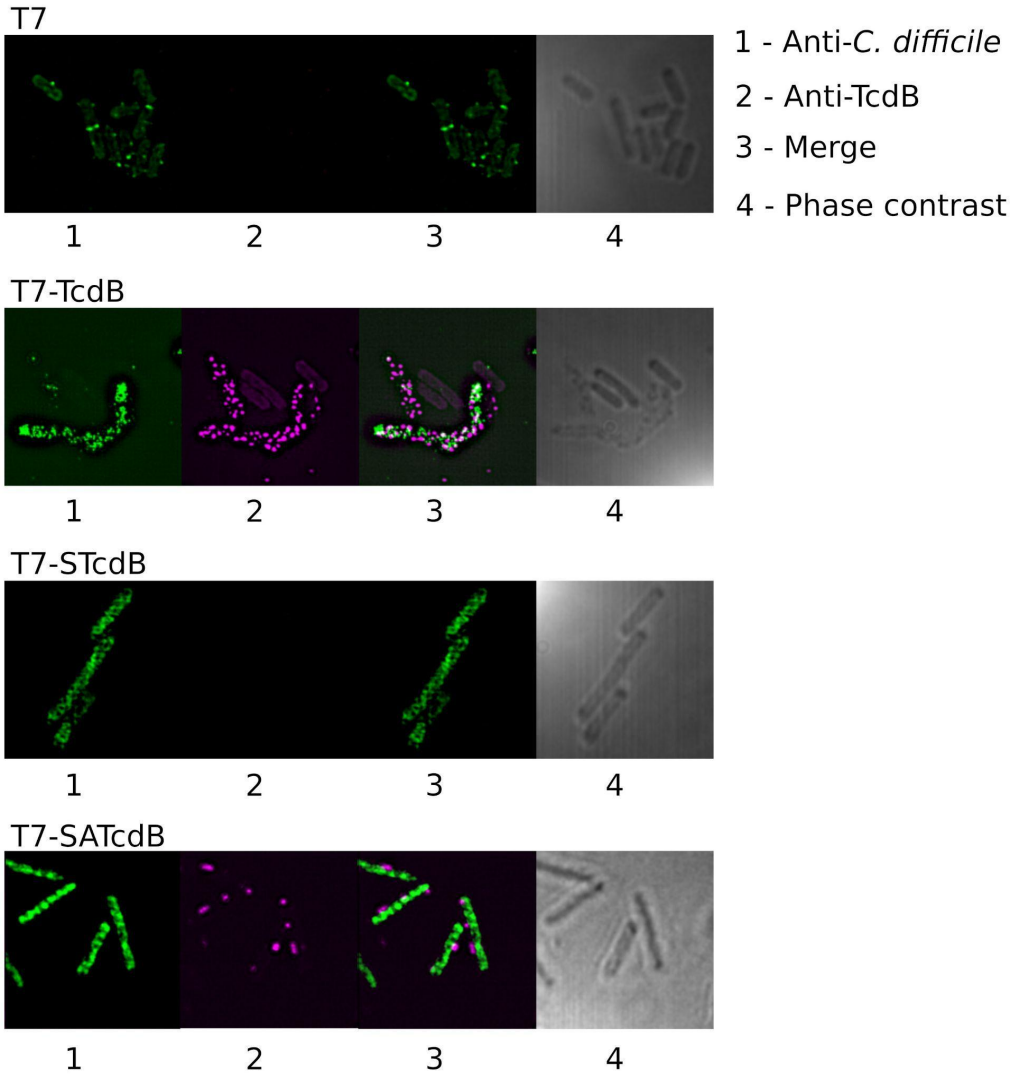


Figure 5.15: The presence of TcdBin recombinant strains of T7 as visualised by confocal microscopy. Representative confocal images of wild type strain T7 and recombinant strains T7-TcdB, T7-STcdB, and T7-SATcdB which have been stained with both mouse anti-TcdB antibody (1:5000) (Native antigen company) and rabbit Anti-Clostridium antibody (Abcam) (1:5000) as primary antibodies, and subsequently Donkey anti-Mouse IgG (H+L) Highly Cross-Adsorbed Secondary Antibody, Alexa Fluor 568 (1:1000) (Magenta), and Goat anti-Rabbit IgG (H+L) Cross-Adsorbed Secondary Antibody, Alexa Fluor 647 (1:1000) (Green).

Surface expression of TcdB was only detected in strain T7-SATcdB. This may be due to the abundance of TcdB that is translocated out of the cytosol as shown by Western immunoblotting of this strain. Its abundance and

less stringent washing during cell staining than applied for FACS staining, may mean that some TcdB remains cell associated. Detection of TcdB can also be seen for T7-TcdB, however, this is only observed for cells which have ruptured as shown by phase contrast images, indicating that this strain is not surface-expressing TcdB.

5.4 Discussion

The aims of this chapter were to generate and purify protein antigen or an antigen fragment for use in ELISA and Western blots, to confirm the presence of episomal plasmids in T7 does not affect viability of the cells (specifically growth rate and sporulation rate), and to assess the expression level and localisation of these antigens in T7 recombinant strains by Western blotting, FACS, and immunofluorescent microscopy.

Expression and purification of recombinant protein antigens

Both TcdB and CD0873 were successfully purified (following several optimisations of the purification process in the case of TcdB). Western blotting confirmed their purity and these purified proteins were then taken forwards for coating ELISA plates for measuring antibody titres from immunised animals (**Chapter 6**) and for use as positive controls for Western blot experiments in this chapter.

Assessment of the growth rate and sporulation rate of recombinant strains compared to the wild type

The growth rate of recombinant strains and wild type were similar with an OD_{600} 0.7-1.0 reached. It was important to assess if strains could grow to densities within this range in order to be able to potentially harvest sufficient spores for subsequent immunisation studies (**Chapter 6**). This experiment could have been expanded to assess the viability of cells at this point, as a measurement of OD will also include lysed cells. For a more accurate measurement of growth rate, serial dilutions of these cultures should be made at various time-points and CFU enumerated as described in **Section 2.1.2.2**.

All recombinant strains were shown to produce a similar number of spores after 5 days of culture, meaning sufficient yields for immunisation studies (**Chapter 6**). Following germination of spores in the small intestine, vegetative cells are reported to take 6 hours to transmit to the large intestine in mice (Padmanabhan, 2013). It is the short terminal portion of the small intestine (ileum) which is the immune inductive site where vegetative cells must express the antigens of interest to induce an immune response. Indeed, such a response has been observed previously using an oral administration of NTCD spores in mice and hamsters (Wang, *et al,* 2018).

Phenotypic assessment of antigen candidates by Western immunoblotting

A difference in banding pattern was observed for T7-STcdB when WCL samples were fractionated and stained by Coomassie. Purity of all recombinant strains was confirmed in **Section 4.3.7** by PCR so contamination with *E. coli* is unlikely. Future work would be focussed on further assessment of these bands. For bands corresponding to the size expected for processed lipoprotein, MS analysis or N-terminal sequencing could be performed to confirm absence of the SP and LC-MS could be conducted to confirm presence of the lipid moiety. A further improvement to the methodology would be the inclusion of a sonication step to better assess the level of intracellular proteins as boiling cells may only release surface proteins.

Western blots have confirmed that both antigens are being expressed in a form which can be recognised by antigen-specific antibodies raised against their full-length naturally produced counterparts. This provides a good level of confidence that any antibodies produced *in vivo* as a result of administration will target the equivalent region (full length CD0873 and the C-terminal region of the TcdB RBD) of naturally occurring antigens also.

The detection of the antigens in the culture supernatant of recombinant strains is very promising. Immune responses stimulated by antigens located solely on the cell surface rely on the whole bacterial cell being taken up by an M cell. NTCD is not known to be one of the few whole organisms taken up by

M cells (Dillon and Lo, 2019). Free antigens stand a higher chance of being taken up by M cells than those attached to the whole bacterial cell, and as such are expected to promote an immune response.

Differences in the localisation of TcdB by the recombinant strains (WCL vs SN) were as expected with the majority of TcdB produced by T7-TcdB found in the cytosol. This is likely due to the absence of a SP to provide instructions to the cell for translocation and post-translational modification. The opposite was found for TcdB produced by T7-SATcdB, its SPAP allowing for translocation across the cytoplasmic membrane for processing of the preprolipoprotein (as inferred from the detection of the cleaved form). Interestingly the non-cleaved (unprocessed) form was also detected, and perhaps it is some of this form mainly that remains cell-associated as shown by immunofluorescence microscopy. It has been shown that lipoproteins that are not processed can remain attached to the cytoplasmic membrane via anchorage with their retained SP (Hutchings *et al*., 2009). The processed form was found more abundantly in the supernatant but also some of the non-processed form which may be explained by sloughing off into the extracellular space.

A lower level of TcdB expression was observed in the T7-STcdB strain when compared to T7-TcdB and T7-SATcdB. and the band size in **Figure 5.12** indicates T7-STcdB is producing TcdB in its processed form. It has been previously observed that inclusion of the AP facilitates the expression of lipoprotein fusions (Chen *et al.,* 2009) and since the construct expressed in T7-STcdB lacks the AP, our findings corroborate those of Chen *et al*., (2009). Therefore, any future expression constructs which are created should include the anchor region to facilitate expression.

Examining the presence of antigen candidates on the cell surface by FACS

FACS analysis suggests an increased amount of CD0873 is produced by T7-0873 compared to the wild type with some retention of this lipoprotein at the cell surface whilst the remainder is released (**Figure 5.11**).

FACS analysis to detect TcdB associated at the cell surface showed no differences between the recombinant stains expressing TcdB and wild type, suggesting TcdB is either retained in the cytosol as expected for T7-TcdB and supported by its absence in the culture supernatant (**Figure 5.11**), or mostly released as shown for T7-SATcdB supernatant (**Figure 5.11**). The FACS data also support the Western blot data for T7-STcdB which was found to express only a low amount of TcdB.

It is also important to note that the antibodies used for FACS may not be the most suitable. Though the manufacturer states these fluorophore-conjugated antibodies are suitable for cell sorting, it would be beneficial to try a selection of different antibodies for future experiments. Although various optimisations of antibody concentration were carried out, further optimising of the protocol including duration of staining could be tried.

Examining the presence of antigen candidates on the cell surface by confocal microscopy

To further explore whether any TcdB remains cell associated in the recombinant strains, confocal microscopy was conducted for individually stained cells using the same anti-TcdB antibody as used for FACS analysis. Analysis on the cellular level revealed some association of TcdB with the cell surface for strain T7-SATcdB. For T7-TcdB, TcdB was detected but only in cells that were lysed as observed by phase contrast. This corroborates the findings above that TcdB remains in the cytosol. The lack of detection of TcdB on the cell surface of T7-STcdB confirms above observations that TcdB in this strain, although translocated out of the cytoplasm and processed (as inferred from its size on a Western blot), very low levels are produced.

5.5 Conclusion

Overall the recombinant strains produced in Chapter 3 have demonstrated the ability to produce antigen as intended. T7-SATcdB and T7-0873 have demonstrated an abundance of antigen in the extracellular milieu (some of which is retained at the cell surface). The successful release of lipidated TcdB and of CD0873 by T7-SATcdB and T7-0873 render these two strains as promising vaccine strains.

Chapter 6. Assessment of the immunogenicity of orally administered T7 recombinant strains in hamsters and mice

6.1 Introduction

Spores from each expression strain developed and described in previous chapters as well as the wildtype NTCD-T7 were isolated and purified and tested for their immunogenicity in both hamsters and mice following oral administration. Specifically, the ability of these vaccine strains to elicit antigen-specific immune responses in the small intestine and serum were compared. Oral administration through the medium of spores was chosen for a number of reasons. Spore preparations can be stored at room temperature being thermostable. Spores naturally resist the harsh condition of the stomach (low pH and proteases) and germinate into metabolically active, vegetative cells in the small intestine (Lawler *et al*., 2020) where antigens can be released for uptake by M cells in the ileum and potentially induce immune responses (Gil *et al*., 2017). Indeed, previous work performed by Wang *et al.* in 2018 has shown antigen-specific immune responses in mice using a similar method.

6.2 Aims and Objectives

- Administer mice and hamsters with spores from wild type T7 and expression strains;
- Measure the titre of antibodies induced by the vaccine strains in serum and small intestinal fluid harvested from these animals;
- Determine the functional properties of antibodies in serum and intestinal fluid in terms of adherence blocking and toxin neutralisation

6.3 Results

6.3.1 Serum IgG titres detected in immunised hamsters by ELISA

The titre of antigen-specific serum IgG was compared between groups by pooling sera from each group (n=4 per group), diluting 1:5 in PBS then quantifying the binding of IgG present to either rCD08730 or rTcdB by indirect ELISA (**Section 2.10.1.2**). 96-well plates were coated with 2.5 µg/ml of each purified antigen. Plates were incubated with diluted sera, washed then incubated with anti-hamster IgG (H +L) highly cross adsorbed- biotin antibody produced in goats (Sigma-Aldrich). Detection was achieved by the addition of streptavidin-HRP (RD Systems, Fisher Scientific) (**Figures 6.1 and 6.2**).

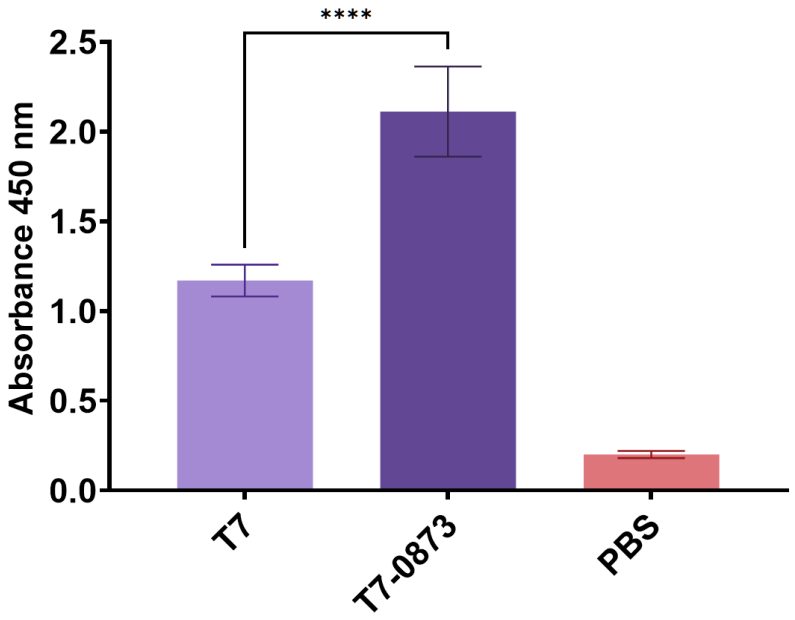


Figure 6.1: Serum IgG responses against rCD0873 from orally immunised hamsters tested by indirect ELISA. Serum was tested for IgG by indirect ELISA using 1:5 diluted serum from hamsters which had been administered with either spores from the wild type T7 strain, or recombinant strain T7-0873 (n=4 for all groups. 3 doses of $1x10^6$ spores at 1, 15, and 30). Using ELISA plates coated with 2.5 µg/ml of recombinant protein rCD0873, IgG responses were detected with goat anti-hamster IgG (H+L) highly cross adsorbed-Biotin antibody (Sigma-Aldrich) followed by incubation with Streptavidin-HRP (Thermo Fisher). Two independent ELISAs were performed with three technical replicates. A parametric one-way ANOVA test was performed followed by Dunn's multiple comparison test. Error bars represent standard error of the mean (SEM). Statistical difference (****) $p < 0.0001$.

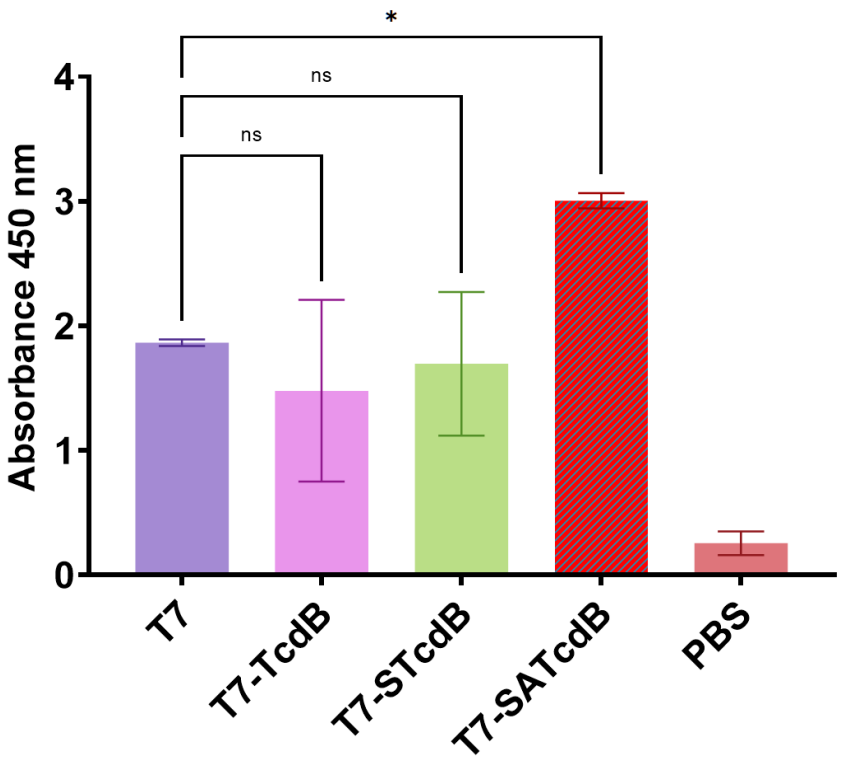


Figure 6.2: Serum IgG responses against rTcdB from orally immunised hamsters tested by indirect ELISA. Serum was tested for IgG by indirect ELISA using 1:5 diluted serum from hamsters which had been administered with either spores from the wild type T7 strain, or spores from recombinant strains T7-TcdB, T7-STcdB, and T7-SATcdB (n=4 for all groups). Using ELISA plates coated with 2.5 µg/ml of recombinant protein rTcdB, IgG responses were detected with goat anti-hamster IgG (H+L) highly cross adsorbed-Biotin antibody (Sigma-Aldrich) followed by incubation with Streptavidin-HRP (Thermo Fisher). Two independent experiments were performed with three technical replicates. A parametric one-way ANOVA test was performed followed by Dunn's multiple comparison test. Error bars represent standard error of the mean (SEM). Statistical difference *p*-value; (ns) not significant, and (*) $p < 0.05$.

The titres of antigen-specific serum IgG in hamsters immunised with spores from recombinant strains were compared to that of the control group (immunised with spores from wild type strain T7). Using a parametric one-way ANOVA, mean absorbance values were directly compared. When probing against rCD0873, hamsters immunised with T7-0873 spores showed a significantly higher (0.8-fold increase) IgG response compared to the wild type T7 group (p <0.0001). When probing against rTcdB, there was no significant

difference found between hamsters inoculated with either T7-TcdB or T7-STcdB when compared to the wild type strain T7 group (p = 0.6289, 0.2-fold decrease, and p = 0.9732, 0.09-fold decrease respectively). However, a significantly higher IgG response was observed in hamsters inoculated with T7-SATcdB compared against wild type strain T7 (p = 0.0139, 0.6-fold increase). An antibody response against rTcdb from material taken from hamsters inoculated with wildtype T7 was unectpected as there should be no factors present in order to cause an immune response of this kind. It is possible this is caused by cross-reactivity of antibodies raised against other factors, or an indication that the assay itself needs to be refined to eliminate background signal.

To investigate the total serum IgA present in the small intestinal fluid (SIF) of these animals, an ELISA was performed against total hamster sIgA using a kit (2B Scientific) according to the manufacturer's instructions (**Figure 6.3**). This methodology is less specific, but was the most suitable option as no individual commercial anti hamster IgA antibodies are available that can be used as a secondary antibody to detect the binding of antigen-specific sIgA to antigen as performed for the above IgG ELISAs.

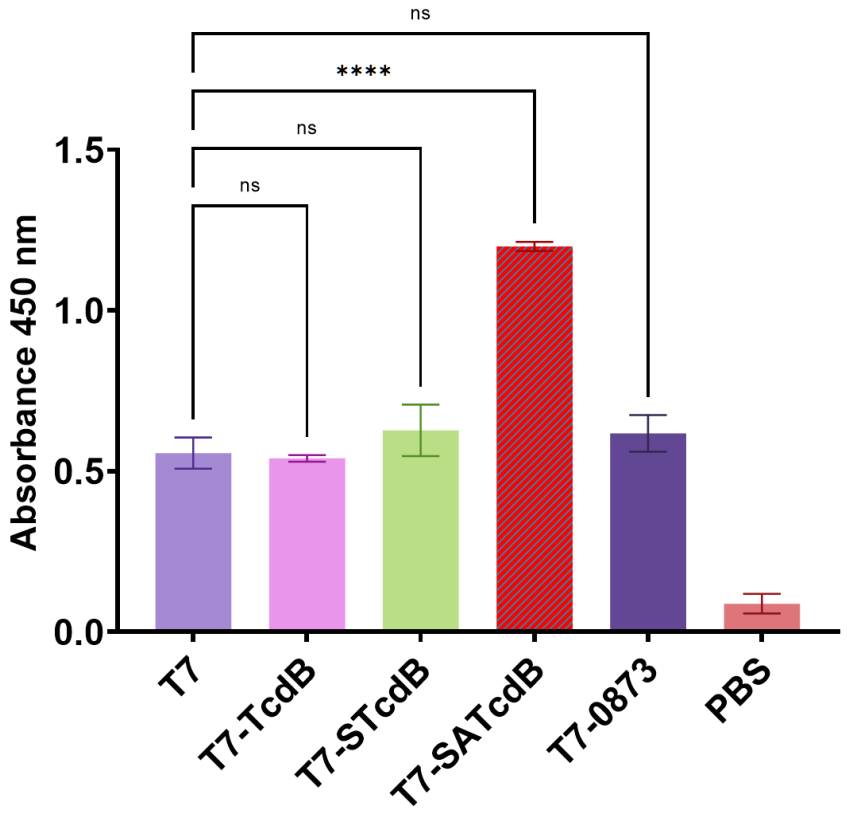


Figure 6.3: Intestinal fluid total secretory IgA responses from orally immunised hamsters tested by indirect ELISA. Total IgA in the small intestine was measured by indirect ELISA (Hamster Secretory Immunoglobulin A (SIgA) ELISA Kit, MyBioSource) using 1:20 diluted small intestinal fluid (SIF) from hamsters which had been administered with either spores from the wild type T7 strain, or spores from recombinant strains T7-TcdB, T7-STcdB, T7-SATcdB, or T7-0873 (n=4 for all groups). A parametric one-way ANOVA test was performed followed by Dunn's multiple comparison test. Error bars represent standard error of the mean (SEM). Statistical difference *p*-value; (ns) not significant and (****) $p < 0.0001$.

The titre of total sIgA in hamsters immunised with recombinant strains were compared to that of the control group, T7. Using a parametric one-way ANOVA, mean absorbance values were compared. The only significant response when compared to the wild type T7 group was seen in hamsters immunised with T7-SATcdB, where an increased level of sIgA was detected (p <0.0001, 1.2 fold increase).

6.3.2 Adherence blocking of *C. difficile* CD630 to Caco-2 cells by immunised hamster serum and intestinal fluid

In order to test the ability of antibodies in both the serum and SIF to block adherence of TCD strain 630 to epithelial cells, an adherence blocking assay was performed using Caco-2 cells (human colorectal epithelial cells) chosen for their ability to mimic the epithelium of the colon of humans in the form of a polarised monolayer. Cells of 630 were pre-incubated with diluted serum or SIF prior to their addition to Caco-2 cells. Adhered bacteria were determined by CFU per 100 Caco-2 cells (**Section 2.10.1.4**) (**Figure 6.4**).

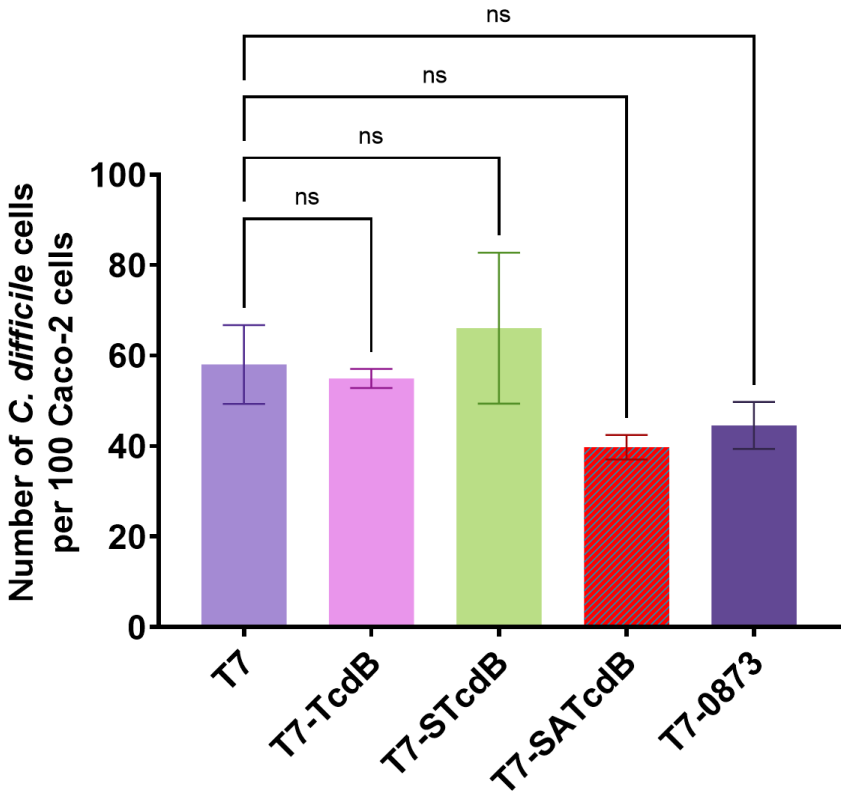


Figure 6.4: Reduction of adherence of cells of *C. difficile* strain 630 to Caco-2 cells by serum of hamsters immunised with recombinant strains of T7. Adherence of *C. difficile* 630 cells to Caco-2 cells when pre-incubated with serum (1:5) from hamsters administered with either spores from the wild type T7 strain or spores from recombinant strains T7-TcdB, T7-STcdB. T7-SATcdB, or T7-CD0873 (n=4 for all groups). Caco-2 cells were washed and average numbers of adherent bacteria enumerated (bacterial CFU per 100 Caco-2 cells shown). This assay was performed using three technical replicates. A parametric one-way ANOVA was performed followed by Dunn's multiple comparison tests. Error bars represent standard error of the mean (SEM). Statistical difference *p*-value; (ns) not significant.

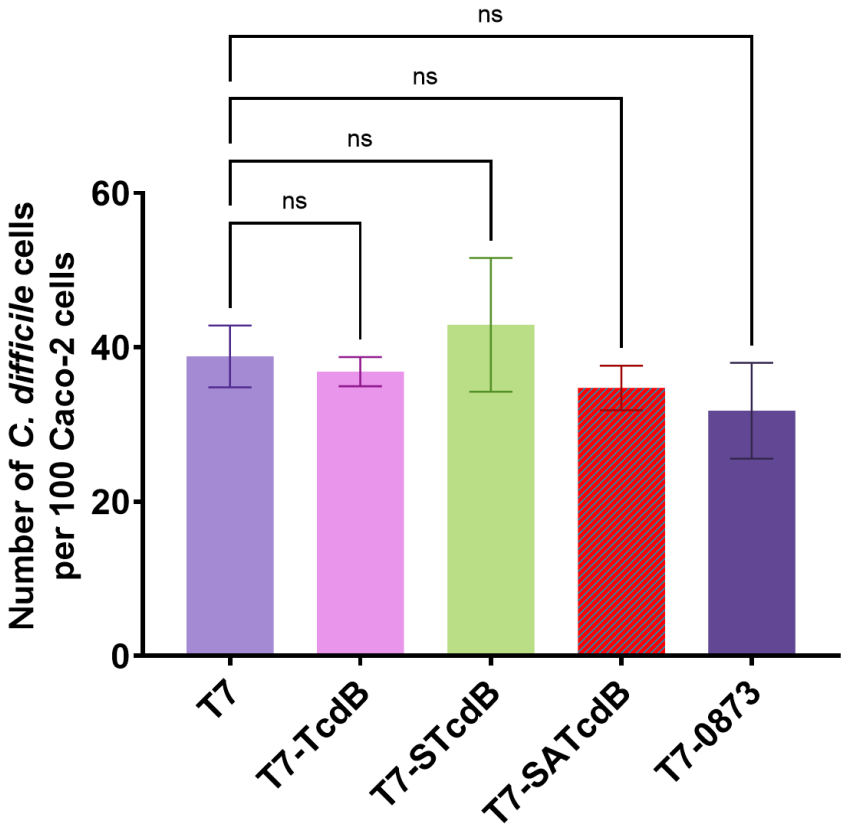


Figure 6.5: Reduction of adherence of cells of *C. difficile* strain 630 to Caco-2 cells by intestinal fluid of hamsters immunised with recombinant strains of T7. Adherence of *C. difficile* 630 to Caco-2 cells when pre-incubated with small intestinal fluid (SIF) (1:2) from hamsters inoculated with either spores from the wild type T7 strain, or spores from recombinant strains T7-TcdB, T7-STcdB. T7-SATcdB, or T7-CD0873 (n=4 for all groups). Caco-2 cells were washed and average numbers of adherent bacteria enumerated (CFU per 100 Caco-2 cells shown). This assay was performed using three technical replicates. A parametric one-way ANOVA was performed followed by Dunn's multiple comparison tests. Error bars represent standard error of the mean (SEM). Statistical difference *p*-value; (ns) not significant.

Although the binding action of cells of strain CD630 was reduced by both the serum and SIF of hamsters administered with the wild type T7 strain (p = 0.0151, 0.4-fold decrease, and p = 0.0111, 0.6-fold decrease respectively), neither serum nor SIF of hamsters immunised with recombinant strains had any significant additive effect. The reduction in binding was greatest for serum of T7-SATcdB and T7-0873-immunised groups withT7-SATcdB showing a 0.5- fold decrease in binding (p = 0.0899) and T7-0873 a 0.3-fold decrease (p = 0.2511) when compared to the wild type. A similar trend was observed when

using hamster SIF: T7-SATcdB showed a 0.2 fold decrease ($p = 0.9846$) and T7-0873 showed a 0.2 fold decrease ($p = 0.8323$) when compared to the wild type.

6.3.3 Toxin neutralisation ability of immunised hamster serum and intestinal fluid as assessed by MTT assay

Toxin neutralisation assays were performed to determine whether the antibodies detected in ELISA experiments were capable of preventing damage (cell rounding) to Vero cells when exposed to full-length toxins, TcdA and TcdB (FL TdA and FL TcdB; 50 ng/ml and 0.25 ng/ml, respectively; Public Health England). The colorimetric detection used for this assay is a 3-(4,5-dimethylthiazol-2-yl)-2,5-diphenyltetrazolium bromide (MTT) which is a yellow dye. Metabolically active, healthy cells produce NADPH-dependent cellular oxidoreductase enzymes which reduce the **MTT** to its insoluble form, formazan. The insoluble crystals are purple and the absorbance of the purple colour can be measured by a plate reader providing quantification of metabolism of cells in each microplate well. Therefore an increased absorbance (570 nm) correlates to a larger proportion of healthy metabolically active cells within a sample whereas a decreased reading indicates cells that are not able to metabolise MTT efficiently due to damage.

Using a series of 2-fold dilutions, serum and SIF were pre-incubated with FL TcdA and FL TcdB for 1 hour before being added to Vero cells that were previously seeded onto 96-well plates at a density of 1 x 10^5/ml (**Section 2.10.1.3**). Absorbance readings were taken at 570 nm wavelength.

Vero cells incubated solely with FL TcdA and FL TcdB were used as a positive control for cytotoxicity, and Vero cells in the absence of toxin were used as a negative control. The degree of toxin neutralisation by antibodies present in pooled biological fluids from each group was measured against these controls. Serum and SIF samples were tested on separate 96-well plates (**Figures 6.6 and 6.7**).

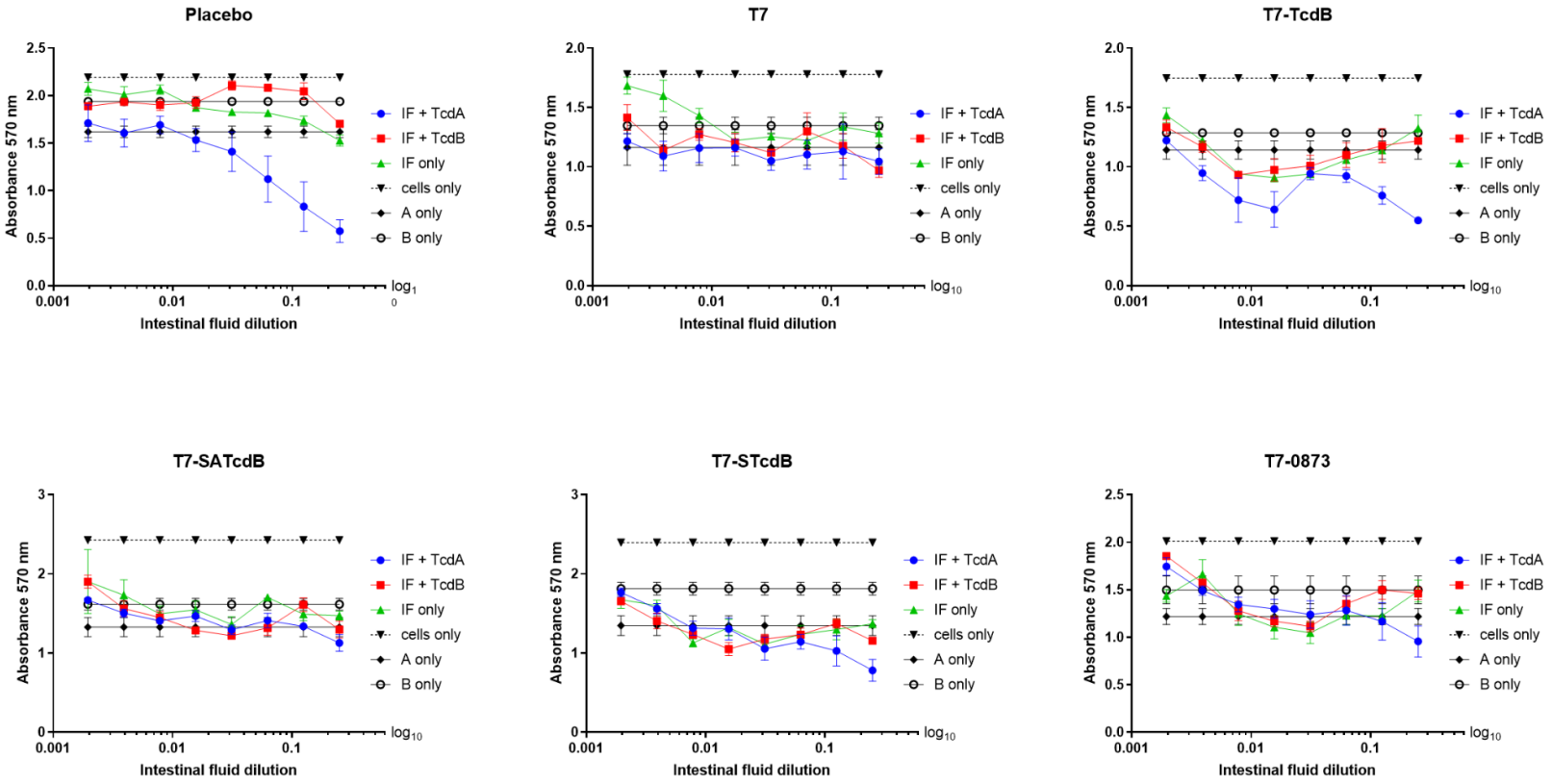


Figure 6.6: MTT assay to measure toxin neutralisation by intestinal fluid of orally immunised hamsters. Small Intestinal fluid (SIF) dilutions (1:2 to 1:128) of hamster groups inoculated with either spores from the wild type T7 strain or spores from recombinant strains T7-TcdB, T7-STcdB. T7-SATcdB, or T7-CD0873 (n=4 for all groups) were pre-incubated with full length (FL) TcdA (50 ng/ml) or FL TcdB (0.25 ng/ml) (Public Health England). Samples were also prepared in the absence of SIF in either the presence of toxins (positive controls; labelled FL TcdA and FL TcdB) or absence of toxins. (negative control; labelled Cells only) These mixes were subsequently added to Vero cells (1 x 10^5/ml). All sample dilutions were tested in triplicate. The metabolic health of the cells was assessed by measuring absorbance at 570 nm.

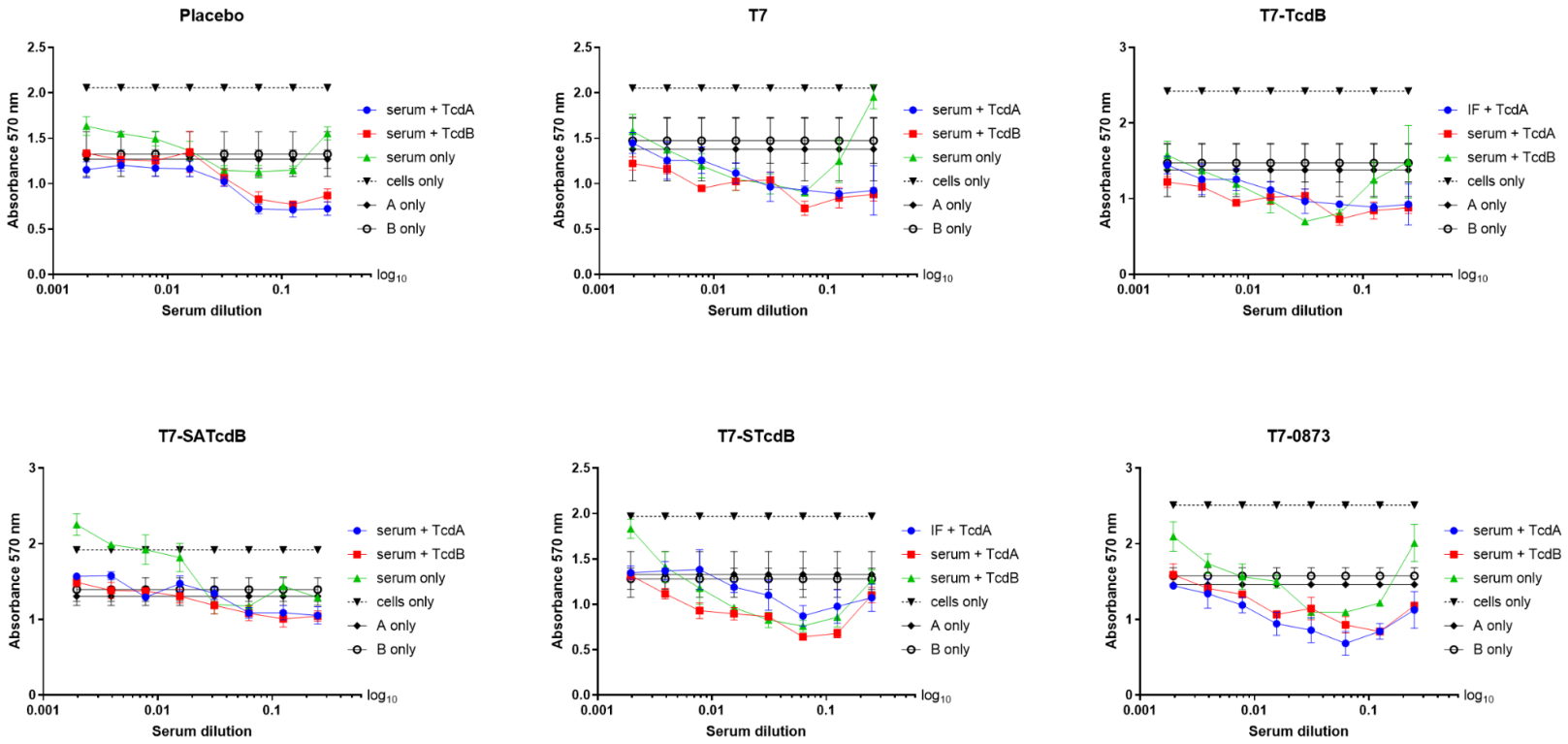


Figure 6.7: MTT assay to measure toxin neutralisation ability of serum of orally immunised hamsters. Serum dilutions (1:2 to 1:128) of hamster groups inoculated with either spores from the wild type T7 strain or spores from recombinant strains T7-TcdB, T7-STcdB. T7-SATcdB, or T7-CD0873 (n=4 for all groups) were pre-incubated with full length (FL) TcdA (50 ng/ml) or FL TcdB (0.25 ng/ml) (Public Health England). Samples were also prepared in the absence of serum in either the presence of toxins (positive controls; labelled FL TcdA and FL TcdB) or absence of toxins. (negative control; labelled Cells only) These mixes were subsequently added to Vero cells (1 x 10^5/ml). All sample dilutions were tested in triplicate. The metabolic health of cells was assessed by measuring absorbance at 570 nm.

In this experiment, no samples displayed the ability to neutralise the cytotoxicity of FL TcdA or FL TcdB.

6.3.3.1 Conclusions from immunogenicity profiles of hamsters immunised with T7 recombinant strains

The ELISAs testing for serum IgG showed that the group immunised with T7-0873 and with T7-SATcdB had significantly higher titres of IgG specific for rCD0873 and rTcdB respectively compared to the other immunised groups. Likewise the ELISA kit to detect total sIgA demonstrated a significantly higher titre of sIgA in the intestinal fluid of the T7-SATcdB-immunised group. This data supports the findings from **Chapter 5** that T7-SATcdB generated much more TcdB antigen than other strains and that this was found predominantly extracellularly. We would anticipate from this finding that the released antigen would be taken up by M cells and induce a sIgA response and potentially a serum IgG response.

Corroborating the phenotypic data for T7-0873 in **Chapter 5**, where CD0873 is abundant extracellularly, a significant serum IgG titre is found in the serum of T7-0873-immunised hamsters supporting the findings of Kayral *et al*., (2021) who found that recombinant CD0873 administered orally to hamsters elicited a strong antigen-specific serum IgG response.

The sera and intestinal fluid of hamsters immunised with T7-SATcdB and T7-0873 also reduced the ability of cells of *C. difficile* strain 630 to adhere to Caco-2 cells. The reduction was not significant which is likely due to the small group sizes used, nonetheless, a trend was evident supporting the higher titres of antibodies detected and the abundance of antigen released by these strains (**Chapter 5**). Finally, no toxin neutralisation effects were observed with any of the groups.

6.3.4 Serum IgG titres detected in immunised mice by ELISA

The titre of antigen-specific serum IgG was compared between groups by quantifying the binding of IgG to either rCD08730 or rTcdB by indirect

ELISA. 96-well plates were coated with 2.5 µg/ml of each purified antigen. Plates were incubated with serum diluted 1:5. This was followed by incubation with rabbit anti-mouse IgG H&L (HRP) at 1:1000 dilution. Absorbance was measured using TMB at 650 nm wavelength (**Figures 6.8 and 6.9**).

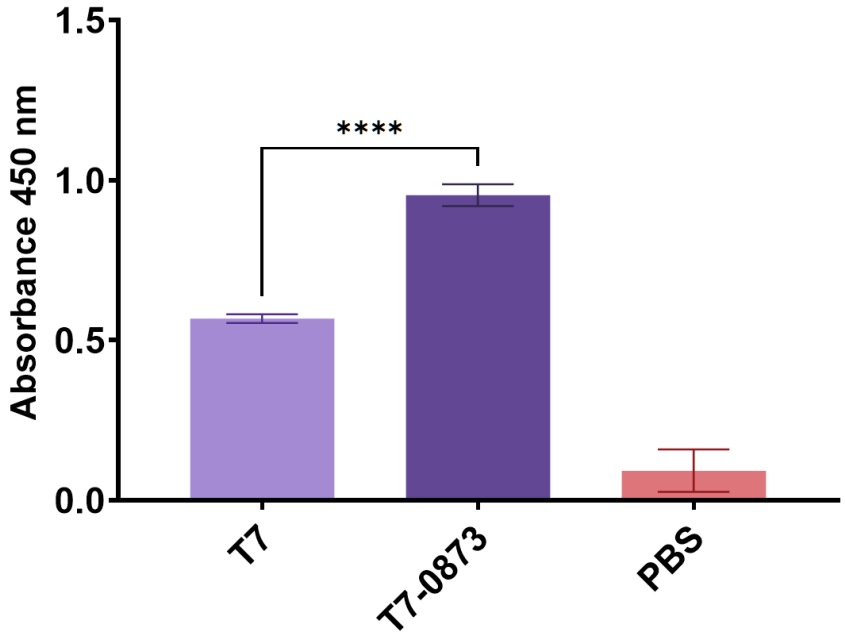


Figure 6.8: Serum IgG responses against CD0873 from orally immunised mice tested by indirect ELISA. Serum was tested for IgG by indirect ELISA using 1:5 diluted serum from mice which had been administered with either spores from the wild type T7 strain or spores from recombinant strain T7-0873 (n=4 for all groups). Using ELISA plates coated with 2.5 µg/ml of recombinant protein rCD0873, IgG responses were detected with rabbit anti-mouse IgG H&L (HRP). Two independent experiments were performed with three technical replicates. A parametric one-way ANOVA test was performed followed by Dunn's multiple comparison test. Error bars represent standard error of the mean (SEM). Statistical difference *p*-value; (****) $p < 0.0001$.

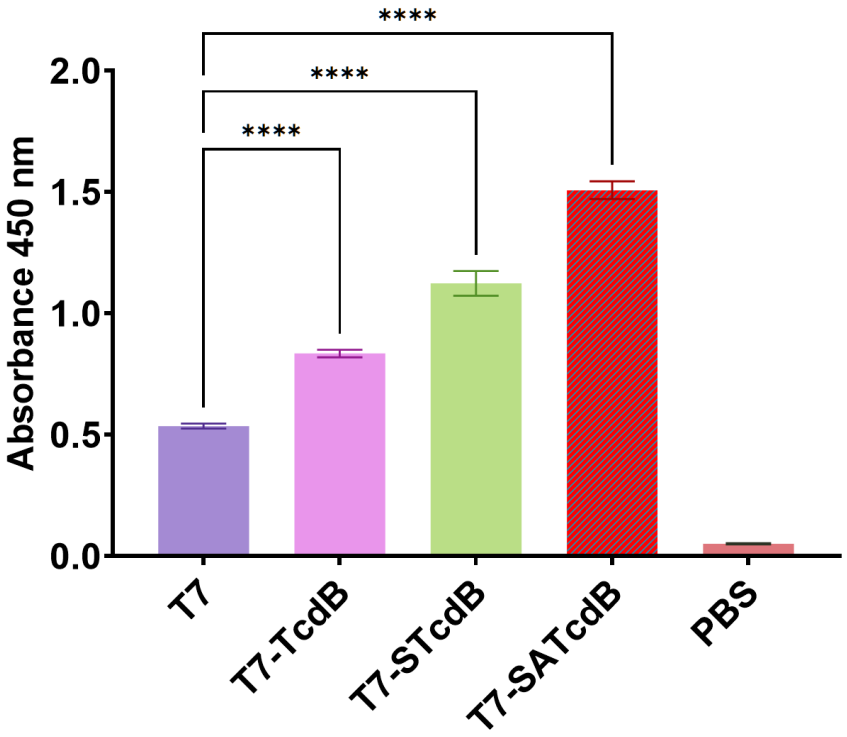


Figure 6.9: Serum IgG responses against TcdB from orally immunised mice tested by indirect ELISA. Serum was tested for IgG by indirect ELISA using 1:5 diluted serum from mice which had been administered with either spores from the wild type T7 strain or spores from recombinant strains T7-TcdB, T7-STcdB, or T7-SATcdB (n=4 for all groups). Using ELISA plates coated with 2.5 µg/ml of recombinant protein rTcdB, IgG responses were detected with rabbit anti-mouse IgG H&L (HRP). Two independent experiments were performed with three technical replicates. A parametric one-way ANOVA test was performed followed by Dunn's multiple comparison test. Error bars represent standard error of the mean (SEM). Statistical difference *p*-value; (****) $p < 0.0001$. The response seen in serum obtained from mice inoculated with wildtype T7 is unexpected as it produces no TcdB itself. It is likely therefore that this value represents the background level of non-specific binding within the assay.

The titre of antigen-specific serum IgG in mice immunised with recombinant strains were compared to that of the control group. Using a parametric one-way ANOVA test, mean absorbance values were compared. Mice immunised with T7-0873 spores showed a significantly higher IgG response when compared to the wild type T7 group when probing against rCD0873 (p <0.0001, 0.7 fold increase). When probing against rTcdB, significant differences were found between mouse groups given T7-TcdB,

T7-STcdB, and T7-SATcdB when compared to the wild type T7 ($p < 0.0001$ for all, 0.6, 1.1, and 1.8-fold increases respectively).

In order to investigate antigen-specific sIgA present in the intestinal fluid of mice, 96-well plates were coated with 2.5 µg/ml of either rTcdB or rCD0873. Plates were incubated with SIF diluted 1:20. This was followed by incubation with rabbit anti-mouse IgA H&L (HRP) at 1:1000 dilution. Absorbance was measured using TMB at 650 nm wavelength (**Figures 6.10 and 6.11**).

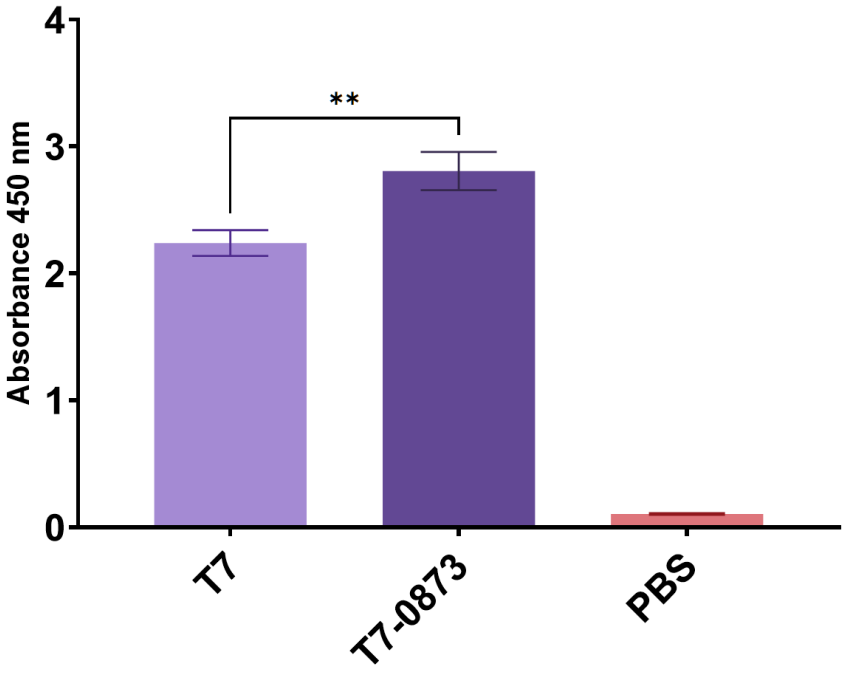


Figure 6.10: Intestinal fluid IgA responses against CD0873 from orally immunised mice tested by indirect ELISA. Small intestinal fluid (SIF) was tested for IgA by indirect ELISA using 1:20 diluted SIF from mice which had been administered with either spores from the wild type T7 strain or spores from recombinant strain T7-0873 (n=4 for all groups). Using ELISA plates coated with 2.5 µg/ml of recombinant protein rCD0873, IgA responses were detected with goat anti-mouse IgG alpha chain (HRP). Two independent experiments were performed with three technical replicates. A parametric one-way ANOVA test was performed followed by Dunn's multiple comparison test. Error bars represent standard error of the mean (SEM). Statistical difference *p*-value; (**) $p < 0.01$. It is hypothesised that T7-0873 provokes a larger antibody response than wildtype T7 because the amount of CD0873 being proceed by the recombinant strain is greater..

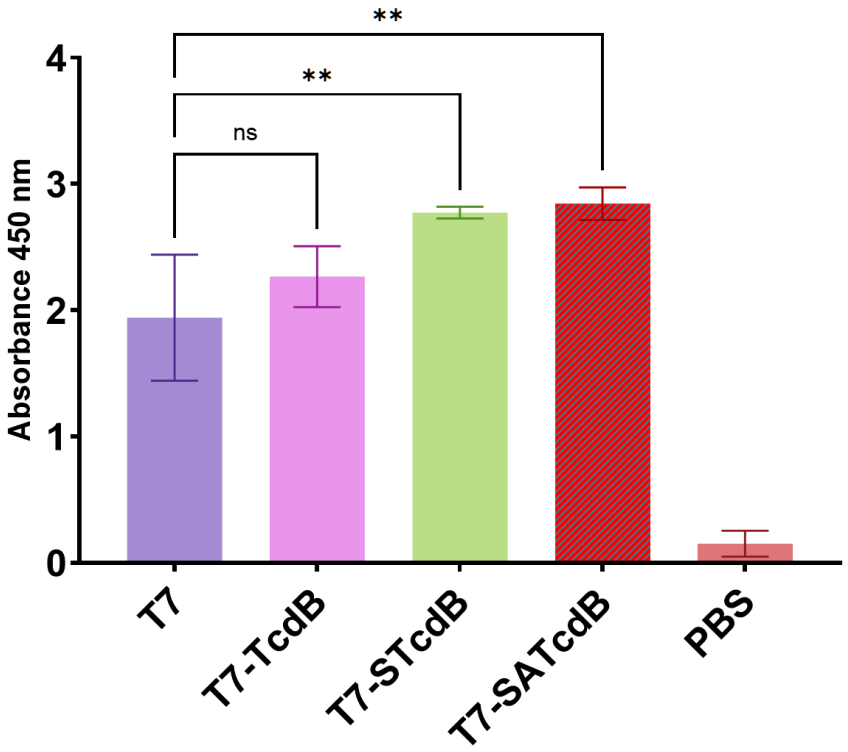


Figure 6.11: Intestinal fluid IgA responses against TcdB from orally immunised mice tested by indirect ELISA. Small intestinal fluid (SIF) was tested for IgA by indirect ELISA using 1:20 diluted SIF from mice which had been administered with either spores from the wild type T7 strain or spores from recombinant strains T7-TcdB, T7-STcdB, or T7-SATcdB (n=4 for all groups). Using ELISA plates coated with 2.5 µg/ml of recombinant protein rTcdB, IgA responses were detected with goat anti-mouse IgG alpha chain (HRP). Two independent experiments were performed with three technical replicates. A parametric one-way ANOVA test was performed followed by Dunn's multiple comparison test. Error bars represent standard error of the mean (SEM). Statistical difference *p*-value; (**) $p < 0.01$.

The titre of antigen-specific sIgA in mice immunised with recombinant strains were compared to that of the control group. Using a parametric one-way ANOVA test, mean absorbance values were compared. Mice immunised with T7-0873 spores showed a significantly higher sIgA response when compared to the wild type T7 group when probing against rCD0873 (p <0.0010, 0.25-fold increase). When probing against rTcdB, significant differences were found between mouse groups immunised with T7-STcdB and T7-SATcdB when compared to the wild type T7 (p = 0.0093, 0.4-fold increase and p =

0.0055, 0.5-fold increase respectively). However, no significant difference was observed in mice given T7-TcdB (p = 0.3958).

6.3.5 Adherence blocking of *C. difficile* CD630 to Caco-2 cells caused by immunised mouse serum and intestinal fluid

In order to test the ability of antibodies in serum and SIF of immunised groups: T7, T7-TcdB, T7-STcdB, T7-SATcdB, and T7-0873 to block adherence of *C. difficile* strain 630 to epithelial cells, an adherence blocking assay was performed using Caco-2 cells. Cells of 630 were pre-incubated with serum or SIF prior to their addition to Caco-2 cells. Adhered bacteria were determined by CFU per 100 Caco-2 cells (**Section 2.10.1.4**) (**Figures 6.12 and 6.13**).

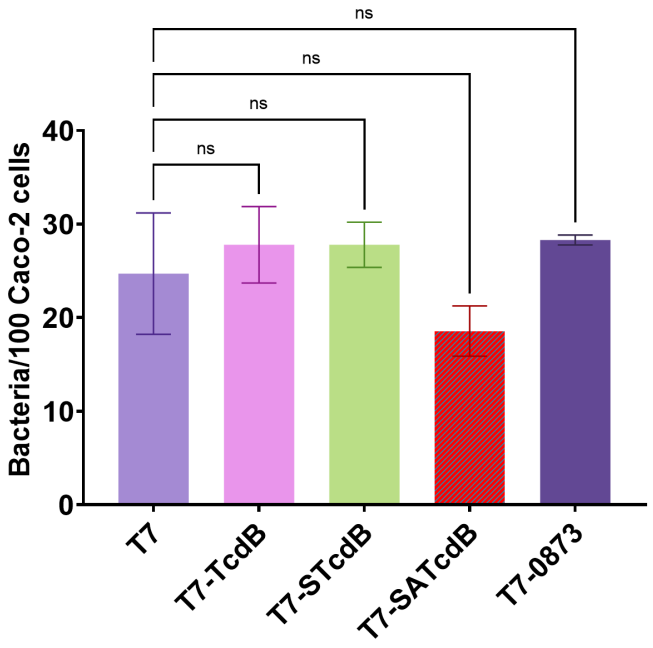


Figure 6.12: Effects of intestinal fluid from mice immunised with recombinant strains of T7 on adherence by cells of *C. difficile* strain 630 to Caco-2 cells. Adherence of *C. difficile* to Caco-2 cells when pre-incubated with small intestinal fluid (SIF) (1:2) from mice given spores of the wild type T7 strain (CDT7) or spores from recombinant strains T7-TcdB, T7-STcdB. T7-SATcdB, or T7-CD0873 (n=4 for all groups). Caco-2 cells were washed and mean numbers of adherent bacteria enumerated by CFU/100 Caco-2 cells. This assay was performed using three technical replicates. A parametric one-way ANOVA test was performed followed by a Dunn's multiple comparison test to compare means of control groups with experimental groups. Error bars represent standard error of the mean (SEM). Statistical difference *p*-value; (ns) not significant.

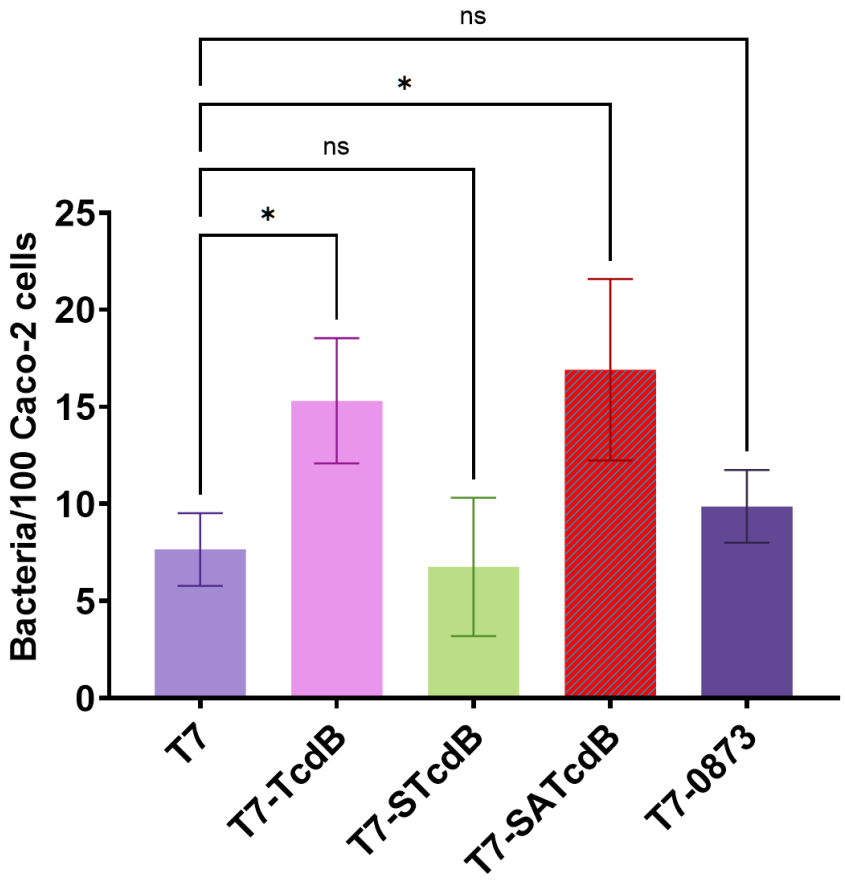


Figure 6.13: Effects of serum from mice immunised with recombinant strains of T7 on adherence by cells of *C. difficile* strain 630 to Caco-2 cells. Adherence of *C. difficile* to Caco-2 cells when pre-incubated with serum (1:5) and from mice given spores of the wild type T7 strain (CDT7) or spores from recombinant strains T7-TcdB, T7-STcdB. T7-SATcdB, or T7-CD0873 (n=4 for all groups). Caco-2 cells were washed, and mean numbers of adherent bacteria enumerated, shown by CFU/100 Caco-2 cells. This assay was performed using three technical replicates. A parametric one-way ANOVA test was performed followed by Dunn's multiple comparison test to compare means of control groups with experimental groups. Error bars represent standard error of the mean (SEM). Statistical difference *p*-value; (ns) not significant, and (*) $p < 0.05$.

Neither SIF nor serum of mice immunised with spores of recombinant strains had any statistically significant effect on reducing the amount of CD630 bound to Caco-2 cells when compared to the wild type T7 strain itself when the data were analysed by a one-way ANOVA test. Some reduction in binding ability was observed in the SIF of T7-SATcdB (0.2-fold decrease, $p = 0.2108$),

and the serum of T7-STcdB (0.1-fold decrease, $p = 0.9902$). However, these results were not found to be statistically significant compared to the wild type.

6.3.6 Toxin neutralisation ability of immunised mouse serum and intestinal fluid as assessed by MTT assay

Toxin neutralisation assays were performed to determine whether the antibodies detected in ELISA experiments were capable of preventing damage to Vero cells when exposed to full-length toxins, TcdA and TcdB (FL TdA and FL TcdB; 50 ng/ml and 0.25 ng/ml, respectively; Public Health England). The MTT assay was used as before (**Section 6.3.3**).

Using a series of 2-fold dilutions, serum and SIF were pre-incubated with FL TcdA and FL TcdB for 1 hour before being added to Vero cells seeded onto 96-well plates at a density of 1 x 10^5/ml (**Section 2.10.1.3**). Absorbance measures were taken at 570 nm wavelength.

Toxin neutralisation assays were performed in the same manner as described above (**Section 6.3.3**) using serum and SIF harvested from immunised mice (**Figures 6.14 and 6.15**).

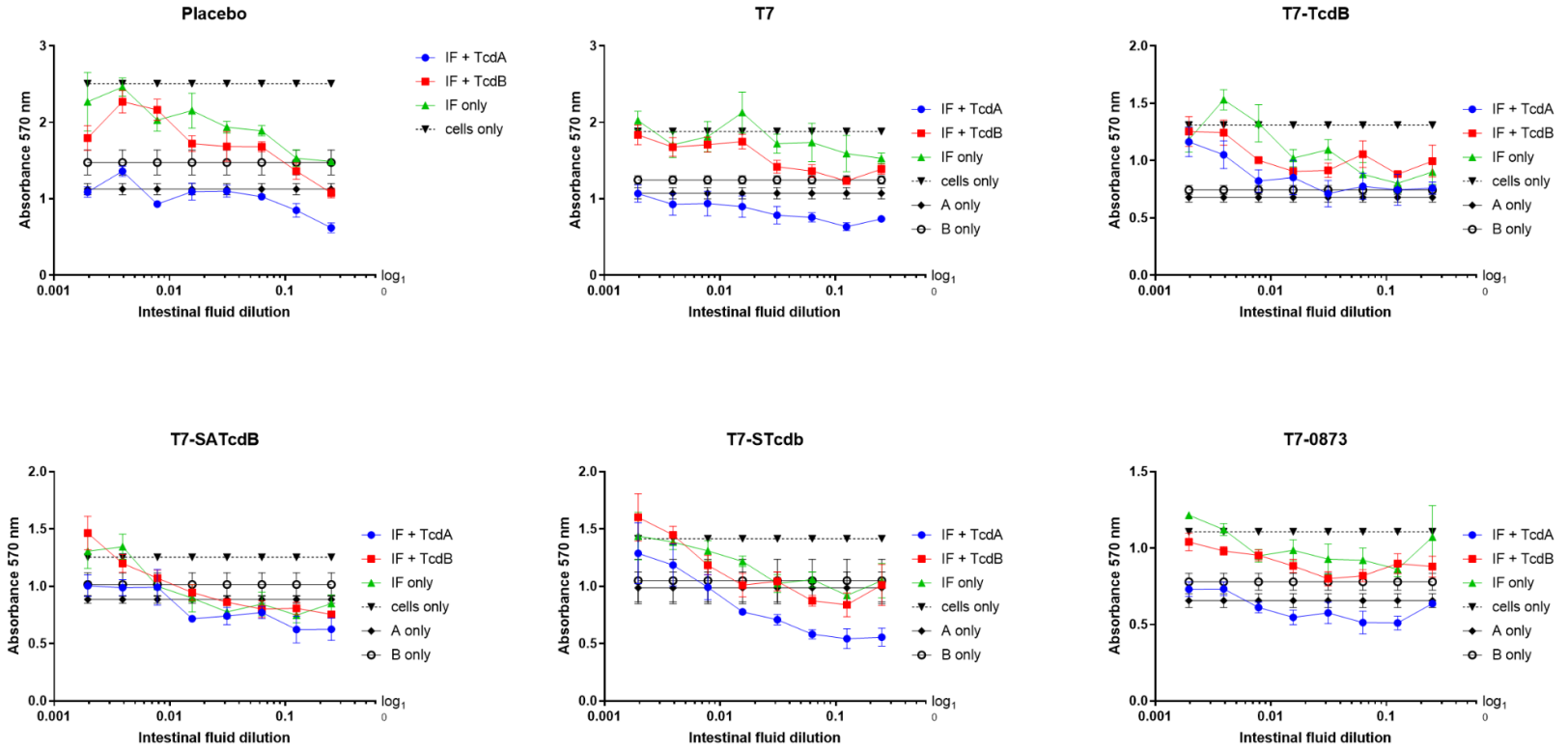


Figure 6.14: MTT assay to measure toxin neutralisation ability of intestinal fluid of orally immunised mice. Small Intestinal fluid (SIF) dilutions (1:2 to 1:128) of mouse groups administered with either spores from the wild type T7 strain or spores from recombinant strains T7-TcdB, T7-STcdB. T7-SATcdB, or T7-CD0873 (n=4 for all groups) were pre-incubated with full length (FL) TcdA (50 ng/ml) or FL TcdB (0.25 ng/ml) (Public Health England). Samples were also prepared in the absence of SIF in either the presence of toxins (positive controls; labelled FL TcdA and FL TcdB) or absence of toxins. (negative control; labelled Cells only) These mixes were subsequently added to Vero cells (1 x 10^5/ml). All sample dilutions were tested in triplicate. Metabolic activity of cells was assessed by measuring absorbance at 570 nm.

As was previously noted in MTT assays performed with hamster SIF, SIF itself has cytotoxic activity. In these experiments, SIF from mice immunised with strains T7-TcdB, T7-STcdB, and T7-SATcdB, was determined to confer some level of protection against FL TcdB as well as a minor level of protection against FL TcdA. This effect is most pronounced in the T7-SATcdB group. No protection against either toxin was observed in the wild type T7 or T7-0873 groups as expected since these strains do not express any toxin or toxin components.

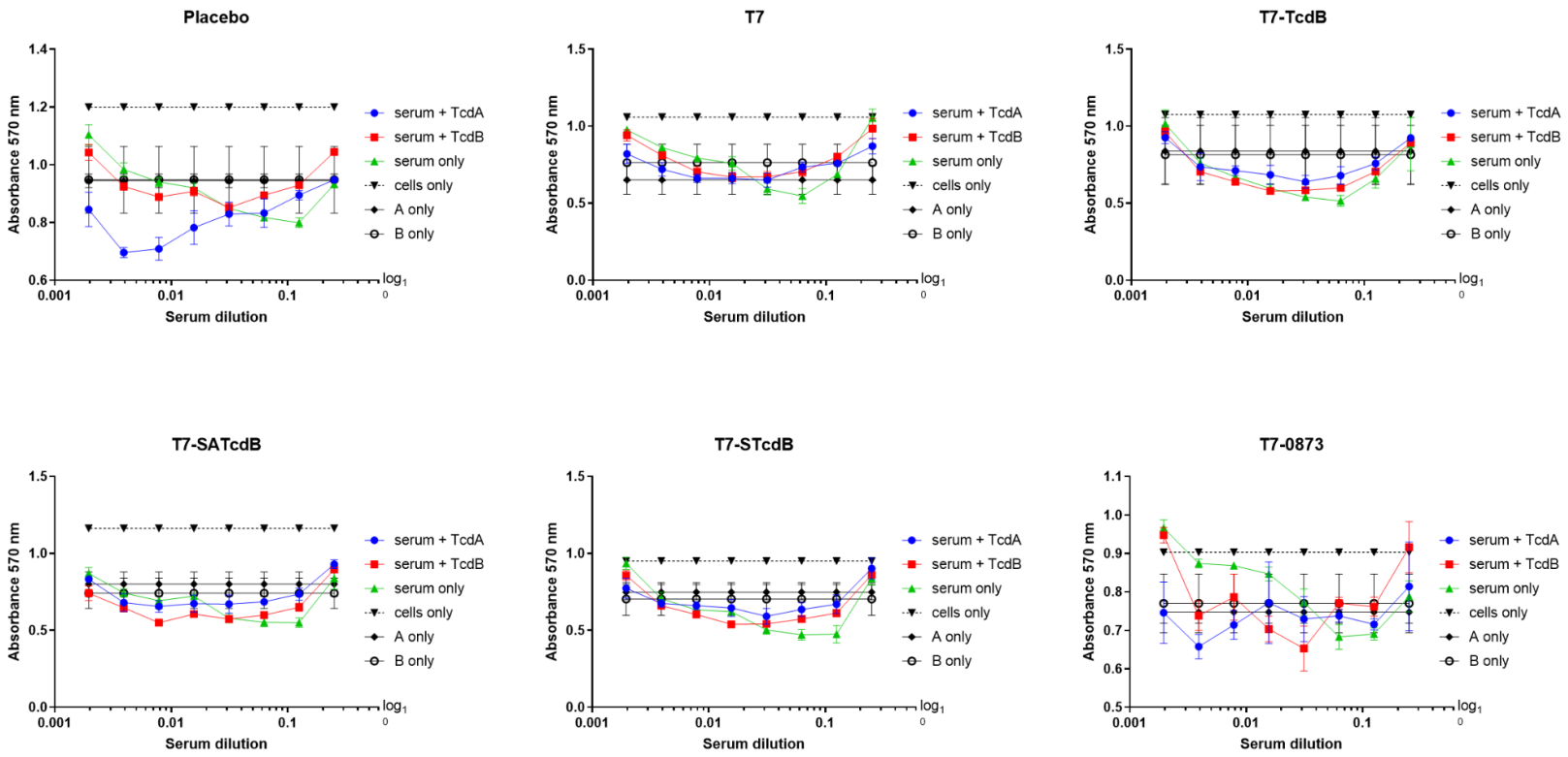


Figure 6.15: MTT assay to measure toxin neutralisation ability of serum collected from orally immunised mice. Serum dilutions (1:2 to 1:128) of hamster groups administered with either spores from the wild type T7 strain or spores from recombinant strains T7-TcdB, T7-STcdB. T7-SATcdB, or T7-CD0873 (n=4 for all groups) were preincubated with full length (FL) TcdA (50 ng/ml) and FL TcdB (0.25 ng/ml) (Public Health England). Samples were also prepared in the absence of SIF in either the presence (positive controls; labelled FL TcdA and FL TcdB) or absence (negative control; labelled Cells only) of toxins. These mixes were subsequently added to Vero cells (1 x 10^5/ml). All sample dilutions were tested in triplicate. Metabolic activity of cells was assessed by measuring absorbance at 570 nm.

In this series of experiments, no protection against FL TcdB or FL TcdA was conferred by serum from any group.

6.3.6.1 Conclusions from immunogenicity profiles of hamsters immunised with T7 recombinant strains

In this study, all recombinant strains elicited significant antigen-specific serum IgG responses compared to the wild type strain. Highest titres of IgG were observed for groups immunised with T7-0873 and T7-SATcdB corroborating the findings for the hamster study. Significant titres of sIgA were found in the intestinal fluid of mice immunised with T7-0873 and T7-SATcdB, also with T7-STcdB, with highest titres were observed for T7-0873 and T7-SATcdB groups again supporting the findings made from the hamster study.

Further corroborating data was obtained when testing for adherence blocking effects, with intestinal fluid of mice administered with T7-SATcdB showing the greatest reduction in adherence of *C. difficile* cells to Caco-2 cells, although this was not significant. As with hamsters, no toxin neutralisation was observed for any vaccinated sera or intestinal fluid of mice. The overall greater immunogenicity observed in mice compared to hamsters, with all groups showing significant antibody titres compared to the wild type control group suggest that there could be more lysis of vegetative cells in mice compared to hamsters, releasing antigen that is normally contained in the cytosol.

6.4 Discussion

The aims of this chapter were to vaccinate mice and hamsters with spores from NTCD strain T7and recombinant strains, compare antibody titres in serum and SIF in these animals and determine the functionality of these antibodies in adherence blocking and toxin neutralisation assays.

Assessment of IgG and IgA titre detected in the serum and intestinal fluid of immunised animals

Titres were different in animals immunised with recombinant spores compared with wild-type T7 spores. This was most significant in both serum and SIF harvested from animals immunised using spores from recombinant strain T7-SATcdB when probing against rTcdB, and T70873 when probing against rCD0873.

The measurement of total sIgA for hamster SIF is not a specific measure of response to *C. difficile* antigens. However, given the significance of the result and its similarity to the anti rCD0873 serum ELISA, it still allows us to infer with some confidence that T7-SATcdB has been effective in producing an immune response in this instance.

Throughout these experiments, T7-0873 and T7-SATcdB have been shown to be the most consistent in producing significantly greater antigen-specific immune responses across all assays when compared to the wild type. These data suggest the recombinant strains are functioning as hypothesised.

Assessment of the efficacy of antibodies within animal tissues to block adherence of CD630 to Caco-2 cells

Although administration of recombinant strains showed no significant prevention of CD630 binding to Caco-2 cells when compared to the wild type, the overall amount of CD630 binding is reduced. This is in agreement with previous experiments performed using this strain (Sambol *et al*., 2002; Nagaro *et al.*, 2013) where colonisation by pathogenic strains was reduced by prior administration of wild type NTCD strains including T7.

Although not statistically significant, reduction in binding was observed with strains T7-SATcdB, and T7-0873 in the SIF and serum of hamsters. This was also seen in the T7-SATcdB SIF group, and T7-STcdB serum group for mice. This possibly indicates that the amount of antibody produced was not sufficient enough to provide full protection from adherence by CD630.

A greater immune response is likely needed to achieve a higher antibody titre. This could be achieved by greater spore load being administered, and reviewing promoter activity in the overexpression constructs, making amendments where necessary.

Assessment of the efficacy of antibodies within animal tissues to prevent the cytotoxic effects of TcdA and TcdB

Reduction of cytotoxicity by FL TcdA was only observed in the SIF of mice immunised with either T7-TcdB or T7-SATcdB. This was very weak. Cross-reactivity with FL TcdA was observed, this implies the shared homology with FL TcdB is enough that only one or the other may need to be included in the finished vaccine. An alignment of the TcdB region expressed by these recombinant strains against FL TcdA confirms a shared homology of 34%. This effect is most prominently seen in SIF of mice immunised with spores of T7-TcdB and the effect was not seen in the hamster model.

It could be hypothesised that there is a greater level of *C. difficile* cell lysis occuring in the T7 strains in mice than in hamsters. As confocal microscopy has shown, T7-TcdB harbours large amounts of rTcdB within its cytosol (**Figure 5.13**). Lysis of these cells would release a large amount of rTcdB into the host which would be more easily taken up by M cells when compared to whole cells. This could be due to the hamster's effectiveness as a model for immune responses (**Section 1.6.1**).

Though an antigen-specific response was observed in the serum and SIF of both animal modes, the properties of these antibodies need to be assessed further. Most significantly, a reduction in *C. difficile* binding to Caco-2 cells was observed in both SIF and serum of the T7-TcdB and T7-SATcdB groups. This result was anticipated. It is hypothesised that immune responses caused by these strains would result in antibodies being raised against cell surface factors such as adhesins, as well as the vaccine candidate included in each construct. These antibodies will bind to the cell surface and block the attachment to host cells by *C. difficile.*

This result is very encouraging as blocking the adherence of pathogens to host tissues is a crucial part of host immunity. SIF from mice immunised with spores of recombinant strains T7-TcdB, and T7-SATcdB was found to be capable of reducing cytotoxic activity of both FL TcdB and FL TcdA but only marginally.

While encouraging, the level of response observed here does not match those necessary for effective vaccine candidates. However, the specificity of the immune response induced *in vivo* lends favour to the use of these vaccine candidates. The relative weakness of the ability to block adherence of *C. difficile* cells and block cytotoxic activity suggests the delivery mechanism needs further optimisation.

The amount of each vaccine candidate expressed by each cell could be increased by further investigation into the promoters used in each construct. T7-TcdB achieves a good level of expression using only the *p.fdx* promoter, while all other constructs encode the CD0873 promoter in combination with *p.fdx*. It is possible that these constructs could express a greater level of TcdB if the native CD0873 promoter were removed from the construct. It could also be worthwhile looking into synthetic promoters which, if highly active, could increase the level of expression above that of *p.fdx*.

Additionally, the stability of the episome plays a vital role in the proportion of the population of T7 recombinant cells which are actively able to produce the vaccine candidates. Integration of the overexpression constructs onto the main chromosome would allow the entire population to produce vaccine candidate proteins without the need for selection. This would potentially lead to a greater immune response *in vivo* as the entire population of T7 recombinant cells would produce vaccine candidates as long as they are extant within the host.

6.5 Conclusion

These results indicate promise for future work using these overexpression constructs in NTCD strains, and demonstrate the first utilisation of natively lipidated vaccine candidates in the generation of an immune response *in vivo*. Further work is needed to refine the expression of these vaccine candidates.

Chapter 7. Discussion

A recombinant non-toxigenic *Clostridioides difficile* spore vaccine directed against toxigenic *C. difficile*

Exploiting a gut commensal spore-former as a vaccine chassis strain

Spore-forming organisms found naturally in the human gut, such as the commensal organism, non-toxigenic *Clostridioides difficile*, have the potential to serve as vaccine chassis strains. Spores of *C. difficile* naturally resist the harsh conditions of the stomach (acidity and proteases) and germinate in the small intestine, specifically in the ileum where the mucosal inductive sites are located (Lawson *et al*., 2016).

These organisms can be genetically engineered to express and release heterologous vaccine antigens once they become vegetative following germination. The ability of spores to stimulate an immune response within a specific target tissue, in this case the gut, along with their thermostable properties, makes them attractive vaccine vehicles for global distribution since the requirement for cold chain transportation and storage is negated, as well as the need for needles.

To this end, we have exploited a natural non-toxigenic *C. difficile* (NTCD) strain, T7. NTCD strains have been tested in mice, hamsters and piglets where they were shown to prevent fatal CDI (Songer *et al*., 2007; Villanno *et al*., 2012; Nagaro *et al*., 2013). Based on the finding that asymptomatic colonisation by NTCD strains tends to decrease the risk of CDI in humans (Shim *et al*., 1998), most studies investigating the candidacy of NTCD as a vaccine against toxigenic *C. difficile* have focused on its utility in promoting resistance against colonisation.

A recent study exploited a NTCD strain to express a fusion protein composed of fragments of TcdA and TcdB (Wang *et al*., 2018) which these workers previously showed, in recombinant form, induced toxin neutralising

antibodies (Wang *et al*., 2015). Immunisation of hamsters with spores of the recombinant strain generated partial protection against CDI with a hypervirulent strain (Wang *et al.*, 2018). In this study, without the inclusion of any mechanism to direct secretion, it is difficult to conceive that the fusion proteins would be released from the cell unless cells were lysed in the host. Dissociation of antigen from the cell is important to facilitate uptake by M cells (i.e., the first stage of generating an intestinal immune response) and therefore inclusion of a mechanism promoting secretion of antigens could lead to increased protection against CDI.

Genome sequencing of strain T7

Illumina sequencing was conducted to generate a shotgun sequence of the T7 genome. The pathogenicity locus (PaLoc) which encodes the toxins was confirmed to be absent, instead being replaced by 115 bp of sequence. Genes encoding other *C. difficile* virulence factors that have shown promise as vaccine candidates were found to be present at a high level of sequence identity to the TCD homologues, and are therefore expected to afford some level of protection against TCD (**Table 3.2**). Indeed, a recent study showed that the membrane fraction of NTCD given as an intra-rectal vaccine in mice resulted in a 99% decrease in *C. difficile* cells in faeces compared to non-vaccinated mice, and given to hamsters, conferred a 30% increase in survival (Senoh *et al*., 2018). This implies that non-toxin factors which are conserved between NTCD and TCD strains are capable of provoking a host immune response which is effective against infection byTCD strains.

Engineering heterologous antigens to be lipidated and released from the cell surface of the vaccine strain

We set out to establish the genetic machinery required to lipidate heterologous antigens and release these from the cell, based on the observation that the lipidation of antigens can increase their immunogenicity up to 10-fold (Fletcher *et al*., 2004). The lipid moiety of bacterial lipoproteins is recognized as a danger signal by the immune system and confers intrinsic immunostimulatory properties to the attached protein.

With knowledge of the molecular pathway for lipoprotein processing, and understanding the role of the signal peptide (Karlyshev *et al*., 2015, da Silva *et al*., 2017, da Silva *et al*., 2019) the aim was to identify a lipoprotein in strain T7 that is naturally abundant in the extracellular milieu, and to engineer recombinant strains of NTCD strain with the signal peptide fused to antigens that are promising vaccine candidates.

Analysis of the extracellular proteome of strain T7 by LC-MS demonstrated that the homologue of lipoprotein CD0873 (sharing 99% sequence identity with the CD0873 of TCD strain 630) was highly abundant in the supernatant at both mid-log phase and early stationary phase. This supports previous findings of Cafardi *et al.*, (2013) who found that CD0873 among 4 other lipoproteins was present in culture supernatants of TCD strain 630. CD0873 is known to be a surface-exposed colonisation factor (Kovacs-Simon *et al*., 2014) which has been shown to be highly immunogenic in parenterally immunised mice (Bradshaw *et al*., 2019).

In the Griffin lab, when recombinant CD0873 was delivered orally to hamsters, it elicited a strong intestinal sIgA response and an antigen-specific serum IgG response with activity in blocking adherence of cells of *C. difficile* to Caco-2 cells (Karyal *et al*., 2021). Furthermore, CD0873-orally vaccinated hamsters were partially protected from infection by a hypervirulent strain of *C. difficile* (Karyal *et al*., 2021).

Exploiting the propensity of CD0873 to be released in the extracellular milieu, its signal peptide was fused in frame with the vaccine candidates, here the terminal portion of the receptor binding domains of TcdA and TcdB since these fragments of both TcdA and TcdB have previously been shown to be immunogenic (Wang, *et al.,* 2015; Liu *et al*., 2017). Expression plasmids were created using the pMTL8000 series of modular plasmids. These allow for easy switching of origins of replication and antibiotic resistance markers for bespoke applications. Here pMTL84123 was utilised, which encodes the pCD6 origin of replication from *C. difficile,* and the p15a origin of replication from *E. coli*.

These fusions were expressed episomally under the native CD0873 promoter, and *p.fdx* promoter in the backbone vector. Including an *Xba*I restriction site between the signal peptide and vaccine candidate resulted in a new signal peptidase II cleavage recognition site as strongly predicted by the lipoprotein prediction programme, LipoP, suggesting this fusion protein should be successfully processed as a lipoprotein.

Given that incorporation of the protein sequence immediately downstream of the signal peptide (the anchor peptide) facilitates a higher level of expression of fusion proteins (Chen *et al*., 2009), constructs were made incorporating both signal and anchor peptide of CD0873 fused in frame with the vaccine candidates. As a control, the TcdB domain was also cloned with its own start codon. We would expect this protein to be localised in the cytoplasm only due to lack of mechanism for translocation out of the cytosol. STcdB possesses the CD0873 SP and its N-terminal cysteine resulting in a functional SP when fused to the TcdB fragment with the *Xba*I site. This is recognised by SPII, as predicted by LipoP. This should result in lipidation and SP cleavage before secretion into the extracellular milieu. T7-SATcdB also possesses a functional SP and should therefore be processed in the same manner as STcdB. However, the presence of both processed and unprocessed forms within the supernatant as detected by Western immunoblotting would suggest that only part of the population is able to be processed, this is possibly due to the amount that is being produced when compared to STcdB (**Figure 7.1**).

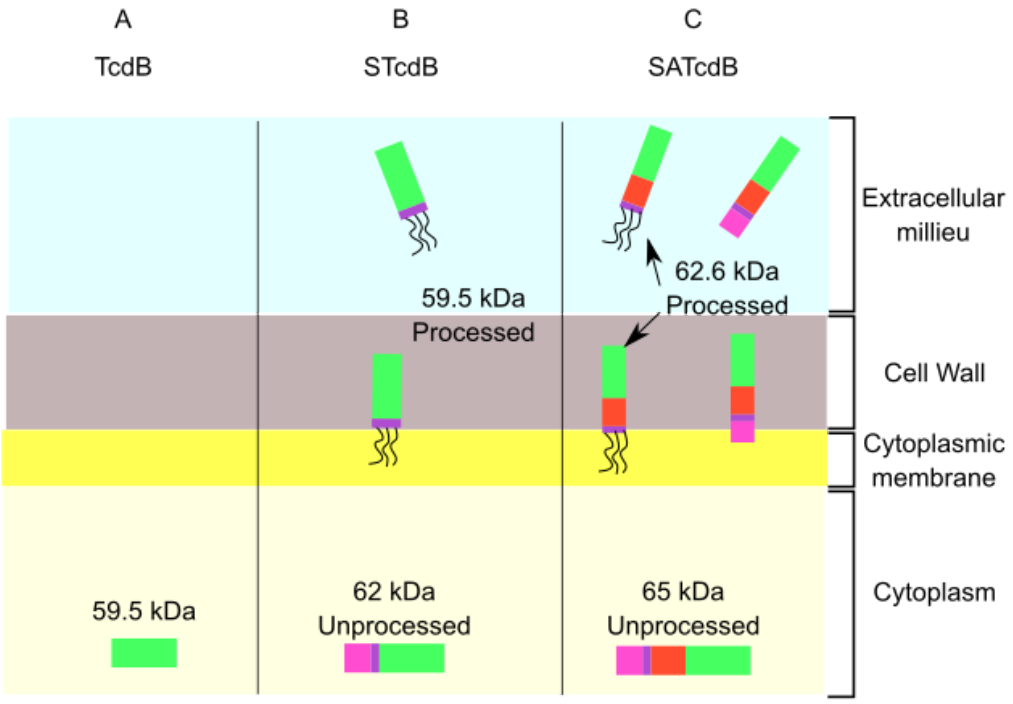


Figure 7.1: Model for the processing and localisation of the TcdB domain of recombinant strains of T7. A. T7-TcdB. The native coding sequence of the TcdB fragment (green) contains no signal peptide (SP) and therefore should only be localised within the cytoplasm. B. T7-STcdB. The presence of the CD0873 SP (pink) and its N-terminal cysteine (purple) results in a functional SP which is recognised by SPII, as predicted by LipoP. This should result in lipidation (represented by black lines) and SP cleavage before secretion into the extracellular milieu. C. T7-SATcdB also possesses a functional SP and should therefore be processed in the same manner as STcdB. However, the presence of both processed and unprocessed forms within the supernatant detected by Western immunoblotting would suggest that only part of the population is able to be processed, this is possibly due to the amount that is being produced when compared to STcdB.

In addition, the full length CD0873 gene was cloned into pMTL84123 (including its putative native promoter) to produce a strain which would overexpress CD0873. This would take advantage of its previously observed immunogenicity and provoke an immune response against this essential colonisation factor expressed by TCD strains (Karyal *et al*., 2021).

All constructs with the exception of SATcdA were successfully conjugated into T7, giving rise to recombinant strains T7-TcdB, T7-STcdB,

T7-SATcdB, and T7-0873. The relative ease with which the other constructs were conjugated would suggest that the problem lies with the SATcdA construct itself. It could be hypothesised that because the *p.fdx* promoter is active in *E. coli* enough of the toxin fragment is synthesised that it has a toxic effect upon the *E. coli* cell. Previous attempts in the Griffin lab to express this fragment of TcdA in *E. coli* have also been unsuccessful suggesting the fragment is not well tolerated well by *E. coli* and therefore too few cells survive in order to successfully conjugate with *C. difficile.* It is worth noting that in both scenarios where RBD has been stably expressed within *E. coli* the ColE1 origin of replication was used (Huang, *et al.,* 2015; Wang, *et al.,* 2018), whereas the p15a origin was used in this study. It is possible that the copy number conferred by the origin affects the level of toxin domain produced adversely affecting *E. coli.*

Phenotypic characterisation of *C. difficile* antigens in recombinant T7 strains

Following conjugation of constructs into T7 and confirmation by PCR and sequencing, Western immunoblots were conducted on whole cell lysates and supernatants of recombinant strains. For strain T7-TcdB, a strong level of TcdB was detected in whole cell lysates but very little in the supernatant (**Figure 5.11**). This was expected due to the lack of mechanism for translocation out of the cytosol. For T7-STcdB, a lower level of TcdB was detected, with its size corresponding to fully processed (cleaved) TcdB-fusion lipoprotein, with comparable levels of localisation in both whole cell lysates and supernatant. For T7-SATcdB, a strong level of TcdB was detected corresponding in size to both processed and unprocessed forms (predominantly processed), with the majority localising to the supernatant. This suggests that a portion of the SATcdB being produced is unable to be processed by the cell, likely due to the amount of antigen being produced. This would also explain why we see non-processed TcdB in the extracellular milieu. The hydrophobic properties of the retained SP of the non-processed form may facilitate its integration into the plasma membrane and some sloughing off from the cell into the supernatant. The observed difference in expression levels between

T7-STcdB and T7-SATcdB is congruent with the work performed by Chen *et al.* in 2009 where the inclusion of the AP of a meningococcal lipoprotein, in addition to its SP was necessary to permit expression of the fused antigen (Dengue envelope protein). Upon analysis of individual cells of T7-SATcdB by confocal microscopy, the presence of TcdB on its cell surface was clearly detected, unlike cells of T7-STcdB or T7-TcdB (**Figure 5.13**). However, FACS analysis of whole populations of cells of T7-SATcdB showed no significant difference to the negative control strain T7 with regard to TcdB surface expression. This indicates further optimisation of the FACS protocol is necessary as the confocal microscopy result was observed several times.

For T7-0873, CD0873 was detected in both whole cell lysates and the supernatant (as observed for T7 which expresses native levels of CD0873). However, FACS analysis revealed that a higher level of CD0873 localised to the cell surface of T7-0873 compared with T7 (**Figure 5.13**). This suggests the recombinant strain is producing a higher amount of CD0873 than that of the wild type strain.

***In vivo* immunogenicity studies**

Mice and hamsters were immunised orally with 1 x 10^6 spores of each recombinant strain; T7-CD0873, T7-TcdB, T7-STcdB and T7-SATcdB and of the parent T7 strain 3 times 2 weeks apart and intestinal fluid and sera were harvested 2 weeks after the last immunisation.

Analysis of the small intestinal fluid (SIF) and serum harvested from these animals showed that both serum IgG and secretory IgA titres were increased when compared to the wild type. This was most significant in both serum and SIF harvested from animals immunised using spores from recombinant strain T7-SATcdB when probing against rTcdB, and T7-0873 when probing against rCD0873. These results correlate with the results of Western immunoblotting performed in **Chapter 5** (**Figures 5.11 and 5.12**) where both T7-0873 and T7-SATcdB were found to release large amounts of their respective antigen into the extracellular milieu. This will have increased the chances of antigen being taken up by M cells inducing subsequent immune

responses. In addition, the presence of the lipid moiety is expected to enhance the immunogenicity of the covalently attached antigen (Fletcher et al., 2004).

The results of the adherence blocking assay for the parent T7 strain (broadly) supports previous work demonstrating the ability of NTCD immunisation to block adherence to epithelial cells by TCD cells (Sambol *et al.,* 2002; Nagaro *et al.,* 2013; Gerding *et al.,* 2015). The blocking property was more pronounced in tissues taken from animals immunised with either T7-0873 or T7-SATcdB, demonstrating the effectiveness of the engineered lipidated antigens that are likely released from cells *in vivo*.

Toxin-blocking assays revealed a minor reduction in toxin activity observed in the SIF of mice only that had been immunised with either T7-TcdB or T7-SATcdB. In these samples, cross-reactivity against TcdA was also observed. Though the delivery mechanism appears to be effective, an increase in antigen production is required to elicit a stronger toxin neutralisation immune response *in vivo.*

Further work

The next step in this study would be to perform a challenge study to demonstrate the protective efficacy of immunised animals against CDI after challenge with a TCD strain. Previous work has indicated that immunisation using NTCD has a significant effect on the level of TCD colonisation in a host (Sambol *et al.,* 2002; Nagaro *et al.,* 2013; Gerding *et al.,* 2015) and it would be of interest to see if introduction of these strains would have an additive effect on this.

The plasmid pMTL84123 used for this project was suitable for expressing TcdB fusion constructs in strain T7 but not for TcdA fusion constructs. It could be hypothesised that use of a different *E. coli* replication origin would have affected the ease with which the SATcdA construct was conjugated into T7. Given the ability of a specific origin to influence the efficiency of replication and plasmid copy number in the host, altering the Gram positive replication origin could have an effect on the copy number of the plasmid within the engineered *C. difficile* strain, and in turn the amount of

antigen produced by the specific transconjugant. As such, creation of a panel of plasmids featuring different Gram negative and Gram positive replicons would allow investigation into the most effective combination in terms of ease of conjugation into T7 and level of antigen produced.

In this study, the *p.fdx* promoter was used to drive expression of the heterologous proteins or fusion proteins. However, it is unknown whether this promoter was the most suitable option. As with replicons, had there been more time, an investigation into the strength of other promoters on antigen expression level would have been conducted.

Here, constructs were maintained episomally. In the absence of antibiotic selection, it is unknown how long plasmids will be stably maintained. Previous work has been performed utilising allelic coupled exchange (ACE) (Ng *et al.*, 2013) and, more recently, CRISPR (S. Wang *et al.*, 2018) to insert desired nucleotide sequences into the chromosome of *C. difficile* at the *pyrE* (uracil biosynthesis) and *spo0A* (sporulation regulation) loci respectively. Integration of the fusion constructs into the chromosome would eliminate the possibility of plasmid loss *in vivo* due to lack of selective pressure and negate the requirement for an antibiotic resistance cassette. However, it would also mean a reduction in the level of expression owing to the fact that there would only be one copy per genome, whereas plasmids exist as multiple copies per cell. It would therefore be of importance to assess the level of expression of these strains compared to strains harbouring plasmids. As such, the studies described in this thesis would need to be repeated with the integrated strains to assess their efficacy.

Here, mice and hamsters were immunised orally with 1 x 10^6 spores of each recombinant strain 3 times 2 weeks apart and intestinal fluid and sera harvested 2 weeks after the last immunisation. An investigation into the optimal number of spores used to immunise animal models should be performed to confirm whether the dosage used is sufficient to elicit the necessary immune response. It would also be of interest to investigate the effect of immunising animals using a combination of recombinant strains

harbouring different antigens to assess whether the elicited response is greater than immunisation with individual strains.

In conclusion, this thesis provides important proof-of-concept data for use of NTCD strains as a delivery device for vaccines. These findings pave the way for exploiting the ability of the signal peptide of CD0873 to lipidate and secrete attached antigens to the extracellular milieu. Results from antibody titre, adhesion-blocking and toxin-neutralising experiments indicate that immune responses against these vaccine candidates are antigen-specific, providing a strong body of evidence for continued development of this vaccine strategy.

8. References

Aubry, Annie., Zou, Wei., Vinogradov, Evguenii., Williams, Dean.,Chen, Wangxue., Harris, Greg., Zhou, Hongyan., Schur, Melissa J., Gilbert, Michel., Douce, Gillian R., Logan, Susan M.. 2020. *In vitro* production and immunogenicity of a *Clostridium difficile* spore-specific BclA3 glycopeptide conjugate vaccine. *Vaccines*. 8, 73.

Abhyankar, W., Hossain, A.H., Djajasaputra, A., Permpoonpattana, P., ter Beek, A., Dekker, H.L., Cutting, S.M., Brul, S., de Koning, L.J. and de Koster, C.G. 2013. In pursuit of protein targets: Proteomic characterization of bacterial spore outer layers. *J Proteome Res*. 12, 4507–4521.

Adler, A., Miller-Roll, T., Bradenstein, R., Block, C., Mendelson, B., Parizade, M., Paitan, Y., Schwartz, D., Peled, N., Carmeli, Y. and Schwaber, M.J. 2015. A national survey of the molecular epidemiology of *Clostridium difficile* in Israel: The dissemination of the ribotype 027 strain with reduced susceptibility to vancomycin and metronidazole. *Diagn Microbiol Infect Dis*. 83, 21–24.

Adlerberth, I., Huang, H., Lindberg, E., Åberg, N., Hesselmar, B., Saalman, R., Nord, C.E., Wold, A.E. and Weintraubb, A. 2014. Toxin-producing *Clostridium difficile* strains as long-term gut colonizers in healthy infants. *J Clin Microbiol*. 52, 173–179.

Aktories, K., Schwan, C. and Jank, T. 2017. *Clostridium difficile* toxin biology. *Annu Rev Microbiol*. 71, 281–307.

Alang, N. and Kelly, C.R. 2015. Weight gain after fecal microbiota transplantation. *Open Forum Infect Dis*. 2, ofv004.

Alves Feliciano, C., Douché, T., Giai Gianetto, Q., Matondo, M., Martin-Verstraete, I. and Dupuy, B. 2019. CotL, a new morphogenetic spore coat protein of *Clostridium difficile*. *Environ Microbiol*. 21, 984–1003.

Babcock, G.J., Broering, T.J., Hernandez, H.J., Mandell, R.B., Donahue, K., Boatright, N., Stack, A.M., Lowy, I., Graziano, R., Molrine, D., Ambrosino, D.M. and Thomas, W.D. 2006. Human monoclonal antibodies directed against toxins A and B prevent *Clostridium difficile*-induced mortality in hamsters. *Infect Immun*. 74, 6339–47.

Bafeta, A., Yavchitz, A., Riveros, C., Batista, R. and Ravaud, P. 2017. Methods and reporting studies assessing fecal microbiota transplantation a systematic review. *Ann Intern Med*. 167, 34–39.

Barketi-Klai, A., Hoys, S., Lambert-Bordes, S., Collignon, A. and Kansau, I. 2011. Role of fibronectin-binding protein A in *Clostridium difficile* intestinal colonization. *J Med Microbiol*. 60, 1155–1161.

Bartlett, J.G., Onderdonk, A.B., Cisneros, R.L. and Kasper, D.L. 1977. Clindamycin-associated colitis due to a toxin-producing species of Clostridium in hamsters. *J Infect Dis*. 136, 701–705.

Battaglioli, E.J., Hale, V.L., Chen, J., Jeraldo, P., Ruiz-Mojica, C., Schmidt, B.A., Rekdal, V.M., Till, L.M., Huq, L., Smits, S.A., Moor, W.J., Jones-Hall, Y., Smyrk, T., Khanna, S., Pardi, D.S., Grover, M., Patel, R., Chia, N., Nelson, H., Sonnenburg, J.L., Farrugia, G. and Kashyap, P.C. 2018. *Clostridioides difficile* uses amino acids associated with gut microbial dysbiosis in a subset of patients with diarrhea. *Sci Transl Med*. 10, eaam7019.

di Bella, S., Ascenzi, P., Siarakas, S., Petrosillo, N. and di Masi, A. 2016. *Clostridium difficile* toxins A and B: Insights into pathogenic properties and extraintestinal effects. *Toxins*. 8, 1–25.

Best, E.L., Freeman, J. and Wilcox, M.H. 2012. Models for the study of *Clostridium difficil*e infection. *Gut Microbes*. 3, 145–167.

Bézay, N., Ayad, A., Dubischar, K., Firbas, C., Hochreiter, R., Kiermayr, S., Kiss, I., Pinl, F., Jilma, B. and Westritschnig, K. 2016. Safety, immunogenicity and dose response of VLA84, a new vaccine candidate against *Clostridium difficile*, in healthy volunteers. *Vaccine*. 34, 2585–2592.

Bignardi, G.E. 1998. Risk factors for *Clostridium difficile* infection. *J Hosp Infect*. 40, 1–15.

Bilsborough, J. and Viney, J.L. 2004. Gastrointestinal dendritic cells play a role in immunity, tolerance, and disease. *Gastroenterology*. 127, 300–309.

Boyaka, P.N. 2017. Inducing mucosal IgA: A challenge for vaccine adjuvants and delivery systems. *J Immunol*. 199, 9–16.

Bradshaw, W.J., Bruxelle, J.-F.F., Kovacs-Simon, A., Harmer, N.J., Janoir, C., Pechine, S., Acharya, K.R., Michell, S.L., Péchiné, S., Acharya, K.R. and Michell, S.L. 2019. Molecular features of lipoprotein CD0873 – a potential vaccine against the human pathogen *Clostridioides difficile* . *J Biol Chem*. 294, 15850–15861.

Brandtzaeg, P. and Prydz, H. 1984. Direct evidence for an integrated function of J chain and secretory component in epithelial transport of immunoglobulins. *Nature*. 311, 71–73.

Broecker, F. Martin C. E. Wegner, E. Mattner, J. Baek, J. Y. Pereira, C. L. Anish, C. Seeberger, P. H. 2016. Synthetic lipoteichoic acid glycans are potential vaccine candidates to protect from *Clostridium difficile* infections. *Cell Chem Biol.* 23, 1014–22

Brülle, J.K., Tschumi, A. and Sander, P. 2013. Lipoproteins of slow-growing Mycobacteria carry three fatty acids and are N-acylated by Apolipoprotein N-Acyltransferase BCG-2070c. *BMC Microbiol*. 13, 1–15.

Bruxelle, J.F., Mizrahi, A., Hoÿs, S., Collignon, A., Janoir, C. and Péchiné, S. 2017. *Clostridium difficile* flagellin FliC: Evaluation as adjuvant and use in a mucosal vaccine against *Clostridium difficile*. *PLoS One*. 12, e0187212.

Buddelmeijer, N. 2015. The molecular mechanism of bacterial lipoprotein modification-How, when and why? *FEMS Microbiol Rev*. 39, 246–261.

Buffie, C.G., Bucci, V., Stein, R.R., McKenney, P.T., Ling, L., Gobourne, A., No, D., Liu, H., Kinnebrew, M., Viale, A., Littmann, E., van den Brink, M.R.M., Jenq, R.R., Taur, Y., Sander, C., Cross, J.R., Toussaint, N.C., Xavier, J.B. and Pamer, E.G. 2015. Precision microbiome reconstitution restores bile acid mediated resistance to *Clostridium difficile*. *Nature*. 517, 205–208.

Cafardi, V., Biagini, M., Martinelli, M., Leuzzi, R., Rubino, J.T., Cantini, F., Norais, N., Scarselli, M., Serruto, D. and Unnikrishnan, M. 2013. Identification of a novel zinc metalloprotease through a global analysis of *Clostridium difficile* extracellular proteins M. Skurnik, ed. *PLoS One*. 8, e81306.

Calabi, E., Calabi, F., Phillips, A.D. and Fairweather, N.F. 2002. Binding of *Clostridium difficile* surface layer proteins to gastrointestinal tissues. *Infect Immun*. 70, 5770–5778.

Calabi, E., Ward, S., Wren, B., Paxton, T., Panico, M., Morris, H., Dell, A., Dougan, G. and Fairweather, N. 2001. Molecular characterization of the surface layer proteins from *Clostridium difficile*. *Mol Microbiol*. 40, 1187–1199.

Calderón-Romero, P., Castro-Córdova, P., Reyes-Ramírez, R., Milano-Céspedes, M., Guerrero-Araya, E., Pizarro-Guajardo, M., Olguín-Araneda, V., Gil, F. and Paredes-Sabja, D. 2018. *Clostridium difficile* exosporium cysteine-rich proteins are essential for the morphogenesis of the exosporium layer, spore resistance, and affect *C. difficile* pathogenesis T. M. Koehler, ed. *PLoS Pathog*. 14, e1007199.

Cerquetti, M., Molinari, A., Sebastianelli, A., Diociaiuti, M., Petruzzelli, R., Capo, C. and Mastrantonio, P. 2000. Characterization of surface layer proteins from different *Clostridium difficile* clinical isolates. *Microb Pathog*. 28, 363–372.

Chandrasekaran, R. and Lacy, D.B. 2017. The role of toxins in *Clostridium difficile* infection. *FEMS Microbiol Rev*. 41, 723–750.

Chapman, S.M.O. 2020. *Identification and characterisation of novel bacteriocins active against Clostridioides difficile.* PhD Thesis, University of Nottingham, Nottingham

Charlton, T.M., Kovacs-Simon, A., Michell, S.L., Fairweather, N.F. and Tate, E.W. 2015. Quantitative lipoproteomics in *Clostridium difficile* reveals a role for lipoproteins in sporulation. *Chem Biol*. 22, 1562–1573.

Chen, H.W., Liu, S.J., Liu, H.H., Kwok, Y., Lin, C.L., Lin, L.H., Chen, M.Y., Tsai, J.P., Chang, L.S., Chiu, F.F., Lai, L. wei, Lian, W.C., Yang, C.Y., Hsieh, S.Y., Chong, P. and Leng, C.H. 2009. A novel technology for the production of a heterologous lipoprotein immunogen in high yield has implications for the field of vaccine design. *Vaccine*. 27, 1400–1409.

Chen, J. and Griffiths, M.W. 1998. PCR differentiation of *Escherichia coli* from other Gram-negative bacteria using primers derived from the nucleotide sequences flanking the gene encoding the universal stress protein. Lett Appl Microbiol. 27, 369–371.

Chen, X., Katchar, K., Goldsmith, J.D., Nanthakumar, N., Cheknis, A., Gerding, D.N. and Kelly, C.P. 2008. A mouse model of *Clostridium difficile*–associated disease. *Gastroenterology*. 135, 1984–1992.

Ciesla, W.P. and Bobak, D.A. 1998. *Clostridium difficile* toxins A and B are cation-dependent UDP-glucose hydrolases with differing catalytic activities. *J Biol Chem*. 273, 16021–16026.

Cohen, S.H., Tang, Y.J. and Silva, Jr., J. 2000. Analysis of the pathogenicity locus in *Clostridium difficile* strains. *The J Infect Dis*. 181, 659–663.

Consortium, T.U., Bateman, A., Martin, M.-J., Orchard, S., Magrane, M., Agivetova, R., Ahmad, S., Alpi, E., Bowler-Barnett, E.H., Britto, R., Bursteinas, B., Bye-A-Jee, H., Coetzee, R., Cukura, A., da Silva, A., Denny, P., Dogan, T., Ebenezer, T., Fan, J., Castro, L.G., Garmiri, P., Georghiou, G., Gonzales, L., Hatton-Ellis, E., Hussein, A., Ignatchenko, A., Insana, G., Ishtiaq, R., Jokinen, P., Joshi, V., Jyothi, D., Lock, A., Lopez, R., Luciani, A., Luo, J., Lussi, Y., MacDougall, A., Madeira, F., Mahmoudy, M., Menchi, M., Mishra, A., Moulang, K., Nightingale, A., Oliveira, C.S., Pundir, S., Qi, G., Raj, S., Rice, D., Lopez, M.R., Saidi, R., Sampson, J., Sawford, T., Speretta, E., Turner, E., Tyagi, N., Vasudev, P., Volynkin, V., Warner, K., Watkins, X., Zaru, R., Zellner, H., Bridge, A., Poux, S., Redaschi, N., Aimo, L., Argoud-Puy, G., Auchincloss, A., Axelsen, K., Bansal, P., Baratin, D., Blatter, M.-C., Bolleman, J., Boutet, E., Breuza, L., Casals-Casas, C., de Castro, E., Echioukh, K.C., Coudert, E., Cuche, B., Doche, M., Dornevil, D., Estreicher, A., Famiglietti, M.L., Feuermann, M., Gasteiger, E., Gehant, S., Gerritsen, V., Gos, A., Gruaz-Gumowski, N., Hinz, U., Hulo, C., Hyka-Nouspikel, N., Jungo, F., Keller, G., Kerhornou, A., Lara, V., le Mercier, P., Lieberherr, D., Lombardot, T., Martin, X., Masson, P., Morgat, A., Neto, T.B., Paesano, S., Pedruzzi, I., Pilbout, S., Pourcel, L., Pozzato, M., Pruess, M., Rivoire, C., Sigrist, C., Sonesson, K., Stutz, A., Sundaram, S., Tognolli, M.,

Verbregue, L., Wu, C.H., Arighi, C.N., Arminski, L., Chen, C., Chen, Y., Garavelli, J.S., Huang, H., Laiho, K., McGarvey, P., Natale, D.A., Ross, K., Vinayaka, C.R., Wang, Q., Wang, Y., Yeh, L.-S., Zhang, J., Ruch, P. and Teodoro, D. 2021. UniProt: the universal protein knowledgebase in 2021. *Nucleic Acids Res*. 49, D480–D489.

Cornely, O.A., Crook, D.W., Esposito, R., Poirier, A., Somero, M.S., Weiss, K., Sears, P. and Gorbach, S. 2012. Fidaxomicin versus vancomycin for infection with *Clostridium difficile* in Europe, Canada, and the USA: A double-blind, non-inferiority, randomised controlled trial. *Lancet Infect Dis*. 12, 281–289.

Corthier, G., Muller, M.C., Wilkins, T.D., Lyerly, D. and L'Hardion, R. 1991. Protection against experimental pseudomembranous colitis in gnotobiotic mice by use of monoclonal antibodies against *Clostridium difficil*e toxin A. *Infect Immun*. 59, 1192–1195.

Corthsy, B. 2009. Secretory immunoglobulin A: Well beyond immune exclusion at mucosal surfaces. *Immunopharmacol Immunotoxicol*. 31, 174–179.

Corver, J., Bakker, D., Brouwer, M.S.M., Harmanus, C., Hensgens, M.P., Roberts, A.P., Lipman, L.J.A., Kuijper, E.J. and van Leeuwen, H.C. 2012. Analysis of a *Clostridium difficile* PCR ribotype 078 100 kilobase island reveals the presence of a novel transposon, Tn6164. *BMC Microbiol*. 12, 130.

Cowardin, C.A., Jackman, B.M., Noor, Z., Burgess, S.L., Feig, A.L. and Petri, W.A. 2016. Glucosylation drives the innate inflammatory response to *Clostridium difficile* toxin A. *Infect Immun*. 84, 2317–2323.

Czepiel, J., Kędzierska, J., Biesiada, G., Birczyńska, M., Perucki, W., Nowak, P. and Garlicki, A. 2015. Epidemiology of *Clostridium difficile* infection: Results of a hospital-based study in Krakow, Poland. *Epidemiol Infect*. 143, 3235–3243.

Dancer, S.J. 2016. Dos and don'ts for hospital cleaning. *Curr Opin Infect Dis*. 29, 415–423.

Darkoh, C., Odo, C. and Dupont, H.L. 2016. Accessory gene regulator-1 locus is essential for virulence and pathogenesis of *Clostridium difficil*e. *mBio*. 7, e01237-16.

David, L.A., Maurice, C.F., Carmody, R.N., Gootenberg, D.B., Button, J.E., Wolfe, B.E., Ling, A. v., Devlin, A.S., Varma, Y., Fischbach, M.A., Biddinger, S.B., Dutton, R.J. and Turnbaugh, P.J. 2014. Diet rapidly and reproducibly alters the human gut microbiome. *Nature*. 505, 559–563.

Deeks, E.D. 2017. Bezlotoxumab: A review in preventing *Clostridium difficile* infection recurrence. *Drugs*. 77, 1657–1663.

DeFilipp, Z., Bloom, P.P., Torres Soto, M., Mansour, M.K., Sater, M.R.A., Huntley, M.H., Turbett, S., Chung, R.T., Chen, Y.-B. and Hohmann, E.L. 2019. Drug-resistant *E. coli* bacteremia transmitted by fecal microbiota transplant. *N Engl J Med*. 381, 2043–2050.

Diaz, O.R., Sayer, C. v., Popham, D.L. and Shen, A. 2018. *Clostridium difficile* lipoprotein GerS is required for cortex modification and thus spore germination. *mSphere*. 3, e00205-18

Díaz-González, F., Milano, M., Olguin-Araneda, V., Pizarro-Cerda, J., Castro-Córdova, P., Tzeng, S.C., Maier, C.S., Sarker, M.R. and Paredes-Sabja, D. 2015. Protein composition of the outermost exosporium-like layer of *Clostridium difficile* 630 spores. *J Proteomics*. 123, 1–13.

Dillon, A. and Lo, D.D. 2019. M cells: Intelligent engineering of mucosal immune surveillance. *Front Immunol*. 10, 1499.

Dingle, T.C., Mulvey, G.L. and Armstrong, G.D. 2011. Mutagenic analysis of the *Clostridium difficile* flagellar proteins, flic and flid, and their contribution to virulence in hamsters. *Infect Immun*. 79, 4061–4067.

Dingsdag, S.A. and Hunter, N. 2018. Metronidazole: an update on metabolism, structure-cytotoxicity and resistance mechanisms. *J Antimicrob Chemother*. 73, 265–279.

Domm, W., Brooks, L., Chung, H.L., Feng, C., Bowers, W.J., Watson, G., McGrath, J.L. and Dewhurst, S. 2011. Robust antigen-specific humoral immune responses to sublingually delivered adenoviral vectors encoding HIV-1 Env: Association with mucoadhesion and efficient penetration of the sublingual barrier. *Vaccine*. 29, 7080–7089.

Eckburg, P.B., Bik, E.M., Bernstein, C.N., Purdom, E., Dethlefsen, L., Sargent, M., Gill, S.R., Nelson, K.E. and Relman, D.A. 2005. Microbiology: Diversity of the human intestinal microbial flora. *Science*. 308, 1635–1638.

Edwards, A.N., Karim, S.T., Pascual, R.A., Jowhar, L.M., Anderson, S.E. and McBride, S.M. 2016. Chemical and stress resistances of *Clostridium difficile* spores and vegetative cells. *Front Microbiol*. 7, 1698.

Edwards, A.N., Nawrocki, K.L. and McBride, S.M. 2014. Conserved oligopeptide permeases modulate sporulation initiation in *Clostridium difficile*. *Infect Immun*. 82, 4276–4291.

Endres, B.T., Begum, K., Sun, H., Walk, S.T., Memariani, A., Lancaster, C., Gonzales-Luna, A.J., Dotson, K.M., Bassères, E., Offiong, C., Tupy, S., Kuper, K., Septimus, E., Arafat, R., Alam, M.J., Zhao, Z., Hurdle, J.G., Savidge, T.C. and Garey, K.W. 2019. Epidemic *Clostridioides difficile* ribotype 027 lineages: Comparisons of Texas versus worldwide strains. *Open Forum Infect Dis*. 6, ofz013

Enoch, D.A., Murray-Thomas, T., Adomakoh, N., Dedman, D., Georgopali, A., Francis, N.A. and Karas, A. 2020. Risk of complications and mortality following recurrent and non-recurrent *Clostridioides difficile* infection: a retrospective observational database study in England. *J Hosp Infect.* 106, 793-803.

Fantappie, L., Irene, C., de Santis, M., Armini, A., Gagliardi, A., Tomasi, M., Parri, M., Cafardi, V., Bonomi, S., Ganfini, L., Zerbini, F., Zanella, I., Carnemolla, C., Bini, L., Grandi, A. and Grandi, G. 2017. Some gram-negative lipoproteins keep their surface topology when transplanted from one species to another and deliver foreign polypeptides to the bacterial surface. *Mol Cell Proteomics*. 16, 1348–1364.

Farrow, K.A., Lyras, D. and Rood, J.I. 2001. Genomic analysis of the erythromycin resistance element Tn5398 from *Clostridium difficile*. *Microbiology*. 147, 2717–2728.

Feuerstadt, P., Stong, L., Dahdal, D.N., Sacks, N., Lang, K. and Nelson, W.W. 2020. Healthcare resource utilization and direct medical costs associated with index and recurrent *Clostridioides difficile* infection: a real-world data analysis. *J Med Econ*. 23, 603-609

de Filippo, C., Cavalieri, D., di Paola, M., Ramazzotti, M., Poullet, J.B., Massart, S., Collini, S., Pieraccini, G. and Lionetti, P. 2010. Impact of diet in shaping gut microbiota revealed by a comparative study in children from Europe and rural Africa. *Proc Natl Acad Sci U S A*. 107, 14691–14696.

Filippone, E.J., Kraft, W.K. and Farber, J.L. 2017. The nephrotoxicity of vancomycin. *Clinical Pharmacology and Therapeutics*. 102, 459–469.

Fimlaid, K.A., Jensen, O., Donnelly, M.L., Francis, M.B., Sorg, J.A. and Shen, A. 2015. Identification of a novel lipoprotein regulator of *Clostridium difficile* spore germination T. M. Koehler, ed. *PLoS Pathog*. 11, e1005239.

Fletcher, J.R., Erwin, S., Lanzas, C. and Theriot, C.M. 2018. Shifts in the gut metabolome and *Clostridium difficile* transcriptome throughout colonization and infection in a mouse model. *mSphere*. 3, e00089-18.

Fletcher, L.D., Bernfield, L., Barniak, V., Farley, J.E., Howell, A., Knauf, M., Ooi, P., Smith, R.P., Weise, P., Wetherell, M., Xie, X., Zagursky, R., Zhang, Y. and Zlotnick, G.W. 2004. Vaccine potential of the *Neisseria meningitidis* 2086 lipoprotein. *Infect Immun*. 72, 2088–2100.

Galdys, A.L., Nelson, J.S., Shutt, K.A., Schlackman, J.L., Pakstis, D.L., Pasculle, A.W., Marsh, J.W., Harrison, L.H. and Curry, S.R. 2014. Prevalence and duration of asymptomatic *Clostridium difficile* carriage among healthy subjects in Pittsburgh, Pennsylvania. *J Clin Microbiol*. 52, 2406–2409.

Gérard, P. 2014. Metabolism of cholesterol and bile acids by the gut microbiota. *Pathogens*. 3, 14.

Gerding, D.N., Johnson, S., Rupnik, M. and Aktories, K. 2014a. *Clostridium difficile* binary toxin CDT. *Gut Microbes*. 5, 15–27.

Gerding, D.N., Johnson, S., Rupnik, M. and Aktories, K. 2014b. *Clostridium difficile* binary toxin CDT: Mechanism, epidemiology, and potential clinical importance. *Gut Microbes*. 5, 15.

Gerding, D.N., Meyer, T., Lee, C., Cohen, S.H., Murthy, U.K., Poirier, A., van Schooneveld, T.C., Pardi, D.S., Ramos, A., Barron, M.A., Chen, H. and Villano, S. 2015. Administration of spores of nontoxigenic *Clostridium difficile* strain M3 for prevention of recurrent *C difficile* infection: A Randomized clinical trial. *J Am Med Assoc.* 313, 1719–1727.

Gerding, D.N., Sambol, S.P. and Johnson, S. 2018. Non-toxigenic *Clostridioides* (formerly clostridium) *difficile* for prevention of *C. difficile* infection: From bench to bedside back to bench and back to bedside. *Front Microbiol*. 9, 1–13.

Gerhard, R., Frenzel, E., Goy, S. and Olling, A. 2013. Cellular uptake of *Clostridium difficile* TcdA and truncated TcdA lacking the receptor binding domain. *J Med Microbiol*. 62, 1414–1422.

Ghose, C., Eugenis, I., Edwards, A.N., Sun, X., McBride, S.M. and Ho, D.D. 2016. Immunogenicity and protective efficacy of *Clostridium difficile* spore proteins. *Anaerobe*. 37, 85–95.

Giannasca, P.J., Zhang, Z.X., Lei, W.D., Boden, J.A., Giel, M.A., Monath, T.P. and Thomas, W.D. 1999. Serum antitoxin antibodies mediate systemic and mucosal protection from *Clostridium difficile* disease in hamsters. *Infect Immun*. 67, 527–38.

Giel, J.L., Sorg, J.A., Sonenshein, A.L. and Zhu, J. 2010. Metabolism of bile salts in mice influences spore germination in *Clostridium difficile*. *PLoS One*. 5, e8740.

Gil, F., Lagos-Moraga, S., Calderón-Romero, P., Pizarro-Guajardo, M. and Paredes-Sabja, D. 2017. Updates on *Clostridium difficile spore biology. Anaerobe.* 45, 3–9.

Girinathan, B.P., Monot, M., Boyle, D., McAllister, K.N., Sorg, J.A., Dupuy, B. and Govind, R. 2017. Effect of tcdR mutation on sporulation in the epidemic *Clostridium difficile* strain R20291. *mSphere*. 2. e00383-16

Govind, R. and Dupuy, B. 2012. Secretion of *Clostridium difficile* toxins A and B requires the holin-like protein tcdE. *PLoS Pathog*. 8. e1002727

Guoyan, Z., Yingfeng, A., Zabed, H., Qi, G., Yang, M., Jiao, Y., Li, W., Wenjing, S. and Xianghui, Q. 2019. *Bacillus subtilis* spore surface display

technology: A review of its development and applications. *J Microbiol Biotechnol*. 29, 179–190.

Gupta, S., Allen-Vercoe, E. and Petrof, E.O. 2016. Fecal microbiota transplantation: In perspective. *Therap Adv Gastroenterol*. 9, 229–239.

Haiko, J. and Westerlund-Wikström, B. 2013. The role of the bacterial flagellum in adhesion and virulence. *Biology*. 2, 1242–1267.

Hall, I.C. 1935. Intestinal flora in new-born infants. *Am J Dis Child*. 49, 390.

Hamilton, M.J., Weingarden, A.R., Unno, T., Khoruts, A. and Sadowsky, M.J. 2013. High-throughput DNA sequence analysis reveals stable engraftment of gut microbiota following transplantation of previously frozen fecal bacteria. *Gut Microbes*. 4, 125–135.

Hammond, G.A. and Johnson, J.L. 1995. The toxigenic element of *Clostridium difficile* strain VPI 10463. *Microb Pathog*. 19, 203–213.

Hammond, G.A., Lyerly, D.M. and Johnson, J.L. 1997. Transcriptional analysis of the toxigenic element of *Clostridium difficile*. *Microb Pathog*. 22, 143–154.

He, L., Peng, X., Chen, Y., Liu, G., Liu, Z., Zhu, J., Liu, Y., Liu, H., Liang, Y., Liu, F., Sun, L., & Peng, Y. (2016). Regulation of IgA class switch recombination in immunoglobulin a nephropathy: Retinoic acid signaling and BATF. *Am J Nephrol,* 43, 179–194.

Heap, J.T., Pennington, O.J., Cartman, S.T. and Minton, N.P. 2009. A modular system for Clostridium shuttle plasmids. *J Microbiol Methods*. 78, 79–85.

Heimann, S.M., Cruz Aguilar, M.R., Mellinghof, S. and Vehreschild, M.J.G.T. 2018. Economic burden and cost-effective management of *Clostridium difficil*e infections. *Med Mal infect*. 48, 23–29.

Hennequin, Claire, Collignon, A. and Karjalainen, T. 2001. Analysis of expression of GroEL (Hsp60) of *Clostridium difficile* in response to stress. *Microb Pathog*. 31, 255–260.

Hennequin, C., Porcheray, F., Waligora-Dupriet, A.J., Collignon, A., Barc, M.C., Bourlioux, P. and Karjalainen, T. 2001. GroEL (Hsp60) of *Clostridium difficile* is involved in cell adherence. *Microbiology*. 147, 87–96.

Hensgens, M.P.M., Goorhuis, A., Dekkers, O.M. and Kuijper, E.J. 2012. Time interval of increased risk for *Clostridium difficile* infection after exposure to antibiotics. *J Antimicrob Chemother*. 67, 742–748.

Higgins, D. and Dworkin, J. 2012. Recent progress in *Bacillus subtilis* sporulation. *FEMS Microbiol Rev*. 36, 131–148.

HogenEsch, H. 2012. Mechanism of immunopotentiation and safety of aluminum adjuvants. *Front Immunol*. 3, 406.

Hollister, E.B., Gao, C. and Versalovic, J. 2014. Compositional and functional features of the gastrointestinal microbiome and their effects on human health. *Gastroenterology*. 146, 1449–1458.

Holmgren, J. and Czerkinsky, C. 2005. Mucosal immunity and vaccines. *Nat Med*. 11, S45.

Holshue, M.L., DeBolt, C., Lindquist, S., Lofy, K.H., Wiesman, J., Bruce, H., Spitters, C., Ericson, K., Wilkerson, S., Tural, A., Diaz, G., Cohn, A., Fox, L.A., Patel, A., Gerber, S.I., Kim, L., Tong, S., Lu, X., Lindstrom, S., Pallansch, M.A., Weldon, W.C., Biggs, H.M., Uyeki, T.M. and Pillai, S.K. 2020. First case of 2019 novel coronavirus in the United States. *N Engl J Med*. 382, 929–936.

Hong, H.A., Ferreira, W.T., Hosseini, S., Anwar, S., Hitri, K., Wilkinson, A.J., Vahjen, W., Zentek, J., Soloviev, M. and Cutting, S.M. 2017. Te spore coat protein CotE facilitates host colonization by *Clostridium difficile. J Infect Dis*. 216, 1452–1459.

Howerton, A., Ramirez, N. and Abel-Santos, E. 2011. Mapping interactions between germinants and *Clostridium difficil*e spores. *J Bacteriol*. 193, 274–282.

Huang, J.-H. 2015. Biochemical and immunological characterizations of the receptor binding domain of *C. difficile* toxin B. *J Vaccines Vaccin*. 06, 1–9.

Huang, J.H., Shen, Z.Q., Lien, S.P., Hsiao, K.N., Leng, C.H., Chen, C.C., Siu, L.K., Chong, P.C.S. and Vedantam, G. 2015. Biochemical and immunological characterization of truncated fragments of the receptor-binding domains of *C. difficil*e Toxin A G. Vedantam, ed. *PLoS One*. 10, e0135045.

Huang, J.H., Wu, C.W., Lien, S.P., Leng, C.H., Hsiao, K.N., Liu, S.J., Chen, H.W., Siu, L.K. and Chong, P. 2015. Recombinant lipoprotein-based vaccine candidates against C. difficile infections. *J Biomed Sci*. 22, 65.

Hundsberger, T., Braun, V., Weidmann, M., Leukel, P., Sauerborn, M. and Eichel-Streiber, C. 1997. Transcription analysis of the genes *tcdA-E* of the pathogenicity locus of *Clostridium difficile*. *Eur J Biochem*. 244, 735–742.

Hutchings, M.I., Palmer, T., Harrington, D.J. and Sutcliffe, I.C. 2009. Lipoprotein biogenesis in Gram-positive bacteria: knowing when to hold ’em, knowing when to fold ’em. *Trends Microbiol*. 17, 13–21.

Irazoki, O., Hernandez, S.B. and Cava, F. 2019. Peptidoglycan muropeptides: Release, perception, and functions as signalling molecules. *Front Microbiol*. 10, 500.

Isticato, R., Cangiano, G., Tran, H.T., Ciabattini, A., Medaglini, D., Oggioni, M.R., de Felice, M., Pozzi, G. and Ricca, E. 2001. Surface display of recombinant proteins on *Bacillus subtilis* spores. *J Bacteriol*. 183, 6294–6301.

Jackson, D.A. and Elsawa, S.F. 2015. Factors regulating immunoglobulin production by normal and disease-associated plasma cells. *Biomolecules*. 5, 20.

Jackson, S., Calos, M., Myers, A. and Self, W.T. 2006. Analysis of proline reduction in the nosocomial pathogen *Clostridium difficile*. *J Bacteriol*. 188, 8487–8495.

Jank, T., Giesemann, T. and Aktories, K. 2007. Rho-glucosylating *Clostridium difficile* toxins A and B: New insights into structure and function. *Glycobiology*. 17, 15R–22R

Janoir, C., Denève, C., Bouttier, S., Barbut, F., Hoys, S., Caleechum, L., Chapetón-Montes, D., Pereira, F.C., Henriques, A.O., Collignon, A., Monot, M. and Dupuy, B. 2013. Adaptive strategies and pathogenesis of *Clostridium difficile* from In vivo transcriptomics. *Infect Immun*. 81, 3757–3769.

Jenior, M.L., Leslie, J.L., Young, V.B. and Schloss, P.D. 2017. *Clostridium difficile* colonizes alternative nutrient niches during infection across distinct murine gut microbiomes. *mSystems*. 2, e00063-17.

Johansen, F.E. and Kaetzel, C.S. 2011. Regulation of the polymeric immunoglobulin receptor and IgA transport: New advances in environmental factors that stimulate pIgR expression and its role in mucosal immunity. *Mucosal Immunol*. 4, 598–602.

Just, I., Selzer, J., Wilm, M., Eichel-Streiber, C. von, Mann, M. and Aktories, K. 1995. Glucosylation of Rho proteins by *Clostridium difficile* toxin B. *Nature*. 375, 500–503.

K. Garg, N., Mangal, S., Khambete, H., K. Sharma, P. and K. Tyagi, R. 2010. Mucosal delivery of vaccines: Role of mucoadhesive/biodegradable polymers. *Recent Pat Drug Deliv Formul*. 4, 114–128.

Kaetzel, C.S., Mestecky, J. and Johansen, F.-E. 2017. Two cells, one antibody: The discovery of the cellular origins and transport of secretory IgA. *J Immunol*. 198, 1765–1767.

Karyal, C., Hughes, Jaime., Kelly, Michelle L., Luckett, Jeni C., Kaye, Philip V., Cockayne, Alan., Minton, Nigel P., Griffin, Ruth. 2021. Colonisation factor CD0873, an attractive oral vaccine candidate against *Clostridioides difficile*. *Microorganisms*. 9, 1–25.

Karlyshev, A. v., Snyder, L.A.S., McFadden, J. and Griffin, R. 2015. Insight into proteomic investigations of *Neisseria meningitidis* serogroup C strain

L91543 from analysis of its genome sequence. *FEMS Microbiol Lett*. 362, 55.

Kelly, C.P. 2012. Can we identify patients at high risk of recurrent *Clostridium difficile* infection? *Clin Microbiol Infect*. 18, 21–27.

Khanna, S., Pardi, D.S., Aronson, S.L., Kammer, P.P., Orenstein, R., St Sauver, J.L., Harmsen, W.S. and Zinsmeister, A.R. 2012. The epidemiology of community-acquired clostridium difficile infection: A population-based study. *Am J Gastroenterol*. 107, 89–95.

Khoruts, A., Dicksved, J., Jansson, J.K. and Sadowsky, M.J. 2009. Changes in the composition of the human fecal microbiome after bacteriotherapy for recurrent *Clostridium difficile*-associated diarrhea. *J Clin Gastroenterol*. 44, 1.

Kirk, J.A., Banerji, O. and Fagan, R.P. 2017. Characteristics of the *Clostridium difficile* cell envelope and its importance in therapeutics. *Microb Biotechnol*. 10, 76–90.

Nagaro, Kristin J., Phillips, S. Tyler., Cheknis, Adam K., Sambol, Susan P., Zukowski, Walter E., Johnson, Stuart., Gerding, Dale N.. 2013. Nontoxigenic *Clostridium difficile* protects hamsters against challenge with historic and epidemic strains of toxigenic BI/NAP1/027 *C. difficile*. *Antimicrob Agents Chemother*. 57, 5266–5270.

Kool, M., Fierens, K. and Lambrecht, B.N. 2012. Alum adjuvant: Some of the tricks of the oldest adjuvant. *J Med Microbiol*. 61, 927–934.

Kovacs- Simon, A. 2013. *Characterisation of lipoproteins of Clostridium difficile and their role in virulence*. PhD Thesis, University of Exeter, Exeter.

Kovacs-Simon, A., Leuzzi, R., Kasendra, M., Minton, N., Titball, R.W. and Michell, S.L. 2014. Lipoprotein CD0873 is a novel adhesin of *Clostridium difficile*. *J Infect Dis*. 210, 274–284.

de la Riva, L., Willing, S.E., Tate, E.W. and Fairweather, N.F. 2011. Roles of cysteine proteases Cwp84 and Cwp13 in biogenesis of the cell wall of *Clostridium difficile*. *J Bacteriol*. 193, 3276–3285.

LaFrance, M.E., Farrow, M.A., Chandrasekaran, R., Sheng, J., Rubin, D.H. and Lacy, D.B. 2015. Identification of an epithelial cell receptor responsible for *Clostridium difficile* TcdB-induced cytotoxicity. *Proc Natl Acad Sci U S A*. 112, 7073–7078.

Lance George, W., Goldstein, E.J.C., Sutter, V.L., Ludwig, S.L. and Finegold, S.M. 1978. Ætiology of antimicrobial-agent-associated colitis. *Lancet*. 311, 802–803.

Lawler, A., Lambert, P. and Worthington, T. 2020. A revised understanding of *Clostridioides difficile* spore germination. *Trends Microbiol*. 28, 744–752.

Lawley, T.D., Clare, S., Walker, A.W., Goulding, D., Stabler, R.A., Croucher, N., Mastroeni, P., Scott, P., Raisen, C., Mottram, L., Fairweather, N.F., Wren, B.W., Parkhill, J. and Dougan, G. 2009. Antibiotic treatment of *Clostridium difficile* carrier mice triggers a supershedder state, spore-mediated transmission, and severe disease in immunocompromised hosts. *Infect Immun*. 77, 3661–3669.

Lawson, P.A., Citron, D.M., Tyrrell, K.L. and Finegold, S.M. 2016. Reclassification of *Clostridium difficile* as *Clostridioides difficile* (Hall and O'Toole 1935) Prévot 1938. *Anaerobe*. 40, 95–99.

Leffler, D.A. and Lamont, J.T. 2015. *Clostridium difficil*e infection D. L. Longo, ed. *N Engl J Med*. 372, 1539–1548.

Leng, C.H., Liu, S.J., Chen, H.W. and Chong, P. 2015. Recombinant bacterial lipoproteins as vaccine candidates. *Expert Rev Vaccines*. 14, 1623–1632.

Leusen, J.H.W. and Nimmerjahn, F. 2013. The role of IgG in immune responses *Mol Cell Mechan Antibody Act*. 85–112.

Libby, J.M., Jortner, B.S. and Wilkins, T.D. 1982. Effects of the two toxins of *Clostridium difficile* in antibiotic-associated cecitis in hamsters. *Infect Immun*. 36, 822–9.

Liu, Y.-W., Chen, Y.-H., Chen, J.-W., Tsai, P.-J. and Huang, I.-H. 2017. Immunization with recombinant TcdB-encapsulated nanocomplex induces protection against *Clostridium difficile* challenge in a mouse model. *Front Microbiol*. 0, 1411.

Lyras, D., O'Connor, J.R., Howarth, P.M., Sambol, S.P., Carter, G.P., Phumoonna, T., Poon, R., Adams, V., Vedantam, G., Johnson, S., Gerding, D.N. and Rood, J.I. 2009. Toxin B is essential for virulence of *Clostridium difficile*. *Nature*. 458, 1176–1179.

MacPherson, A.J., McCoy, K.D., Johansen, F.E. and Brandtzaeg, P. 2008. The immune geography of IgA induction and function. *Mucosal Immunol*. 1, 11–22.

Makino, S. and Moriyama, R. 2002. Hydrolysis of cortex peptidoglycan during bacterial spore germination. *Medical Science Monitor*. 8, RA119-27

Maldarelli, G.A., de Masi, L., von Rosenvinge, E.C., Carter, M. and Donnenberg, M.S. 2014. Identification, immunogenicity, and cross-reactivity of type IV pilin and pilin-like proteins from *Clostridium difficile*. *Pathog Dis*. 71, 302–314.

Mason, HS., Ball, JM., Shi, JJ., Jiang, X., Estes, MK., Arntzen, CJ., Nakanishi, U., Matsumura, A., Uozumi, A., Hiroi, T., Morita, S., Tanaka, K., Takaiwa, F. and Kiyono, H. 2007. Expression of Norwalk virus capsid protein in transgenic tobacco and potato and its oral immunogenicity in mice. *Proc Natl Acad Sci U S A*. 93, 5335–5340.

McDonald, L.C., Killgore, G.E., Thompson, A., Owens, R.C., Kazakova, S. v., Sambol, S.P., Johnson, S. and Gerding, D.N. 2005. An epidemic, toxin gene–variant strain of *Clostridium difficile*. *N Engl J Med*. 353, 2433–2441.

McFarland, L. v. 1999. Epidemiology, Risk factors and treatments for antibiotic-associated diarrhea. *Dig Dis*. 16, 292–307.

McGovern, B.H., Ford, C.B., Henn, M.R., Pardi, D.S., Khanna, S., Hohmann, E.L., O'Brien, E.J., Desjardins, C.A., Bernardo, P., Wortman, J.R., Lombardo, M.-J., Litcofsky, K.D., Winkler, J.A., McChalicher, C.W.J., Li, S.S., Tomlinson, A.D., Nandakumar, M., Cook, D.N., Pomerantz, R.J., Auninš, J.G. and Trucksis, M. 2020. SER-109, an investigational microbiome drug to reduce recurrence after *Clostridioides difficile* infection: Lessons learned from a phase 2 trial. *Clin Infect Dis*. 72, 2132–2140.

Mestecky, J., Russell, M.W. and Elson, C.O. 2014. Perspectives on mucosal vaccines: is mucosal tolerance a barrier? *J Immunol*. 179, 5633–5638.

Mészáros, B., Erdős, G., & Dosztányi, Z. (2018). IUPred2A: context-dependent prediction of protein disorder as a function of redox state and protein binding. *Nucleic Acids Res*, 46, W329–W337

Miller-Roll, T., Na'amnih, W., Cohen, D., Carmeli, Y. and Adler, A. 2016. Molecular types and antimicrobial susceptibility patterns of *Clostridium difficile* isolates in different epidemiological settings in a tertiary care center in Israel. *Diagn Microbiol Infect Dis*. 86, 450–454.

Miquel-Clopés, A., Bentley, E.G., Stewart, J.P. and Carding, S.R. 2019. Mucosal vaccines and technology. *Clin Exp Immunol*. 196, 205–214.

Mora, J.R., Iwata, M., Eksteen, B., Song, S.Y., Junt, T., Senman, B., Otipoby, K.L., Yokota, A., Takeuchi, H., Ricciardi-Castagnoli, P., Rajewsky, K., Adams, D.H. and von Andrian, U.H. 2006. Generation of gut-homing IgA-secreting B cells by intestinal dendritic cells. *Science*. 314, 1157–1160.

Mori, N. and Takahashi, T. 2018. Characteristics and immunological roles of surface layer proteins in *Clostridium difficile*. *Ann Lab Med*. 38, 189–195.

Mowat, A.McI. 2003. Anatomical basis of tolerance and immunity to intestinal antigens. *Nat Rev Immunol*. 3, 331–341.

Na, X., Kim, H., Moyer, M.P., Pothoulakis, C. and LaMont, J.T. 2008. gp96 is a human colonocyte plasma membrane binding protein for *Clostridium difficile* toxin A. *Infect Immun*. 76, 2862–2871.

Navalkele, B.D. and Chopra, T. 2018. Bezlotoxumab: An emerging monoclonal antibody therapy for prevention of recurrent *Clostridium difficile* infection. *Biologics*. 12, 11–21.

Negri, A., Potocki, W., Iwanicki, A., Obuchowski, M. and Hinc, K. 2013. Expression and display of *Clostridium difficile* protein FliD on the surface of Bacillus subtilis spores. *J Med Microbiol*. 62, 1379–1385.

Nelson, R.L., Suda, K.J. and Evans, C.T. 2017. Antibiotic treatment for *Clostridium difficile*-associated diarrhoea in adults. *Cochrane Database Syst Rev*. 3, CD004610

Ng, Y.K., Ehsaan, M., Philip, S., Collery, M.M., Janoir, C., Collignon, A., Cartman, S.T. and Minton, N.P. 2013. Expanding the repertoire of gene tools for precise manipulation of the *Clostridium difficile* genome: Allelic exchange using *pyrE* alleles M. R. Popoff, ed. *PLoS One*. 8, e56051.

Nguyen, C.T., Li, J., Anders, S., Garcia-Diaz, J., Staffeld-Coit, C. and Hand, J. 2018. Comparison of outcomes with vancomycin or metronidazole for mild-to-moderate *Clostridium difficile* associated diarrhea among solid organ transplant recipients: A retrospective cohort study. *Transpl Infect Dis*. 20, e12867.

Nguyen, M.T. and Götz, F. 2016. Lipoproteins of Gram-positive bacteria: key players in the immune response and virulence. *Microbiol Mol Biol Rev*. 80, 891–903.

Nguyen, M.T., Uebele, J., Kumari, N., Nakayama, H., Peter, L., Ticha, O., Woischnig, A.K., Schmaler, M., Khanna, N., Dohmae, N., Lee, B.L., Bekeredjian-Ding, I. and Götz, F. 2017. Lipid moieties on lipoproteins of commensal and non-commensal staphylococci induce differential immune responses. *Nat Commun*. 8, 1–12.

Nicholson, W.L. 2020. Spore‐forming bacteria as model organisms for studies in astrobiology *Extremophiles as Astrobiological Models*. 275–290.

O'Brien, J.B., McCabe, M.S., Athié-Morales, V., McDonald, G.S.A., Ní Eidhin, D.B. and Kelleher, D.P. 2005. Passive immunisation of hamsters against *Clostridium difficile* infection using antibodies to surface layer proteins. *FEMS Microbiol Lett*. 246, 199–205.

Oleszycka, E. and Lavelle, E.C. 2014. Immunomodulatory properties of the vaccine adjuvant alum. *Curr Opin Immunol*. 28, 1–5.

Olling, A., Seehase, S., Minton, N.P., Tatge, H., Schröter, S., Kohlscheen, S., Pich, A., Just, I. and Gerhard, R. 2012. Release of TcdA and TcdB from *Clostridium difficile* cdi 630 is not affected by functional inactivation of the tcdE gene. *Microb Pathog*. 52, 92–100.

Padmanabhan, P., Grosse, J., Asad, A.B.M.A., Radda, G.K. and Golay, X. 2013. Gastrointestinal transit measurements in mice with 99mTc-DTPA-labeled activated charcoal using NanoSPECT-CT. *Eur J Nucl Med Mol Imaging*. 3, 60.

Paiva, A.M.O., Jong, L. de, Friggen, A.H., Smits, W.K. and Corver, J. 2019. The C-terminal domain of *Clostridioides difficile* TcdC is exposed on the bacterial cell surface. *bioRxiv*., 202, e00771.

Paredes-Sabja, D. and Sarker, M.R. 2012. Adherence of *Clostridium difficile* spores to Caco-2 cells in culture. *J Med Microbiol*. 61, 1208–1218.

Paredes-Sabja, D. and Sarker, M.R. 2011. Germination response of spores of the pathogenic bacterium *Clostridium perfringens* and *Clostridium difficile* to cultured human epithelial cells. *Anaerobe*. 17, 78–84.

Paredes-Sabja, D., Setlow, P. and Sarker, M.R. 2011. Germination of spores of Bacillales and Clostridiales species: Mechanisms and proteins involved. *Trends Microbiol*. 19, 85–94.

Paredes-Sabja, D., Setlow, P. and Sarker, M.R. 2009. SleC is essential for cortex peptidoglycan hydrolysis during germination of spores of the pathogenic bacterium *Clostridium perfringens*. *J Bacteriol*. 191, 2711–2720.

Paredes-Sabja, D., Shen, A. and Sorg, J.A. 2014. *Clostridium difficile* spore biology: Sporulation, germination, and spore structural proteins. *Trends Microbiol*. 22, 406–416.

Pasteur, S. 2013. Study of a candidate *Clostridium difficile* toxoid vaccine (Cdiffense) in subjects at risk fo*r C. Difficile* infection. *Phase III clinical trial*. [Online]. [Accessed 31 May 2019]. Available from: https://clinicaltrials.gov/ct2/show/NCT01887912?term=clostridium+difficile+vaccine+sanofi&rank=2.

Péchiné, S., Bruxelle, J.F., Janoir, C. and Collignon, A. 2018. Targeting *Clostridium difficile* surface components to develop immunotherapeutic strategies against *clostridium difficile* infection. *Front Microbiol*. 9, 1009.

Péchiné, S., Denève, C., Le Monnier, A., Hoys, S., Janoir, C. and Collignon, A. 2011. Immunization of hamsters against *Clostridium difficile* infection using the Cwp84 protease as an antigen. *FEMS Immunol Med Microbiol*. 63, 73–81.

Péchiné, S., Hennequin, C., Boursier, C., Hoys, S. and Collignon, A. 2013. Immunization using GroEL decreases *Clostridium difficile* intestinal colonization M. R. Popoff, ed. *PLoS One*. 8, e81112.

Péchiné, S., Janoir, C. and Collignon, A. 2005. Variability of *Clostridium difficile* surface proteins and specific serum antibody response in patients with *Clostridium difficile*-associated disease. *J Clin Microbiol*. 43, 5018–5025.

Peng, Z., Jin, D., Kim, H.B., Stratton, C.W., Wu, B., Tang, Y.W. and Suna, X. 2017. Update on antimicrobial resistance in *Clostridium difficile:* Resistance mechanisms and antimicrobial susceptibility testing. *J Clin Microbiol*. 55, 1998–2008.

Pepin, J., Saheb, N., Coulombe, M.-A., Alary, M.-E., Corriveau, M.-P., Authier, S., Leblanc, M., Rivard, G., Bettez, M., Primeau, V., Nguyen, M., Jacob, C.-E. and Lanthier, L. 2005. Emergence of fluoroquinolones as the predominant risk factor for *Clostridium difficile*-associated diarrhea: A cohort study during an epidemic in Quebec. *Clin Infect Dis*. 41, 1254–1260.

Perez-Lopez, A., Behnsen, J., Nuccio, S.P. and Raffatellu, M. 2016. Mucosal immunity to pathogenic intestinal bacteria. *Nat Rev Immunol*. 16, 135–148.

PFIZER INC., 2017. A Phase 3, Placebo-Controlled, Randomized, Observer-Blinded Study To Evaluate The Efficacy, Safety, And Tolerability Of A Clostridium Difficile Vaccine In Adults 50 Years Of Age And Older. [online]. Available from: https://clinicaltrials.gov/ct2/show/NCT03090191%0Ahttps://www.clinicaltrialsregister.eu/ctr-search/trial/2016-003866-14/SE/ [Accessed 13 May 2019].

Phalipon, A, Cardona, A. Kraehenbuhl, J, P. Edelman, L. Sansonetti, P, J. Corthésy, B. 2002. Secretory component: A new role in secretory IgA-mediated immune exclusion *in vivo*. *Immunity* 17, 107–15.

Phelps, C.J., Lyerly, D.L., Johnson, J.L. and Wilkins, T.D. 1991. Construction and expression of the complete *Clostridium difficile* toxin A gene in Escherichia coli. *Infect Immun*. 59, 150–153.

Phetcharaburanin, J., Hong, H.A., Colenutt, C., Bianconi, I., Sempere, L., Permpoonpattana, P., Smith, K., Dembek, M., Tan, S., Brisson, M.C., Brisson, A.R., Fairweather, N.F. and Cutting, S.M. 2014. The spore-associated protein BclA1 affects the susceptibility of animals to colonization and infection by *Clostridium difficile. Mol Microbiol*. 92, 1025–1038.

Piepenbrink, K.H., Maldarelli, G.A., Martinez De La Peña, C.F., Dingle, T.C., Mulvey, G.L., Lee, A., von Rosenvinge, E., Armstrong, G.D., Donnenberg, M.S. and Sundberg, E.J. 2015. Structural and evolutionary analyses show unique stabilization strategies in the type IV pili of *Clostridium difficile*. *Structure*. 23, 385–396.

Pizarro-Guajardo, M., Calderón-Romero, P., Castro-Córdova, P., Mora-Uribe, P. and Paredes-Sabja, D. 2016. Ultrastructural variability of the exosporium layer of *Clostridium difficile* spores. *Applied and Environ Microbiol*. 82, 2202–2209.

Pizarro-Guajardo, M., Ravanal, M.C., Paez, M.D., Callegari, E. and Paredes-Sabja, D. 2018. Identification of *Clostridium difficile* immunoreactive spore proteins of the epidemic strain R20291. *Proteomics Clin Appl*. 12, 1700182.

Popham, D.L., Helin, J., Costello, C.E. and Setlow, P. 1996. Muramic lactam in peptidoglycan of *Bacillus subtilis* spores is required for spore outgrowth but not for spore dehydration or heat resistance. *Proc Natl Acad Sci U S A*. 93, 15405–15410.

Potot, S., Serra, C.R., Henriques, A.O. and Schyns, G. 2010. Display of recombinant proteins on *Bacillus subtilis* spores, using a coat-associated enzyme as the carrier. *Applied and Environ Microbiol*. 76, 5926–5933.

Price, A.B., Larson, H.E. and Crow, J. 1979. Morphology of experimental antibiotic-associated enterocolitis in the hamster: A model for human pseudomembranous colitis and antibiotic-associated diarrhea. *Gut*. 20, 467–475.

Qiu, H., Cassan, R., Johnstone, D., Han, X., Joyee, A.G., McQuoid, M., Masi, A., Merluza, J., Hrehorak, B., Reid, R., Kennedy, K., Tighe, B., Rak, C., Leonhardt, M., Dupas, B., Saward, L., Berry, J.D. and Nykiforuk, C.L. 2016. Novel clostridium difficile anti- Toxin (TcdA and TcdB) humanized monoclonal antibodies demonstrate in vitro neutralization across a broad spectrum of clinical strains and in vivo potency in a hamster spore challenge model. *PLoS One*. 11, e0157970

Rakoff-Nahoum, S., Paglino, J., Eslami-Varzaneh, F., Edberg, S. and Medzhitov, R. 2004. Recognition of commensal microflora by toll-like receptors is required for intestinal homeostasis. *Cell*. 118, 229–241.

Relations, M. 2015. Nearly half a million Americans suffered from *Clostridium difficile* infections in a single year | CDC Online Newsroom | CDC. *Centers for Disease Control and Prevention*. [Online]. [Accessed 7 May 2019]. Available from: https://www.cdc.gov/media/releases/2015/p0225-clostridium-difficile.html.

Riley, T. v., Lyras, D. and Douce, G.R. 2019. Status of vaccine research and development for *Clostridium difficile*. *Vaccine*. 37, 7300-7306.

Rohlfing, A.E., Eckenroth, B.E., Forster, E.R., Kevorkian, Y., Donnelly, M.L., Benito de la Puebla, H., Doublié, S. and Shen, A. 2019. The CspC pseudoprotease regulates germination of *Clostridioides difficile* spores in response to multiple environmental signals D. A. Garsin, ed. *PLoS Genet*. 15, e1008224.

Rosales-Mendoza, S., Cervantes-Rincón, T., Romero-Maldonado, A., Monreal-Escalante, E. and Nieto-Gómez, R. 2021. Transgenic plants expressing a *Clostridium difficile* spore antigen as an approach to develop low-cost oral vaccines. *Biotech Prog*. 37, e3141.

Rossez, Y., Wolfson, E.B., Holmes, A., Gally, D.L. and Holden, N.J. 2015. Bacterial Flagella: Twist and Stick, or Dodge across the Kingdoms J. B. Bliska, ed. *PLoS Pathog*. 11, e1004483.

Rupnik, M., Wilcox, M.H. and Gerding, D.N. 2009. *Clostridium difficile* infection: New developments in epidemiology and pathogenesis. *Nat Rev Microbiol*. 7, 526–536.

Sambol, S.P., Merrigan, M.M., Tang, J.K., Johnson, S. and Gerding, D.N. 2002. Colonization for the prevention of *Clostridium difficile* disease in hamsters. *J Infect Dis*. 186, 1781–1789.

San-Juan-Rodriguez, A., Parekh, N., Newman, T. and Hernandez, I. 2018. Pricing of monoclonal antibodies in the United States. *Glo J Qual Saf Healthcare*. 1, 4.

Schmaler, M., Jann, N.J., Ferracin, F., Landolt, L.Z., Biswas, L., Götz, F. and Landmann, R. 2009. Lipoproteins in *Staphylococcus aureus* mediate inflammation by TLR2 and iron-dependent growth *in vivo* . *J Immunol*. 182, 7110–7118.

Sebaihia, M., Wren, B.W., Mullany, P., Fairweather, N.F., Minton, N., Stabler, R., Thomson, N.R., Roberts, A.P., Cerdeño-Tárraga, A.M., Wang, H., Holden, M.T.G.T., Wright, A., Churcher, C., Quail, M.A., Baker, S., Bason, N., Brooks, K., Chillingworth, T., Cronin, A., Davis, P., Dowd, L., Fraser, A., Feltwell, T., Hance, Z., Holroyd, S., Jagels, K., Moule, S., Mungall, K., Price, C., Rabbinowitsch, E., Sharp, S., Simmonds, M., Stevens, K., Unwin, L., Whithead, S., Dupuy, B., Dougan, G., Barrell, B. and Parkhill, J. 2006. The multidrug-resistant human pathogen *Clostridium difficile* has a highly mobile, mosaic genome. *Nature Genetics*. 38, 779–786.

Senoh, M., Iwaki, M., Yamamoto, A., Kato, H., Fukuda, T. and Shibayama, K. 2018. Development of vaccine for *Clostridium difficile* infection using membrane fraction of nontoxigenic *Clostridium difficile*. *Microb Pathog*. 123, 42–46.

Setlow, P. 2003. Spore germination. *Curr Opin Microbiol*. 6, 550–556.

Setlow, P. (2006). Spores of *Bacillus subtilis*: Their resistance to and killing by radiation, heat and chemicals. *J Appl Microbiol*, 101, 514–525.

Shahmirzadi, S. v., Nguyen, M.-T. and Götz, F. 2016. Evaluation of *Staphylococcus aureus* Llpoproteins: Role in nutritional acquisition and pathogenicity. *Front Microbiol*. 7, 1404.

Shim, J.K., Johnson, S., Samore, M.H., Bliss, D.Z. and Gerding, D.N. 1998. Primary symptomless colonisation by *Clostridium difficile* and decreased risk of subsequent diarrhoea. *Lancet*. 351, 633–636.

da Silva, R.A.G., Churchward, C.P., Karlyshev, A. V., Eleftheriadou, O., Snabaitis, A.K., Longman, M.R., Ryan, A. and Griffin, R. 2017. The role of apolipoprotein N-acyl transferase, Lnt, in the lipidation of factor H binding protein of *Neisseria meningitidis* strain MC58 and its potential as a drug target. *Br J Pharmacol*. 174, 2247–2260.

da Silva, R.A.G., Karlyshev, A. v., Oldfield, N.J., Wooldridge, K.G., Bayliss, C.D., Ryan, A. and Griffin, R. 2019. variant signal peptides of vaccine antigen, FHbp, Impair Processing Affecting Surface Localization And Antibody-mediated Killing In Most Meningococcal Isolates. *Front Microbiol*. 10, 2847.

Slieman, T.A. and Nicholson, W.L. 2001. Role of dipicolinic acid in survival of *Bacillus subtilis* spores exposed to artificial and solar UV radiation. *Applied and Environ Microbiol*. 67, 1274–1279.

Small, J.D. 1968. Fatal enterocolitis in hamsters given lincomycin hydrochloride. *Lab Anim Care*. 18, 411–420.

Smits, L.P., Bouter, K.E.C., de Vos, W.M., Borody, T.J. and Nieuwdorp, M. 2013. Therapeutic potential of fecal microbiota transplantation. *Gastroenterology*. 145, 946–953.

Smits, W.K., Lyras, D., Lacy, D.B., Wilcox, M.H. and Kuijper, E.J. 2016. *Clostridium difficile* infection. *Nat Rev Dis Primers*. 2, 1–20.

Sorg, J.A. and Sonenshein, A.L. 2008. Bile salts and glycine as cogerminants for *Clostridium difficile* spores. *J Bacteriol*. 190, 2505–2512.

Spigaglia, P. 2016. Recent advances in the understanding of antibiotic resistance in *Clostridium difficile* infection. *Ther Adv Infect Dis*. 3, 23–42.

Spigaglia, P., Mastrantonio, P., & Barbanti, F. 2018. Antibiotic resistances of *Clostridium difficile*. *Adv Exp Med Bio*. 1050, 137–159.

Stavnezer, J., Guikema, J.E.J. and Schrader, C.E. 2008. Mechanism and regulation of class switch recombination. *Ann Rev Immunol*. 26, 261.

Steiner, E., Dago, A.E., Young, D.I., Heap, J.T., Minton, N.P., Hoch, J.A. and Young, M. 2011. Multiple orphan histidine kinases interact directly with Spo0A to control the initiation of endospore formation in *Clostridium acetobutylicum*. *Mol Microbiol*. 80, 641–654.

Takeoka, A., Takumi, K., Koga, T. and Kawata, T. 1991. Purification and characterization of S layer proteins from *Clostridium difficile* GAI 0714. *Journal of General Microbiology*. 137, 261–267.

Tang-Feldman, Y.J., Ackermann, G., Henderson, J.P., Silva, J. and Cohen, S.H. 2002. One-step cloning and expression of *Clostridium difficile* toxin B gene (tcdB). *Mol Cell Probes*. 16, 179–183.

Tao, L., Zhang, J., Meraner, P., Tovaglieri, A., Wu, X., Gerhard, R., Zhang, X., Stallcup, W.B., Miao, J., He, X., Hurdle, J.G., Breault, D.T., Brass, A.L. and Dong, M. 2016. Frizzled proteins are colonic epithelial receptors for *C. difficile* toxin B. *Nature*. 538, 350–355.

Tariq, R., Pardi, D. S., Bartlett, M. G., & Khanna, S. (2019). Low cure rates in controlled trials of fecal microbiota transplantation for recurrent

clostridium difficile infection: A systematic review and meta-analysis. *Clin Infect Dis*, 68, 1351–1358.

Tasteyre, A., Barc, M.C., Collignon, A., Boureau, H. and Karjalainen, T. 2001. Role of FliC and FliD flagellar proteins of *Clostridium difficile* in adherence and gut colonization. *Infect Immun*. 69, 7937–7940.

Tasteyre, A., Barc, M.C., Karjalainen, T., Dodson, P., Hyde, S., Bourlioux, P. and Borriello, P. 2000. A *Clostridium difficile* gene encoding flagellin. *Microbiology*. 146, 957–966.

Tasteyre, A., Karjalainen, T., Avesani, V., Delmée, M., Collignon, A., Bourlioux, P. and Barc, M.C. 2001. Molecular characterization of fliD gene encoding flagellar cap and its expression among *Clostridium difficile* isolates from different serogroups. *J Clin Microbiol*. 39, 1178–1183.

Tedesco, F.J., Barton, R.W. and Alpers, D.H. 1974. Clindamycin associated colitis. A prospective study. *Ann Intern Med*. 81, 429–433.

Thanissery, R., Winston, J.A. and Theriot, C.M. 2017. Inhibition of spore germination, growth, and toxin activity of clinically relevant *C. difficile* strains by gut microbiota derived secondary bile acids. *Anaerobe*. 45, 86–100.

Theriot, C.M., Bowman, A.A. and Young, V.B. 2016. Antibiotic-induced alterations of the gut microbiota alter secondary bile acid production and allow for *Clostridium difficile* spore germination and outgrowth in the large intestine. *mSphere*. 1, e0004.

Tian, J.H., Glenn, G., Flyer, D., Zhou, B., Liu, Y., Sullivan, E., Wu, H., Cummings, J.F., Elllingsworth, L. and Smith, G. 2017. *Clostridium difficile* chimeric toxin receptor binding domain vaccine induced protection against different strains in active and passive challenge models. *Vaccine*. 35, 4079–4087.

Tulli, L., Marchi, S., Petracca, R., Shaw, H.A., Fairweather, N.F., Scarselli, M., Soriani, M. and Leuzzi, R. 2013. Cbpa: A novel surface exposed adhesin of *Clostridium Difficile* targeting human collagen. *Cell Microbiol*. 15, 1674–1687.

Uddin, A.N., Bejugam, N.K., Gayakwad, S.G., Akther, P. and D'Souza, M.J. 2009. Oral delivery of gastro-resistant microencapsulated typhoid vaccine. *J Drug Target*. 17, 553–560.

Usui, Y., Ayibieke, A., Kamiichi, Y., Okugawa, S., Moriya, K., Tohda, S. and Saito, R. 2020. Impact of deoxycholate on *Clostridioides difficile* growth, toxin production, and sporulation. *Heliyon*. 6, e03717.

Vardakas, K.Z., Polyzos, K.A., Patouni, K., Rafailidis, P.I., Samonis, G. and Falagas, M.E. 2012. Treatment failure and recurrence of *Clostridium difficile* infection following treatment with vancomycin or metronidazole: A systematic review of the evidence. *Int J Antimicrob Agents*. 40, 1–8.

Venugopal, A.A. and Johnson, S. 2012. Fidaxomicin: A novel macrocyclic antibiotic approved for treatment of *Clostridium difficile* infection. *Clin Infect Dis*. 54, 568–574.

Villano, S.A., Seiberling, M., Tatarowicz, W., Monnot-Chase, E. and Gerding, D.N. 2012. Evaluation of an oral suspension of VP20621, spores of nontoxigenic *Clostridium difficile* strain M3, in healthy subjects. *Antimicrob Agents Chemother*. 56, 5224–5229.

Voth, D.E. and Ballard, J.D. 2005. *Clostridium difficile* toxins: Mechanism of action and role in disease. *Clin Microbiol Rev*. 18, 247–263.

Waligora, A.J., Hennequin, C., Mullany, P., Bourlioux, P., Collignon, A. and Karjalainen, T. 2001. Characterization of a cell surface protein of *Clostridium difficil*e with adhesive properties. *Infect Immun*. 69, 2144–2153.

Wang, S., Wang, Y., Cai, Y., Kelly, C.P. and Sun, X. 2018. Novel chimeric protein vaccines against *Clostridium difficile* infection. *Front Immunol*. 9, 2440.

Wang, Y., Wang, S., Bouillaut, L., Li, C., Duan, Z., Zhang, K., Ju, X., Tzipori, S., Sonenshein, A.L. and Sun, X. 2018. Oral immunization with nontoxigenic *Clostridium difficile* strains expressing chimeric fragments of TcdA and TcdB elicits protective immunity against *C. difficile* infection in both mice and hamsters. *Infect Immun*. 86, e00489-18.

Watanakunakorn, C. 1984. Mode of action and in-vitro activity of vancomycin. *J Antimicrob Chemother*. 14, 7–18.

Wetzel, D. and McBride, S.M. 2020. The impact of pH on *Clostridioides difficile* sporulation and physiology. *Applied and Environ Microbiol*. 86, e02706-19.

Wheeldon, L.J., Worthington, T. and Lambert, P.A. 2011. Histidine acts as a co-germinant with glycine and taurocholate for *Clostridium difficile* spores. *J Appl Microbiol*. 110, 987–994.

Wilcox, M.H., Gerding, D.N., Poxton, I.R., Kelly, C., Nathan, R., Birch, T., Cornely, O.A., Rahav, G., Bouza, E., Lee, C., Jenkin, G., Jensen, W., Kim, Y.-S., Yoshida, J., Gabryelski, L., Pedley, A., Eves, K., Tipping, R., Guris, D., Kartsonis, N. and Dorr, M.-B. 2018. Bezlotoxumab for prevention of recurrence of *Clostridium difficile* infection. *Drug Ther Bull*. 56, 57–60.

Wilcox, M.H., Gerding, D.N., Poxton, I.R., Kelly, C., Nathan, R., Birch, T., Cornely, O.A., Rahav, G., Bouza, E., Lee, C., Jenkin, G., Jensen, W., Kim, Y.S., Yoshida, J., Gabryelski, L., Pedley, A., Eves, K., Tipping, R., Guris, D., Kartsonis, N. and Dorr, M.B. 2017. Bezlotoxumab for Prevention of Recurrent *Clostridium difficile* Infection. *N Engl J Med*. 376, 305–317.

Wilson, K.H. 1983. Efficiency of various bile salt preparations for stimulation of *Clostridium difficile* spore germination. *J Clin Microbiol*. 18, 1017–1019.

Wilson, K.H., Kennedy, M.J. and Fekety, F.R. 1982. Use of sodium taurocholate to enhance spore recovery on a medium selective for *Clostridium difficile*. *J Clin Microbiol*. 15, 443–446.

Wilson, K.H. and Sheagren, J.N. 1983. Antagonism of toxigenic *Clostridium difficile* by nontoxigenic *C. difficile*. *J Infect Dis*. 147, 733–736.

Wright, A., Drudy, D., Kyne, L., Brown, K. and Fairweather, N.F. 2008. Immunoreactive cell wall proteins of *Clostridium difficile* identified by human sera. *J Med Microbiol*. 57, 750–756.

Yuan, P., Zhang, H., Cai, C., Zhu, S., Zhou, Y., Yang, X., He, R., Li, C., Guo, S., Li, S., Huang, T., Perez-Cordon, G., Feng, H. and Wei, W. 2015. Chondroitin sulfate proteoglycan 4 functions as the cellular receptor for *Clostridium difficile* toxin B. *Cell Res*. 25, 157–168.

Zückert, W.R. 2014. Secretion of bacterial lipoproteins: Through the cytoplasmic membrane, the periplasm and beyond. *Biochimica et Biophysica Acta - Molecular Cell Res*. 1843, 1509–1516.